161

0-315-12475-X

■✶ National Library
of Canada

Bibliothèque nationale
du Canada

Canadian Theses Division   Division des thèses canadiennes

Ottawa, Canada
K1A 0N4

60386

PERMISSION TO MICROFILM — AUTORISATION DE MICROFILMER

• Please print or type — Écrire en lettres moulées ou dactylographier

Full Name of Author — Nom complet de l'auteur

MANAT TIPTANATORANIN

Date of Birth — Date de naissance	Country of Birth — Lieu de naissance
4TH MAY 1950	THAILAND

Permanent Address — Résidence fixe

1705 CORNELL DRIVE , ALAMEDA , CALIFORNIA 94501

U.S.A

Title of Thesis — Titre de la thèse

NMR METHODS OF DETERMINING THE SOLVATION NUMBER IN

PARAMAGNETIC METAL ION-CONTAINING SOLUTIONS

University — Université

UNIVERSITY OF ALBERTA

Degree for which thesis was presented — Grade pour lequel cette thèse fut présentée

Ph. D.

Year this degree conferred — Année d'obtention de ce grade	Name of Supervisor — Nom du directeur de thèse
1982	ROBERT B. JORDAN

Permission is hereby granted to the NATIONAL LIBRARY OF CANADA to microfilm this thesis and to lend or sell copies of the film.

The author reserves other publication rights, and neither the thesis nor extensive extracts from it may be printed or otherwise reproduced without the author's written permission.

L'autorisation est, par la présente, accordée à la BIBLIOTHÈQUE NATIONALE DU CANADA de microfilmer cette thèse et de prêter ou de vendre des exemplaires du film.

L'auteur se réserve les autres droits de publication; ni la thèse ni de longs extraits de celle-ci ne doivent être imprimés ou autrement reproduits sans l'autorisation écrite de l'auteur.

Date	Signature
7th OCTOBER 1982	

NL-91 (4/77)

CANADIAN THESES ON MICROFICHE

I.S.B.N.

THESES CANADIENNES SUR MICROFICHE

National Library of Canada
Collections Development Branch

Canadian Theses on
Microfiche Service

Ottawa, Canada
K1A 0N4

Bibliothèque nationale du Canada
Direction du développement des collections

Service des thèses canadiennes
sur microfiche

NOTICE

The quality of this microfiche is heavily dependent
upon the quality of the original thesis submitted for
microfilming. Every effort has been made to ensure
the highest quality of reproduction possible.

If pages are missing, contact the university which
granted the degree.

Some pages may have indistinct print especially
if the original pages were typed with a poor typewriter
ribbon or if the university sent us a poor photocopy.

Previously copyrighted materials (journal articles,
published tests, etc.) are not filmed.

Reproduction in full or in part of this film is gov-
erned by the Canadian Copyright Act, R.S.C. 1970,
c. C-30. Please read the authorization forms which
accompany this thesis.

AVIS

La qualité de cette microfiche dépend grandement de
la qualité de la thèse soumise au microfilmage. Nous
avons tout fait pour assurer une qualité supérieure
de reproduction.

S'il manque des pages, veuillez communiquer
avec l'université qui a conféré le grade.

La qualité d'impression de certaines pages peut
laisser à désirer, surtout si les pages originales ont été
dactylographiées à l'aide d'un ruban usé ou si l'univer-
sité nous a fait parvenir une photocopie de mauvaise
qualité.

Les documents qui font déjà l'objet d'un droit
d'auteur (articles de revue, examens publiés, etc.) ne
sont pas microfilmés.

La reproduction, même partielle, de ce microfilm
est soumise à la Loi canadienne sur le droit d'auteur,
SRC 1970, c. C-30. Veuillez prendre connaissance des
formules d'autorisation qui accompagnent cette thèse.

THIS DISSERTATION
HAS BEEN MICROFILMED
EXACTLY AS RECEIVED

LA THÈSE A ÉTÉ
MICROFILMÉE TELLE QUE
NOUS L'AVONS REÇUE

Canada

THE UNIVERSITY OF ALBERTA

NMR METHODS OF DETERMINING THE SOLVATION NUMBER

IN PARAMAGNETIC METAL ION-CONTAINING SOLUTIONS

by

MANAT TIPTANATORANIN

A THESIS

SUBMITTED TO THE FACULTY OF GRADUATE STUDIES AND RESEARCH

IN PARTIAL FULFILMENT OF THE REQUIREMENTS FOR THE DEGREE

OF DOCTOR OF PHILOSOPHY

DEPARTMENT OF CHEMISTRY

EDMONTON, ALBERTA

FALL   1982

THE UNIVERSITY OF ALBERTA

RELEASE FORM

NAME OF AUTHOR   MANAT TIPTANATORANIN

TITLE OF THESIS   NMR METHODS OF DETERMINING THE

                      SOLVATION NUMBER IN PARAMAGNETIC METAL

                      ION-CONTAINING SOLUTIONS

DEGREE FOR WHICH THESIS WAS PRESENTED   Ph.D.

YEAR THIS DEGREE GRANTED   1982

      Permission is hereby granted to THE UNIVERSITY OF

ALBERTA LIBRARY to reproduce single copies of this

thesis and to lend or sell such copies for private,

scholarly or scientific research purposes only.

      The author reserves other publication rights, and

neither the thesis nor extensive extracts from it may

be printed or otherwise reproduced without the author's

written permission.

PERMANENT ADDRESS:

1705 Cornell Drive

Alameda, California 94501

DATED .....October..4....., 1982.

THE UNIVERSITY OF ALBERTA

FACULTY OF GRADUATE STUDIES AND RESEARCH

The undersigned certify that they have read, and recommend to the Faculty of Graduate Studies and Research, for acceptance, a thesis entitled

"NMR METHODS OF DETERMINING THE SOLVATION NUMBER

IN PARAMAGNETIC METAL ION-CONTAINING SOLUTIONS"

submitted by Manat Tiptanatoranin in partial fulfilment of the requirements for the degree of Doctor of Philosophy.

....
Supervisor

....
External Examiner

....

....

....

........October 4,....1982.

To My Parents

ABSTRACT

The solvation numbers (n) of the nickel(II),
NipyDPT^{2+}, and NiTRI^{2+} complexes in acetonitrile have been
determined using nmr spectroscopy. The nmr method of
determining the solvation number involves measurements of
the bulk solvent proton chemical shift ($\Delta\omega_{obsd}$) and
transverse relaxation rate (R_{2obsd}) at various temperatures.
The R_{2obsd} values were measured as a function of the
separation (t_{CP}) between successive 180° pulses in the
Carr-Purcell-Meiboom-Gill pulse sequence. From the
modified Bloch equations, a general theoretical expression
for the t_{CP} dependence of R_{2obsd} has been derived for
two-site exchange systems without restrictions on the
relative magnitudes of the relaxation rates or populations
of the two sites. Non-linear least-squares fitting of the
R_{2obsd}-t_{CP} data to the theoretical equation yielded the
solvent exchange rate (τ_m^{-1}) and the chemical shift of the
solvent molecule coördinated to the paramagnetic metal
complex in solution ($\Delta\omega_m$).

Two important facts emerge from the R_{2obsd}-t_{CP}
study of the three nickel(II) complexes in acetonitrile.
The $\Delta\omega_m$ value obtained from the analysis is independent
of the initially assumed n value in the slow exchange
region where R_{2obsd} is controlled by τ_m^{-1}. Anomalies are
observed in the temperature dependencies of the calculated

τ_m^{-1} and $\Delta\omega_m$ in the intermediate exchange region, where R_{2obsd} is a maximum, when the wrong n value has been assumed. The slow exchange region $R_{2obsd}-t_{CP}$ data determine reliably the $\Delta\omega_m$ value which can be combined with $n\Delta\omega_m$ from the chemical shift analysis to give the solvation number. The intermediate exchange region data provide an excellent criterion for the selection of the solvation number.

A third method for determining the solvation number is achieved by placing restrictions on the temperature dependence of all parameters in the $R_{2obsd}-t_{CP}$ analysis and analysing the data at all temperatures together. No assumption on the n value is necessary with this method.

General limitations of the $R_{2obsd}-t_{CP}$ method of determining the solvation number originated from both the chemical natures of the systems studied and from limitations in instrumentation of the pulsed nmr method. These limitations are discussed in detail.

The $R_{2obsd}-t_{CP}$ solvation number study gives the solvation numbers of six, one, and two respectively for the Ni^{2+}, $NipyDPT^{2+}$, and $NiTRI^{2+}$ complexes in acetonitrile. For all the nickel(II) complexes in acetonitrile, except the $NiTRI^{2+}$ complex, the solvation numbers determined agree with the total ligand coordination number of six around the nickel(II) centre. The solvation

number of two obtained for the NiTRI^{2+} complex in acetonitrile seems to be inconsistent with the expected octahedral ligand geometry of the nickel(II) complex since the TRI ligand is a tridendate. Possible explanations for this apparent inconsistency are discussed in Chapter IV. Further studies are needed to clarify some of the possibilities discussed.

ACKNOWLEDGEMENTS

TABLE OF CONTENTS

Chapter III   RESULTS AND DISCUSSION

x

LIST OF TABLES

LIST OF FIGURES

xx

Chapter I

INTRODUCTION

When a salt or coordination complex of a metal ion is dissolved in some coordinating solvent it is often difficult to determine the number of solvent molecules coordinated to the metal ion. This number will be referred to as the solvation number, and the purpose of this work is to apply and assess an nmr method for its determination. To illustrate the problem with a simple system one might consider what happens when $CoCl_2$ is dissolved in acetonitrile (AN); possible species are $(AN)_5CoCl^+$, $(AN)_4CoCl_2$, $(AN)_3CoCl^+$, and $(AN)_2CoCl_2$. These possibilities are distinguishable if one has a method of determining the solvation number of cobalt (II) in the system.

The solvation number is obviously important to an understanding of the chemistry of dissolved metal ions. The number of coordinated solvent molecules will affect the overall ligand geometry, it is likely to affect the chemical reactivity, and it is required in calculating specific rate constants for solvent exchange from the coordination sphere.

The earlier methods for determining solvation number have been reviewed by Lincoln[1]. In systems which are kinetically inert, isolation and analysis are satisfactory methods. For inert systems or those that can be cooled to a temperature where ligand exchange is slow on

the nmr time scale, then simple integration of the bulk and coordinated solvent resonances can be used to determine the solvation number. This method is particularly convenient for diamagnetic species, but in paramagnetic complexes the coordinated solvent peak is broadened making detection difficult and integration uncertain.

The solvation number can also be determined from chemical shift measurements on solutions containing a labile paramagnetic ion which causes large solvent shifts. Dysprosium(III) has been used for this purpose. If Dy^{3+} is dissolved in a solvent of concentration [s] then the observed chemical shift is

$$\Delta\omega_{obsd} = q\Delta\omega_m [Dy^{3+}]/[s] ,$$

where q is the solvation number of the Dy^{3+} ion and $\Delta\omega_m$ is the chemical shift of the solvent molecules coordinated to Dy^{3+}. If another metal (M) is added to the solution at some concentration [m] and has a solvation number n, then the observed shift due to the dysprosium(III) is

$$\Delta\omega'_{obsd} = q\Delta\omega_m [Dy^{3+}]/([s] - n[m]).$$

Then n can be calculated from the values of $\Delta\omega_{obsd}$ and $\Delta\omega'_{obsd}$. The main disadvantage of this method is that it requires relatively high concentration of M so that n[m] is significant relative to [s] to make $\Delta\omega'_{obsd}$ significantly different from $\Delta\omega_{obsd}$.

For kinetically labile systems less direct methods are generally required. The electronic spectrum of the transition metal ion contains bands due to d-d transitions which are usually sensitive to the ligand geometry and provide a guide to coordination number. It may even be possible to compare the reflectance spectrum of a solid of known structure to its solution spectrum and demonstrate coordination geometry in solution. The method is primarily a probe of geometry and could differentiate octahedral $(AN)_4CoCl_2$ from tetrahedral $(AN)_2CoCl_2$, but it would be more difficult to distinguish two tetrahedral species such as $(AN)_3CoCl^+$ and $(AN)_2CoCl_2$. Of course this method is not applicable to ions without electronic transitions sensitive to ligand geometry.

For labile paramagnetic ions two indirect nmr methods can be used to estimate the solvation number. If the metal ion is dissolved to some concentration [m] in the coordinating solvent of concentration [s], and solvent exchange between bulk and coordinated solvent is fast on the nmr time scale, then the measured longitudinal relaxation rate of bulk solvent nuclei is given by

$$R_{1obsd} = \frac{n[m]}{[s]} R_{1m} \ ,$$

and the chemical shift of bulk solvent resonance is given by

$$\Delta\omega_{obsd} = \frac{n[m]}{[s]} \Delta\omega_m \ ,$$

where R_{1m} and $\Delta\omega_m$ are the longitudinal relaxation rate and chemical shift of the coordinated solvent nucleus respectively, and n is the solvation number. The R_{1obsd} and $\Delta\omega_{obsd}$ can be measured easily but n, R_{1m}, and $\Delta\omega_m$ are unknown. However if one chooses a standard system of known n value, then R_{1m} and/or $\Delta\omega_m$ can be determined for a particular metal ion - solvent system. It is assumed that R_{1m} or $\Delta\omega_m$ are relatively independent of other ligands on the metal ion in the same metal ion - solvent system. Then a measurement of R_{1obsd} or $\Delta\omega_{obsd}$ with known [m] and [s], can be combined with the assumed R_{1m} or $\Delta\omega_m$ to calculate n. Hunt[2] has shown that $\Delta\omega_m$ for oxygen-17 is relatively independent of other ligands for a number of nickel(II) complexes in water. The method has also been applied to manganese(II) - $^{17}OH_2$ systems[3]. This method has the advantage of using relatively simple measurements on rapidly exchanging systems, but suffers from concern about the validity of the assumption that $\Delta\omega_m$ or R_{1m} is constant. This assumption would be especially tenuous if the ligand coordination geometry of the standard and the test systems happened to be different.

Richards and coworkers[4] seem to have been the first to propose and apply a pulsed nmr method for the determination of solvation numbers. The method was applied to nickel(II) perchlorate in acetonitrile by Richards and coworkers[4]. They concluded that the solvation number.

was four, i.e., $Ni(AN)_4^{2+}$ is the dominant species. This implies a tetrahedral geometry for the $Ni(AN)_4^{2+}$ complex since a square planar nickel(II) complex would be diamagnetic. However, the electronic spectrum of the nickel(II) ion in acetonitrile is entirely consistent with an octahedral coordination complex[5] (n=6). Richards and coworkers[6] also applied the pulsed nmr method to cobalt(II) in methanol and found a solvation number of six. This is consistent with the electronic spectrum and previous nmr integration results in the slow exchange region.

The pulsed nmr method has the advantage that it does not involve any assumptions. But the validity of the method could be considered suspect because of the anomalous results found for nickel(II) in acetonitrile. The purpose of this thesis is to investigate the application of the pulsed nmr method in order to determine if it is valid, under what conditions it can be applied, and what is the best method of analysing the experimental results. The nickel(II)-acetonitrile system was reinvestigated first, and then two other nickel(II) complexes in acetonitrile were studied to assess the sensitivity of the method to variation in solvation number. The two additional nickel(II) complexes studied were: (acetonitrile) [N-(2-pyridylmethylene)-N-[3-(2-pyridylmethylene)amino] propyl] - 1, 3-propanediamine - N,N',N'',N''',N'''']nickel(II) hexafluorophosphate {[NipyDPT(CH$_3$CN)] (PF$_6$)$_2$} , structure

I, and tris(acetonitrile)tribenzo[b, f, j]-[1, 5, 9]tri-
azacycloduodecinenickel(II) perchorate { [NiTRI(CH$_3$CN)$_3$]
(ClO$_4$)$_2$ }, structure II.

Theoretical considerations necessary for the nmr
method of determining the solvation number can be divided
into two sections, the temperature dependence of the relax-
ation rates and the exchange parameters and the pulse
separation dependence of the transverse relaxation rate.

Temperature Dependence of Relaxation Rates and Chemical Shifts

The Bloch phenomenological equations[8,9] describ-
ing the time dependence of the net nuclear magnetization
in a sample in terms of the longitudinal and transverse
relaxation processes were extended by McConnell[10] to take
into account the effect of chemical exchange. Swift and
Connick[11] solved the modified Bloch equations for the
case of bulk solvent molecules undergoing exchange with a
much smaller number of solvent molecules coordinated to a
dissolved paramagnetic ion. This two-site exchange system
can be represented by

$$MS_n + S^* \rightleftharpoons MS_{n-1}S^* + S \qquad (1-1),$$
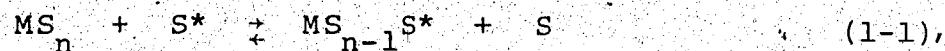
where S* represents an arbitrary bulk solvent molecule
exchanging with any of n equivalent solvent molecules
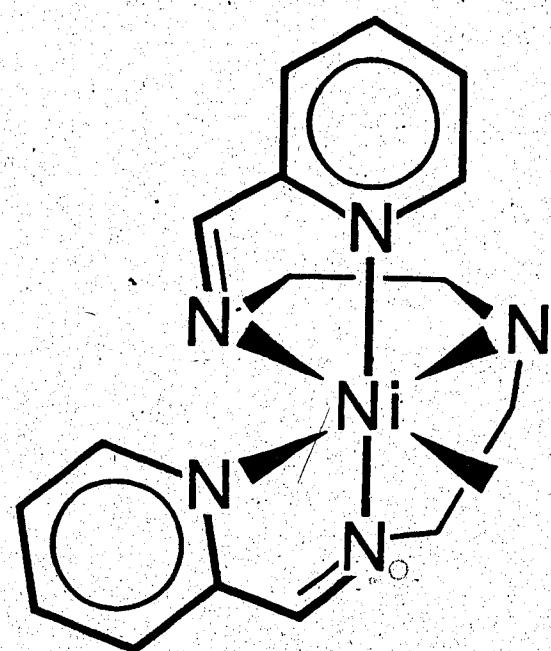
I NipyDPT^{2+}
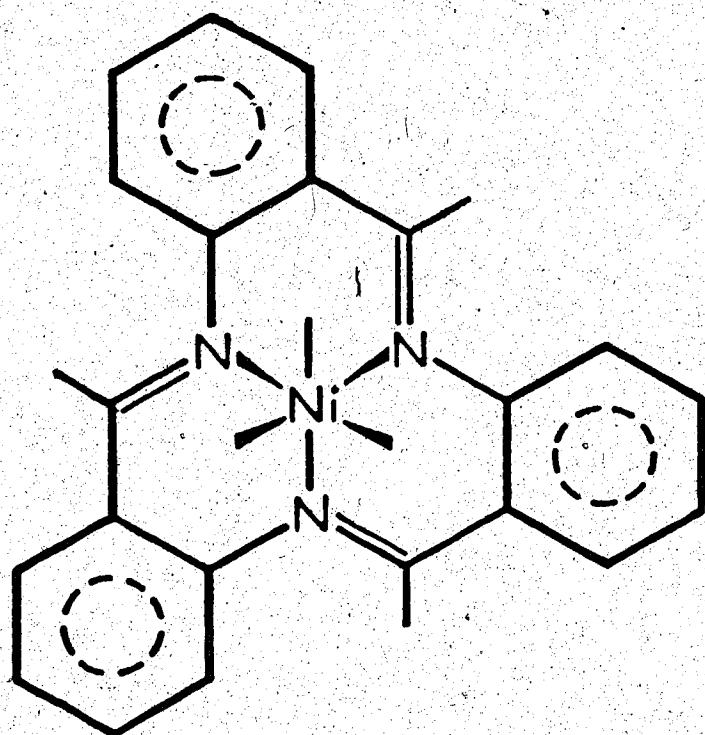
II NiTRI^{2+}

coordinated to the metal ion M. Under the slow passage

conditions of the conventional continuous wave (CW) nmr

method, the bulk solvent transverse relaxation rate

(R_{2obsd}), and the chemical shift of the bulk solvent

$(\Delta\omega_{obsd})$ are given by

$$R_{2obsd} = P_m \tau_m^{-1} \left[\frac{R_{2m}(R_{2m} + \tau_m^{-1}) + \Delta\omega_m^2}{(R_{2m} + \tau_m^{-1})^2 + \Delta\omega_m^2} \right] + R_{2solv} + P_m R_{2o} \quad (1\text{-}2)$$

and

$$-\Delta\omega_{obsd} = \frac{P_m \Delta\omega_m}{(1+R_{2m}\tau_m)^2 + (\tau_m \Delta\omega_m)^2} \quad (1\text{-}3) ,$$

where R_{2m} and R_{2solv} are the transverse relaxation rates

of the coordinated solvent molecules and of the pure

solvent respectively, $\Delta\omega_m$ is the chemical shift between

the resonances of the coordinated solvent and the pure

solvent, τ_m is the average lifetime of the solvent

molecules in the first coordination sphere, P_m is the

ratio between the populations of the coordinated and the

bulk solvent molecules given by

$$P_m = \frac{n[m]}{[s]} \quad (1\text{-}4),$$

where n is the number of solvent molecules in the first

coordination sphere of the metal ion of molal concentra-

tion [m], [s] is the molal concentration of the bulk

solvent, R_{2o} is the outer-sphere contribution to the

observed relaxation rate (R_{2obsd}). In equation (2) the outer-sphere contribution (R_{2o}) arises from the interaction of the solute with the solvent molecules beyond the first coordination sphere; this effect will be discussed later.

Luz and Meiboom[12] solved the modified Bloch equations[10] to obtain the following expression for the bulk solvent nuclear longitudinal relaxation rate,

$$R_{1obsd} = \frac{P_m}{T_{1m} + \tau_m} + R_{1solv} + P_m R_{1o} \qquad (1-5),$$

where R_{1obsd}, R_{1m} (= $1/T_{1m}$), and R_{1solv} are the longitudinal relaxation rates of the bulk solvent, the coordinated solvent, and the pure solvent respectively; R_{1o} is the outer-sphere contribution arising from solvent molecules beyond the first coordination sphere.

In order to describe the temperature dependence of R_{2obsd}, R_{1obsd}, and $\Delta\omega_{obsd}$, the temperature dependence of the parameters given in equations (1-2), (1-3), and (1-5) must be considered. The average lifetime (τ_m) of the solvent molecules in the first coordination sphere, can be expressed as a function of temperature by the transition state theory equation

$$\tau_m^{-1} = (kT/h) \exp [-\Delta H^{\ddagger}/(RT) + \Delta S^{\ddagger}/R] \qquad (1-6),$$

where k is Boltzmann's constant, h is Planck's constant,

T is the absolute temperature, R is the universal gas constant, and $\Delta H^{\ddagger}$ and $\Delta S^{\ddagger}$ are the activation enthalpy and entropy respectively.

It was shown by Bloembergen[13] that the Fermi contact shift can be expressed as

$$\Delta \omega_m = \frac{(-A/\hbar) \cdot \omega_o \mu_{eff} \beta \sqrt{S(S+1)}}{3k\gamma_I T} \tag{1-7},$$

where $A/\hbar$ (radians s^{-1}) is the hyperfine coupling constant between the unpaired electrons of the metal having electron spin quantum number S and nuclei in the coordinated solvent molecule, ω_o is the operating frequency of the nmr spectrometer, β is the Bohr magneton and γ_I is the nuclear magnetogyric ratio. If μ_{eff}, the effective magnetic moment of the complex, is independent of temperature, then $\Delta \omega_m$ is given by

$$\Delta \omega_m = C_\omega/T \tag{1-8},$$

where C_ω is a constant containing the constants in equation (1-7).

Theoretical expressions for the relaxation rates of the solvent molecules coordinated to a paramagnetic species were derived by Solomon and Bloembergen[14,15]. The magnetic interaction between the nuclear spin and electron spin can be divided into dipole-dipole and Fermi contact or hyperfine contributions. The dipolar relaxation is a result of a through-space interaction whereas the hyperfine contribution is a result of the finite probability of

transferring electron spin density through chemical bonds
to the probe nucleus of the coordinated solvent molecules.
The dipolar and scalar contributions are given by the
first and second terms respectively in the following
equations.

$$R_{1m} = \frac{2}{15} <1/r_i^6>(\gamma_I g\beta)^2 S(S+1) f_D(\tau_{D1}) \qquad (1-9)$$

$$+ \frac{2}{3}(A/\hbar)^2 S(S+1) f_e(\tau_{e1})$$

and

$$R_{2m} = \frac{1}{15} <1/r_i^6>(\gamma_I g\beta)^2 S(S+1) f_D(\tau_{D2}) \qquad (1-10)$$

$$+ \frac{1}{3}(A/\hbar)^2 S(S+1) f_e(\tau_{e2})$$

The terms R_{1m} and R_{2m} in equations (1-9) and (1-10) are
commonly referred to as the inner-sphere relaxation rates.
In equations (1-9) and (1-10), $<1/r_i^6>$ is the average magnitude
of the reciprocal of the sixth power of the vector con-
necting the interacting spins, g is the electronic g-
factor. The correlation time functions, $f_D(\tau_{D1})$, $f_D(\tau_{D2})$,
$f_e(\tau_{e1})$, and $f_e(\tau_{e2})$ are functions of the dipolar (τ_{D1} and
τ_{D2}) and electronic (τ_{e1} and τ_{e2}) correlation times as
given by Connick and Fiat[16].

$$f_D(\tau_{D1}) = 3\tau_{D1} + \frac{7\tau_{D2}}{1+(\omega_e\tau_{D2})^2} \qquad (1-11),$$

$$f_D(\tau_{D2}) = 7\tau_{D1} + \frac{13\tau_{D2}}{1 + (\omega_e\tau_{D2})^2} \qquad (1-12),$$

$$f_e(\tau_{e1}) \doteq \frac{\tau_{e2}}{1 + (\omega_e\tau_{e2})^2} \qquad (1-13),$$

and

$$f_e(\tau_{e2}) = \tau_{e1} + \frac{\tau_{e2}}{1 + (\omega_e\tau_{e2})^2} \qquad (1-14).$$

The correlation times τ_{D1}, τ_{D2}, τ_{e1}, and τ_{e2} are given by

$$\tau_{D1}^{-1} = \tau_{e1}^{-1} + \tau_r^{-1} = (R_{1e} + \tau_m^{-1}) + \tau_r^{-1} \qquad (1-15)$$

and

$$\tau_{D2}^{-1} = \tau_{e2}^{-1} + \tau_r^{-1} = (R_{2e} + \tau_m^{-1}) + \tau_r^{-1} \qquad (1-16),$$

where R_{1e} and R_{2e} are the longitudinal and transverse relaxation rates of the electron spin, τ_r is the rotational tumbling correlation time of the molecule. Equations (1-11) to (1-14) were derived under the conditions $\omega_I \ll \omega_e$, $(\omega_I\tau_{e1,2})^2 \ll 1$, and $(\omega_I\tau_{D1,2})^2 \ll 1$, where ω_e and ω_I are the Larmor frequencies of the electron and nucleus respectively.

Theoretical expressions for the average electron spin relaxation rates ($<R_{1e}>$ and $<R_{2e}>$) have been developed by McLauchlan[17]

$$<R_{1e}> = C_e\left[\frac{\tau_c}{1 + (\omega_e\tau_c)^2} + \frac{4\tau_c}{1 + (2\omega_e\tau_c)^2}\right] \qquad (1-17)$$

and

$$<R_{2e}'>=C_e/2 \left[3\tau_c + \frac{5\tau_c}{1 + (\omega_e\tau_c)^2} + \frac{2\tau_c}{1 + (2\omega_e\tau_c)^2} \right] \quad (1\text{-}18),$$

where C_e is a function of electron spin quantum number
and the zero-field splitting energy of the paramagnetic
complex. Equations (1-17) and (1-18) are valid under the
condition $\tau_c^{-1} > R_{2e}$. Bloembergen and Morgan[18] have de-
rived the same functional dependence for R_{1e} as given by
equation (1-17) and their treatment identifies the correla-
tion time (τ_c) with the correlation time for distortion
of the complex caused by random molecular collisions.

Previous works with nickel(II)[19,20] indicate
that the rotational tumbling rate τ_r^{-1} may be less than
R_{2e}, so that if $\tau_c = \tau_r$, then equations (1-17) and (1-18) are
not valid. However if τ_c is related to complex distortion
then it may be true that $\tau_c^{-1} > R_{2e}$. These complications
are not particularly important for the present study be-
cause no attempt is made to calculate R_{1m} and R_{2m} from
first principles. It will be useful to remember that R_{1e}
and R_{2e} are the only factors in equations (1-15) and (1-16)
which depend on the magnetic field strength (H_o), since
$\omega_e = \gamma_e H_o$.

The field dependence of R_{1e} and R_{2e} is such
that they should increase with decreasing field (i.e. ω_e),
and this will generally translate into a decrease in
$f_D(\tau_{D1,2})$ and $f_e(\tau_{e1,2})$. This neglects the ω_e dependence

explicit in equations (1-11) through (1-14)which would cause
an increase in $f_D(\tau_{D1,2})$ and $f_e(\tau_{e1,2})$ with decreasing
ω_e. Since R_{1m} and R_{2m} depend directly on $f_D(\tau_{D1,2})$ and
$f_e(\tau_{e1,2})$ it is clear that R_{1m} and R_{2m} may have a com-
plicated frequency dependence. However for nickel(II)
the first effect dominates and R_{1m} and R_{2m} tend to de-
crease if anything with decreasing ω_e.

In principle the feature described above could
lead to a complicated temperature dependence for R_{1m} and
R_{2m}. In practice[21] it is found satisfactory to assume
that there is one dominant correlation time which may be
related to the solvent viscosity through the Debye-Stokes-
Einstein relationship. Then

$$R_{1,2m} \propto \tau \propto \frac{4\pi r^3}{3kT} \eta \qquad (1-19).$$

The solvent viscosity (η) usually has an exponential
temperature dependence so that the temperature dependence
of R_{1m} and R_{2m} can be described by

$$R_{1,2m} = (\frac{C_{1,2m}}{T}) \exp(\frac{E_{1,2m}}{RT}) \qquad (1-20),$$

where $C_{1,2m}$ are constants, $E_{1,2m}$ are the effective
activation energies of the relaxation rates, and R is the
universal gas constant.

It will sometimes be assumed that $E_{1m} = E_{2m}$ in
the data analysis. This assumption implies that the same
correlation time controls R_{1m} and R_{2m}.

In this work the values of R_{1m} and R_{2m} are inferred from the bulk solvent relaxation rates under conditions where the inner-sphere contributions are the dominant factor and are inseparable from P_m. An example of such conditions is when solvent exchange is fast and the relaxation rate is given by

$$R_{1,2obsd} = P_m R_{1,2m} + P_m R_{1,2o} + R_{1,2solv} \ .$$

Then the inner-sphere contributions to R_{2obsd} are given by

$$\frac{n[m]}{[s]} \left(\frac{C_{1,2m}}{T}\right) \exp \left(\frac{E_{1,2m}}{RT}\right) \ .$$

Non-linear least-squares analysis of $R_{1,2obsd}$ data was carried out to obtain the fitting parameters. Since only $[m]/[s]$ is known the pre-exponential parameter in the least-squares fits contained n. In subsequent analysis procedures different values of n will be used in fitting the data and it is convenient to express the inner-sphere contributions as

$$R_{1,2m} = \left(\frac{C'_{1,2m}}{nT}\right) \exp \left(\frac{E_{1,2m}}{RT}\right) \qquad (1-21),$$

where $C'_{1,2m} = nC_{1,2m}$. Then, when different values of n are assumed, the inner-sphere contributions will automatically be scaled accordingly.

The outer-sphere contributions to the observed relaxation rates arise from dipole-dipole interaction between the electron spin of the paramagnetic species and the nuclear spin of the solvent molecules beyond the first coordination sphere. Luz and Meiboom[12] assumed that the outer-sphere contributions can be estimated by approximating the outer-sphere nucleus distribution by a continuum and averaging the dipole-dipole interaction over the volume between the sphere of closest approach with radius d and infinity;

$$R'_{1o} = \frac{1}{15} p(\gamma_I g\beta)^2 S(S + 1) f_D(\tau_{D1}) \int_d^\infty \frac{4\pi r^2 dr}{r^6} \qquad (1-22)$$

and

$$R'_{2o} = \frac{2}{15} p(\gamma_I g\beta)^2 S(S + 1) f_D(\tau_{D2}) \int_d^\infty \frac{4\pi r^2 dr}{r^6} \qquad (1-23),$$

where $p = \rho N_o[m] \times 10^{-3}$ is the number of the paramagnetic species per mL of the solution, ρ is the density of the solution, $[m]$ is the molal concentration of the paramagnetic species, and N_o is Avogadro's number. The superscript prime is used in equations (1-22) and (1-23) to indicate that $R'_{1,2o}$ are dependent on the metal ion concentration. Integration of equations (1-22) and (1-23) gives

$$R'_{1o} = \frac{8\pi\rho N_o[m] \times 10^{-3}(\gamma_I g\beta)^2 S(S + 1)}{45d^3} f_D(\tau_{D1}) \qquad (1-24)$$

and

$$R'_{2o} = \frac{4\pi\rho N_o [m] \times 10^{-3} (\gamma_I g\beta)^2 S(S+1)}{45d^3} f_D (\tau_{D2}) \qquad (1-25).$$

Following the argument used in obtaining $R'_{1,2m}$ given by equations (1-19) and (1-20), the functional form of the outer-sphere contributions can be expressed as

$$R'_{1,2o} = (\frac{C'_{1,2o}}{T}) \exp (\frac{E_{1,2o}}{RT}) \qquad (1-26),$$

where $C'_{1,2o}$ contain constants in equations (1-24) and (1-25) including ρ and $[m]$, and $E_{1,2o}$ are the effective activation energies of the relaxation. The outer-sphere contributions in equation (1-26) are divided by $P_m = n[m]/[s]$, and the equation is rearranged keeping the unknown n to give:

$$R_{1,2o} = (\frac{K_{1,2o}}{nT}) \exp (\frac{E_{1,2o}}{RT}) \qquad (1-27),$$

where $K_{1,2o}$ now contain [s] in addition to the constants in equations (1-24) and (1-25), and $R_{1,2o}$ are the outer-sphere contributions normalized to unit P_m. In fact $R_{1,2o}$ are the terms which appear on the right of equations (1-2) and (1-5) given previously. In subsequent analyses $C_{1,2o} = K_{1,2o}/n$ will be used in equation (1-27) since different n values will be assumed.

The temperature dependence of the observed relaxation rates and the chemical shift can now be considered. The dependencies of R_{2obsd} and $\Delta\omega_{obsd}$ will be discussed together first and a brief description of the variation of R_{1obsd} with temperature will follow.

The temperature dependence of R_{2obsd} and $\Delta\omega_{obsd}$ is obtained by substitution of the appropriate temperature functions into equations (1-2) and (1-5). The various limiting conditions for R_{2obsd} and $\Delta\omega_{obsd}$ and their temperature dependence are summarized in Table 1 and Figure 1.

In the low temperature limit (region I) the solvent exchange is too slow to affect the bulk solvent relaxation and the outer-sphere contribution (R_{2o}) controls R_{2obsd}; R_{2obsd} decreases with increasing temperature. Since the outer-sphere chemical shift is usually small, the observed chemical shift is close to zero.

As the temperature increases τ_m^{-1} becomes larger and the limiting conditions in region II begin to apply. The two limiting conditions (a) $\Delta\omega_m^2 \gg R_{2m}^2$, τ_m^{-2} and (b) $R_{2m}^2 \gg \Delta\omega_m^2$, τ_m^{-2} give the same result for the bulk solvent relaxation rate, i.e., R_{2obsd} is directly proportional to τ_m^{-1}, and increases as the temperature increases. Since the solvent exchange rate is smaller than either R_{2m} or $\Delta\omega_m$, each time the solvent nuclei enter the coordination sphere they are effectively relaxed or are effectively dephased. Thus the bulk solvent relaxation rate is controlled by the rate at which the coordinated solvent molecules return to the bulk solvent.

The observed chemical shift in region II increases rapidly with increasing temperature for both

Table 1

Temperature dependence of R_{2obsd} and $\Delta\omega_{obsd}$ as given by equations (1-2) and (1-5) under various limiting conditions.

Region[a]	Limiting conditions	$R_{2obsd} - R_{2solv}$	$-\Delta\omega_{obsd}$
I	τ_m^{-1} too small to affect R_{2obsd} and $\Delta\omega_{obsd}$	$P_m R_{2o}$	0
II	(a) $\Delta\omega_m^2 \gg R_{2m}^2,\ \tau_m^{-2}$	$P_m \tau_m^{-1} + P_m R_{2o}$	$\dfrac{P_m \tau_m^{-2}}{\Delta\omega_m}$
	(b) $R_{2m}^2 \gg \Delta\omega_m^2,\ \tau_m^{-2}$	$P_m \tau_m^{-1} + P_m R_{2o}$	$P_m \Delta\omega_m \left(\dfrac{\tau_m^{-1}}{R_{2m}}\right)^2$
III	$\tau_m^{-2} \gg \Delta\omega_m^2 > R_{2m}\tau_m^{-1}$	$P_m \tau_m \Delta\omega_m^2 + P_m R_{2o}$	$P_m \Delta\omega_m$
IV	$R_{2m}\tau_m^{-1} \gg R_{2m}^2,\ \Delta\omega_m^2$	$P_m R_{2m} + P_m R_{2o}$	$P_m \Delta\omega_m$

(a) The exchange regions given above are designated according to Figure 1.
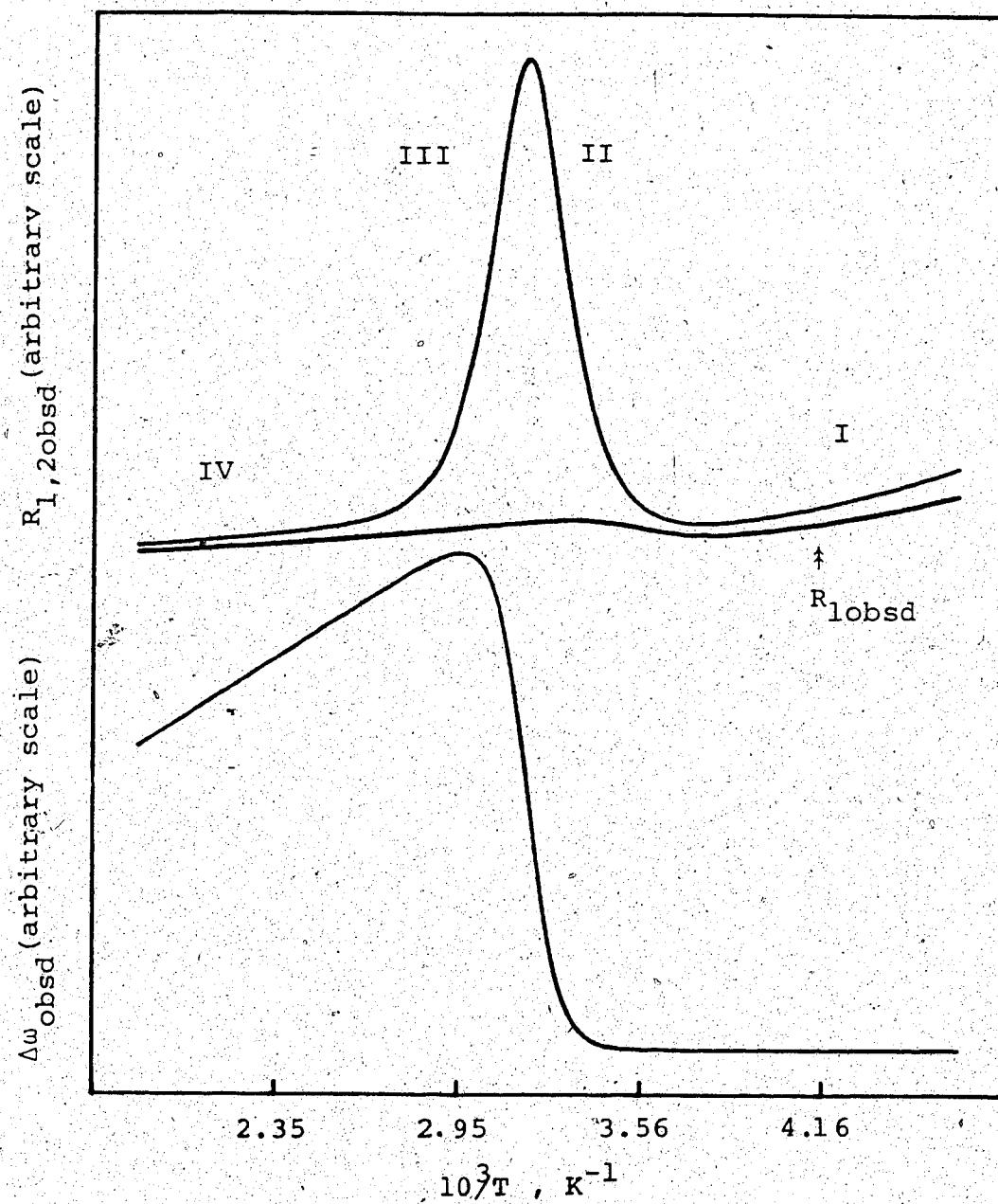
Figure 1 Illustration of the temperature dependence of
R_{2obsd}, $\Delta\omega_{obsd}$, and R_{1obsd} for a two-site chemical
exchange system. The four exchange regions are
designated as the outer-sphere control(I), the
slow exchange(II), the fast exchange(III), and
the inner-sphere control(IV) regions.

limiting conditions because of the τ_m^{-2} term (Table 1).
The two limiting conditions could be distinguished by the
opposite frequency dependence of $\Delta\omega_{obsd}$. If the limiting
condition $\Delta\omega_m^2 >> R_{2m}^2, \tau_m^{-2}$ applies, an increase in
magnetic field strength should result in a decrease in
$\Delta\omega_{obsd}$ since $\Delta\omega_{obsd}$ is inversely proportional to $\Delta\omega_m$
which is directly proportional to the field strength.
If $R_{2m}^2 >> \Delta\omega_m^2, \tau_m^{-2}$ applies, then $\Delta\omega_{obsd}$ would increase
with increasing field strength, but would be difficult to
measure relative to the linewidth.

In region III the solvent exchange rate has
increased to the extent that $\tau_m^{-1} > \Delta\omega_m$ and $\tau_m^{-1} > R_{2m}$. The
average lifetime of solvent molecules in the first co-
ordination sphere is now too short for relaxation to
occur effectively through either the R_{2m} or the $\Delta\omega_m$
mechanism each time the solvent enters the coordination
sphere. Since $R_{2obsd} \cong P_m \tau_m \Delta\omega_m^2$ then R_{2obsd} decreases
rapidly with increasing temperature because τ_m becomes
smaller. The average lifetime is too short to affect the
observed chemical shift. The temperature dependence of
$\Delta\omega_{obsd}$ is small and due to the change in $\Delta\omega_m$ given by
equation (1-8).

In region IV, $R_{2m}\tau_m^{-1} >> R_{2m}^2 > \Delta\omega_m^2$, the ex-
change rate is so fast that no dephasing of the coordinat-
ed solvent molecules occurs. Then R_{2obsd} is a weighted
average of the relaxation rates in the two sites and is

controlled primarily by R_{2m} because of its magnitude

relative to R_{2solv}. The value of R_{2obsd} is expected to

decrease with increasing temperature but more slowly than

in region III because the activation energy for R_{2m} is

usually less than that for τ_m^{-1}.

It should be pointed out that if the limiting

condition $R_{2m}^2 \gg \Delta\omega_m^2, \tau_m^{-2}$ applies to region II, then

the limiting condition $\tau_m^{-2} \gg \Delta\omega_m^2 > R_{2m}\tau_m^{-1}$ will never

apply, and the chemical exchange is never controlled by

$\Delta\omega_m$. Such an exchange system consists of regions I, II,

and IV. The work of this thesis does not deal with such

a system.

For future reference the four regions are des-

ignated as the outer-sphere control region (I), slow

exchange region (II), the fast exchange region (III), and

the inner-sphere control region (IV). The region between

II and III, where R_{2obsd} is a maximum (Figure 1), shall

be referred to as the intermediate exchange region.

The temperature dependence of R_{1obsd} can be de-

scribed by reference to equation (1-5) and Figure 1. Be-

ginning at low temperature, there is an outer-sphere region

where the solvent exchange is too slow to affect the re-

laxation of the bulk solvent, then the exchange-controlled

region ($\tau_m^{-1} \ll R_{1m}$), and finally the inner-sphere

controlled region ($\tau_m^{-1} \gg R_{1m}$). Since the longitudinal

relaxation is not affected by the chemical shift

mechanism, the solvent exchange has less effect on R_{1obsd} than on R_{2obsd}. However in this work, use has been made of R_{1obsd} data to obtain R_{1o} and R_{1m} which in turn provide estimates of R_{2o} and R_{2m}.

Dependence of R_{2obsd} on Pulse Separation

The transverse relaxation rate can be measured by the Carr-Purcell-Meiboom-Gill(CPMG) pulse method[22-24]. In the CPMG pulse sequence ($90_x, -t_{CP}/2-180_y, -t_{CP}-180_y, -\ldots$), the net magnetization is tipped into the $+y'$ axis in the rotating frame[24] by a $90°$ pulse applied along the $+x'$ axis. The macroscopic magnetization (m_i) of the nuclei in the sample dephases for a time $t_{CP}/2$, a $180°$ pulse is applied along the $+y'$ axis causing m_i to flip through $180°$, and the magnetization rephases in time interval $t_{CP}/2$, at which time an echo occurs and sampling takes place. Measurement of the successive echo amplitudes allows one to determine the transverse relaxation rate. The time separation t_{CP} is an experimental variable.

If the nuclei being observed are exchanging between sites (with sufficiently different relaxation rates and/or precessional frequencies, then the transverse relaxation rate may show a dependence on the value of t_{CP}. The conditions under which such a dependence is observable have been discussed by Carver and Richards[25] and by Jen[26]. A simple qualitative description can be given for the t_{CP} dependence under certain circumstances.

Assume that nuclei are being observed in site A with precessional frequency ω_a, as they undergo exchange with nuclei in site B with precessional frequency ω_b. After a 90° pulse the A nuclei will begin to dephase in the x'-y' plane due to natural processes, but if the B site exchange into the A site they will be precessing at ω_b and cause the rate of dephasing in the A site to increase. The result is the well known increase in transverse relaxation rate due to chemical exchange. In the pulse experiment the series of 180° pulses serve to rephase the nuclear magnetization in the x'-y' plane. If the interval between the 180° pulses (t_{CP}) is sufficiently short relative to $|\omega_a - \omega_b|$ then the dephasing due to chemical exchange and precessional frequency change will not have a chance to occur before another 180° rephasing pulse is applied. In this short t_{CP} limit the system will appear as if no exchange were occurring. As t_{CP} is increased, the dephasing will become more and more effective in increasing the transverse relaxation rate until in the long t_{CP} limit the relaxation rate will be the same as that measured from a continuous wave(CW) experiment. A similar qualitative explanation has been given by Jen[26].

A theoretical expression for the dependence of R_{2obsd} on t_{CP} was derived first by Luz and Meiboom[27] for the case of equal relaxation rates and populations in the two exchanging sites. The approximations used re-

stricted their formulation to conditions of short t_{CP} and fast exchange relative to the chemical shift difference between the two sites. Following Luz and Meiboom[27], Allerhand and Gutowsky[28,29] developed the exact solution of the modified Bloch equations[10] to obtain the dependence of R_{2obsd} on t_{CP} for the two-site exchange with equal relaxation rates and populations. Later Carver and Richards[25] derived a general theoretical expression of the t_{CP} dependence of R_{2obsd} for the two-site exchange without restriction on the relative magnitudes of relaxation rates and populations of the two sites. The general expression given by Carver and Richards was derived independently by Jen[26]. Gutowsky *et al.*[30] extended the general two-site exchange expression to include spin coupling between the two sites and showed that their formulations can be applied to exchange between any number of spin-coupled sites. The effect of the chemical exchange between more than two uncoupled sites on the dependence of R_{2obsd} on t_{CP} was studied also by Allerhand and Thiele[31] and by Jen[32]. Recently a combination of multiple pulse sequences for measuring transverse relaxation rates with Fourier transformation of the resulting echoes was proposed by Frahm[33]; the proposed method was in principle neither restricted to exchanges between sites of equal relaxation rates nor populations.

In this work, the method of Allerhand and

Gutowsky[28,29] has been used to develop the expressions for the dependence of R_{2obsd} on t_{CP} for a two-site exchange system without restriction on the relative relaxation rates or populations of the two sites. The result is the same as that given by Carver and Richards[25]. An outline of the derivation follows.

The modified Bloch equations[10] for the magnetization between $180°$ pulses, when an rf field is absent, can be written in complex form[34]

$$dG_a/dt = -\alpha_a G_a + \tau_b^{-1} G_b \qquad (1-32),$$

and

$$dG_b/dt = \tau_a^{-1} G_a - \alpha_b G_b$$

where

$$G_k = u_k + iv_k \qquad (1-33)$$

and

$$\alpha_k = R_{2k} + \tau_k^{-1} - i(\omega_k - \omega) \qquad (1-34).$$

u_k and v_k are the components of magnetization of site k along the +x' and +y' axes in the rotating frame and R_{2k}, τ_k, and ω_k are the transverse relaxation rate, average lifetime, and nuclear precessional frequency of site k. If $(\alpha_a - \alpha_b)^2 + 4\tau_a^{-1}\tau_b^{-1} \neq 0$ the general solutions of equations (1-32) are

$$G_a(t) = A_+ \exp(-\phi_+ t) + A_- \exp(-\phi_- t)$$

$$G_b(t) = \beta_+ A_+ \exp(-\phi_+ t) + \beta_- A_- \exp(-\phi_- t) \qquad (1\text{-}35),$$

where $A_\pm$ are the integration constants to be determined from the boundary conditions and $\phi_\pm$ and $\beta_\pm$ are functions of the relaxation rates and exchange parameters of the two sites given by

$$2\phi_\pm = (\alpha_a + \alpha_b) \pm [(\alpha_a - \alpha_b)^2 + 4\tau_a^{-1}\tau_b^{-1}]^{\frac{1}{2}} \qquad (1\text{-}36)$$

and

$$\beta_\pm = -(\phi_\pm - \alpha_a)\tau_b \qquad (1\text{-}37).$$

The complex magnetization at various times are designated as follows:

G_a and G_b for the values of $G_a(t)$ and $G_b(t)$ at the nth echo $\qquad (1\text{-}38)$

G_a^i and G_b^i for the values of $G_a(t)$ and $G_b(t)$ at time $t_{CP}/2$ after the nth echo (just before the 180° pulse is applied)

G_a' and G_b' for the values of $G_a(t)$ and $G_b(t)$ at time of the (n+1)th echo.

The boundary conditions are

$G_a(0) = 0$; $G_b(0) = 0$ t=0, time before the 90° pulse is applied

$\qquad (1\text{-}39a)$

$G_a(0^+) = M_a$; $G_b(0^+) = M_b$ just after the 90° pulse is applied.

The application of a $180°$ pulse at $t_{CP}/2$ after the $90°$ pulse converts the magnetization into its complex conjugate. Hence

$$G_a(t_{CP}^+/2) = G_a^*(t_{CP}/2)$$

$$G_b(t_{CP}^+/2) = G_b^*(t_{CP}/2)$$

(1-39b).

Equation (1-35) describes the time dependence of the magnetization for the nth echo, from which it can be shown that

$$A_\pm = [(\beta_\mp G_a - G_b)/(\beta_\mp - \beta_\pm)]\exp(\phi_- t)$$ (1-40).

By defining

$$S^2 = \tau^{-2} - (\omega_a - \omega_b)^2 + 2i\tau^{-1}(P_a - P_b)(\omega_a - \omega_b) + (R_{2a} - R_{2b})^2$$

$$+ 2(R_{2a} - R_{2b})(P_b - P_a)\tau^{-1} - 2i(R_{2a} - R_{2b})(\omega_a - \omega_b)$$ (1-41),

where P_a and P_b are the populations of the two sites and

$$\tau^{-1} = \tau_a^{-1} + \tau_b^{-1}$$ (1-42),

it can be shown that

$$\beta_- - \beta_+ = S\tau/P_a$$ (1-43)

and

$$\beta_- \beta_+ = - P_b/P_a \qquad (1-44).$$

It should be mentioned that the term S in equation (1-41) differs from that of Allerhand and Gutowsky[28] since in this work no restriction is placed on the magnitudes of R_{2a} and R_{2b} and P_a and P_b, whereas Allerhand and Gutowsky assumed (i) $R_{2a} = R_{2b}$ and (ii) $R_{2a} = R_{2b}$ and $P_a = P_b$.

By combining equation (1-35) with equations (1-40), (1-43), and (1-44) for the magnetization at time $t_{CP}/2$ after the echo and just before the next 180° pulse, one obtains

$$G_a^i = -P_- G_a + Q G_b \qquad (1-45)$$

and

$$G_b^i = (P_b/P_a) Q G_a + P_+ G_b \qquad (1-46),$$

where

$$P_\pm = [P_a/(S\tau)](\beta_- E_- - \beta_+ E_+) \qquad (1-47),$$

$$Q = [P_a/S\tau](E_- - E_+) \qquad (1-48),$$

and

$$E_\pm = \exp(-\phi_\pm t_{CP}/2) \qquad (1-49).$$

After the 180° pulse, the boundary condition (1-39b) applies and equations (1-45) and (1-46) become

$$G_a^i = -P_-^* G_a^* + Q^* G_b^*$$

(1-50)

and

$$G_b^i = (P_b/P_a) Q^* G_a^* + P_+^* G_b^*$$

(1-51).

In a similar manner the (n+1)th echo at time $t+t_{CP}$ are given by

$$G_a' = -P_- G_a^{i*} + Q G_b^{i*}$$

(1-52)

and

$$G_b' = (P_b/P_a) Q G_a^{i*} + P_+ G_b^{i*}$$

(1-53).

If equations (1-52) and (1-53) are combined with equations (1-50) and (1-51) then one obtains the recursion relations, which give the relative amplitudes of any echo in terms of the immediately preceding one;

$$G_a' = a_- G_a^* + b G_b^*$$

(1-54)

and

$$G_b' = (P_b/P_a) b^* G_a + a_+ G_b^*$$

(1-55),

where

$$a_\pm = P_\pm P_\pm^* + (P_b/P_a) Q Q^*$$

(1-56)

and

$$b = P_+^* Q - P_- Q^* = b_1 + i b_2$$

(1-57).

b_1 and b_2 are the real and imaginary parts.
Separation of the real and imaginary parts of equations (1-54) and (1-55) yields the recursion relations

$$u_a' = a_- u_a + b_1 u_b + b_2 v_b$$

$$u_b' = (P_b/P_a) u_a + a_+ u_b - (P_b/P_a) b_2 v_a \qquad (1-58).$$

$$v_a' = b_2 u_b - a_- v_b - b_1 v_b$$

$$v_b' = -(P_b/P_a)(b_2 u_a + b_1 v_a) - a_+ v_b$$

In principle it is possible to use an iterative procedure to determine the relaxation rates and the exchange parameters from the observed echo amplitudes. However such a procedure would be very time consuming especially when many echoes are observed. Thus it is desirable to have a closed formula for the t_{CP} dependence of R_{2obsd}.

The recursion relations given in equation (1-58) can be solved and, according to Allerhand and Gutowsky[29], the solutions for the nth echo as a function of magnetization at $t = 0$ (after the $90°$ pulse) are given by

$$u_a = c_1 A_1 \lambda_1^n + c_2 A_2 \lambda_2^n + c_3 A_3 \lambda_3^n + c_4 A_4 \lambda_4^n$$

$$u_b = c_1 B_1 \lambda_1^n + c_2 B_2 \lambda_2^n + c_3 B_3 \lambda_3^n + c_4 B_4 \lambda_4^n$$

$$v_a = c_1 C_1 \lambda_1^n + c_2 C_2 \lambda_2^n + c_3 C_3 \lambda_3^n + c_4 C_4 \lambda_4^n \qquad (1-59),$$

$$v_b = c_1 D_1 \lambda_1^n + c_2 D_2 \lambda_2^n + c_3 D_3 \lambda_3^n + c_4 D_4 \lambda_4^n$$

where c_j's are integration constants to be determined
from the initial magnetization after the application of
the 90° pulse; A_j's, B_j's, C_j's, and D_j's are functions
of $a_\pm$, b_1, b_2, P_a, P_b, and λ_j's are the solutions of
the recursion relations in equation (1-58) given by

$$\lambda_j = \pm[(p+q)/2]^{\frac{1}{2}} \pm [(p-q)/2]^{\frac{1}{2}} \qquad (1-60),$$

where

$$p = \tfrac{1}{2}(a_+^2 + a_-^2) + (P_b/P_a)(b_1^2 - b_2^2) \qquad (1-61)$$

and

$$q = a_+a_- - (P_b/P_a)(b_1^2 + b_2^2) \qquad (1-62).$$

According to the signs in equation (1-60) the four
roots are designated $\lambda_1(++)$, $\lambda_2(+-)$, $\lambda_3(-+)$, and $\lambda_4(--)$
respectively. Allerhand and Gutowsky[29] showed that the
λ_j's can be expressed in terms of experimental variables
using relationships between sums and products of hyper-
bolic functions. From such relationships they concluded
that

$$\lambda_1 > \lambda_2 > 0 \text{ and } \lambda_3 < \lambda_4 < 0$$

and
$$\qquad (1-63).$$
$$\lambda_1 = -\lambda_4 \text{ and } \lambda_2 = -\lambda_3$$

The fact that λ_1 is greater than λ_2 was confirmed by
various numerical evaluations of λ_1 and λ_2 by Carver

and Richards[25].

The amplitude of the nth echo now is consider-ed. It is directly proportional to the u-component of the complex magnetization. Addition of u_a and u_b in equation (1-59) and taking into account the fact that $\lambda_1 = \lambda_4$ and $\lambda_2 = -\lambda_3$, then one obtains

$$u(t) = K_1 \exp[(t/t_{CP})\ln(\lambda_1)] + K_2 \exp[(t/t_{CP})\ln(\lambda_2)] \qquad (1\text{-}64),$$

where

$$K_1 = c_1(A_1 + B_1) + (-1)^n c_4(A_4 + B_4)$$

and

$$K_2 = c_2(A_2 + B_2) + (-1)^n c_3(A_3 + B_3) .$$

Equation (1-64) indicates that the observed echo amplitude consists of two terms decaying exponentially at different rates, but since $\lambda_1 >> \lambda_2$ simple exponential decay of the echo train should be observed. Small ripples may be observed due to the K_1 term since it consists of two terms decaying in and out of phase for every other echo. The magnitude of the ripple obviously depends on the ratio $c_1(A_1 + B_1)/c_4(A_4 + B_4)$. Carver and Richards[25] indicated that direct examination of the echo amplitudes using the recursion relations shows that such modulation of the echo amplitude is insignificant.

Following the argument presented above one

expects to see simple exponential decay of the echo train. By definition

$$u(t) = C \exp(-R_{2obsd}t) \qquad (1-65),$$

where R_{2obsd} is the effective decay rate. A comparison of equations (1-64) and (1-65) indicates that

$$R_{2obsd} \cong -(1/t_{CP}) \ln \lambda_1 \qquad (1-66),$$

where

$$\lambda_1 = f(R_{2a}, R_{2b}, \tau_a^{-1}, \tau_b^{-1}, P_a, P_b, \Delta\omega_a, \Delta\omega_b).$$

Thus from the observed echo amplitudes as a function of time one can derive the exchange parameters and relaxation rates from the effective relaxation rate of the bulk solvent (R_{2obsd}) in a two-site exchange system.

A computer programme has been constructed based on the following equations

$$R_{2obsd} = -(1/t_{CP})\ell n\lambda_1$$

$$\lambda_1 = [(p+q)/2]^{\frac{1}{2}} + (p-q)/2]^{\frac{1}{2}}$$

$$p = \frac{1}{2}(a_+^2 + a_-^2) + (P_b/P_a)(b_1^2 - b_2^2)$$

$$q = a_+ a_- - (P_b/P_a)(b_1^2 + b_2^2)$$

$$a_\pm = P_\pm P_\pm^* + (P_b/P_a)QQ^*$$

$$b = b_1 + ib_2 = P_+^* Q - P_- Q^*$$

$$P_\pm = [P_a/S\tau)](\beta_{\mp} E_- - \beta_\pm E_+)$$

$$Q = [P_a/(S\tau)](E_- - E_+)$$

$$E_\pm = \exp(-\phi_\pm t_{CP}/2)$$

$$\beta_\pm = (\alpha_a - \phi_\pm)(\tau/P_a)$$

$$\phi_\pm = [(\alpha_a+\alpha_b)/2] \pm \frac{1}{2}[(\alpha_a-\alpha_b)^2 + 4P_a P_b \tau^{-2}]^{\frac{1}{2}}$$

$$S = (P_a/\tau)(\beta_- - \beta_+)$$

$$\alpha_a = R_{2a} + \tau_a^{-1} - i\Delta\omega_a$$

$$\alpha_b = R_{2b} + \tau_b^{-1} - i\Delta\omega_b$$

$$\tau_a^{-1} = P_b\tau^{-1}$$

$$\tau_b = P_a\tau^{-1}$$

$$P_a + P_b = 1$$

(1-67)

In a metal-ion-solvent system it has been conventional to use the subscript m for the coordinated site, thus the terms P_m, $\Delta\omega_m$, R_{2m}, and τ_m^{-1} shall be used and the parameters in equation (1-67) are redefined as

$$P_a = 1/(1 + P_m)$$

$$\tau^{-1} = \tau_m^{-1} P_a^{-1}$$

$$R_{2a} = R_{2solv}$$

$$R_{2b} = R_{2m}$$

$$\Delta\omega_a = P_b \Delta\omega_m$$

$$\Delta\omega_b = -P_a \Delta\omega_m$$

(1-68).

Numerical evaluation of the dependence of R_{2obsd} on t_{CP} according to equation (1-67) for the slow and fast exchange regions is shown in Figure 2 . The oscillation pattern found in the slow exchange region was also noted in the numerical evaluations of Jen[26] and Carver and Richards[25] and was described by Jen as an effect of the trigonometric functions at some long t_{CP} values.

The variation of R_{2obsd} with t_{CP} in the various exchange regions in Figure 1 now is considered. From equations (1-66) and (1-67), it can be seen that the dependence of R_{2obsd} on t_{CP} is complicated because λ_1 is a complicated function of the relaxation rates, populations
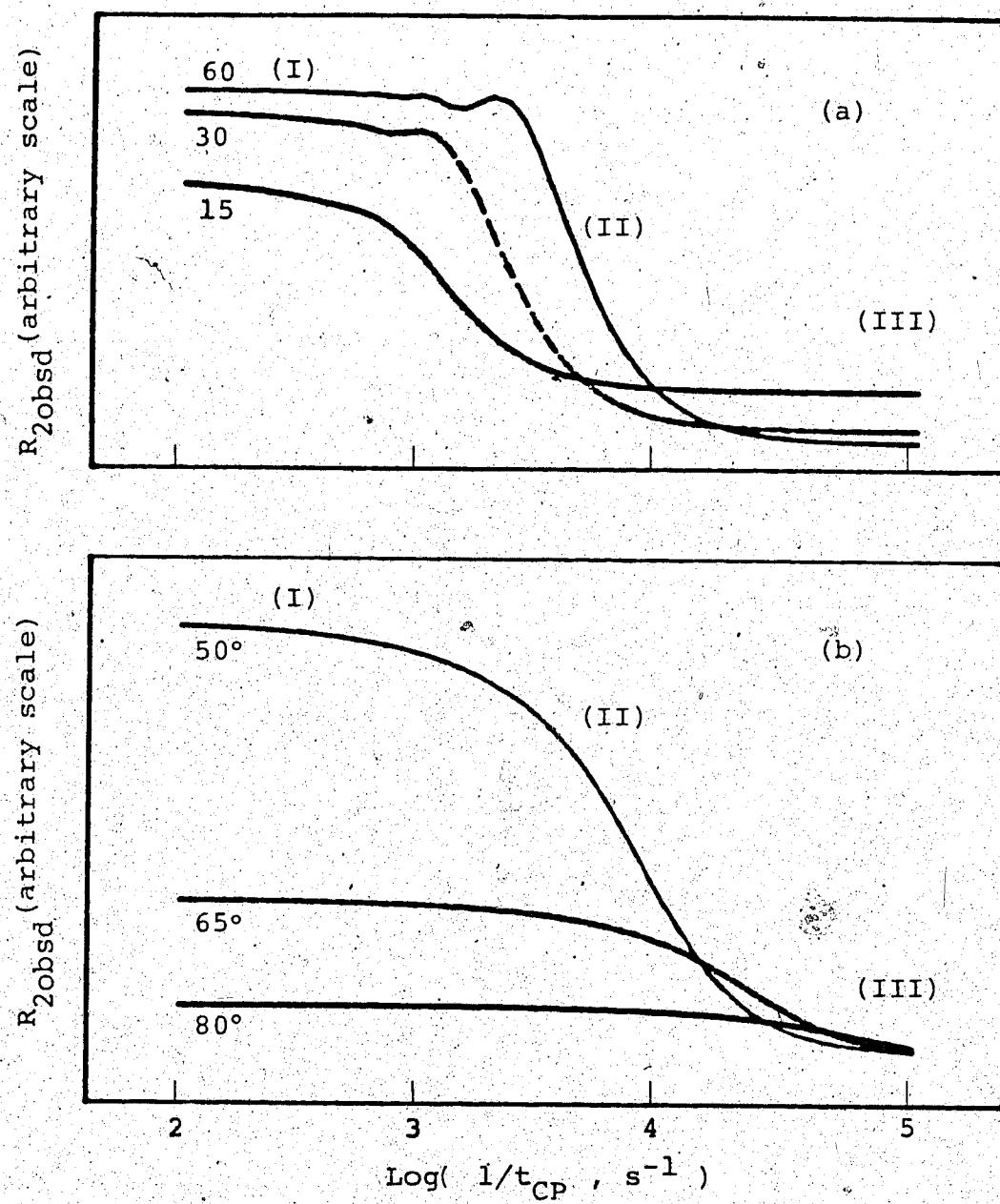
Figure 2. Illustrations of the variation of R_{2obsd} with t_{CP} in (a) the slow exchange region at 15, 30, and 60 MHz (b) the fast exchange region at 50°, 65°, and 80°C. The three regions of t_{CP} value are designated: the long t_{CP} (I), the intermediate t_{CP} (II), and the short t_{CP} (III) regions.

of nuclei, and the precessional frequencies in the two sites. Therefore numerical evaluation of R_{2obsd} according to equation (1-67) will be used to illustrate the basic features of the variation of R_{2obsd} with t_{CP} in the various exchange regions discussed previously.

First it should be pointed out that in the inner-sphere and the outer-sphere control regions R_{2obsd} remains unaffected by the choice of t_{CP}. A variation of R_{2obsd} with t_{CP} will be observed only in the slow, the intermediate, and the fast exchange regions. Secondly, in the intermediate exchange region, the dependence of R_{2obsd} on t_{CP} is too complicated to be described qualitatively. However it will be shown later (Chapter III) that from this exchange region the $R_{2obsd} - t_{CP}$ data provide useful information for the determination of the solvation number.

The variation of R_{2obsd} with t_{CP} in the slow and fast exchange regions is illustrated by plots of R_{2obsd} versus $\log(1/t_{CP})$ in Figure 2. The basic features of the variation of R_{2obsd} with t_{CP} in both the slow and fast exchange regions consist of three regions of t_{CP} values, designated as the long t_{CP} region (I), the intermediate t_{CP} region (II), and the short t_{CP} region (III).

In the slow exchange region, the full effect of relaxation due to R_{2m} or $\Delta\omega_m$ is observed when t_{CP} is long(Region I). Thus R_{2obsd} is large and corresponds to

the linewidth of the conventional continuous wave nmr sig-
nal in equation (1-2), and is given by

$$(R_{2obsd})_{long\ t_{CP}} = P_m \tau_m^{-1} + R_{2solv} + P_m R_{2o} \qquad (1-69).$$

Since 180° pulses cause the macroscopic magnetization of
the nuclei (m_i) in the sample to rephase and the chemical
exchange enhances dephasing of m_i, successive pulsing com-
petes with enhanced dephasing brought about by the chemi-
cal exchange. In the slow exchange region ($\Delta\omega_m^2 >> R_{2m}^2$, τ_m^{-2}),
solvent molecules reside in the first coordination sphere
long enough so that $\Delta\omega_m$ effectively causes dephasing. Con-
sequently, the pulsing rate, i.e., rephasing rate of m_i,
competes directly with $\Delta\omega_m$. Following the argument
presented above, one expects that there exists a value
of t_{CP} at which the pulsing rate will overcome half of
the influence of $\Delta\omega_m$, and this value of t_{CP} corresponds
to approximately the mid-point of the change in R_{2obsd}
with t_{CP},

$$(1/t_{CP})_{mid-point} \simeq \Delta\omega_m/2 \qquad (1-70).$$

Equation (1-70) indicates that, in the slow exchange
region, the mid-point of the R_{2obsd}-$1/t_{CP}$ curve is
frequency dependent; it should shift to the longer t_{CP}

values (smaller $1/t_{CP}$) with decreasing resonance fre-
quency as shown in Figure 2(a). It should be mentioned
that equation (1-70) only provides an estimate for $\Delta\omega_m$
from the experimental results. A mathematical treatment
of the point of inflexion in the plot of $\ln R_{2obsd}$ $versus$
$\ln(1/t_{CP})$ for both the slow and the fast exchange region
is given by Campbell $et\ al.$[6].

In the fast exchange region (Figure 2b), R_{2obsd}
corresponds to the conventional nmr linewidth in the
long t_{CP} region and is given by

$$(R_{2obsd})\ \text{long } t_{CP} = P_m \tau_m \Delta\omega_m^2 + R_{2solv} + P_m R_{2o} \qquad (1-71).$$

In this exchange region the solvent residence time is
too short for $\Delta\omega_m$ to cause dephasing of m_i effectively,
and according to equation (1-71) dephasing of m_i by $\Delta\omega_m$
is reciprocally dependent on the exchange rate. Thus the
pulsing rate competes directly with τ_m^{-1}. Therefore it
is expected that when the pulsing equals half the ex-
change rate, this will correspond to the mid-point of the
change of R_{2obsd} with t_{CP}.

$$(1/t_{CP})_{\text{mid-point}} \cong \tau_m^{-1}/2 \qquad (1-72).$$

Equation (1-72) indicates that the mid-point of the
R_{2obsd} - $1/t_{CP}$ curve in the fast exchange region should
have the strong temperature dependence of τ_m^{-1}. This is

illustrated in Figure 2(b). The higher the temperature the larger the pulsing rate at the mid-point of the $R_{2obsd} - 1/t_{CP}$ curve.

In the short t_{CP} region (III) the same information is obtained from the slow and the fast exchange regions. The pulsing rate now is so fast that it completely overcomes the dephasing caused by $\Delta\omega_m$. This situation is equivalent to $\Delta\omega_m = 0$ in Swift and Connick's equation (1-2), and the equation is reduced to

$$(R_{2obsd})_{short\ t_{CP}} = [P_m/(T_{2m}+\tau_m)]+R_{2solv}+P_m R_{2o}$$

(1-73)

This equation was obtained by Campbell *et al.*[6] using a mathematical approach.

In the case that the short t_{CP} region is not accessible experimentally, a comparison of equation (1-73) and equation (1-5) helps to provide a lower limit estimate for R_{2m} since $R_{2m} \geq R_{1m}$ and $R_{2o} \geq R_{1o}$.

The extent to which R_{2obsd} is affected by the t_{CP} effect is determined by the long and the short t_{CP} regions, or by the long t_{CP} region and R_{1obsd} if the short t_{CP} region is not available. The t_{CP} effect is maximum in the intermediate exchange region since R_{2obsd} has the maximum difference from R_{1obsd} in this region (Figure 1).

Chapter II

EXPERIMENTAL

1. Preparation and Characterization of Hexakis
(acetonitrile)nickel(II)perchlorate { [Ni(CH$_3$CN)$_6$](ClO$_4$)$_2$}

The title compound was prepared from nickel carbonate (Baker and Adamson) and perchloric acid (McArthur chemical) in acetonitrile (Fisher) as described by Wickenden and Krause[35]. The product was crystallized twice by dissolving in acetonitrile and precipitating with ether. The preparation was carried out entirely under a dry nitrogen atmosphere.

This compound was identified by a comparison of its infra-red spectrum with the previously reported result[35]. The coordinated acetonitrile is characterized by ν_{C-N} at 2300 cm^{-1}. The infra-red spectrum of the compound showed no OH absorption in the 3500 cm^{-1} region.

Elemental analysis of this compound by pyrolysis was unsuccessful, thus separate analyses of the nickel(II) and the perchlorate ion content of the complex were carried out. The nickel(II) was analysed by atomic absorption spectroscopy and the perchlorate ion was determined gravimetrically as tetraphenylarsonium perchlorate.

Three sample solutions were prepared from a weighed amount of the solid complex in a given amount of

42

doubly distilled water. The solid complex was trans-
ferred in a glovebag filled with dry nitrogen. A Varian
Techtron model AA-6 atomic absorption spectrometer was
calibrated over the concentration range of 15 to 30 µg/ml
using standard nickel(II) solutions prepared from 1000
µg/ml standard nickel(II) stock solution (Fisher). The
absorbance readings were taken at 352.4 nm, and each
reading was taken over a three second period. An air/
acetylene mixture was used for the reducing flame.

For the analysis of the perchlorate ion, a two
fold molar excess of tetraphenylarsonium chloride was
added to a solution of the sample in about 100 ml of 2.5 M
sodium chloride and 0.1 M HCl at $90^{\circ}C$. The mixture was
allowed to cool for 2-3 hours and the white precipitate
of tetraphenylarsonium perchlorate was collected, washed
with ice cold water, and dried at $110^{\circ}C$ for several hours
before weighing. The results of the analysis are given
as follows.

Anal. Calcd for $[Ni(CH_3CN)_6](ClO_4)_2$: Ni, 11.7;
ClO_4, 39.5. Found: Ni, 11.8, 12.1, and 11.0, average
11.6 ± 0.6; ClO_4 40.6, 40.0, and 37.6, average 39.4 ± 1.6.

2. Preparation and Characterization of (Acetontrile) [*N*-(2-pyridylmethylene)-*N'*-[3-(2-pyridylmethylene) amino]propyl]-1,3-propanediamine-*N*,*N'*,*N''*,*N'''*,*N''''*] nickel(II)hexafluorophosphate{ [NipyDPT(CH$_3$CN)](PF$_6$)$_2$}

The aquo complex of this compound [NipyDPTOH$_2$](PF$_6$)$_2$ [a] was prepared by minor modifications of the method described by Spencer and Taylor[36]. The product was recrystallized twice from warm water.

Anal. calcd for C$_{18}$H$_{25}$N$_5$NiO.2PF$_6$: C, 31.98; H, 3.73; N, 10.36. Found: C, 31.82; H, 3.75; N, 10.28.

The compound was also characterized by comparison of its infra-red spectrum to that reported by Spencer and Taylor[36]. The aquo complex was dissolved in acetonitrile, and then the solvent was removed under vacuum, and the procedure was repeated three times. The infra-red spectrum of the resulting product indicated that water had been removed and replaced by acetonitrile as supported by the sharp peak at about 2300 cm^{-1}.

3. Preparation and Characterization of

    Tris(acetonitrile)tribenzo b,f,j -1,5,9 tri-

    azacycloduodecinenickel(II) perchlorate

    $\{[NiTRI(CH_3CN)_3](ClO_4)_2\}$

The aquo complex $[NiTRI(OH_2)_3](ClO_4)_2$[a] was pre-
pared by the method described by Taylor *et al.*[37a] ,
after converting o-nitrobenzaldehyde to o-aminobenzalde-
hyde as described by Smith and Opie[38]. The nitrate salt
was converted to the perchlorate salt by the addition of
a sodium perchlorate solution to an aqueous solution of
the nitrate salt. The product was filtered, washed with
a solution of sodium perchlorate and finally with water.
It was dried for a few days under vacuum over $CaSO_4$. The
electronic spectrum of a sample of $[NiTRI(OH_2)_3](ClO_4)_2$ in
dilute $HClO_4$ agreed with that reported by Taylor and
Busch[37b].

A portion of the aquo complex was dissolved in
acetonitrile, and then the solvent was removed under
vacuum, and the procedure was repeated three times. The
infra-red spectrum of the product (Nujol mull) indicated
that water had been removed and replaced by acetonitrile
(ν_{C-N} at 2300 cm^{-1}).

---

[a] The author is grateful to Dr. R.B. Jordan for preparing
$[NiTRI(OH_2)_3](ClO_4)_2$.

Anal. Calcd for $C_{27}H_{24}N_6Ni \cdot 2ClO_4$: C, 46.98;
H, 3.48; N, 12.18. Found: C, 46.63; H, 3.37; N, 12.26.

4. Sample Preparation

The solvent acetonitrile (Fisher) was purified
by triple vacuum distillation from Linde 3A molecular
sieves. Only the middle fraction of each distillation
was retained. The solvent was always stored over
molecular sieves and was vacuum distilled into a contain-
er just before use.

All samples were prepared in a glovebag filled
with dry nitrogen. The general procedure consisted of
transferring the solid complex into a small pre-weighed
flask which was then reweighed. The solvent was trans-
ferred into the flask containing the solid and the
contents were reweighed   An aliquot of the solution was
poured into an nmr tube. In the case of samples for chem-
ical shift measurements, the nmr tube contained a small
amount of 1,4-dimethoxybenzene as internal standard. The
nmr tube was removed from the glovebag and degassed using
the freeze-thaw technique. The tube was then sealed.

5. Instrumentation

The C.W. proton nmr spectra were recorded on
Varian Associates model A56/60 and HA-100, Perkin Elmer
model R32, and Bruker model WP-80 spectrometers equipped

with standard commercial temperature control units. In
all spectrometers the sample was maintained at constant
temperature by passing a thermostatically controlled
nitrogen gas around the sample tube. Temperatures on the
Varian A56/60 and the Perkin Elmer R32 instruments were
determined by a comparison of the peak to peak separation
of pure methanol or ethylene glycol samples with calibra-
tion charts published by Varian Associates. Temperatures
on the HA-100 and WP-80 instruments were measured by means
of a copper-constantan thermocouple. In all cases the
temperature was measured before and after a spectral run
and found to be constant to ± 0.5°C. About 5 minutes were
allowed for thermal equilibration in the sample tube.
About 15 minutes were allowed when the temperature was
measured with a copper-constantan thermocouple since the
sample tube was not allowed to spin. Normal precautions
were taken to prevent signal saturation and to ensure
proper phasing. Chemical shift measurements were re-
producible on all instruments to about ± 1 Hz.

Longitudinal (R_1) and transverse (R_2) relaxation
rates were measured with a Bruker SXP4-100 pulsed nmr
spectrometer and a 14-kGauss Varian Associates electro-
magnet and V3506 magnetic field flux stabilizer. Temp-
eratures were controlled by a standard Bruker B-ST 100/700
temperature control unit, and were measured with a Doric
Trendicator 400 digital thermometer using a copper-

48

constantan thermocouple. The nmr spectrometer can be
operated under control of a Nicolet 1180 minicomputer and
a Nicolet 293A programmable pulser. Data collection and
analysis were done by the Nicolet 1180 system.

The nmr system consists of the standard com-
ponents of a pulsed spectrometer and only the more unique,
or particularly pertinent features will be described.
The system has four independent pulse lines, and the phase
of the radio frequency (rf) pulse is continuously adjust-
able on each line. The system can be tuned to the re-
quired radio frequency by adjustment of two variable
capacitors on the high power amplifier and the probe arm
respectively. The detection system consists of a pre-
amplifier followed by an amplifier which can be operated
in either the diode or the phase sensitive mode. Diode
detection gives a signal which is the square root of the
sum of the squares of the absorption and dispersion
signals and is unaffected by moderate changes in magnetic
field or radio frequency. However the phase sensitive
detection gives a better signal to noise ratio, has better
linearity over the full dynamic range of the amplifier
and has better time constant characteristics. The latter
feature especially necessitated the use of phase sensitive
detection during pulse sequences when pulse repetition and
data collection occurred in a few tenths of a millisecond.
The detector also contains an rf filter with

bandwidths adjustable from 100 kHz to 100 Hz.

The spectrometer was tuned to obtain a maximum power transmission to the sample. In a one pulse sequence with a repetition time of about ten times the T_1 of the sample and using diode detection, the free induction decay (FID) should be a maximum after a $90°$ pulse and a minimum after a $180°$ pulse. With an initial pulse length much less than a normal $90°$ pulse the tuning capacitors were adjusted to give a maximum signal. Then the pulse length was increased until the amplitude of the FID decreased to about 80% of its maximum value. Then the tuning capacitors were adjusted to give a minimum signal amplitude. Finally the pulse length was increased to give a null signal for a $180°$ pulse length. The final $180°$ pulse length can be determined under computer control by an iterative programme which adjusts the pulse length until a minimum signal amplitude is detected. The $90°$ pulse length was taken as half the $180°$ value. The $90°$ pulse lengths were in the range of 2-5 µs.

The relative phases of the rf pulses on each pulse line were adjusted by observing the FID in the phase sensitive mode after a $90°$ pulse. For the first pulse line the appropriate adjustment was made on the phase shifter to give a maximum signal immediately after the pulse. This will be referred to as the $+x'$ phase. The phase of the second pulse line was adjusted to give a

positive-going null signal after the pulse, and is referred to as the +y' phase. The third line was adjusted to give a maximum negative signal amplitude after the pulse (i.e., 180° out of phase to the first line) and is referred to as the -x' phase.

Longitudinal relaxation rates were measured normally by the conventional 180-τ-90 pulse sequence under computer control. The sequence actually has the form $[180-\tau_o-90]-[wait]-[180-(\tau_o+\Delta)-90]-[wait]-[180-(\tau_o+2\Delta)-90]$... where τ_o, Δ, and the wait time are input initially. Typically the wait time was ten times T_1 and τ was incremented to about $\tau_o+20\Delta$ so that $\tau_o+20\Delta \simeq 3\ T_1$. The FID was detected in the diode mode after the 90° pulse, digitized, and integrated over a fixed region. The relaxation rate R_1 was determined from a nonlinear least-squares fit of the integrated intensities (I_t) to the equation[39]

$$I_t = A + B[1-\exp(-t/T_1)] \qquad (2-1)$$

where A and B are fitting constants, t is $\tau_o+n\Delta$, and T_1 is the relaxation time (= $1/R_1$). Since the FID after a 90° pulse decays with a time constant of about 5 ms, due to magnetic field inhomogeneity, diode detection was used for these measurements. This is an advantage because the diode signal is not significantly affected by the field or frequency drifts that may occur over the

several minutes often required for the R_1 measurements. This method of measurements has a precision of about ±1% for solutions containing paramagnetic ions, and about ± 5% for pure acetonitrile.

In the case of the rather long relaxation times of pure acetonitrile the R_1 was also measured by the triplet pulse sequence [40-42]. This sequence is more difficult to set up experimentally, and is more sensitive to pulse length errors than the simple [180-τ-90] sequence, but gives a saving in time because the wait period of ~ 10 T_1 is not involved. The pulse sequence used was 180_x,-τ-$[90_x,-180_{-x},-90_x,]$-τ-$[90_x,-180_{-x},-90_x,]$-τ-... where subscripts refer to phases of the rf pulses described previously. In a typical experiment τ was about 1 second and the intratriplet spacing, between the $90_x,-180_{-x},-90_x,$ pulses was 1 millisecond. The spacing must be much smaller than T_1 so that no significant relaxation occurs while the triplet is applied. The signal was detected after the first $90°$ pulse in the triplet using the phase sensitive detection mode. The -x′ phase was readjusted during the triplet pulse sequence so that the FID amplitudes after the first two pulses of the triplet were symmetrical about zero amplitude and the pulse lengths readjusted until the FID amplitude after the third phase of the triplet was minimized. The R_1 was determined by the nonlinear least-squares fit of

the signal intensities to equation (2-1). Typical pre-
cision of this method of measurements was about ± 5%.

The transverse relaxation rates (R_2) were
measured by the Carr-Purcell-Meiboom-Gill (CPMG) pulse
sequence[22-24], ($90_x, -t_{CP}/2-180_y, -t_{CP}-180_y, -t_{CP}-180_y, ...$).
The magnetization rephases to produce an echo with a
maximum intensity at a time $t_{CP}/2$ after each $180°$ pulse.
The intensity of the successive echoes was measured with
phase sensitive detection and collected on the Nicolet
1180 minicomputer. Since the $180°$ pulse length is much
shorter than t_{CP}, the echo maxima are separated by t_{CP}.
The R_2 values were determined by a nonlinear least-
squares fit of the intensities to the equation

$$I_t = A + B \exp(-t/T_2) \qquad (2-2),$$

where A and B are fitting parameters, t is real time,
and T_2 is the relaxation time (= $1/R_2$). Typical pre-
cision of the CPMG method was ± 5% or better.

The relative phases of the pulses on the CPMG
sequence compensate for inevitable pulse length errors.
Small adjustments in the phase of the $180°$ pulse can be
made during trial experiments to optimize the exponential
appearance of the echo intensity decay curves. With the
experimental system used in this work the main problem
with the R_2 measurement was the change in the field

during the measurement. This problem was not of major significance because most relaxation times were relatively short. However the effect did seem to place an upper limit of 20 to 50 ms on the t_{CP} value range.

The lower limit of the t_{CP} value was controlled by the need to maintain a constant sample temperature. When a series of 180° pulses is applied to the sample rapidly some of the rf power is converted into heat. Blank experiments with a typical sample size and thermostatting gas flow rate indicated that the t_{CP} of 0.1 ms and duration of 1-2 s for the pulse train the sample temperature was increased by less than 0.5°C. Thus a lower limit of t_{CP} = 0.1 ms was used in the experiments. This limit probably could be extended with smaller samples, faster gas flow rates, and shorter durations of pulses, but the necessity to detect the signal between the 180° pulses, and the ring-down time of the receiver system probably gives a lower limit of about 0.05 ms.

The nmr sample was maintained at constant temperature by passing thermostatically controlled nitrogen gas around the sample tube. Temperatures were determined before and after each experiment by means of a copper-constantan thermocouple, and found to be reproducible to better than ± 0.5°C. At least 15 minutes were allowed for thermal equilibration in the sample tube. Precautions were taken to align the sample tube

in the sample coil and in between the magnet poles to minimize the magnetic field gradient.

Electronic spectra were measured on a Cary 219 spectrophotometer and infra-red spectra on Perkin Elmer 457 and 421 spectrophotometers.

6. Treatment of Data

An iterative nonlinear least-squares programme was used to analyse the $\Delta\omega_{obsd}-1/T$, $R_{1obsd}-$, and $R_{2obsd}-1/T$, and $R_{2obsd}-t_{CP}$ data. The programme is based on a general model

$$\hat{Y}_i = f(X_{i1}, X_{i2}, \ldots X_{im}; b_1, b_2, \ldots b_k)$$

which predicts the value $\hat{Y}$, of a dependent variable Y, where f contains m independent variables X_i and k parameters, and given n data points

$$(Y_i, X_{i1}, X_{i2}, \ldots X_{im}), \quad i=1,2, \ldots n$$

this programme calculates the best fit values of the coefficients b_j either by minimizing the function

$$\Phi = \sum_{i=1}^{n} (Y_i - \hat{Y}_i)^2$$

which is referred to as absolute residual minimization,

or by minimizing

$$\Phi = \sum_{i=1}^{n} (1 - Y_i / \hat{Y}_i)^2$$

which is referred to as relative residual minimization.

The least-squares analysis of all the R_{1obsd}- and R_{2obsd}-$1/T$ as well as R_{2obsd}-t_{CP} data was based on the relative residual minimization since the measured relaxation rates have the same relative uncertainty. Then each point of the data carries the same influence in the least-squares analysis.

Each point of the chemical shift data has the same absolute uncertainty. Thus the larger the value, the smaller the relative uncertainty, and the chemical shift data were analysed based on the absolute residual minimization where larger values carry more influence in the least-squares analysis.

The uncertainty limits of the fitted parameters calculated by the least-squares programme are equivalent to the 95% confidence limits.

Chapter III

RESULTS AND DISCUSSION

The contents of this chapter are divided into four major sections. Section I deals with solvent acetonitrile relaxation rate measurements, the results of which were used for the calculations in the remaining three sections. Sections II, III, and IV contain the chemical shift measurements, the longitudinal and transverse relaxation rate measurements, and the data analysis for the determination of the solvation numbers of nickel(II), NipyDPT^{2+}, and NiTRI^{2+} complexes in acetonitrile respectively.

I. Solvent Acetonitrile Proton Relaxation Rates

The relaxation rates in acetonitrile have been studied several times previously[43-46]. As a result, a detailed study was not attempted in this work. In addition, the solvent proton relaxation rates are not of great importance in the interpretation of results discussed in subsequent sections of this thesis.

It is known that the acetonitrile solvent proton longitudinal relaxation rate (R_{1solv}) is controlled by proton-proton dipolar relaxation[47]. The proton

transverse relaxation rate (R_{2solv}) has contributions from the dipolar mechanism (R_{2solv}^{o}) and from scalar coupling between the protons and nitrogen-14 (S=1). The quadrupolar relaxation of the nitrogen-14 causes a fluctuating local field at the protons to provide this relaxation mechanism. Allerhand and Thiele[31] developed the theory for the dependence of R_{2solv} on the separation (t_{CP}) of the 180° pulses of the CPMG pulse train for the limiting case of fast quadrupolar relaxation $|2\pi J_{NH}T_{1N}| << 1$, and found that

$$R_{2solv} = R_{2solv}^{o} + \frac{4}{3}\pi^2 S(S+1)J_{NH}^2 T_{1N} \text{ x}$$

$$\{ 1 - (2T_{1N}/t_{CP})\tanh[t_{CP}/(2T_{1N})] \}$$

(3-1),

where S is the nuclear spin quantum number of nitrogen-14 , J_{NH} is the proton-nitrogen-14 coupling constant in Hz, and T_{1N} is the nitrogen longitudinal relaxation time (= $1/R_{1N}$).

In the short t_{CP} limit, when $t_{CP} \lesssim 0.3T_{1N}$, R_{2solv} becomes independent of t_{CP} and equation (3-1) is reduced to

$$R_{2solv} = R_{2solv}^{o}$$

(3-2)

which should equal R_{1solv} because the acetonitrile

molecule has only the dipolar relaxation mechanism. In

the long t_{CP} limit, when $t_{CP} >> T_{1N}$, R_{2solv} again becomes

independent of t_{CP} and equation (3-1) is reduced to

$$R_{2solv} = R_{2solv}^{o} + \frac{4}{3}\pi^2 S(S+1)J_{NH}^2 T_{1N} \qquad (3-3).$$

From this limit one can determine $J_{NH}^2 T_{1N}$, and in the

intermediate region the variation of R_{2solv} with t_{CP}

defines T_{1N}. Thus a study of the t_{CP} dependence of

R_{2solv} allows one to determine R_{2solv}^{o}, J_{NH}, and T_{1N}.

Gutowsky et al.[43] studied the t_{CP} dependence

of R_{2solv} in acetonitrile and obtained $R_{1N} = 2.0 \times 10^2$

s^{-1}, $J_{NH} = 1.38$ Hz , and $R_{2solv}^{o} = 8.93 \times 10^{-2}$ s^{-1} at 26°C.

Since this early study, Woessner et al.[45] have directly

measured the nitrogen relaxation rate and found

$R_{1N} = 2.27 \times 10^2$ s^{-1} at 25°C, while a measurement of the

^{1}H-^{15}N coupling constant[48] indicates that $J_{NH} = 1.28$ Hz

for ^{14}N. These discrepancies, and the general concern

of this work with t_{CP} - R_{2solv} variations, are the

reason for a reinvestigation of the earlier work of

Gutowsky et al.[43].

Selected results of R_{2solv} measurements as a

function of t_{CP} are shown in Figure 3, and the results

are similar to the values of Gutowsky et al.[43]. The para-
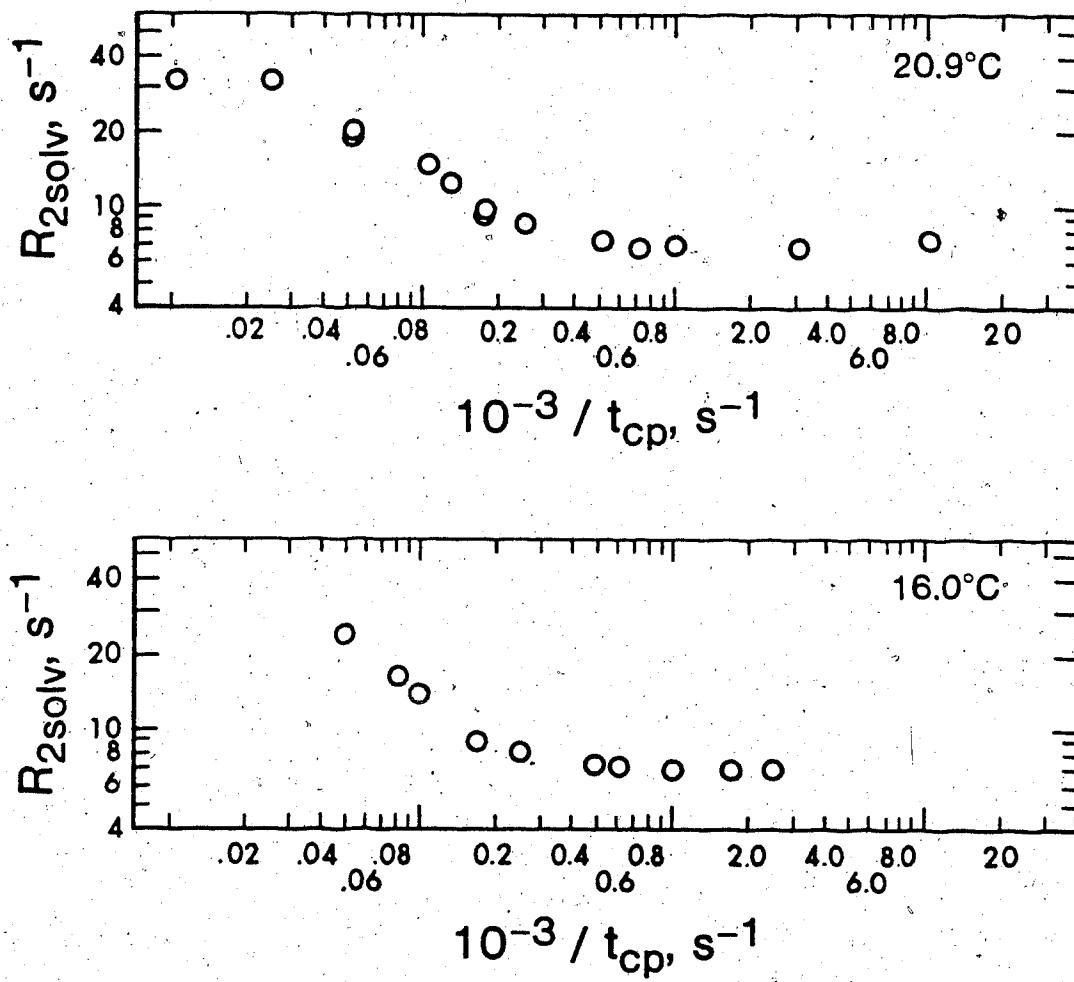
Figure 3 Selected plots of R_{2solv} *versus* $1/t_{CP}$ for pure acetonitrile at $20.9°C$ and $16.0°C$ and 60 MHz.

meters from a least-squares analysis of these results

are summarized in Table 2. In Fit I (Table 2) the best

fit of the three parameters R°_{2solv}, R_{1N}, and J_{NH} was

obtained. If J_{NH} and R_{1N} are fixed at the value from di-

rect measurements[48,44], then the data are not well fitted

as can be seen from the fact that the standard error of

the fit increases by a factor of 2 to 5. Samples of

the fit are given in Table 3.

The t_{CP} study gives the expected value of

R_{2solv} in the short t_{CP} limit, but the value of J_{NH} is

too large, and R_{1N} is not well defined. Numerical calcu-

lation shows that the problem can be traced to the poorly

defined long t_{CP} limit. Since $T_{1N} \cong 5 \times 10^{-3}$ s, then

the long t_{CP} limit $(t_{CP} \gg T_{1N})$ is satisfied only if

$t_{CP} \gtrsim 5 \times 10^{-2}$ s. With the apparatus used in this

study, and probably also by Gutowsky et al.[43], measurements

at such long t_{CP} values are much less accurate largely

due to magnetic field fluctuations. The useful lesson

from this analysis is that R_{2solv} cannot be reliably

measured for $t_{CP} \gtrsim 20$ ms with our instrumentation. It

is noteworthy that such instrumental problems generally

give too large values of R_{2solv}, and this is the direct-

ion of deviation between the predicted and experimental

values from this study and that of Gutowsky et al.[43].

Table 2

Non-linear least-squares fit to equation (3-2) for pure acetonitrile at 60 MHz.

$^\circ$C	Fit[a]	$10^2 R^\circ_{2solv}$, s^{-1}	$10^2 R_{1N}$[b], s^{-1}	J_{NH}, Hz	10^2S.E.[c]
20.9	I	7.01±0.28	1.64±0.46	1.56±0.09	2.5
	II	7.30±0.95	2.08±2.41	1.28	11.0
	III	6.72	2.33±1.90	1.28	12.0
16.0	I	7.00±0.62	2.01±0.05	1.52±0.13	5.7
	II	7.54±0.91	1.52±0.65	1.28	11.7
	III	7.00	1.56±0.52	1.28	12.6
10.5	I	7.30±0.73	1.65±0.38	1.50±0.11	5.3
	II	8.02±1.20	1.32±0.66	1.28	12.7
	III	7.30	1.39±0.53	1.28	14.0

(a) Fit I R°_{2solv}, R_{1N}, and J_{NH} are fitting parameters.

Fit II J_{NH} is held constant at the value given.

Fit III R°_{2solv} and J_{NH} are held constant at the values given.

(b) R_{1N} values from direct measurements, equation (3-4), are 2.37 x 10^2, s^{-1}, 2.49 x 10^2 s^{-1}, and 2.64 x 10^2 s^{-1} at 20.9°, 16.0°, and 10.5°C respectively.

<u>Table 2(cont'd)</u>

(c) Standard errors of the fits are based on relative

residual minimization. See Chapter II for explanation.

Table 3

Comparison of the three-parameter and the two-parameter fits to equation (3-1) for pure acetontrile at 20.9°C and 60 MHz .

t_{CP},ms	$10^2 R_{2solv}$,s^{-1}	Fitted values[a]	
		I	II
20.0	23.6	23.9	18.4
12.0	16.5	16.1	13.9
10.0	14.1	13.9	12.5
6.0	9.42	9.87	9.63
4.0	8.36	8.35	8.42
2.0	7.40	7.36	7.60
1.6	7.19	7.23	7.49
1.0	7.33	7.10	7.38
0.6	7.00	7.04	7.33
0.4	7.00	7.02	7.32

(a) The three-parameter (I) and the two-parameter (II) fits correspond to Fit I and Fit II at 20.9°C of Table 2 respectively.

The main concern here is to have an expression which predicts the t_{CP} and temperature dependence of the solvent relaxation rates. Fortunately previous studies can be relied on to give this dependence. The study of the temperature dependence of R_{1N} ($-40°$ to $+60°$ C) by Bopp[44], and the value $T_{1N} = (4.38 \pm 0.07) \times 10^{-3}$ s obtained by Woessner et al.[45] can be combined to give

$$R_{1N} = 12.9\exp\left(\frac{1.7 \times 10^3}{RT}\right) \qquad (3\text{-}4).$$

The temperature dependence of R_{1solv} was measured in the present study (Figure 4). The results are fitted by a normal exponential temperature dependence, and since $R_{2solv}^° = R_{1solv}^°$, then

$$R_{1solv} = R_{2solv}^° = 5.70 \times 10^{-3}\exp\left(\frac{1.44 \times 10^3}{RT}\right) \qquad (3\text{-}5).$$

The value of R_{2solv} at various temperatures and t_{CP} values now can be calculated by substitution of equations (3-4) and (3-5) into (3-1) and by assuming that the directly measured $J_{NH} = 1.28$ Hz[48] is temperature independent. Finally it should be reemphasized that the values of R_{2solv} are not very important to the analysis in the following sections because the values are always much less than the relaxation rate measured in the presence of the paramagnetic ions.
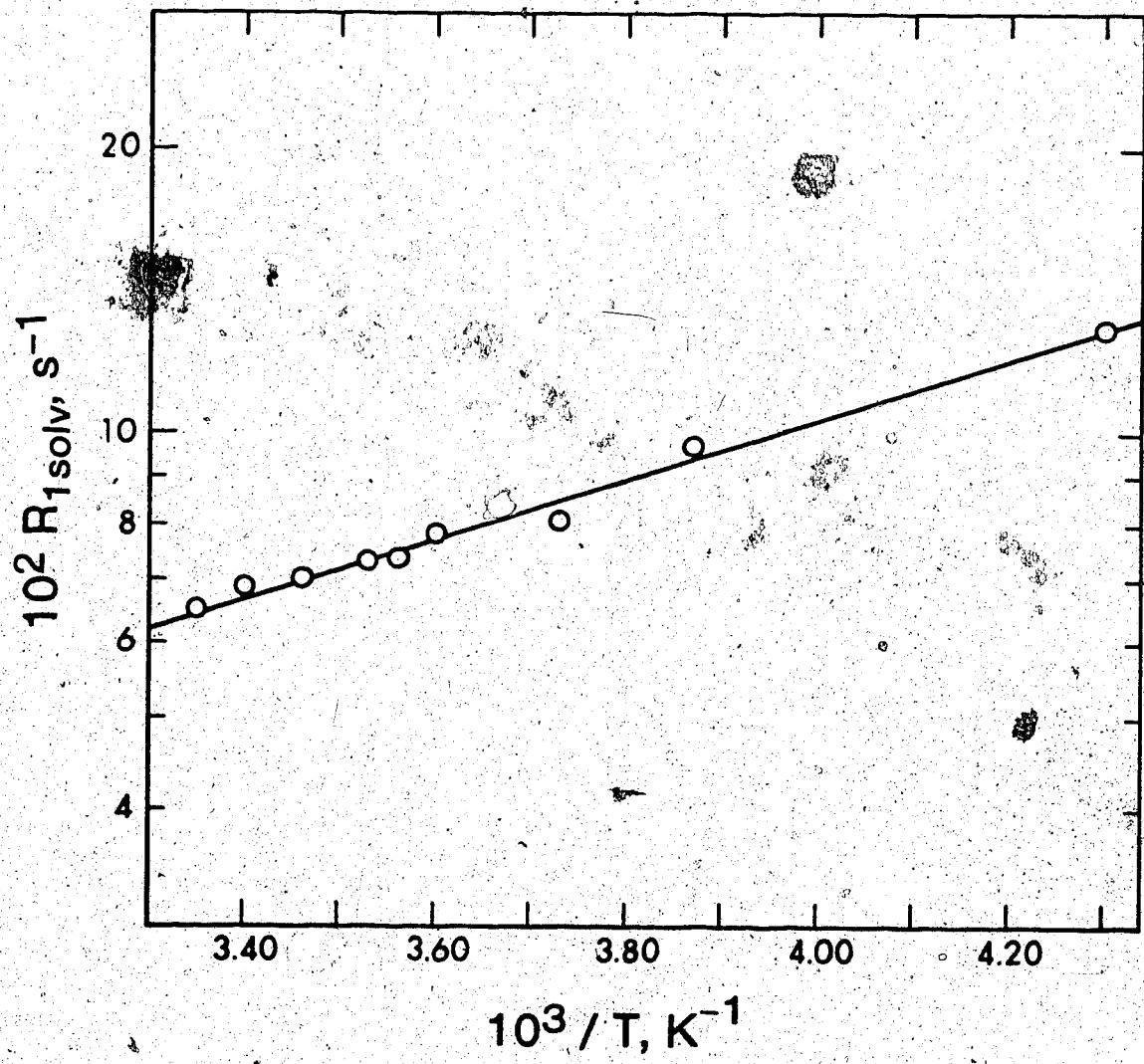
Figure 4 Plot of R_{1solv} *versus* 1/T for pure acetonitrile at 60 MHz.

II Determination of the Solvation Number of Nickel(II) in Acetonitrile

A Chemical Shift Measurements

The chemical shifts were measured at 60 and 90 MHz on Varian 56/60A and Perkin Elmer R32 spectrometers. The chemical shift of the solvent $(\Delta \nu_s^o)$ was measured relative to that of the phenyl protons of 1,4-dimethoxybenzene in solutions containing about 4%(w/w) of the internal standard. The shift of the solvent resonance in the presence of nickel(II) ions $(\Delta \nu_s)$ was measured relative to the same internal standard then

$$\Delta \nu_{obsd} = \Delta \nu_s - \Delta \nu_s^o$$

or

$$\Delta \omega_{obsd} = \Delta \omega_s - \Delta \omega_s^o \; .$$

The nickel(II) ions always caused upfield shifts of the solvent resonance.

The temperature dependence of $\Delta \omega_{obsd}$, given by equation (1-3), can be rewritten by defining $K_\omega = nC_\omega$ and by combining equations (1-8) and (1-4) with (1-3)

$$\Delta \omega_{obsd} = \frac{[m]}{[s]} \left[\frac{K_\omega / T}{(1 + \tau_m R_{2m})^2 + (\tau_m K_\omega n^{-1} T^{-1})^2} \right] \qquad (3-6).$$

Equation (3-6) predicts that $\Delta \omega_{obsd}$ should be directly

proportional to [m] at a constant temperature. The variation of $\Delta\omega_{obsd}$ with the molality of nickel(II) is shown in Figure 5 and clearly corresponds to the prediction of equation (3-6).

The main purpose of these chemical shift measurements is to determine K_ω since this value is used in conjunction with the value of $\Delta\omega_m$ from the R_{2obsd} $- t_{CP}$ analysis to calculate the solvation number n, since

$$n = \frac{K_\omega}{\Delta\omega_m T}$$

Chemical shift measurements in the fast exchange region $(1 \gg \tau_m R_{2m}, [\tau_m K_\omega/n^{-1}T^{-1}]^2)$ give the best value of K_ω because then

$$\Delta\omega_{obsd} = \frac{[m]K_\omega}{[s]T}$$

In this region K_ω can be determined independent of any knowledge of τ_m, R_{2m}, and n.

The nickel(II)-acetonitrile system reaches this fast exchange limit at about 60° C and measurements were extended to 80° C, the boiling point of acetonitrile. Beyond this point distillation of solvent into the

cooler parts of the sample tube might cause changes in the nickel(II) molality. The linearity of the plot in Figure 5 shows that this is not a problem up to $80°C$.

The chemical shift results are given in Table 4. The values show a relatively small increase with decreasing temperature in the fast exchange region ($>60°C$), but then decrease rapidly with decreasing temperature mainly because τ_m is increasing and $(\tau_m K_\omega n^{-1} T^{-1})^2$ is no longer small with respect to 1 in equation (3-6).

In order to fit the temperature dependence of $\Delta\omega_{obsd}$ it is necessary to know the temperature dependence of τ_m and R_{2m}. In principle these parameters can be obtained from the shift measurements alone, but in practice, the shift becomes smaller and less accurate in the region where $\Delta\omega_{obsd}$ decreases rapidly with decreasing temperature and τ_m and R_{2m} cannot be accurately determined from the shifts. Therefore the temperature dependence of τ_m was given by equation (1-6) with $\Delta H^{\ddagger} = 15.4_4 \times 10^3$ cal mol^{-1}, as determined from the $R_{2obsd} - t_{CP}$ study described in the next section, while $\Delta S^{\ddagger}$ was a fitting parameter. The temperature dependence of R_{2m} was obtained from fitting to equation (1-20) the results of Merbach et al.[49] on the linewidths
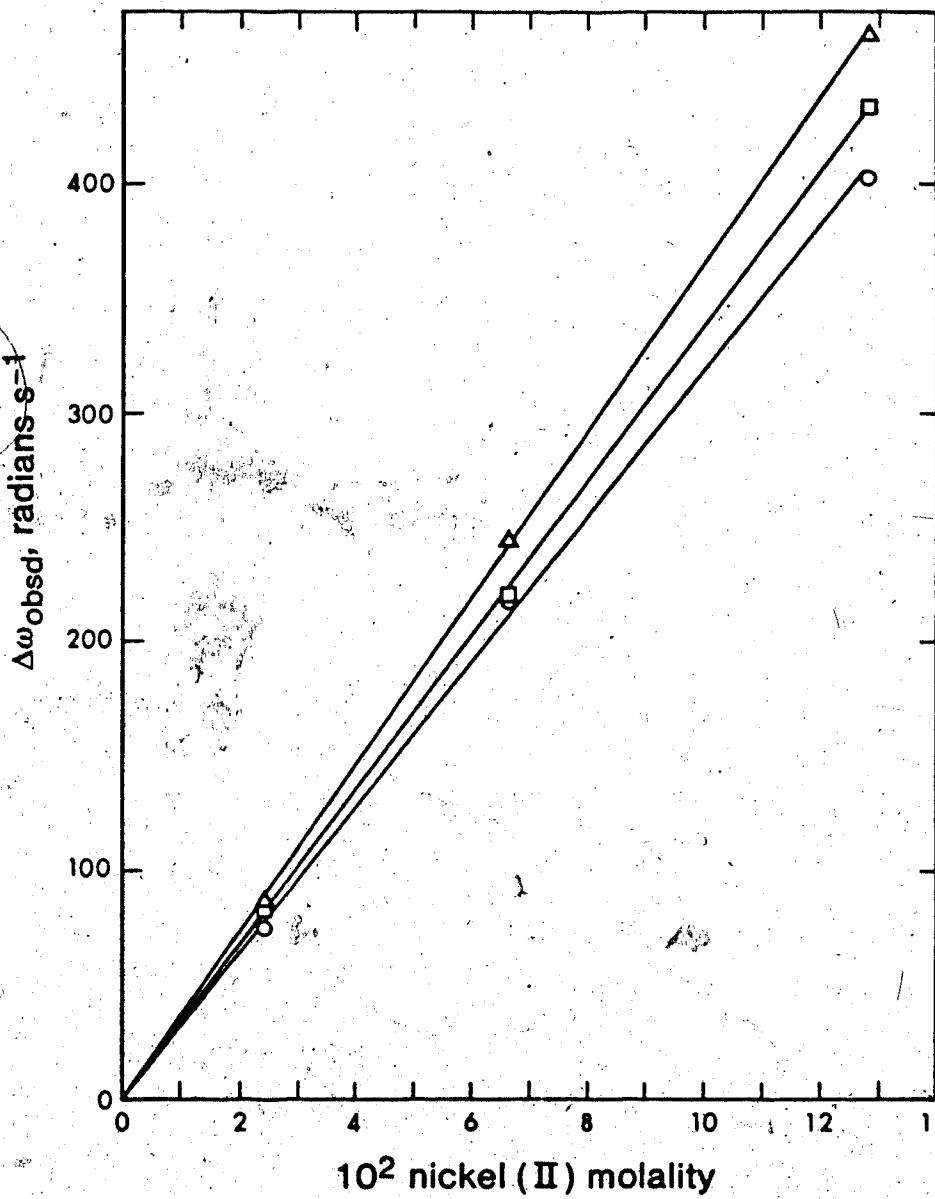
Figure 5 Plots of $\Delta\omega_{obsd}$ *versus* nickel(II) molality
for the nickel(II) solutions in acetonitrile
at: $50°$(○), $60°$(△), and $80°C$(□) and 90 MHz.

Table 4

Comparison of the experimental and calculated(least-squares) values of $\Delta\omega_{obsd}$ at various temperatures for the nickel(II)-acetonitrile system at 60 and 90 MHz.

		Chemical shift, radians s^{-1}	
Sample[a]	°C	Experimental	Calculated
			60 MHz
B	80	298	300
	70	278	304
	60	295	296
	50	254	247
	40	119	129
C	80	138	119
	70	141	120
	60	148	117
	50	110	98
	40	50.3	51.2
E	80	47.1	57.1
	70	47.1	57.8
	60	47.1	56.3

Table 4(cont'd)

Sample[a]	°C	Chemical shift, radians s^{-1}	
		Experimental	Calculated
			90 MHz
B	80	434	441
	70	452	450
	60	465	452
	50	402	419
	35	188	186
C	80	220	227
	70	239	232
	60	245	233
	50	220	216
	35	101	96
E	80	82	84
	70	82	85.7
	60	88	86
	50	75	80

(a) The sample labels given correspond to the nickel(II) concentrations of 0.1277(B), 0.06593(C), and 0.02431 (E) molal respectively.

of the coordinated solvent peaks to give

$$R_{2m} = (\frac{8.70 \times 10^4}{T}) \exp(\frac{3.78 \times 10^2}{RT}) \qquad (3-7).$$

It should be noted that the $(\tau_m R_{2m})$ term in equation (3-6) is never very significant so that even a 50% change in C_{2m} causes less than 2% change in K_ω. For this reason the same C_{2m} and E_{2m} values were used at 60 MHz and 90 MHz. The initial values for K_ω and $\Delta S^{\ddagger}$ were obtained from a qualitative evaluation of the limiting shift in the fast exchange region and from the $R_{2obsd} - t_{CP}$ analysis respectively.

The results of various nonlinear least-squares fits are summarized in Table 5. The value of K_ω at 90 MHz has been normalized to 60 MHz by multiplying by 60/90. It is clear that the data at the two frequencies give the same K_ω value within the 95% confidence limits. The 90 MHz values are considered to be most reliable because the shifts are larger, and the value of $K_\omega = 1.99 \times 10^7$ radians s^{-1}K from Fit II will be used in future calculations.

The observed and predicted values from Fits II and IV are compared in Table 4. The differences are generally about $\pm$ 12 radians s^{-1} ($\pm$ 2 Hz). This is considered reasonable since the values represent the

73

Table 5

Least-squares best fits of the $\Delta\omega_{obsd}$ – 1/T data for the nickel(II)-acetonitrile system at 60 MHz and 90 MHz.

Fit[a]	$10^{-4}\Delta H^{\ddagger}$ [b] cal mol^{-1}	$\Delta S^{\ddagger}$ cal mol^{-1} K^{-1}	$10^{-4}C_{2m}$ [b] s^{-1}	$10^{-2}E_{2m}$ [b] cal mol^{-1}	$10^{-7}K_{\omega}$ rad s^{-1} K	S.E.[c]
I	1.544	10.2 ±0.3	8.70	3.78	1.97±0.08	15.1
II	1.544	10.2 ±0.2	8.70	3.78	1.99±0.05	8.3
III	1.544	11.6 ±0.2	8.70	3.78	1.98±0.05	8.5
IV	1.544	8.72±0.44	8.70	3.78	2.04±0.18	16.6

(a) I   Combined 60 MHz and 90 MHz data.

II   90 MHz data.

III 90 MHz data with the assumed n value of 3 (see text)

IV   60 MHz data.

(b) Parameter held constant at the value given.

(c) Standard errors of the fits are based on the absolute residual minimization.

difference between the two shift measurements each of

which has an uncertainty of about $\pm$ 6 radians s^{-1}.

It may have occurred to the reader that the
solvation number n appears in the denominator of
equation (3-6), and it has been necessary to assume a
value for n to carry out the fitting procedure just
described. This assumption is not critical to the
evaluation of K_ω as shown by comparison of Fits II and
III in Table 5. When n is changed from 6 to 3 the value
of K_ω only changes by 0.5%. The value of $\Delta S^{\ddagger}$ changes
with n, as expected from equation (3-6), so that
(τ_m/n) remains the same, but K_ω is unaffected. In fact
K_ω is determined primarily from the limiting shift in
the fast exchange region.

B Relaxation Rate Measurements of Nickel(II) Solutions

The relaxation rates (R_{1obsd} and R_{2obsd}) are predicted to have a direct dependence on the nickel(II) concentration according to equations (1-2) and (1-5). Measurements of R_{1obsd} as a function of nickel(II) molality were carried out at $25°$ C and 60 MHz, and the linearity of the plot of R_{1obsd} versus nickel(II) molality (Figure 6) confirms the direct dependence of the relaxation rate on nickel(II) concentration. These observations also confirm the reliability of the sample preparation method.

Measurements of R_{2obsd} as a function of t_{CP} of the nickel(II) solution in acetonitrile were made at 60 MHz in the temperature range of $50°$ to $4.9°$ C. Measurements at lower temperatures were not attempted, primarily because the change in R_{2obsd} between the long and short t_{CP} limits at $4.9°$ C is already small and measurements at lower temperatures would not yield a very meaningful $R_{2obsd} - t_{CP}$ dependence. Furthermore, information concerning R_{2o}, which could be obtained from studies at lower temperatures, is available already from the literature[49]. At temperatures greater than $50°$ C R_{2obsd} could not be measured reliably since dis-
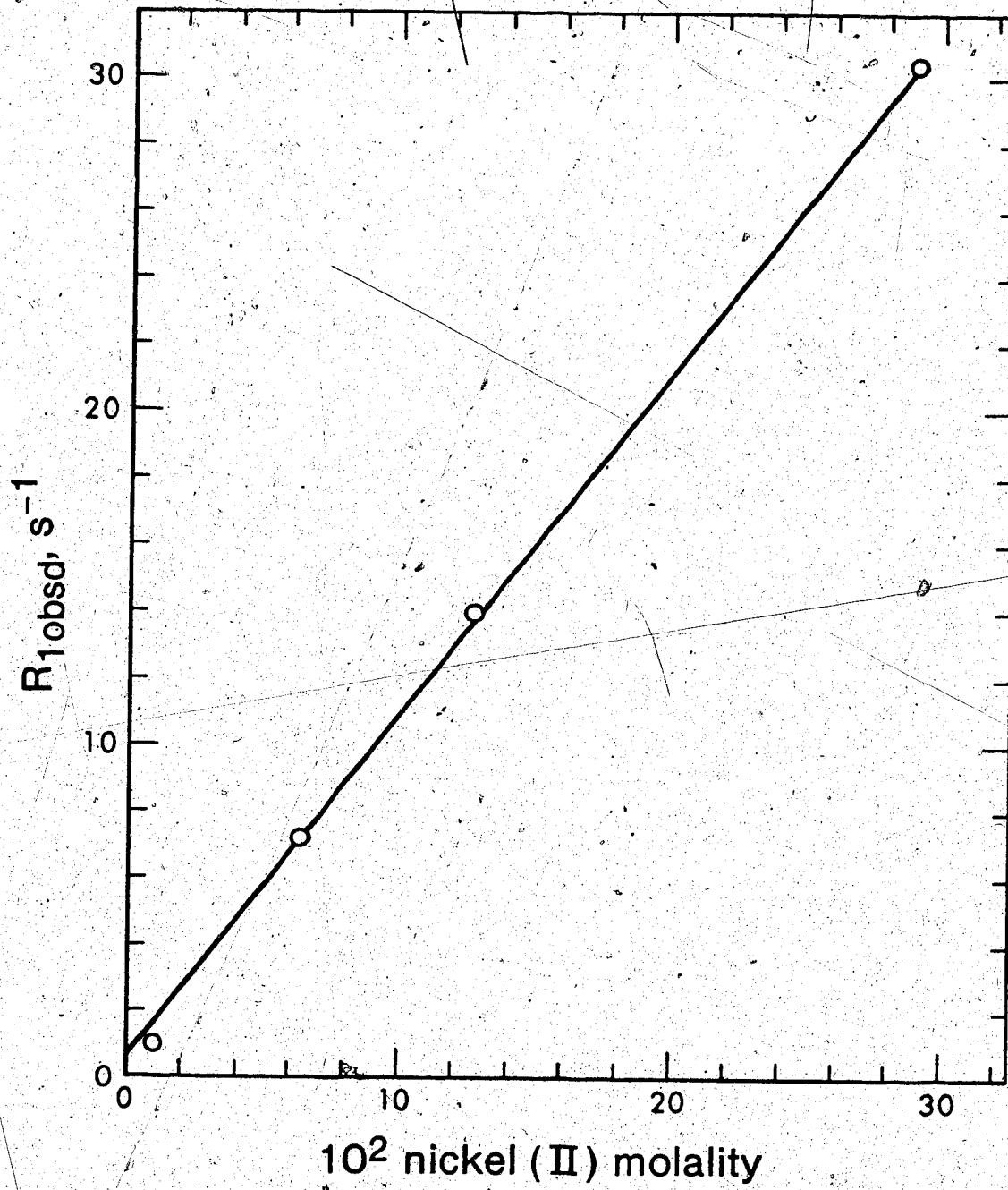
Figure 6 Plot of R_{1obsd} *versus* nickel(II) molality for the nickel(II) solutions in acetonitrile at $25°C$ and 60 MHz.

tillation of solvent into cooler sections of the sample
tube caused the nickel(II) concentration to change.

Selected plots of R_{2obsd} *versus* $1/t_{CP}$ are
shown in Figure 7. The full results are given in
Appendix A. The R_{2obsd} in the long t_{CP} limit, which is
equivalent to the R_2 obtained from the linewidth of
conventional nmr signal, increases with decreasing
temperature to a maximum value at about $40°C$, then de-
creases with decreasing temperature. This agrees with
the variation of R_2 with $1/T$ found by Merbach *et al.*[49]
from the linewidth method.

The results in Figure 7 show that the long
t_{CP} limit, and the intermediate t_{CP} region, are well
defined at each temperature. However, the short t_{CP}
limit is absent at all temperatures, due to the
experimental limitation on t_{CP} discussed in Chapter II.
The lack of data at the short t_{CP} limit could present
a problem in data analysis. Therefore, further
studies were carried out at lower magnetic fields to
better define this region. The value of R_{2obsd} undergoes
about half of its change with t_{CP} when $\Delta\omega_m/2 \doteq 1/t_{CP}$.
The lower magnetic field will lower $\Delta\omega_m$. Therefore
the change in R_{2obsd} will appear at longer t_{CP} values,
and the short t_{CP} will be more accessible.
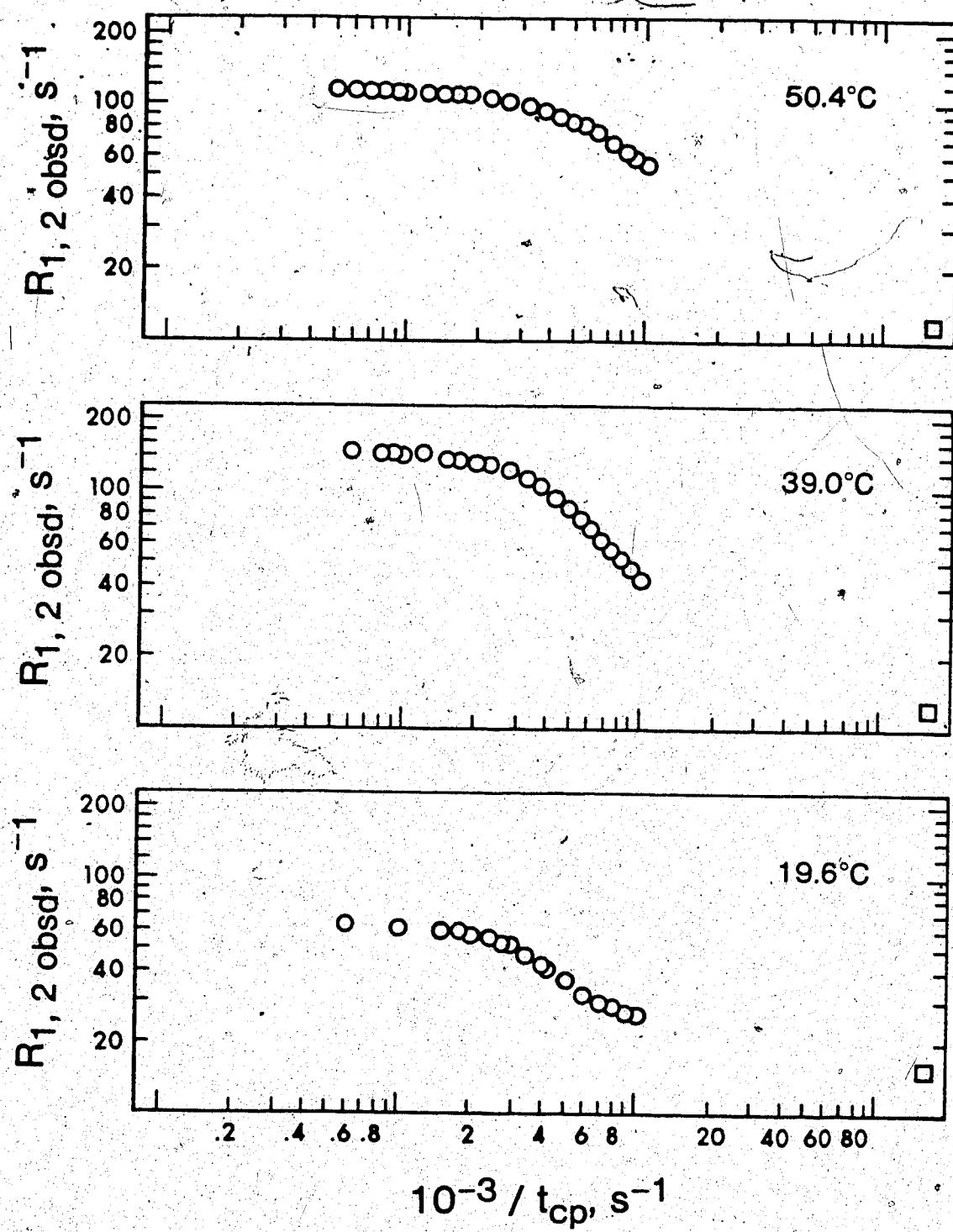
Figure 7 Plots of R_{2obsd} *versus* $1/t_{CP}$(O) for the 0.1277 molal nickel(II) solution in acetonitrile from selected data and temperatures at 60 MHz. R_{1obsd} is shown as ▢.

At 30 MHz the short t_{CP} limit still could not

be reached at least between 20° and 35°C. However at

15 MHz the short t_{CP} limit was sufficiently well defined

to be useful. The t_{CP} dependence of R_{2obsd} was studied

from 10° to 30°C at 15 MHz with the results shown in

Figure 8. The mid-point of the R_{2obsd} - $1/t_{CP}$ plots at

10.3°C (15 MHz) corresponds to the $1/t_{CP}$ value of about

a quarter of the value at 19.6°C and 60 MHz as expected

from equation (1-70). The values of R_{1obsd} were also

measured at 15 MHz. They provide a lower limit for

R_{2obsd} in the short t_{CP} limit since $R_{2obsd} \geq R_{1obsd}$.

The latter relationship is always satisfied by the results.

The goal of the R_{2obsd} - t_{CP} analysis is to

determine $\Delta\omega_m$. Then, from the chemical shift measurements

which give K_ω, and knowing that $\Delta\omega_m = K_\omega/(nT)$, it will be

possible to calculate the solvation number n. However

inspection of equations (1-67) and (1-68) shows that

$P_m = n[m]/[s]$ must be specified in order to fit the data.

In other words a value of n must be assumed to calculate

P_m. This appears to lead to a cyclical argument in

which n must be specified in order to evaluate n. The

analysis below will show that this is actually not the

case, and that $\Delta\omega_m$ can be evaluated independent of the

initially assumed n value. In addition, if an incorrect

n is assumed certain anomalies appear in the fitting
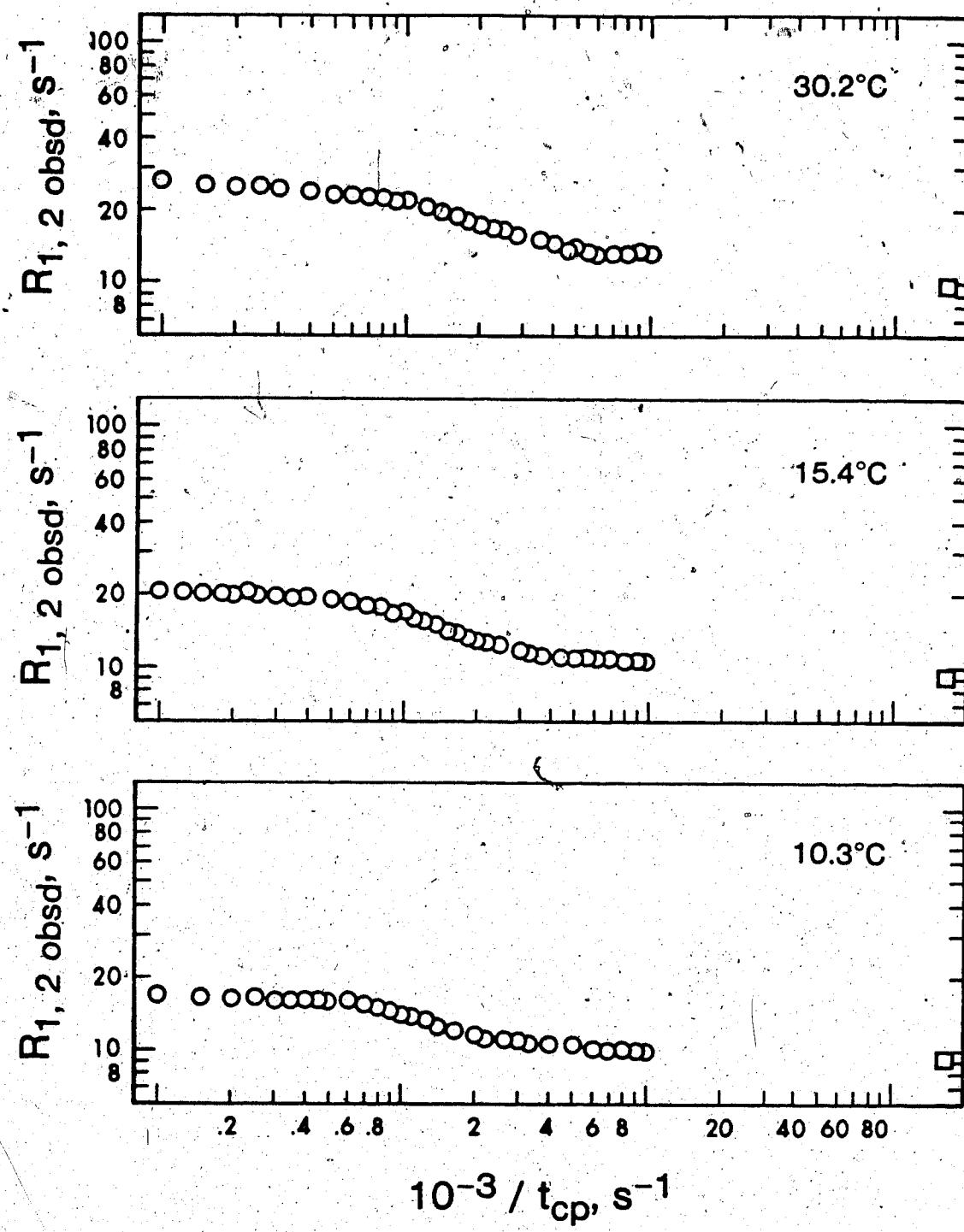
Figure 8 Plots of R_{2obsd} *versus* $1/t_{CP}$ (O) for the 0.06593 molal nickel(II) solution in acetonitrile from selected data and temperatures at 15 MHz. R_{1obsd} is shown as □.

parameters which give a clear indication of the in-
correct initial assumption.

In order to evaluate further the validity of
the analysis, the influence of changes in R_{2m} and R_{2o}
will be investigated. These two parameters generally
are the least well defined by the data because their
contribution is smaller than that of τ_m^{-1} and $\Delta\omega_m$. One
would hope to find that reasonable changes in R_{2m} and
R_{2o} do not have a major influence on τ_m^{-1} and $\Delta\omega_m$. These
will be investigated after the least-squares procedure
is described.

C. Least-Squares Analysis of R_{2obsd} - t_{CP} Data

The variation of R_{2obsd} with t_{CP} was fitted by an iterative non-linear least-squares method to equations (1-67) and (1-68). The various fitting procedures used are described in the following sections.

In general there are two factors which must be considered in the analysis. First of all, because of the potentially large number of parameters, it will be necessary to keep some parameters fixed. These parameters generally will be those which are least important to the ultimate goal of determining the solvation number, and those which are poorly defined by the data. Fortunately the same parameters often belong to these two classes. However it is still necessary to decide on the best values of these fixed parameters.

Secondly, it is necessary to provide initial values of the fitting parameters for the iterative least-squares programme. These values can be determined from a qualitative evaluation of limiting regions of the data, from R_1 measurements, and from previous experimental work.

The solvent acetonitrile proton relaxation rates (R_{2solv}) have been discussed already and always

were held constant at the values given by equations
(3-1), (3-4), and (3-5) with J_{NH} = 1.28 Hz. These
values are all reasonably well defined, but are not very
important to the analysis because $R_{2obsd} \gg R_{2solv}$ for
the nickel(II) solutions in acetonitrile. The following
discussion will be concerned primarily with the values
for the outer-sphere (R_{2o}) and the inner-sphere (R_{2m})
contributions.

The outer-sphere contribution was calculated
from the results of Merbach *et al.*[49] who studied the
system down to $-45°$ C at 60 MHz. and found well defined
values of R_{2o}. These results were refitted to equation
(1-27) to obtain

$$R_{2o} = (\frac{4.93 \times 10^4}{nT}) \exp(\frac{1.44 \times 10^3}{RT}) \qquad (3-8).$$

The pre-exponential constant in equation (3-8) has been
reduced by 10% from the value indicated by the data of
Merbach *et al.*[49] because the (R_{2obsd}/P_m) of the latter
have been found to be about 10% greater than those
measured in this work. The R_{2o} values are in the range
of 240 to 400 s^{-1} compared with (R_{2obsd}/P_m) values of
about 4000 s^{-1}. Thus the outer-sphere term is generally
a minor contribution, and was fixed at the value given
by equation (3-8) in the least-squares fits.

The activation energy for R_{2o} (1.44 x 10^3 cal mol^{-1}) is in reasonable agreement with that for the viscosity of acetonitrile (1.84 x 10^3 cal mol^{-1})[50]. This is expected if molecule tumbling is the important correlation time for the outer-sphere interaction.

The values of τ_m^{-1}, $\Delta\omega_m$, and R_{2m} were treated as fitting parameters in the least squares analysis. Satisfactory initial guesses of τ_m^{-1} can be obtained from the slow exchange region below 35°C, and $\Delta\omega_m$ can be estimated from the $1/t_{CP}$ value at which R_{2obsd} had undergone half the total change with t_{CP}. In other temperature ranges τ_m^{-1} and $\Delta\omega_m$ can be estimated by simple extrapolation using the expected temperature dependence given by equations (1-6) and (1-8) respectively. Since the short t_{CP} limit was not defined at 60 MHz R_{2m} values initially were estimated from R_{1m} as discussed previously in Chapter I.

The results of these fits are summarized in Table 6. The results in Table 6 clearly illustrate that $\Delta\omega_m$ and τ_m^{-1} obtained from the least-squares fit are essentially insensitive to the value of R_{2m}. Results are compared for fits in which R_{2m}, τ_m^{-1}, and $\Delta\omega_m$ were fitting parameters, and for fits in which only τ_m^{-1} and $\Delta\omega_m$ were parameters, and R_{2m} was given by equation (3-7).

Table 6

Effect of the variation of R_{2m} on τ_m^{-1} and $\Delta\omega_m$ from the least-squares analysis of the $R_{2obsd}-t_{CP}$ data for the nickel(II) solutions in acetonitrile at 60 MHz[a].

Temp, °C	Sample[b]	R_{2m}[c], s^{-1}	$10^{-3}\tau_m^{-1}$, s^{-1}	$10^{-4}\Delta\omega_m$, radians s^{-1}
50.4	B	824(484)	20.0(22.5)	1.18(1.24)
40.2	B	194(509)	10.7(9.46)	1.38(1.39)
35.0	B	35(523)	10.1(8.87)	1.32(1.32)
24.7	B	758(553)	4.54(4.24)	1.09(1.20)
16.4	B	312(580)	1.88(1.97)	1.11(0.949)
4.9	E	406(620)	0.579(0.576)	1.24(1.08)

(a) The first numbers in columns 3 to 5 are from the three-parameter fits and numbers in brackets are from the two-parameter fits. All fits were analysed with n=4.

(b) The sample labels given correspond to the nickel(II) concentrations of 0.1277(B) and 0.0243(E) molal.

(c) The R_{2m} values in brackets are fixed at those calculated from equation (3-7).

The results presented in Table 6 are at selected temperatures where the differences in R_{2m} values are largest. Comparison of the results shows that even a greater than 50% change in R_{2m} causes less than a 15% change in $\Delta\omega_m$ and even less in τ_m^{-1}.

The general procedure for the least-squares analysis of the 15 MHz data is similar to that used at 60 MHz. However, there are independent measurements of the outer-sphere contribution, and this factor is relatively more important than at 60 MHz. The value of R_{2o} was determined from an analysis of the lower temperature data, which in the long t_{CP} limit, is given by equation (1-69). The value of τ_m^{-1} is known from the 60 MHz results of Merbach et al.[49] and those presented here. At $10.3\degree C$ τ_m^{-1} was fixed at 743 s^{-1} and the least-squares analysis of the $R_{2obsd} - t_{CP}$ data gave $R_{2o} = (3.25 \pm 0.27) \times 10^2$ s^{-1}. The temperature dependence of R_{2o} (E_{2o}) was assumed to be the same as that of the viscosity of acetonitrile[50], and R_{2o} was calculated at any temperature from

$$R_{2o} = \left(\frac{2.11 \times 10^4}{nT}\right) \exp\left(\frac{1.84 \times 10^3}{RT}\right) \qquad (3\text{-}9).$$

The importance of this contribution will be discussed subsequently. However, it may be noted that even if R_{2o}

is omitted, the fitting of the $R_{2obsd} - t_{CP}$ data in the slow exchange region yields essentially correct $\Delta\omega_m$ values.

The outer-sphere contribution is much more important at 15 MHz than at 60 MHz, and the 15 MHz data have been selected to indicate the sensitivity of τ_m^{-1} and $\Delta\omega_m$ to R_{2o}. The results in Table 7 compare values from fits with R_{2o} calculated from equation (3-9) to those of the extreme case where R_{2o} is omitted entirely. Even with this extreme assumption $\Delta\omega_m$ values are affected by less than 15%. In fact in the slow exchange region ($<21°$ C) the change is only about 10%. This is expected because $\Delta\omega_m$ is essentially defined by the change of R_{2obsd} in the intermediate t_{CP} region. It is also clear that τ_m^{-1} is much more sensitive to changes in R_{2o}, especially in the slow exchange region. This is expected because in this region, in the long t_{CP} limit, R_{2obsd} is given to a fair approximation by $P_m (\tau_m^{-1} + R_{2o})$. This fact actually was used to evaluate R_{2o} since τ_m^{-1} values are known from studies reported in this work at 60 MHz and previously reported by Merbach *et al.*[49].

The next question is the effect of the initially assumed n value on the fitting parameters, especially τ_m^{-1} and $\Delta\omega_m$. The least-squares results for the assumption that n=6 or n=4 at 60 MHz and 15 MHz are given in Table 8 and Table 9 respectively.

Table 7

Comparison of the parameters obtained from fits with and without the outer-sphere contribution for the 0.0659-molal nickel(II) solution in acetontrile at 15 MHz[a].

Temp, °C	$10^{-3}R_{2m}$, s^{-1}	$10^{-3}\tau_m^{-1}$, s^{-1}	$10^{-3}\Delta\omega_m$, rad s^{-1}
30.3	0.634(1.04)	3.99 (3.33)	2.59(2.98)
25.0	0.670(1.07)	2.66 (2.83)	2.70(3.16)
21.0	0.589(0.963)	1.87 (2.45)	2.84(3.08)
10.3	0.492(1.12)	0.745(1.35)	3.27(2.91)

(a) The parameters obtained from fits without the outer-sphere contribution are given in brackets. The n value of 6 was assumed in both fits.

Table 8

Comparison of the results of the $R_{2obsd}-t_{CP}$ least-squares analysis assuming n=6 and n=4 for the nickel(II)-acetonitrile solution at 60 MHz.

Temp, °C [a]	$10^{-2}R_{2m}$, s^{-1}		$10^{-3}\tau_m^{-1}$, s^{-1}		$10^{-4}\Delta\omega_m$, rad s^{-1}		10^2 S.E. [b]	
	n=6	n=4	n=6	n=4	n=6	n=4	n=6	n=4
50.4(B)	3.8±2.8	8.2±3.4	23.5±3.0	20.0±2.6	0.992±0.078	1.18±0.06	0.88	0.80
40.2(B)	3.8±1.3	1.9±6.0	11.2±1.2	10.7±6.5	1.00 ±0.01	1.38±0.16	1.50	4.07
40.0(A)	3.0±2.0	2.4±4.7	11.6±1.7	9.94±5.37	1.03 ±0.02	1.39±0.17	1.92	3.03
39.0(B)	3.1±1.4	1.7±5.1	12.0±1.3	10.7±5.6	1.00 ±0.02	1.38±0.14	1.55	3.49
35.4(C)	5.7±0.4	2.0±3.4	5.03±0.18	9.54±4.87	1.20 ±0.04	1.31±0.18	1.27	4.36
35.0(B)	5.2±0.7	0.4±5.0	5.16±0.26	10.1±5.9	1.19 ±0.05	1.32±0.16	1.51	4.25
30.2(C)	4.8±0.8	4.0±1.8	3.90±0.26	7.61±3.42	1.16 ±0.08	1.17±0.20	2.03	3.36
29.8(C)	4.2±0.4	3.7±1.0	3.72±0.06	6.94±0.83	1.22 ±0.03	1.22±0.08	1.02	2.50
29.8(B)	7.4±1.0	6.8±2.7	3.93±0.29	7.36±3.61	1.13 ±0.08	1.17±0.26	2.04	4.18
25.1(C)	5.7±0.5	7.1±1.4	2.71±0.07	4.57±0.41	1.16 ±0.04	1.15±0.10	1.28	2.42
24.7(B)	6.1±0.7	7.6±1.4	2.61±0.10	4.54±0.59	1.12 ±0.06	1.09±0.12	1.44	2.87
19.6(B)	5.0±0.8	7.1±0.9	1.66±0.08	2.66±0.14	1.12 ±0.09	1.09±0.08	2.08	1.70

Table 8(cont'd)

Temp, °C [a]	$10^{-2}R_{2m}$, s^{-1}		$10^{-3}\tau_m^{-1}$, s^{-1}		$10^{-4}\Delta\omega_m$, rad s^{-1}		10^2S.E. [c]	
	n=6	n=4	n=6	n=4	n=6	n=4	n=6	n=4
16.4(B)	2.2±0.6	3.1±0.8	1.22±0.06	1.88±0.09	1.12±0.08	1.11±0.08	2.37	2.15
4.9(E)	2.7±1.0	4.1±1.5	0.385±0.018	0.579±0.028	1.24±0.02	1.24±0.20	1.50	1.51

(a) Sample labels given in brackets correspond to nickel(II) molality of 0.2903(A), 0.1277(B), 0.06593(C), and 0.02431(E) respectively.

(b) Standard errors of the fits are based on relative residual minimization.

Table 9

Comparison of the results of the $R_{2obsd}-t_{CP}$ least-squares analysis assuming n=6 and n=4 for the nickel(II)-acetonitrile system at 15 MHz.

Temp, °C [a]	$10^{-2}R_{2m}$, s^{-1}		$10^{-3}\tau_m^{-1}$, s^{-1}		$10^{-3}\Delta\omega_m$, radians s^{-1}		10^2S.E. [b]	
	n=6	n=4	n=6	n=4	n=6	n=4	n=6	n=4
30.3(C)	6.34±0.53	10.3±3.4	3.99±0.84	3.43±2.95	2.59±0.07	3.93±1.35	2.12	2.77
30.1(B)	6.18±0.30	9.64±2.9	3.82±0.47	3.49±1.91	2.82±0.04	4.23±1.43	1.31	2.71
25.0(B)	5.94±0.56	8.00±3.4	2.49±0.71	3.29±4.03	2.95±0.30	4.11±2.04	1.33	4.80
25.0(C)	6.70±0.96	9.48±4.5	2.66±1.06	3.34±4.20	2.70±0.32	3.86±1.94	2.21	4.40
21.0(C)	5.89±0.37	7.55±3.2	1.87±0.36	2.97±3.62	2.84±0.34	3.66±1.86	1.36	4.72
20.7(B)	6.13±0.68	8.04±4.0	1.97±0.66	2.92±4.30	2.95±0.56	3.85±2.63	1.50	4.57
15.4(C)	5.14±0.23	6.31±1.2	1.13±0.07	2.38±1.39	3.12±0.25	3.01±0.79	1.59	1.85
10.3(C)	4.92±0.34	6.54±0.45	0.745±0.04	1.31±0.16	3.27±0.36	3.10±0.45	1.95	1.89

Table 9(cont'd)

(a) Sample lables given in brackets correspond to the nickel(II) concentrations of

0.1277(B) and 0.06593(C) molal.

(b) Standard errors of the fits are based on relative residual minimization.

In general it is true that the uncertainty limits for the parameters, and the standard errors of the fits are larger for n=4 than for n=6. However both assumptions of n provide satisfactory fits of the data. This is illustrated for data in the fast exchange region (50.4°C) in Table 10 and in the slow exchange region (24.7°C) in Table 11. Thus the goodness of the fit does not provide a useful criterion for the correct choice of n.

The trends and uncertainties in τ_m^{-1} and $\Delta\omega_m$ can be understood qualitatively when their relationship to the limiting region and the t_{CP} variation is noted. In the slow exchange region the long t_{CP} limit gives $(P_m\tau_m^{-1})$ and the t_{CP} variation of R_{2obsd} gives $\Delta\omega_m$. Thus, for temperatures <30°C at 60 MHz and <20° at 15 MHz, the value of τ_m^{-1} with n=4 is close to 6/4 times the value with n=6 as expected since $(P_m\tau_m^{-1})$ is defined by the experiments. In this same region $\Delta\omega_m$ is essentially independent of the assumed n value because $\Delta\omega_m$ is defined by the t_{CP} variation. The results in Table 8 and Table 9 clearly establish this observation which is crucial to the application of this method to determine n. Just to reiterate this important fact, $\Delta\omega_m$ determined from the t_{CP} study in the slow exchange region is independent of the value of n assumed.

Table 10

Comparison of the observed relaxation rates and the fitted values, with n=6 and n=4 for the 0.1277 molal nickel(II) solution in acetonitrile at 50.4 °C and 60 MHz.

t_{CP}, ms	R_{2obsd}, s^{-1}	$R_{2(calcd)}{}^a$, s^{-1}	
		n=6	n=4
2.00	114	116	116
1.67	113	115	115
1.43	113	115	114
1.25	113	114	114
1.11	112	113	113
1.00	113	112	112
0.833	111	111	111
0.741	109	110	110
0.625	109	108	108
0.556	108	107	107
0.500	106	105	105
0.454	105	104	104
0.417	102	102	102
0.385	102	101	101
0.345	100	98.8	99.0
0.312	97.3	96.6	96.9
0.290	95.4	94.8	95.1
0.267	92.9	92.7	92.9

Table 10(cont'd)

t_{CP}, ms	R_{2obsd}, s^{-1}	$R_{2(calcd)}^{a}$, s^{-1}	
		n=6	n=4
0.250	91.6	90.9	91.1
0.233	88.2	88.7	88.9
0.217	86.2	86.5	86.6
0.204	84.2	84.3	84.4
0.192	81.9	82.2	82.2
0.182	80.8	80.1	80.0
0.172	77.9	78.0	77.9
0.163	75.9	75.3	75.1
0.154	72.9	73.3	73.1
0.147	70.6	71.3	71.2
0.139	68.6	68.8	68.6
0.132	66.0	66.3	66.3
0.122	62.4	63.0	62.9
0.116	61.3	60.9	60.8
0.111	58.6	58.9	58.9
0.105	56.3	56.5	56.6
0.100	54.9	54.3	54.5

(a) Standard errors of the fits based on relative residual minimization are (a) 8.8×10^{-3} for n=6 and (b) 8.0×10^{-3} for n=4 .

Table 11

Comparison of the observed relaxation rates and the fitted values with n=6 and n=4 for the 0.1277 molal nickel(II) solution in acetonitrile at $24.7°C$ and 60 MHz .

t_{CP}, ms	R_{2obsd}, s^{-1}	$R_{2\ calc'd}$, s^{-1} n=6	n=4
2.00	84.0	85.7	87.3
1.00	83.4	84.2	84.9
0.667	83.2	83.0	83.8
0.556	83.2	83.4	82.8
0.500	83.7	82.7	81.0
0.454	82.6	81.1	79.4
0.400	77.9	77.5	76.3
0.364	74.6	73.9	73.2
0.333	69.7	70.1	69.9
0.303	66.6	65.7	65.9
0.278	62.5	61.7	62.1
0.250	56.4	56.8	57.4
0.227	52.3	52.7	53.4
0.200	47.4	47.7	48.3
0.194	46.5	46.7	47.2
0.179	44.1	43.9	44.2
0.167	41.2	41.8	42.0
0.158	36.9	40.2	40.3

Table 11 (cont'd)

t_{CP}, ms	R_{2obsd}, s^{-1}	R_2 cal'd, s^{-1}	
		n=6	n=4
0.149	38.9	38.9	38.9
0.143	37.5	37.8	37.7
0.135	36.2	36.6	36.4
0.125	35.5	35.1	34.7
0.118	35.4	34.0	33.5

(a) Standard errors of the fits based on relative residual minimization are 1.4×10^{-2} for n=6 and 2.4×10^{-2} for n=4 .

In the fast exchange region the long t_{CP} limit gives $P_m \tau_m' \Delta \omega_m^2$ and the t_{CP} dependence of R_{2obsd} gives τ_m^{-1}. Thus, for temperatures $\geq 40^\circ$C at 60 MHz τ_m^{-1} is relatively independent of the assumed n value, but $\Delta \omega_m$ is expected to be larger with n=4 by $\sqrt{6/4}$. The data at 60 MHz show the expected behavior. However at 15 MHz the highest temperature studied is not really in the fast exchange limit.

The interdependence of τ_m^{-1}, $\Delta \omega_m$, and n in the region where R_{2obsd} is a maximum, between the fast and slow exchange regions, is too complex to understand or describe in a simple qualitative way. However this region is very useful as a criterion for establishing the correct n value. A great deal of previous work has shown that $\Delta \omega_m$ should vary as $1/T$ as described by equation (1-8). Thus $\Delta \omega_m$ is expected to decrease slowly as the temperature increases, and by about 20% for the 5° to 50°C range of this study. The results in Table 8 and Table 9 show that $\Delta \omega_m$ undergoes a rather abrupt increase as one proceeds from the slow exchange region to the intermediate exchange region (35-40°C at 60 MHz, > 20°C at 15 MHz) when n=4 is used. However for n=6 no such discontinuity appears and the values of $\Delta \omega_m$ decrease with increasing temperature as expected.

A similar problem occurs with the τ_m^{-1} values.

These should show an exponential increase with increasing temperature as given by equation (1-6). However, in the intermediate exchange region the τ_m^{-1} values remain rather constant when n=4 is chosen, whereas for n=6 the expected smooth change with temperature is observed.

The sensitivity to the value of n has been tested by further analysis of the 60 MHz data using n=5. With n=5 a change of 5 degrees in the intermediate exchange (35-40°C) results in no change in the τ_m^{-1} values, instead of the expected doubling of τ_m^{-1}. Thus the temperature dependence of τ_m^{-1} is anomalous even with n=5. However, the anomalous temperature dependence of $\Delta\omega_m$ could not be deduced with confidence when n=5 is assumed. This is because the intrinsic change in $\Delta\omega_m$ with temperature, according to equation (1-8), is small compared with the magnitude of the uncertainty limits of the $\Delta\omega_m$ value.

In summary two important facts emerge from this analysis. The value of $\Delta\omega_m$ is independent of the initially assumed n value in the slow exchange region. The expected temperature dependencies of τ_m^{-1} and $\Delta\omega_m$ in the intermediate exchange region are only observed if the correct n value has been assumed.

The general validity of the data and analysis presented here can be assessed by comparison of the

τ_m^{-1} values obtained with those of Merbach $et\ al.$[44] from a linewidth study. The values are compared in Table 12, based on n=6 as assumed by Merbach $et\ al.$[49]. The agreement is very good in general for two nmr studies using quite different methods.

Calculations of the solvation number now can be made from the values of $\Delta\omega_m$ at various temperatures together with the parameter K_ω from the chemical shift studies. The value of K_ω = 1.99 x 10^7 radians s^{-1}K, normalized to 60 MHz, but obtained from the 90 MHz chemical shift measurements, was used. With the 15 MHz $\Delta\omega_m$ values the value of K_ω was 15/60 of 1.99 x 10^7 radians s^{-1}K. The calculated solvation numbers are given in Table 13 and Table 14. The average values of the solvation number calculated from the 60 MHz and the 15 MHz results are 5.9$_6$ ± 0.3$_6$ and 5.8$_5$ ± 0.3$_4$ respectively. The two average values agree well within the error limits. The solvation number of six for the nickel(II)-acetonitrile system is thus concluded. This is in agreement with the conclusion made by Merbach $et\ al.$[49] from a comparison of the bound and free solvent shifts , and the conclusion from the study of electronic spectra by Wickenden and Krause[35], but differs from the conclusion of Campbell $et\ al.$[4].

Table 12

Comparison of the τ_m^{-1} values from the $R_{2obsd}-t_{CP}$ least-squares analysis and those obtained from the linewidth measurements (Merbach *et al.*[49]) for the nickel(II)-acetonitrile system at 60 MHz .

	$10^{-3}\,\tau_m^{-1}$, s^{-1}	
$^\circ$C (Sample) [a]	This work	Merbach's [b]
50.4(B)	23.5±3.0	23.8
40.2(B)	11.2±1.2	10.6
40.0(A)	11.6±1.7	10.4
39.0(B)	12.0±1.3	9.58
35.4(C)	5.03±0.18	7.08
35.0(B)	5.16±0.26	6.84
30.2(C)	3.90±0.26	4.52
29.8(C)	3.72±0.06	4.36
29.8(B)	3.93±0.29	4.36
25.1(C)	2.71±0.07	2.87
24.7(B)	2.61±0.10	2.77
19.6(B)	1.66±0.08	1.72
16.4(B)	1.22±0.06	1.27
4.9(E)	0.385±0.018	0.403

Table 12(cont'd)

(a)   Sample labels given in brackets correspond to nickel

(II) molality of 0.2903(A), 0.1277(B), 0.06593(C),

and 0.0243(E) respectively.

(b)   Merbach and coworkers' values are calculated from

equation (1-6) with $\Delta H^{\ddagger} = 1.544 \times 10^4$ cal mol^{-1} and

$\Delta S^{\ddagger} = 9.056$ cal mol^{-1}K^{-1} .

Table 13

Calculations of the solvation number of the nickel(II) ion in acetonitrile from the 60 MHz R_{2obsd}-t_{CP} analysis.

$^{\circ}$C (Sample)[a]	$10^{-4}\Delta\omega_m$, rad s^{-1}	n_{calcd}[b]
50.4(B)	0.992	6.2_0
40.2(B)	1.00	6.3_5
40.0(A)	1.03	6.1_7
39.0(B)	1.00	6.3_7
35.4(C)	1.20	5.3_8
35.0(B)	1.19	5.4_3
30.2(C)	1.16	5.6_6
29.8(C)	1.22	5.3_8
29.8(B)	1.13	5.8_1
25.1(C)	1.16	5.7_5
24.7(B)	1.12	5.9_7
19.6(B)	1.12	6.0_7
16.4(B)	1.22	6.1_4
4.9(E)	1.24	5.7_7

Table 13(cont'd)

(a) Sample labels given in brackets correspond to nickel
(II) concentrations of 0.2903(A), 0.06593(B), and
0.02431(E) molal respectively .

(b) Calculated from $K\omega = 1.99 \times 10^7$ radians s^{-1} from the
chemical shift studies and $\Delta\omega_m$ at the temperatures
given .

Table 14

Calculations of the solvation number of the nickel(II) ion in acetonitrile from the 15 MHz R_{2obsd} analysis.

$^{\circ}C$	Sample [a]	$10^{-3}\Delta\omega_m$ radians s^{-1}	n_{calcd} [b]
30.2	C	2.59	6.3_3
30.1	B	2.82	5.8_2
25.0	B	2.95	5.6_6
25.0	C	2.70	6.1_8
21.0	C	2.84	5.9_5
20.7	B	2.95	5.7_4
15.4	C	3.12	5.5_3
10.3	C	3.27	5.3_7

(a) The nickel(II) concentrations are 0.1277 and 0.06593 molal for samples B and C respectively.

(b) Calculated from $K_{\omega}=4.97_5 \times 10^6$ radians s^{-1} from the chemical shift studies and $\Delta\omega_m$ at the temperatures given.

D Multiple Temperature Least-Squares Analysis of R_{2obsd} - t_{CP} Data

The determination of the solvation number de-
scribed in the previous section is based on the least-
squares analysis of the R_{2obsd} - t_{CP} data carried out
at individual temperatures. Such an analysis does not
place any restrictions on the temperature dependence of
τ_m^{-1}, $\Delta\omega_m$, and R_{2m}. In this section the temperature
dependencies of τ_m^{-1}, $\Delta\omega_m$, and R_{2m} according to equations
(1-6), (1-8), and (1-21) are used in the analysis of the
R_{2obsd} - t_{CP} data at various temperatures. The main
purpose of this analysis is to determine if the restrict-
ions placed on the temperature dependence of the para-
meters give a better determination of C_ω from which the
solvation number can be calculated.

The procedure for the least-squares analysis
of the multiple temperature R_{2obsd} - t_{CP} data is slightly
modified from that described in the individual temperature
analysis. Now the ratio [m]/[s] is treated as an
independent variable in addition to t_{CP} and temperature.
The value of n is allowed to vary so that other para-
meters obtained from the fit are free from the influence
of an assumed n value. The parameters which are in-
herently independent of n, namely, $\Delta H^{\ddagger}$, E_{2m}, and E_{2o} are
kept constant in the analysis. The fitting parameters

generally are C_ω, $\Delta S^\ddagger$, C_{2m}, C_{2o}, and n. Deviations from this general procedure will be discussed for each set of data.

The 60 MHz data were analysed to determine if $\Delta H^\ddagger$ from the analysis agrees with the value reported[49]. The analysis was carried out using the R_{2m} and R_{2o} values described by equations (3-7) and (3-8) respectively; the n value of six was assumed. The initial values of $\Delta H^\ddagger$ and $\Delta S^\ddagger$ and C_ω were taken from the individual analyses, and from the chemical shift studies respectively. The $\Delta H^\ddagger$ obtained, $(15.8 \pm 0.4) \times 10^3$ cal mol^{-1} (Fit I of Table 15), agrees within the 95% confidence limits with the value of 15.4_4 Kcal mol^{-1} obtained by Merbach *et al.*[49]. Thus $\Delta H^\ddagger$ was held fixed at $15.4_4 \times 10^3$ cal mol^{-1} in subsequent analyses, and the temperature dependence of the outer-sphere (E_{2o}) and the inner-sphere (E_{2m}) contributions given by equations (3-7) and (3-8) were also held fixed. Since the R_{2m} values given by equation (3-7) were obtained independently the C_{2m} was held constant, while the outer-sphere coefficient (C_{2o}) was allowed to vary in the least-squares analysis. The results of the analysis are given in Table 15.

At 15 MHz the temperature dependence of the outer-sphere contribution was given by equation (3-9).

Table 15

Results of the least-squares analysis of the multiple temperature $R_{2obsd}-t_{CP}$ data[a]
of the nickel(II) solutions in acetonitrile at 60 MHz.

Fit[b]	$10^{-3}C_\omega$ radians s^{-1} K	$10^{-3}\Delta H^\ddagger$ calmol^{-1}	$\Delta S^\ddagger$ calmol^{-1}K^{-1}	$10^{-4}C_{2m}$ s^{-1}	$10^{-2}E_{2m}$ calmol^{-1}	$10^{-3}C_{2o}$ s^{-1}	$10^{-3}E_{2o}$ calmol^{-1}	n	$10^2 x$ S.E.[e]
I	3.16±0.04	15.8±0.4	10.3±1.3	8.53±0.78	3.78	8.22[d]	1.44	6	4.70
II	3.41±0.09	15.4_4	9.18±0.07	8.50[c]	3.78	8.24±0.74	1.44	5.38±0.22	4.03
III	3.19±0.03	15.4_4	9.05±0.04	8.50[c]	3.78	7.17±0.48	1.44	6	4.53
IV	4.08±0.06	15.4_4	9.08±0.13	8.50[c]	3.78	12.06±2.31	1.44	4	7.13

(a) The data consist of 422 points from five samples in the temperature range of
50 to 4.9 °C. The full fit of the data is given in Appendix A.

(b) If error limits are not given, parameters were held constant at the values
given.

(c) $C_{2m}=8.50 \times 10^4$ s^{-1} was used instead of the value indicated in equation (3-7)
because Fit I indicated that a smaller value of C_{2m} is preferrable.

Table 15(cont'd)

(d) This value is based on the assumed solvation number of 6.

(c) Standard errors of the fits are based on relative residual minimization.

The R_{2m} values from the individual temperature analysis (Table 9) were fitted to equation (1-21) to give

$$R_{2m} = \left(\frac{1.28 \times 10^8}{nT}\right) \exp\left(\frac{-2.82 \times 10^3}{RT}\right) \qquad (3\text{-}10)$$

Since the R_{2m} values in equation (3-10) are based on the R_{2o} values described in equation (3-9) which are based on $\Delta H^{\ddagger} = 15.4_4 \times 10^3$ cal mol^{-1} and the assumed temperature dependence ($E_{2o} = 1.84 \times 10^3$ cal mol^{-1}), C_{2m} and C_{2o} were fixed in the analysis. The results of the analysis are given in Table 16.

With these constraints on the temperature dependencies it is possible in principle to determine n as a least-squares fitting parameter of the data. This would provide a method independent of the K_ω value from the shift measurements. To assess this possibility best-fit values of n were determined at 60 MHz and 15 MHz. The sensitivity of the fitting to n was investigated by assuming fixed values of 6 or 4 and examining the quality of the fits.

When n is treated as a fitting parameter (Fit II of Table 15 and Fit I of Table 16) the best-fit values are 5.38 ± 0.22 and 5.88 ± 0.11 at 60 MHz and 15 MHz respectively. These values do not agree within the 95% confidence limits. The discussion below indicates that the overall fit is not very sensitive to the n value

111

Table 16

Results of the least-squares analysis of the multiple temperature R_{2obsd}-t_{CP} data[a] of the nickel(II) solutions in acetonitrile at 15 MHz.

Fit[b]	$10^{-5}C_\omega$ radians s⁻¹K	$10^{-4}\Delta H^\ddagger$ calmol⁻¹	$\Delta S^\ddagger$ calmol⁻¹K⁻¹	$10^{-7}C_{2m}$[c] s⁻¹	$10^{-3}E_{2m}$ calmol⁻¹	$10^{-3}C_{2o}$[c] s⁻¹	$10^{-3}E_{2o}$ calmol⁻¹	n[c]	$10^2 \times$ S.E.[d]
I	8.25±0.22	1.54$_4$	9.25±0.09	2.10	-2.82	3.51	1.84	5.88±0.11	3.36
II	8.08±0.12	1.54$_4$	9.17±0.05	2.10	-2.82	3.51	1.84	6	3.42
III	10.9 ±0.3	1.54$_4$	9.72±0.10	3.15	-2.82	5.27	1.84	4	7.67

(a) The data consist of 325 points from two samples in the temperature range of 30° to 10°C. The full fit of data is given in Appendix A.

(b) If error limits are not given, parameters were held constant at the values given.

(c) The values of C_{2m}=2.10 x 10^7 and C_{2o}=3.15 x 10^3 s⁻¹ are based on n=6 and the values of C_{2m}=3.15 x 10^7 and C_{2o}=5.27 x 10^3 s⁻¹ are based on n=4.

(d) Standard errors of the fits are based on relative residual minimization.

because of compensations in C_ω, $\Delta S^\ddagger$, and C_{2o}. It seems that the best-fit n values are not a very reliable measure of the true n value.

The results of the analysis with assumed n values of 6 and 4 are given in Fits III and IV of Table 15 (60 MHz), and Fits II and III of Table 16 (15 MHz). The standard error of the fits is about 2 times smaller with n=6 than n=4 at both frequencies. A comparison of the difference between experimental and calculated (least-squares) R_{2obsd} values (Appendix A) indicates that the differences are about 10% or less in both cases. Although the differences with n=6 are generally smaller than with n=4 the fit with the latter value is not so bad as to allow it to be excluded. Thus one cannot determine decisively the solvation number on the basis of the fit alone.

The solvation number still can be calculated from the parameter C_ω and the K_ω of 1.99 x 10^7 radians s^{-1}K at 60 MHz determined from the chemical shift studies. The calculated solvation numbers, and the 95% confidence limits, are: 6.2 ± 0.2 (n=6) and 4.9 ± 0.2 (n=4) at 60 MHz, and 6.2 ± 0.2 (n=6) and 4.6 ± 0.2 (n=4) at 15 MHz. It is clear that the calculated solvation number differs from the assumed n value when the incorrect n value is chosen, and the calculated value agrees with the assumed

n value when the correct n value is chosen. Thus the consistency of the calculated and the assumed n value helps to establish the correct choice of the solvation number.

The inconsistency of the calculated solvation number and the assumed n value when an incorrect n value is chosen can be explained qualitatively. When n is held constant at an incorrect value, e.g., smaller than the correct value, the least-squares analysis is forced to select larger $\Delta\omega_m$ values, i.e. larger C_ω, so that the data in the long t_{CP} limits at various temperatures are well fitted in the fast exchange region. In the slow exchange region, where $\Delta\omega_m$ is independent of n, the least-squares fit selects C_ω close to the correct value. Thus the fitted parameter C_ω is the weighted average of $\Delta\omega_m$ values in the fast and the slow exchange region, i.e. the fitted C_ω value is between the incorrect and the correct one. Consequently the value of the calculated solvation number is between the assumed n value and the correct one.

Calculations of the solvation number now can be made from K_ω and C_ω free from any assumption on n. From $K_\omega = (1.99 \pm 0.05) \times 10^7$ radians $s^{-1}K$ at 60 MHz from the shift studies and $C_\omega = (3.41 \pm 0.09) \times 10^7$ radians $s^{-1}K$ at 60 MHz (Fit II of Table 15) one calculates the

solvation number of 5.82 ± 0.29. The 15 MHz equivalent of the K_ω given above and $C_\omega = (8.25 \pm 0.22) \times 10^5$ radians $s^{-1} K$ (Fit I of Table 16) yield the solvation number of 6.03 ± 0.30. The two solvation numbers calculated agree well within the 95% confidence limits.

III   Determination of the Solvation Number of NipyDPT^{2+}

    in Acetonitrile

       In the previous section a method for the de-
termination of the solvation number using the pulsed nmr
method was demonstrated for $\dot{N}i(NCCH_3)_6^{2+}$. It is of
interest to determine if the same method and analysis
procedures can be applied to a system with a smaller
solvation number. For this purpose the NipyDPT^{2+}-
acetonitrile system has been chosen for study.

       The general experimental procedures to obtain
the R_{2obsd} - t_{CP} data are the same as those employed in
the previous study. The experimental results and dis-
cussion are presented in the order: the chemical shift
studies, the relaxation rate measurements and analysis
at individual temperatures, and the multiple temperature
analysis of the R_{2obsd} - t_{CP} data.

A   Chemical Shift Measurements

       The chemical shifts were measured at 100 MHz on
a Varian HA-100 spectrometer. At lower frequencies the
observed chemical shifts are too small because of low
solubility of NipyDPT$(PF_6)_2$ in acetonitrile. The
chemical shifts of both solvent and the NipyDPT^{2+} solu-
tions in acetonitrile were measured relative to that of

the methoxy protons of 1,4-dimethoxybenzene in solutions

containing about 6-8%(w/w) of the internal standard.

The NipyDPT^{2+} complex always caused upfield shifts

of the solvent resonance. The direct dependency of

$\Delta\omega_{obsd}$ on nickel(II) molality, predicted by equation

(3-6), is confirmed by the linearity of the plot of

$\Delta\omega_{obsd}$ *versus* nickel(II) molality shown in Figure 9.

This linearity also shows the reliability of sample

preparation.

The chemical shifts were measured from +40° to

-40° C to cover the fast and the slow exchange regions.

Since samples with different nickel(II) molality were

used, the observed chemical shift values were normalized

by dividing by nickel(II) molality. The average values

of $\Delta\omega_{obsd}/[m]$ were plotted against 1/T as shown in

Figure 10. The values of $\Delta\omega_{obsd}/[m]$ increase gradually

with decreasing temperature to about -17° C

(1/T = 3.9 x 10^{-3}K^{-1}) then decrease rapidly with de-

creasing temperature as expected from equation (3-6)

when the system approaches the slow exchange region.

To obtain the constant K_{ω}, the least-squares

analysis of the $\Delta\omega_{obsd}$ - 1/T data was carried out using

the procedure described for the nickel(II)-acetonitrile

system. The analysis was done with $\Delta H^{\ddagger}$ = 11.67 x 10^3

cal mol^{-1}, the value obtained from the study of Jordan
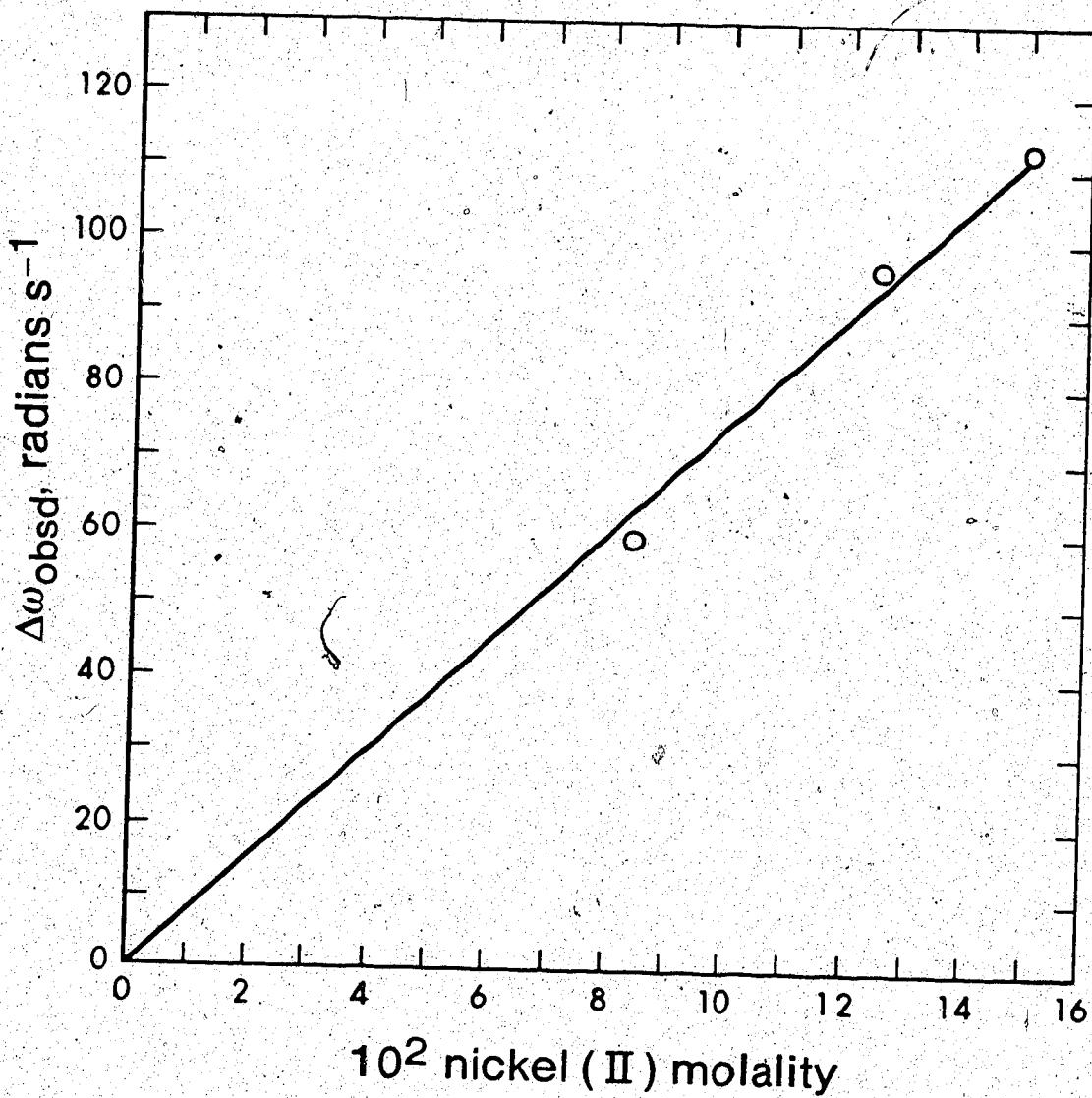
Figure 9 Plot of $\Delta\omega_{obsd}$ *versus* nickel(II) molality for the NipyDPT^{2+} solutions in acetonitrile at 0°C and 100 MHz.
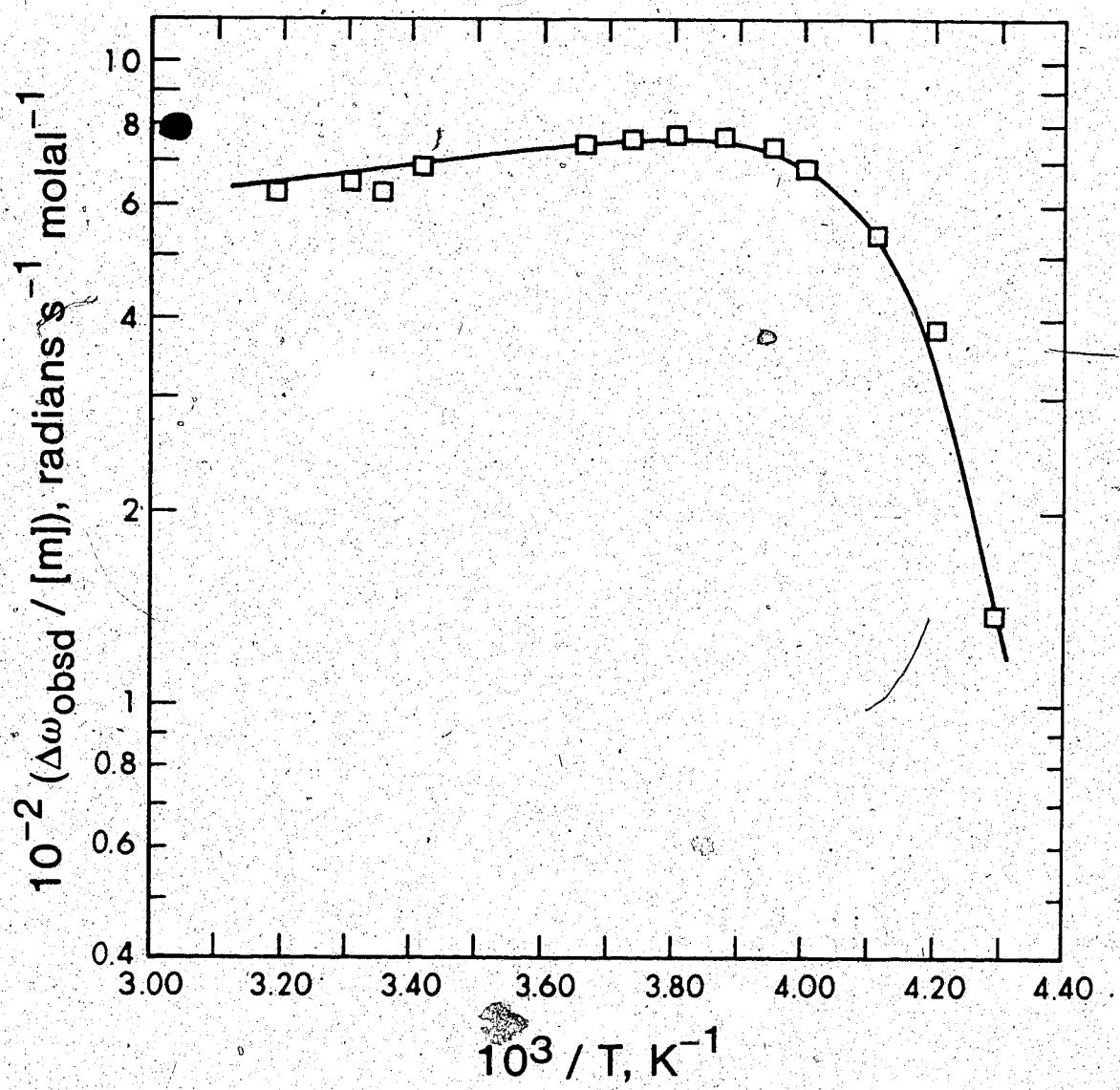
Figure 10 Plot of $\Delta\omega_{obsd}/[m]$ *versus* $1/T$ for for the $NipyDPT^{2+}$ solutions in acetonitrile at 100 MHz.

et al.[51]. The inner-sphere contribution given in reference 51 was fixed in the analysis and an n value of one was assumed while K_ω and $\Delta S^{\ddagger}$ were treated as fitting parameters. The results of various two-parameter fits are given in Table 17. The adequacy of the fit is shown in Table 18 where the experimental and calculated values of $\Delta\omega_{obsd}$ differ generally by less than about 10 radians s^{-1} (<1.5 Hz). This agreement is considered to be satisfactory since the $\Delta\omega_{obsd}$ measurement has an uncertainty of about ± 6 radians s^{-1} (1Hz).

From Table 17 K_ω values from various fits agree reasonably well within the 95% confidence limits. The K_ω value of 3.00 x 10^6 radians $s^{-1}K$ from Fit IV is selected for future calculations since Fit IV is based on all of the data.

Table 17

Least-squares best fits[a] of the $\Delta\omega_{obsd}$-1/T data for the NipyDPT^{2+} solutions in acetonitrile at 100 MHz.

Fit	Nickel(II) molality	$\Delta S^{\ddagger}$ cal mol^{-1}K^{-1}	$10^{-6}K_{\omega}$[c] radians s^{-1}K	S.E.[d]
I	0.08302	11.0±0.2	2.85±0.07	1.3
II	0.1249	10.3±0.3	3.07±0.15	4.4
III	0.1496	10.3±0.2	3.00±0.11	3.7
IV	Combined data [b]	10.4±0.2	3.00±0.09	4.4

(a) $\Delta H^{\ddagger}$, C_{2m}, and E_{2m} were held fixed at 1.167×10^4 cal mol^{-1}, 1.25×10^4 s^{-1}, and 1.68×10^3 cal mol^{-1} respectively.

(b) Data of the three samples were fitted together.

(c) The K_{ω} values given have been normalized to 60 MHz by multiplying by 60/100.

(d) Standard errors of fits are based on absolute residual minimization.

Table 18

Comparison of the experimental and calculated values of $\Delta\omega_{obsd}$ at various temperatures for the NipyDPT^{2+} solutions in acetonitrile at 100 MHz.

Nickel(II) molality	Temp °C	$\Delta\omega_{obsd}$, radians s^{-1} Experimental	Calculated[a]
0.0832	25	52.2	57.1
	0	59.1	62.0
	-5	61.3	62.9
	-10	61.6	63.5
	-15	62.2	63.5
	-20	59.7	61.7
	-25	57.2	56.4
	-30	49.0	44.8
	-35	37.7	27.9
	-40	20.7	12.9
0.1249	40	79.8	81.8
	30	81.0	84.5
	20	87.3	87.3
	0	96.1	93.3
	-5	98.3	94.6
	-10	99.9	95.5
	-15	97.4	95.3
	-20	96.8	92.8

Table 18(cont'd)

Nickel(II) molality	Temp °C	$\Delta\omega_{obsd}$, radians s^{-1}	
		Experimental	Calculated[a]
0.1249	-25	88.0	84.8
	-30	66.6	67.4
	-35	41.5	42.0
	-40	6.9	19.4
0.1496	40	93.6	98.0
	20	102	105
	0	112	112
	-5	114	113
	-10	117	114
	-15	116	114
	-20	108	111
	-25	98.6	102
	-30	77.3	80.8
	-35	54.7	50.3
	-40	16.3	23.3

(a) Calculated values of $\Delta\omega_{obsd}$ are from Fit I, II, and III of Table 17.

B Relaxation Rate Measurements and Data Analysis

The R_{1obsd} was measured as a function of nickel(II) molality at $25\,^{\circ}C$ and 54.7 MHz and was found to be a linear function of nickel(II) molality. This confirms the direct dependence of the relaxation rate on nickel(II) concentration predicted by equation (1-5) and suggests the reliability of the sample preparation.

The R_{2obsd} of the $NipyDPT^{2+}$-acetonitrile system was measured as a function of t_{CP} at 60 MHz from $-32.3\,^{\circ}C$ to $-46.8\,^{\circ}C$. This temperature range covers the slow exchange region and the intermediate exchange region, where R_{2obsd} is a maximum. Measurements above $-32.3\,^{\circ}C$, in the fast exchange region, were not attempted because it was found in the nickel(II)-acetonitrile system that the solvation number could be determined best from results in the slow and the intermediate exchange regions. Measurements at temperatures lower than $-46.8\,^{\circ}C$ could not be carried out because the solution solidified.

Selected R_{2obsd} values are plotted against $1/t_{CP}$ in Figure 11. The full results are given in Appendix B. From Figure 11 it can be seen that the R_{2obsd} variation with temperature in the long t_{CP} limit agrees with that found by Jordan et al.[51]. In the long t_{CP} limit, R_{2obsd} increases slightly with decreasing tempera-
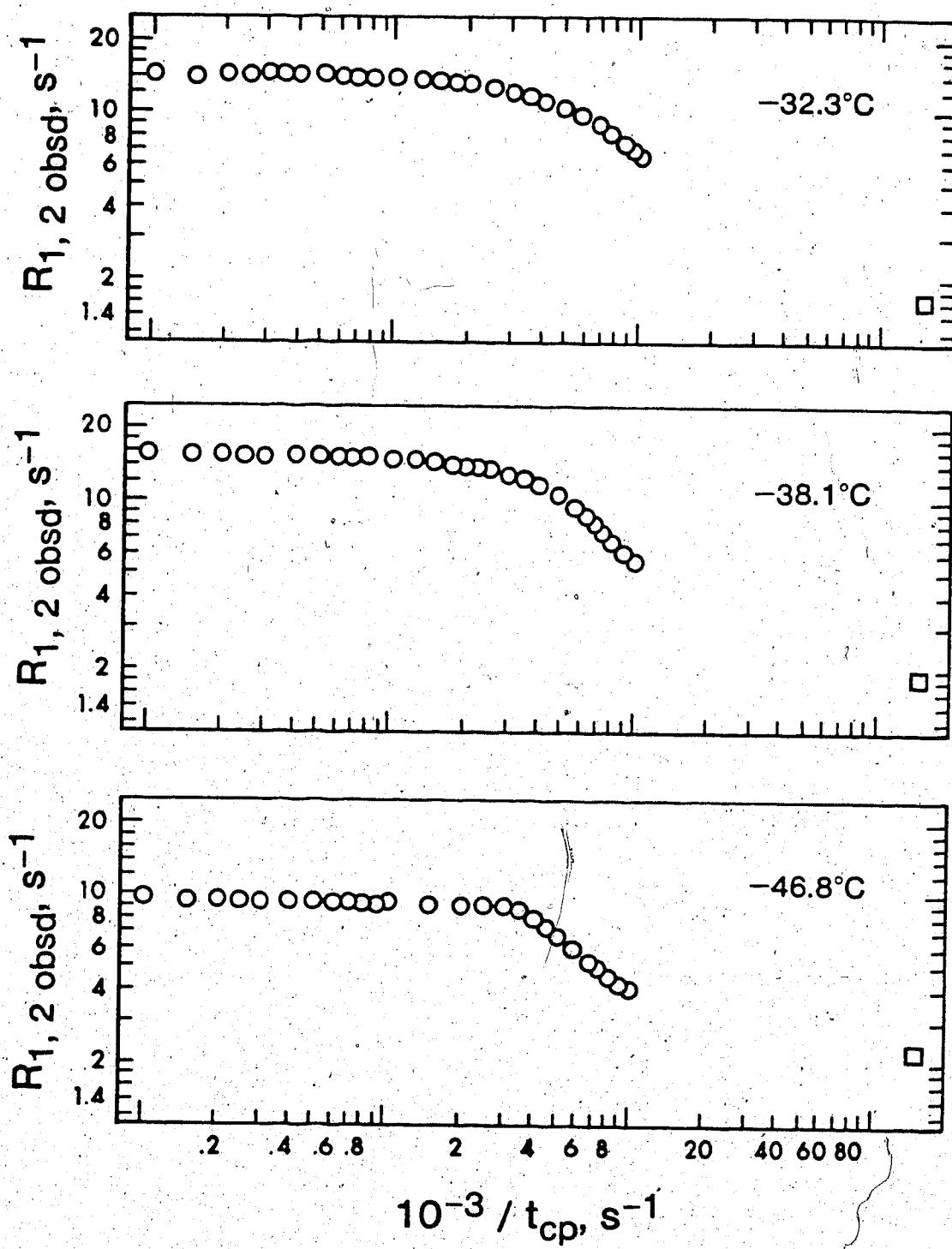
Figure 11   Plots of R_{2obsd} *versus* $1/t_{CP}$ (O) for the 0.04936 molal NipyDPT^{2+} solution in acetonitrile from selected data and temperatures at 60 MHz. R_{1obsd} is shown as □.

ture from $-32.3°$ to $-38.1°C$ then decreases with decreasing temperature. The magnitude of R_{2obsd} agrees within 10% with that found by Jordan $et\ al.$[51].

It is apparent (Figure 11) that the long t_{CP} limit and the intermediate t_{CP} region are well defined at each temperature but the short t_{CP} limit is absent at all temperatures due to the instrumental limitation. Lowering the magnetic field to a 10 MHz proton resonance frequency did not help to make the short t_{CP} limit accessible. However the R_{2obsd} measurements at 10 MHz provide another set of data for the determination of the solvation number.

It should be mentioned here that lowering the resonance frequency from 60 MHz to 10 MHz shifts the intermediate exchange region, where R_{2obsd} is a maximum, from $-38°C$ (at 60 MHz) to a lower temperature. This is expected because R_{2obsd} is a maximum when

$$P_m \tau_m \Delta\omega_m^2 = P_m \tau_m^{-1} \qquad (3-11).$$

If $\Delta\omega_m$ is decreased 6 times by the change in frequency then τ_m^{-1} must decrease similarly to satisfy this condition. A consideration of the temperature dependencies of $\Delta\omega_m$ and τ_m^{-1} shows that the maximum temperature (T_{m2}) at a new frequency (ν_2) can be estimated from that

(T_{m1}) at another frequency (ν_1) by an iterative solution of the equation

$$(1/T_{m2}) = (1/T_{m1}) + (R/\Delta H^{\ddagger})[\ln(\nu_1/\nu_2) + \ln(T_{m2}/T_{m1})]$$

$$(3-12)$$

In the present case R_{2obsd} is expected to be a maximum at $-53°C$ at 10 MHz. Since the solution solidified at $-47°C$ the 10 MHz data must all be in the fast exchange region which was found to be poor for the determination of the solvation number in the nickel(II)-acetonitrile system. For this reason measurements of R_{2obsd} at 10 MHz were carried out at two selected temperatures only.

The least-squares analysis of the $R_{2obsd} - t_{CP}$ data was carried out using the procedure described in the study of the nickel(II)-acetonitrile system. The goals of the analysis are to determine $\Delta\omega_m$ and to determine if the criteria for selecting the correct solvation number established in the study of the nickel(II)-acetonitrile system also apply for NipyDPT^{2+} in acetonitrile.

The analysis at 60 MHz was carried out using the inner-sphere and outer-sphere contributions given by Jordan et al.[51]. In their treatment of the data the R_{1obsd} values were first fitted to equation (1-5) to give

$$R_{1m} = \left(\frac{3.42 \times 10^3}{nT}\right) \exp\left(\frac{1.68 \times 10^3}{RT}\right) \qquad (3\text{-}13).$$

Then the assumption $E_{1m} = E_{2m} = E_{1o} = E_{2o}$ was made. With this assumption and the values of the parameters contained in the pre-exponential terms in equations (1-21) and (1-27) the ratio $(C_{2o}/C_{2m}) = 0.688$ was calculated for the NipyDPT^{2+} complex in acetonitrile[51], and finally the R_{2m} and R_{2o} from the least-squares analysis were given by

$$R_{2m} = \left(\frac{5.07 \times 10^3}{nT}\right) \exp\left(\frac{1.68 \times 10^3}{RT}\right) \qquad (3\text{-}14)$$

$$R_{2o} = \left(\frac{3.49 \times 10^3}{nT}\right) \exp\left(\frac{1.68 \times 10^3}{RT}\right) \qquad (3\text{-}15)$$

The initial values of the fitting parameter τ_m^{-1} and $\Delta\omega_m$ were obtained using the procedure described in Section II. Two-parameter (τ_m^{-1} and $\Delta\omega_m$) and three-parameter (τ_m^{-1}, R_{2m}, and $\Delta\omega_m$) fits were carried out and the results are given in Table 19 and Table 20. Further discussion will be given after the analysis of the 10 MHz data is described.

At 10 MHz the inner-sphere and outer-sphere contributions needed for the least-squares analysis were obtained using the procedure described for the 60 MHz analysis. First, R_{1obsd} at various temperatures in the fast exchange region was fitted to the equation

Table 19

Effect of the change in R_{2m} value[a] on τ_m^{-1} and $\Delta\omega_m$ from the R_{2obsd}-t_{CP} least-squares analysis for the NipyDPT^{2+} solution in acetonitrile at 60 MHz.

°C	$10^{-2}R_{2m}$, s^{-1}	$10^{-3}\tau_m^{-1}$, s^{-1}	$10^{-4}\Delta\omega_m$, radians s^{-1}
-32.3	9.22(2.64[b])	18.4(22.6)	1.36(1.45)
-38.1	4.92(3.04[b])	11.9(13.6)	1.47(1.45)
-42.2	6.33(3.66[b])	6.81(6.54)	1.53(1.62)
-46.8	6.97(3.99[b])	4.42(4.30)	1.58(1.69)

(a) The illustration is made by comparing the three-parameter and the two parameter least-squares fits of the R_{2obsd}-t_{CP} data using the assumed n value of 1. The results of the two-parameter fit are given in brackets.

(b) The R_{2m} values of the two-parameter fit are fixed at the values given in brackets.

Table 20

Comparison of the $R_{2obsd}-t_{CP}$ least-squares best fits with n=1 and n=2 for the 0.04936 molal NipyDPT^{2+} solution in acetonitrile at 60 MHz.

°C	$10^{-2}R_{2m}$, s^{-1}		$10^{-3}\tau_m^{-1}$, s^{-1}		$10^{-4}\Delta\omega_m$, radians s^{-1}		10^2S.E. [a]	
	n=1	n=2	n=1	n=2	n=1	n=2	n=1	n=2
-32.3	9.22±7.74	1.02±4.32	18.4±4.9	26.5±5	1.?5±0.08	1.00±0.13	1.16	1.12
-38.1	4.92±1.75	-2.49±5.61	11.9±1.9	22.9±2.	1.47±0.05	1.03±0.15	1.10	2.35
-42.2	6.33±1.36	5.26±1.21	6.81±0.26	2.85±0.06	1.53±0.06	1.52±0.08	1.26	1.91
-46.8	6.97±0.92	4.31±0.52	4.42±0.07	2.04±0.02	1.58±0.04	1.57±0.04	0.90	0.95

(a). Standard errors of the fits are based on relative residual minimization.

$$R_{1obsd} = P_m R_{1m} + P_m R_{1o} + R_{1solv} \qquad (3-16)$$

to obtain R_{1m} and R_{1o} described by equations (1-21) and (1-27) under the assumption $E_{1m} = E_{1o}$ and $(C_{2o}/C_{2m}) = 0.688$. Then, using R_{1m} and R_{1o} as the lower limits, R_{2m} and R_{2o} are given by

$$R_{2m} \geq R_{1m} = \left(\frac{4.81 \times 10^3}{nT}\right) \exp\left(\frac{4.56 \times 10^3}{RT}\right) \qquad (3-17)$$

and

$$R_{2o} \geq R_{1o} = \left(\frac{3.3 \times 10^3}{nT}\right) \exp\left(\frac{4.56 \times 10^3}{RT}\right). \qquad (3-18).$$

Both the inner-sphere and outer-sphere contributions were fixed to values given by equations (3-17) and (3-18) in the analysis. The n value of 1 as concluded from the 60 MHz analysis was used. The results of the two-parameter (τ_m^{-1} and $\Delta\omega_m$) fit are given in Table 21.

The influence of R_{2m} on the fitting parameters τ_m^{-1} and $\Delta\omega_m$ is examined in Table 19. The results are compared for three-parameter fits (R_{2m}, τ_m^{-1}, and $\Delta\omega_m$) and two-parameter fits (R_{2m} held fixed at the value given, τ_m^{-1} and $\Delta\omega_m$ are fitting parameters). A change in R_{2m} by a factor of two changes $\Delta\omega_m$ by only about 7% and τ_m^{-1} by even less. This indicates that the inner-sphere contribution does not have significant influence on τ_m^{-1} and $\Delta\omega_m$ consistent with the observation on the nickel(II)-acetonitrile system.

Table 21

Least-squares best fits of the R_{2obsd}-t_{CP} data for the 0.04936 molal NipyDPT^{2+} solution in acetonitrile at 10 MHz.

°C	R_{2m}^a s^{-1}	$10^{-4}\tau_m^{-1}$ s^{-1}	$10^{-3}\Delta\omega_m$ radians s^{-1}	10^2S.E.^{b}
-27.1	49.7	2.07±0.23	2.07±0.08	3.6
-32.8	52.0	1.39±0.20	2.21±0.11	6.1

(a) R_{2m} was held constant at the value given.

(b) Standard errors of the fits are based on relative residual minimization.

The question raised in the study of the nickel(II)-acetonitrile system about the effect of the initially assumed n value on τ_m^{-1} and $\Delta\omega_m$ finds the same answer with the $NipyDPT^{2+}$-acetonitrile system. The quality of the fit is not significantly affected, but anomalies appear in the temperature dependencies of τ_m^{-1} and $\Delta\omega_m$ when an incorrect initial assumption of n is made.

First of all the quality of the fits with n=1 and n=2 can be assessed from the results in Table 20. The uncertainty limits of the parameters and the standard error of the fit are larger for n=2 than for n=1. However the experimental and the calculated values of R_{2obsd} with n=1 and n=2 agree quite well (Table 20); the two values at $-38.1°$ C, where the standard errors of the fits are most different, are compared in Table 22. Thus the uncertainty limits of the parameters and the standard errors of the fits do not provide criteria for selection of the solvation number.

When n=2 is assumed anomalies in the temperature dependencies of τ_m^{-1} and $\Delta\omega_m$ are observed in the intermediate exchange region. Between $-38.1°$ and $-32.3°$ C, τ_m^{-1} remains essentially constant instead of approximately doubling as expected from the $\Delta H^{\ddagger}$ value. The abrupt change in $\Delta\omega_m$ between $-42.2°$ and $-38.1°$ is also anomalous. However with n=1 the normal temperature

Table 22

Comparison of the experimental and calculated values of R_{2obsd} with n=1 and n=2 for the 0.04936 molal NipyDPT^{2+} solution in acetonitrile at -38.1°C and 60 MHz.

t_{CP}, ms	R_{2obsd}, s^{-1}	$R_{2(calcd)}$[a], s^{-1}	
		n=1	n=2
10.0	15.5	16.4	16.0
6.67	15.4	15.6	16.0
5.00	15.5	15.6	15.9
3.33	15.4	15.5	15.8
2.50	15.5	15.4	15.7
2.00	15.2	15.3	15.5
1.67	15.2	15.2	15.4
1.43	15.0	15.1	15.3
1.25	15.3	15.0	15.2
1.00	14.8	14.8	15.0
0.800	15.0	14.6	14.7
0.667	14.6	14.4	14.4
0.571	14.0	14.1	14.1
0.500	13.9	13.9	13.8
0.444	13.7	13.7	13.5
0.400	13.7	13.5	13.2
0.364	13.3	13.3	12.9

Table 22(cont'd)

t_{CP}, ms	R_{2obsd}, s^{-1}	$R_{2(calcd)}$ [a], s^{-1}	
		n=1	n=2
0.333	12.9	13.0	12.6
0.308	12.6	12.7	12.3
0.286	12.5	12.4	12.0
0.267	12.1	12.1	11.7
0.250	11.7	11.8	11.4
0.227	11.2	11.2	11.0
0.208	10.6	10.6	10.5
0.192	10.0	10.1	10.0
0.178	9.50	9.53	9.53
0.161	8.76	8.77	8.86
0.149	8.06	8.19	8.32
0.135	7.39	7.46	7.61
0.125	6.86	6.92	7.06
0.117	6.48	6.52	6.62
0.111	6.16	6.16	6.22
0.106	6.02	5.91	5.91
0.100	5.65	5.56	5.49

(a)   Standard errors of the fits based on relative
residual minimization are (a) 1.10×10^{-2} for n=1
and (b) 2.35×10^{-2} for n=2.

dependencies of τ_m^{-1} and $\Delta\omega_m$, predicted by equations (1-6) and (1-8), are observed.

For the purpose of calculating the solvation number it is important that $\Delta\omega_m$ can be determined independent of the assumed n value. The results in Table 20 show that this is the case in the slow exchange region ($-42.2°$ and $-46.8°$ C).

Two important observations from this analysis agree with those from the nickel(II)-acetonitrile system. The value of $\Delta\omega_m$ is independent of the initially assumed n value in the slow exchange region. The expected temperature dependencies of τ_m^{-1} and $\Delta\omega_m$ in the intermediate exchange region are observed only when the correct n value has been assumed in the analysis.

The solvation number now can be calculated from $K_\omega = 3.00 \times 10^6$ radians s^{-1}K at 60 MHz from the chemical shift studies and $\Delta\omega_m$ at various temperatures from the analysis of the $R_{2obsd} - t_{CP}$ data with n=1. The calculated values of the solvation number are given in Table 23 for both the 60 MHz and the 10 MHz data. The average solvation number with one standard error calculated from the 60 MHz data is 0.87 ± 0.04 and the average solvation number calculated from the 10 MHz data is 0.96 ± 0.02.

Table 23

Calculations of the solvation number of the NipyDPT^{2+}-acetonitrile system from the 60 MHz and 10 MHz data.

°C	$10^{-4}\Delta\omega_m$ radians s^{-1}	n_{calcd}^a
		60 MHz
-32.3	1.36	0.92
-38.1	1.47	0.87
-42.2	1.53	0.85
-46.8	1.58	0.84
	-------------	
		10 MHz
-27.1	0.027	0.98
-32.8	0.221	0.94

(a) Calculated from $n = K_\omega (\Delta\omega_m T)^{-1}$ with $K_\omega = 3.00 \times 10^6$ radians s^{-1} K (at 60 MHz) from the chemical shift studies and $\Delta\omega_m$ from the R_{2obsd}-t_{CP} analysis with n=1 from (i) Table 19 for 60 MHz calculations. (ii) Table 21 for 10 MHz calculations

C Multiple Temperature Analysis of the R_{2obsd}-t_{CP} Data

Multiple temperature analysis of the R_{2obsd}-t_{CP} data described in the study of nickel(II)-acetonitrile system was applied to the NipyDPT^{2+}-acetonitrile system. The analysis was carried out for the 60 MHz data only because there is no slow exchange region data at 10 MHz.

The results of various fitting procedures are summarized in Table 24. The effect of changing the assumed solvation number from 1 to 2 is shown by Fits III and IV. In these fits R_{2m} and R_{2o} were fixed at values given by equations (3-14) and (3-15) respectively and the fitting parameters are C_ω and $\Delta S^{\ddagger}$. The standard error of the fit is about 6 times worse when n=2, and the inadequacy of the fit can be seen from the difference between the experimental and calculated R_{2obsd} values in Appendix B. When n=2 the differences are often in the range of 20%, whereas when n=1 the differences are 2-3%. Clearly n=1 is the preferable choice of the solvation number.

The solvation number calculated from $n = K_\omega/C_\omega = 1.46 \pm 0.11$ (Fit IV) is inconsistent with the initial assumption of n=2. However the calculated $n = 0.89 \pm 0.04$ from Fit III is in much better agreement with the initial assumption of n=1. These observations are a further criterion for choosing n=1.

Table 24

Least-squares best fits of the multiple temperature R_{2obsd}-t_{CP} data for the 0.04936 molal NipyDPT^{2+} solution in acetonitrile at 60 MHz.

Fit[a]	$10^{-6}C_\omega$ rad s^{-1}K	$10^{-4}\Delta H^{\ddagger}$ calmol^{-1}	$\Delta S^{\ddagger}$ calmol^{-1}K^{-1}	$10^{-3}C_{2m}$[b] s^{-1}	$10^{-3}E_{2m}$ calmol^{-1}	$10^{-3}C_{2o}$[b] s^{-1}	$10^{-3}E_{2o}$ calmol^{-1}	n	$10^2 \times$ S.E.[c]
I	3.24±0.11	1.167	10.1±0.1	5.07	1.68	3.49	1.68	1.05±0.04	2.53
II	3.52±0.14	1.167	10.1±0.1	0.8±1.7	1.68	7.1±1.7	1.68	0.91±0.06	1.79
III	3.37±0.03	1.167	10.2±0.03	5.07	1.68	3.49	1.68	1	2.72
IV	2.06±0.10	1.167	9.33±0.20	2.54	1.68	1.75	1.68	2	17.2

(a) If no error limits are given parameters were held constant at the values given.

(b) The values of C_{2m} = 5.07 x 10^3 and C_{2o} = 3.49 x 10^3 s^{-1} are based on n=1 and the values C_{2m} = 2.54 x 10^3 and C_{2o} = 1.75 x 10^3 s^{-1} are based on n=2.

Table 24(cont'd)

(c) Standard errors of the fits are based on relative residual minimization.

The additional fits in Table 24 use C_ω, $\Delta S^\ddagger$ and n (Fit I) and C_ω, $\Delta S^\ddagger$, C_{2m}, C_{2o}, and n (Fit II) as fitting parameters. Both of these fits give a good representation of the data, as can be seen by comparison of the standard errors to that of Fit III. Since n is a fitting parameter in both fits the results are independent of initial assumptions about n. The C_ω values from these fits differ by less than 10% so that C_ω is relatively independent of the magnitudes of R_{2m} and R_{2o}. It should be noted that Fit II actually yields an unrealistic value for R_{2m} in that it is smaller than R_{1m}, see equation (3-13). For this reason Fit II will not be used in the solvation number calculation.

The value of C_ω = (3.24 ± 0.11) x 10^6 radians s^{-1}K from Fit I can be combined with the K_ω = (3.00 ± 0.06) x 10^6 radians s^{-1}K from the chemical shift measurements to obtain a solvation number of 0.93 ± 0.06. This result is consistent with that from the individual temperature fits, and can be taken to indicate that one acetonitrile molecule is coordinated to the metal in the NipyDPT^{2+}-acetonitrile system.

IV Determination of the Solvation Number of NiTRI^{2+} in Acetonitrile

The nmr method to determine the solvation number has been applied to the nickel(II)-acetonitrile and the NipyDPT^{2+}-acetonitrile systems. The method gave consistent results for these systems which have quite different solvation numbers. Now the method will be applied to a system in which three coordination sites are occupied by a stable Schiff base ligand, namely, tribenzo[b,f,j]-[1,5,9]triazacyclododecinenickel(II) perchlorate{NiTRI(ClO$_4$)$_2$}.

Since the information about the exchange rate, the inner-sphere and the outer-sphere contributions of the NiTRI^{2+}-acetonitrile system were not available, a relatively extensive study of the temperature dependence of R$_{2obsd}$ and R$_{1obsd}$ was undertaken. The analysis of these results constitutes the first part of this section, while the remainder describes experiments and analyses similar to those in the previous two sections.

A   Measurements and Analysis of R_{2obsd} as a Function of Temperature

The R_{1obsd} of the $NiTRI^{2+}$ solutions in acetonitrile was measured and plotted as a function of sample molality at 26.4°C and 53.14 MHz and was found to be a linear function of $NiTRI^{2+}$ molality. This observation confirms the direct dependence of R_{1obsd} on $NiTRI^{2+}$ concentration predicted by equation (1-5) and shows the reliability of the sample preparation.

In order to determine the exchange rate and the inner-sphere and the outer-sphere contributions, values of R_{2obsd} at long t_{CP} values and R_{1obsd} were measured from 35.6°C to -35.0°C at 53.14 MHz . Measurements at higher temperatures were not attempted since distillation of the solvent caused a noticeable change in complex concentration. Measurements at temperatures lower than -35.0 were impossible because the solute crystalized. However the outer-sphere contribution is reasonably defined by the experiments down to -35.0°C.

Plots of R_{1obsd} and R_{2obsd} *versus* 1/T are shown in Figure 12. Measurements of R_{2obsd} and R_{1obsd} were also carried out at 10 MHz from 32.0° to -41.6°C and the results are given in Figure 13. As shown in Figure 12 and 13, R_{2obsd} increases with decreasing temperature to a maximum, at about 30°C at 53 MHz and about 10°C at 10 MHz,
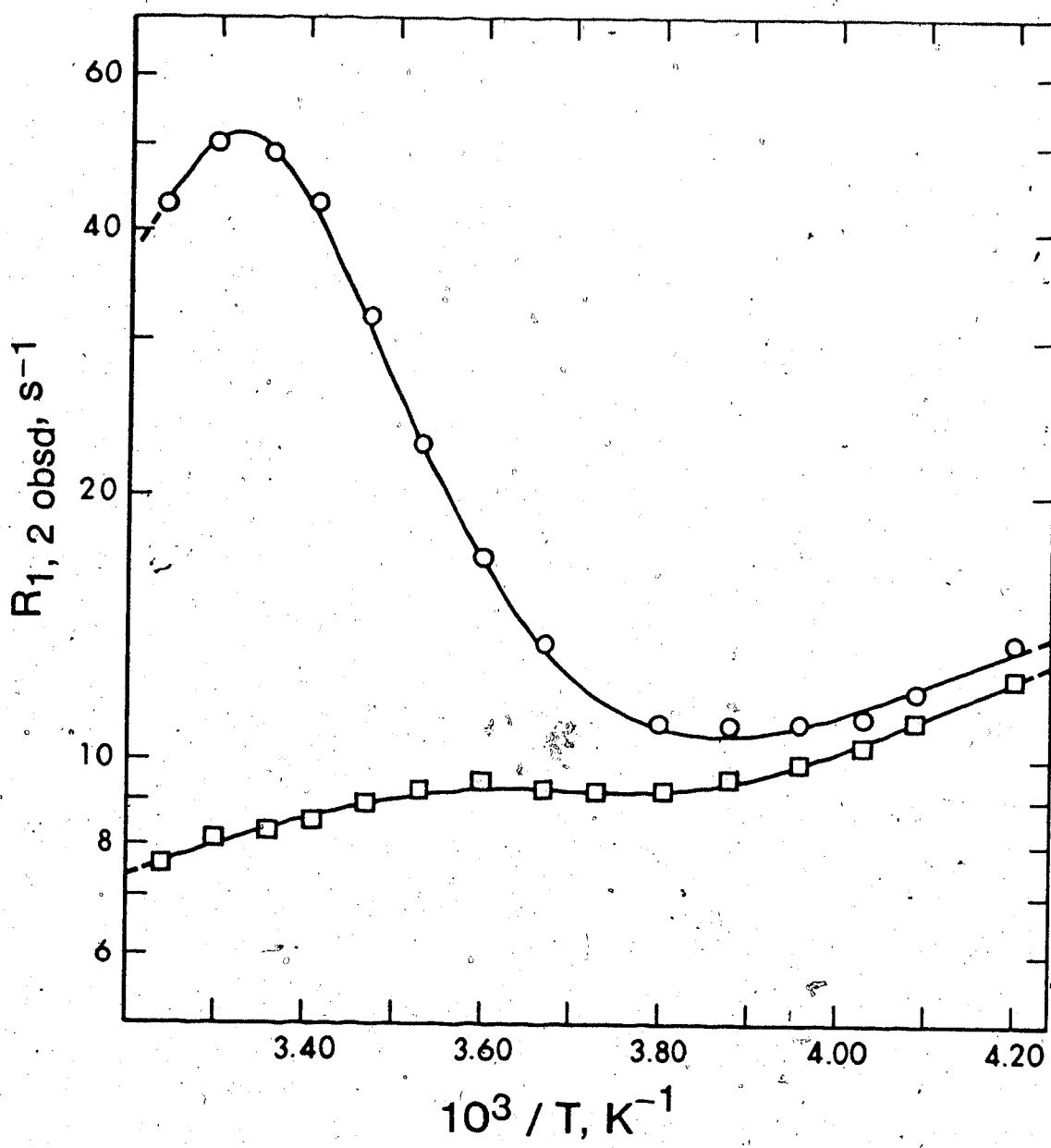
Figure 12 Plots of R_{2obsd} *versus* l/T (O) and R_{1obsd} *versus* l/T (□) for the 0.1199 molal $NiTRI^{2+}$ solution in acetonitrile at 53 MHz .
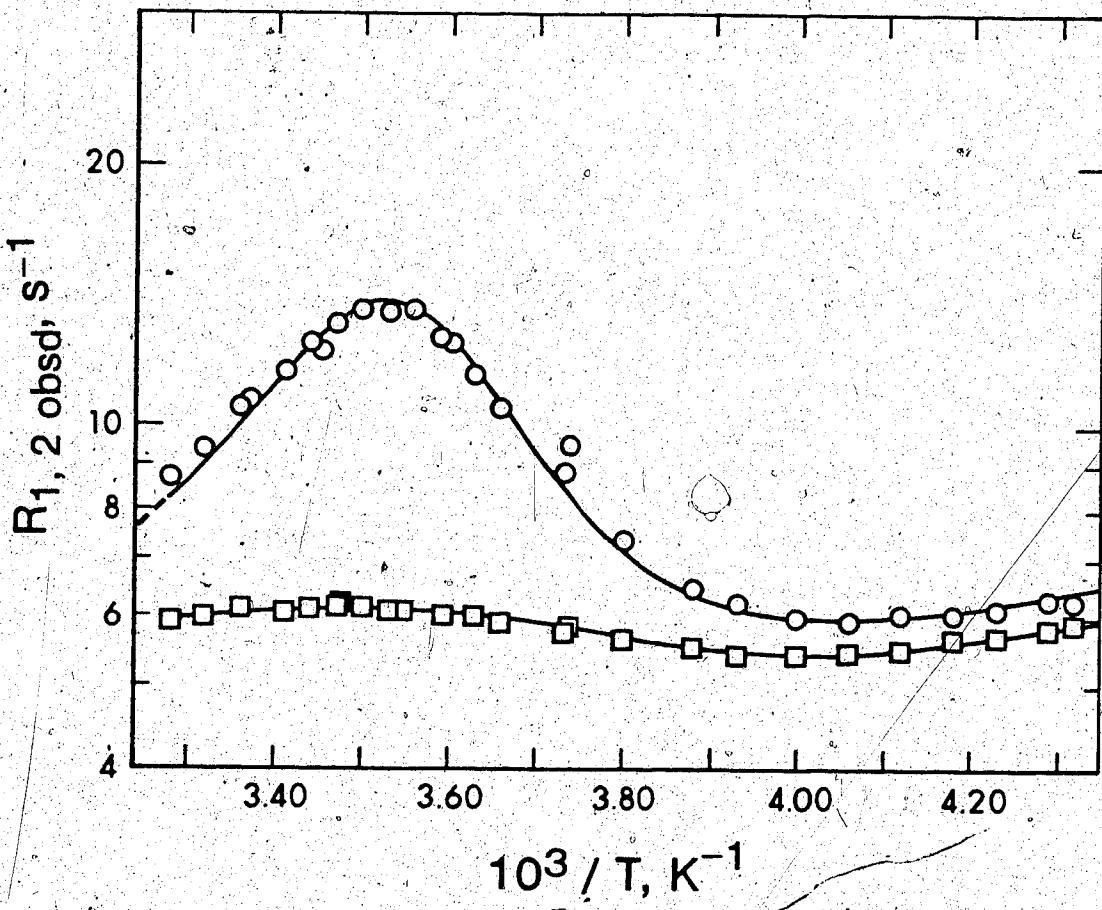
<u>Figure 13</u>   Plots of R_{2obsd} *versus* 1/T (O) and R_{1obsd}

versus 1/T (□) for the 0.1199 molal NiTRI^{2+}

solution in acetonitrile at 10 MHz .

and decreases rapidly with decreasing temperature, goes

through a minimum at about $-17°C$ (3.9×10^{-3} K^{-1}) at

53 MHz and $-23°C$ ($1/T = 4.0 \times 10^{-3} K^{-1}$) at 10 MHz, then gradually

increases with decreasing temperature. These observa-

tions agree with the predictions of equation (1-2). The

variations of R_{1obsd} with temperature at both frequencies

are consistent with equation (1-5). The decrease of

R_{1obsd} with decreasing temperature after the maximum is

not rapid because τ_m^{-1} has a small influence on R_{1obsd}

as expected from equation (1-5).

It is clear from Figures 12 and 13 that the

outer-sphere contributions to both R_{2obsd} and R_{1obsd} are

reasonably well defined by the data at both frequencies.

The slow exchange regions at both frequencies are well

defined, however the exchange parameters $\Delta H^{\ddagger}$ and $\Delta S^{\ddagger}$

obtained at 53 MHz are more reliable because τ_m^{-1} makes

a larger contribution to R_{2obsd} at 53 MHz than at 10 MHz.

Thus $\Delta H^{\ddagger}$ and $\Delta S^{\ddagger}$ will be derived from the least-squares

analysis of the 53 MHz data. Since the inner-sphere

contributions to R_{2obsd} are not defined by the data at

either frequency, it was necessary to use the estimate

of the inner-sphere contribution from the R_{1obsd} data

based on the fact that $R_{2m} \geq R_{1m}$ and the fitting pro-

cedure described below.

The R_{1obsd} - 1/T data were fitted to
equations (1-5), (1-6), (1-21), and (1-27) and the
R_{2obsd} - 1/T data were fitted to equations (1-2), (1-6),
(1-8), (1-21), and (1-27) using an iterative non-linear
least-squares programme. In fitting the R_{2obsd} - 1/T
data the inner-sphere contribution was always kept
constant at the value estimated from the analysis of the
R_{1obsd} - 1/T data. To fit the R_{1obsd} - 1/T data, $\Delta H^{\ddagger}$ and
$\Delta S^{\ddagger}$ were kept constant since τ_m^{-1} is a small contribution
to R_{1obsd}.

The analysis was carried out first with the
53 MHz data while keeping only the inner-sphere constant,
the analysis of the R_{2obsd} - 1/T data was carried out
using the initial guesses for $\Delta H^{\ddagger}$, $\Delta S^{\ddagger}$, C_{2o}, and E_{2o}
from the plot of R_{2obsd} *versus* 1/T (Figure 12), and C_{ω}
from the chemical shift studies (given in the next
section). The n values of 2 and 3 were assumed. The
analysis gave the preliminary values for $\Delta H^{\ddagger}$ and $\Delta S^{\ddagger}$
which in turn were used in the R_{1obsd} - 1/T data analysis
to obtain the best values of C_{1m} and E_{1m}. With the
limitation noted the fitting process was repeated to
optimize to self-consistency between the R_1 and R_2 data
sets. The results are summarized in Tables 25 and 26.

At 10 MHz the analyses of the R_{2obsd} - 1/T and
R_{1obsd} - 1/T data were carried out using the procedure

Least-squares best fits of the R_{2obsd}-1/T data for the 0.1199 molal NiTRI^{2+} solution in acetonitrile at 53 MHz.

Table 25

Fit	$10^{-3}\Delta H^{\ddagger}$ cal mol^{-1}	$\Delta S^{\ddagger}$ cal mol^{-1}K^{-1}	$10^{-4}C_{2m}$ a s^{-1}	$10^{-2}E_{2m}$ cal mol^{-1}	$10^{-6}C_{\omega}$ radians s^{-1}K	$10^{-4}C_{2o}$ s^{-1}	$10^{-3}E_{2o}$ cal mol^{-1}	n	10^{2}S.E. b
I	$15.5_6\pm1.9_5$	10.5 ± 0.6	3.36	4.91	1.88 ± 0.12	1.04 ± 1.81	1.43 ± 0.84	3	2.09
II	$15.5_6\pm1.9_4$	11.3 ± 6.6	4.94	5.02	2.82 ± 0.18	1.60 ± 2.72	1.43 ± 0.85	2	2.09

(a) The parameters C_{2m} and E_{2m} were held constant at the values given. The values of C_{2m} of 3.36×10^4 and 4.94×10^4 s^{-1} are based on n=3 and n=2 respectively.

(b) Standard errors of the fits are based on relative residual minimization.

147

Table 26

Least-squares best fits of the R_{1obsd}^{-1}/T data for the 0.1199 molal NiTRI^{2+} solution in acetonitrile at 53 MHz.

Fit	$10^{-3}\Delta H^{\ddagger a}$ calmol^{-1}	$\Delta S^{\ddagger a}$ calmol^{-1}K^{-1}	$10^{-4}C_{1m}$ s^{-1}	$10^{-2}E_{1m}$ calmol^{-1}	$10^{-3}C_{1o}$ s^{-1}	$10^{-3}E_{1o}$ calmol^{-1}	n	10^2S.E.^{b}
I	15.5$_6$	10.5	3.36±4.87	4.91±8.89	5.09±3.10	1.73±0.30	3	1.12
II	15.5$_6$	11.3	4.94±7.16	5.02±8.90	7.72±4.70	1.72±0.31	2	1.12

(a) The parameters $\Delta H^{\ddagger}$ and $\Delta S^{\ddagger}$ were held constant at the values given.

(b) Standard errors of the fits are based on relative residual minimization.

described for the 53 MHz data except that, in the R_{2obsd} analysis, $\Delta H^{\ddagger}$ was fixed at the value given by the 53 MHz analysis. The results are given in Tables 27 and 28.

The values of $\Delta H^{\ddagger}$ and E_{2o} (Tables 25 and 27), and E_{1m} (Tables 26 and 28) obtained from fits with the assumed n values of 2 and 3 agree well within the 95% confidence limits as expected since these parameters are inherently independent of the n value. Although the fitting parameters C_{1m} and C_{2o} are based on the assumed n value, the product nC_{1m} and nC_{2o} are constants as shown in Tables 25 to 28. The inner-sphere and outer-sphere contributions now can be given for future calculations:

At 53 MHz

$$R_{2m} \geq R_{1m} = (\frac{1.01 \times 10^5}{nT}) \exp(\frac{4.91 \times 10^2}{RT}) \qquad (3-19)$$

and

$$R_{2o} = (\frac{3.12 \times 10^4}{nT}) \exp(\frac{1.43 \times 10^3}{RT}) \qquad (3-20)$$

At 10 MHz

$$R_{2m} \geq R_{1m} = (\frac{6.74 \times 10^5}{nT}) \exp(\frac{-9.11 \times 10^2}{RT}) \qquad (3-21)$$

and

$$R_{2o} = (\frac{1.25 \times 10^5}{nT}) \exp(\frac{3.93 \times 10^2}{RT}) \qquad (3-22)$$

Table 27

Least-squares best fits of the $R_{2obsd}-1/T$ data for the 0.1199 molal $NiTRI^{2+}$ solution in acetonitrile at 10 MHz.

Fit[a]	$10^{-3}\Delta H^{\ddagger}$ cal mol^{-1}	$\Delta S^{\ddagger}$ cal mol^{-1} K^{-1}	$10^{-5}C_{2m}$ s^{-1}	$10^{-2}E_{2m}$ cal mol^{-1}	$10^{-5}C_{\omega}$ rad s^{-1} K	$10^{-4}C_{2o}$ s^{-1}	$10^{-2}E_{2o}$ cal mol^{-1}	n	$10^2 x$ S.E.[b]
I	15.5_6	10.7 ± 0.2	2.24	-9.11	3.60 ± 0.19	4.17 ± 0.15	3.93	3	2.90
II	15.5_6	11.5 ± 0.2	3.38	-9.13	5.40 ± 0.28	6.24 ± 0.23	3.94	2	2.90

(a) If no error limits are given, parameters were held constant at the values given.

(b) Standard errors of the fits are based on relative residual minimization.

Table 28

Least-squares best fits of the R_{lobsd}-1/T data for the 0.1199 molal NiTRI^{2+} solution in acetonitrile at 10 MHz.

Fit[a]	$10^{-3}\Delta H^{\ddagger}$ cal mol^{-1}	$\Delta S^{\ddagger}$ cal mol^{-1} K^{-1}	$10^{-5}C_{lm}$ s^{-1}	$10^{-2}E_{lm}$ cal mol^{-1}	$10^{-4}C_{lo}$ s^{-1}	$10^{-2}E_{lo}$ cal mol^{-1}	n	10^{2}S.E.[b]
I	15.5_6	10.5	2.24±1.95	-9.11±5.27	3.86±1.23	3.93±1.54	3	0.77
II	15.5_6	11.3	3.38±2.93	-9.13±5.27	5.77±2.15	3.94±1.54	2	0.77

(a) If no error limits are given, parameters were held constant at the values given.

(b) Standard errors of the fits are based on relative residual minimization.

151

152

B Chemical Shift Measurements

The chemical shifts were measured at 60 MHz and
80 MHz on Varian A56/60 and Bruker WP-80 spectrometers
respectively. The chemical shifts of both solvent and
the NiTRI^{2+} solutions in acetonitrile were measured
relative to that of the methoxy protons and the phenyl
protons of 1,4-dimethoxybenzene in solutions containing
about 7-11%(w/w) of the internal standard; the average
values of the shifts are used in the subsequent analysis.
The NiTRI^{2+} complex always caused upfield shifts of the
solvent resonance.

The chemical shifts were measured from 100°C
to 25.6°C at 60 MHz and from 110°C to 30°C at 80 MHz to
cover the fast and the slow exchange regions. Figures
14 and 15 show plots of $\Delta\omega_{obsd}$ *versus* 1/T at 60 MHz and
80 MHz respectively. The value of $\Delta\omega_{obsd}$ increases
gradually with decreasing temperature above 57°C
(1/T = 3.02 x 10^{-3} K^{-1}) at 60 MHz and 61°C (1/T =
3.0 x 10^{-3} K^{-1}) at 80 MHz then decreases rapidly with de-
creasing temperature when the slow exchange region is
reached as expected from equation (3-6).

To obtain K_ω, the least-squares analysis of
the $\Delta\omega_{obsd}$ - 1/T data was carried out using the procedure
described in Section II. The analysis employed

153
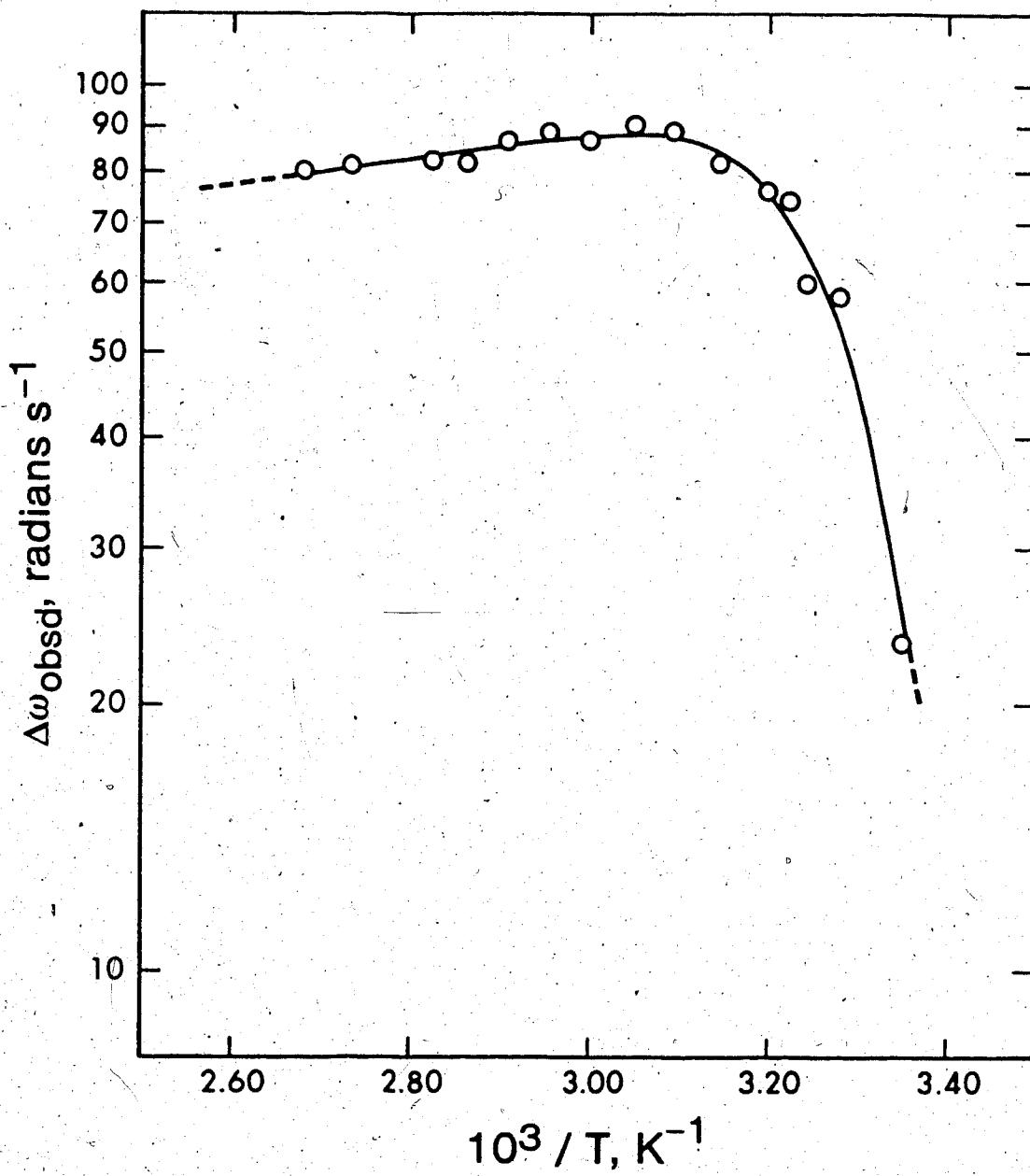
Figure 14 Plot of $\Delta\omega_{obsd}$ *versus* 1/T for the 0.1199 molal
NiTRI^{2+} solution in acetonitrile at 60 MHz.
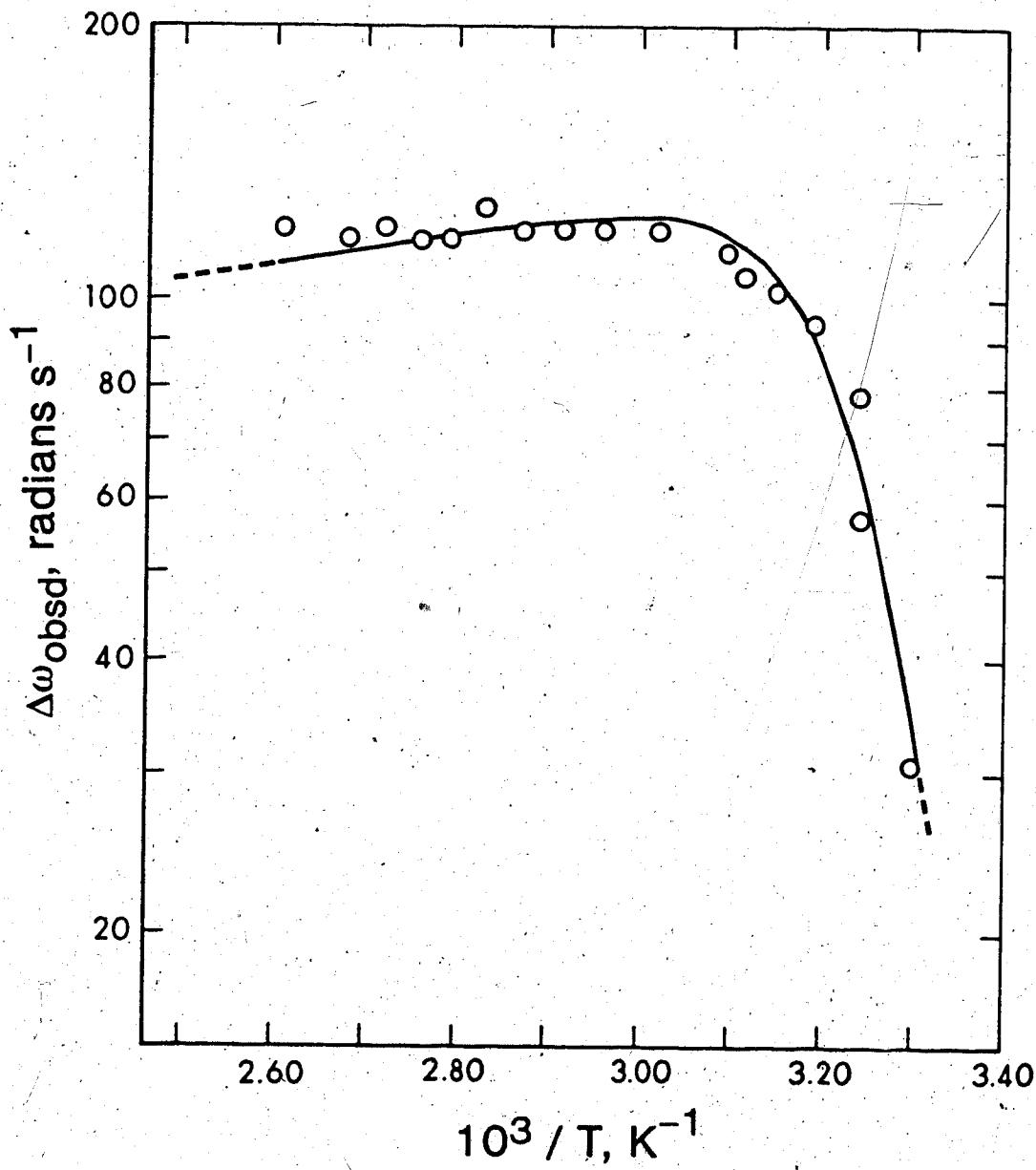
Figure 15 Plot of $\Delta\omega_{obsd}$ *versus* 1/T for the 0.1199 molal NiTRI^{2+} solution in acetonitrile at 80MHz .

$\Delta H^{\ddagger} = 15.5_6 \times 10^3$ cal mol^{-1} given by the $R_{2obsd} - 1/T$ analysis at 53.14 MHz described previously. The inner-sphere contribution was fixed at the value given by equation (3-19). The results of various fits are given in Table 29.

The adequacy of the fit is shown in Table 30 where the experimental and the calculated (least-squares) values of $\Delta \omega_{obsd}$ differ by less than 7 radians s^{-1} (1.1 Hz) for all but 5 of the 32 data points. This agreement is considered good since the $\Delta \omega_{obsd}$ measurement has an uncertainty of about ± 6 radians s^{-1} (1 Hz).

From Table 29, the K_{ω} value is insensitive to a change in the n value which is consistent with the results observed from the nickel(II)-acetonitrile system. The K_{ω} values from fits at 60 MHz and 80 MHz do not agree within the 95% confidence limits. However the values only differ by about 6%. The $K_{\omega} = (5.59 \pm 0.18) \times 10^6$ radians s^{-1}K from fit V is chosen for future calculations since it represents both the 60 MHz and 80 MHz data.

Table 29

Least-squares best fits of the $\Delta\omega_{obsd}$-1/T data for the NiTRI^{2+} solutions in acetonitrile at 60 MHz and 80 MHz.

Fit[a]	n	$\Delta S^{\ddagger}$ calmol^{-1}K^{-1}	10^{-6}Kω [b] radians s^{-1}K	S.E.[c]
I	3	9.87±0.26	5.70±0.24	6.15
II	2	10.7 ±0.3	5.70±0.25	6.15
III	3	10.2 ±0.2	5.36±0.16	2.84
IV	2	11.0 ±0.2	5.36±0.16	2.84
V	2	10.8 ±0.2	5.59±0.18	5.53

(a) Fits I and II (60 MHz) as well as Fits III and IV (80 MHz) are obtained from single sets of data, whereas Fit V is obtained from a combination of the 60 and 80 MHz data.

(b) The values given have been nomalized to 53.14 MHz.

(c) Standard errors of the fits are based on absolute residual minimization.

Table 30

Comparison of the experimental and the calculated (least-squares) $\Delta\omega_{obsd}$ values for the 0.1199 molal $NiTRI^{2+}$ solution in acetonitrile at 60 MHz and 80 MHz.

°C	Chemical shift, rad s^{-1}	
	Experimental	Calculated
		60 MHz
100.0	80.1	83.0
93.0	81.7	84.6
81.0	82.5	87.4
76.0	82.0	88.5
70.0	87.2	89.9
65.0	88.7	90.9
60.0	87.2	91.6
54.5	90.4	91.6
50.0	88.8	90.5
45.0	81.7	86.5
39.0	76.2	74.8
37.0	74.6	68.6
35.0	59.7	61.3
32.0	58.1	48.9
25.5	23.6	23.2

Table 30(cont'd)

	Chemical shift, rad s^{-1}	
°C	Experimental	Calculated
		80 MHz
110.0	119	108
100.0	117	111
94.7	121	112
89.6	116	114
85.2	117	115
79.9	126	117
75.0	118	118
69.8	119	120
64.7	119	121
57.7	119	121
50.0	112	117
48.0	107	114
44.7	102	107
40.6	94.3	92.7
35.7	78.5	67.9
35.4	57.2	66.2
29.9	30.8	37.0

C Measurements and Analysis of $R_{2obsd} - t_{CP}$ Data

Measurements of R_{2obsd} as a function of t_{CP} were carried out at 53.14 MHz in the temperature range of $35.6°$ to $-0.3°C$. No attempts were made to measure R_{2obsd} at temperatures lower than $-0.3°C$ since the change in R_{2obsd} between the long and short t_{CP} limits would be too small to give meaningful $R_{2obsd} - t_{CP}$ dependencies. Selected plots of R_{2obsd} *versus* $1/t_{CP}$ are shown in Figure 16. The full results are given in Appendix C. The results in Figure 16 show that the long t_{CP} limit and the intermediate t_{CP} value region are well defined by the data but the short t_{CP} limit is not. It was necessary to carry out measurements at a lower resonance frequency so that the short t_{CP} limit would become accessible. Therefore $R_{2obsd} - t_{CP}$ measurements at 10 MHz were carried out in the temperature range of $20.0°$ to $-6.1°C$ which covers the fast exchange to the slow exchange regions (Figure 13). Selected R_{2obsd} *versus* $1/t_{CP}$ plots are given in Figure 17. From Figure 17 the long t_{CP} limit, the intermediate t_{CP} value region, and the short t_{CP} limit are well defined by the data.

To determine $\Delta\omega_m$ and to determine if the criterion for selecting the correct solvation number established in the study of the nickel(II)-acetonitrile
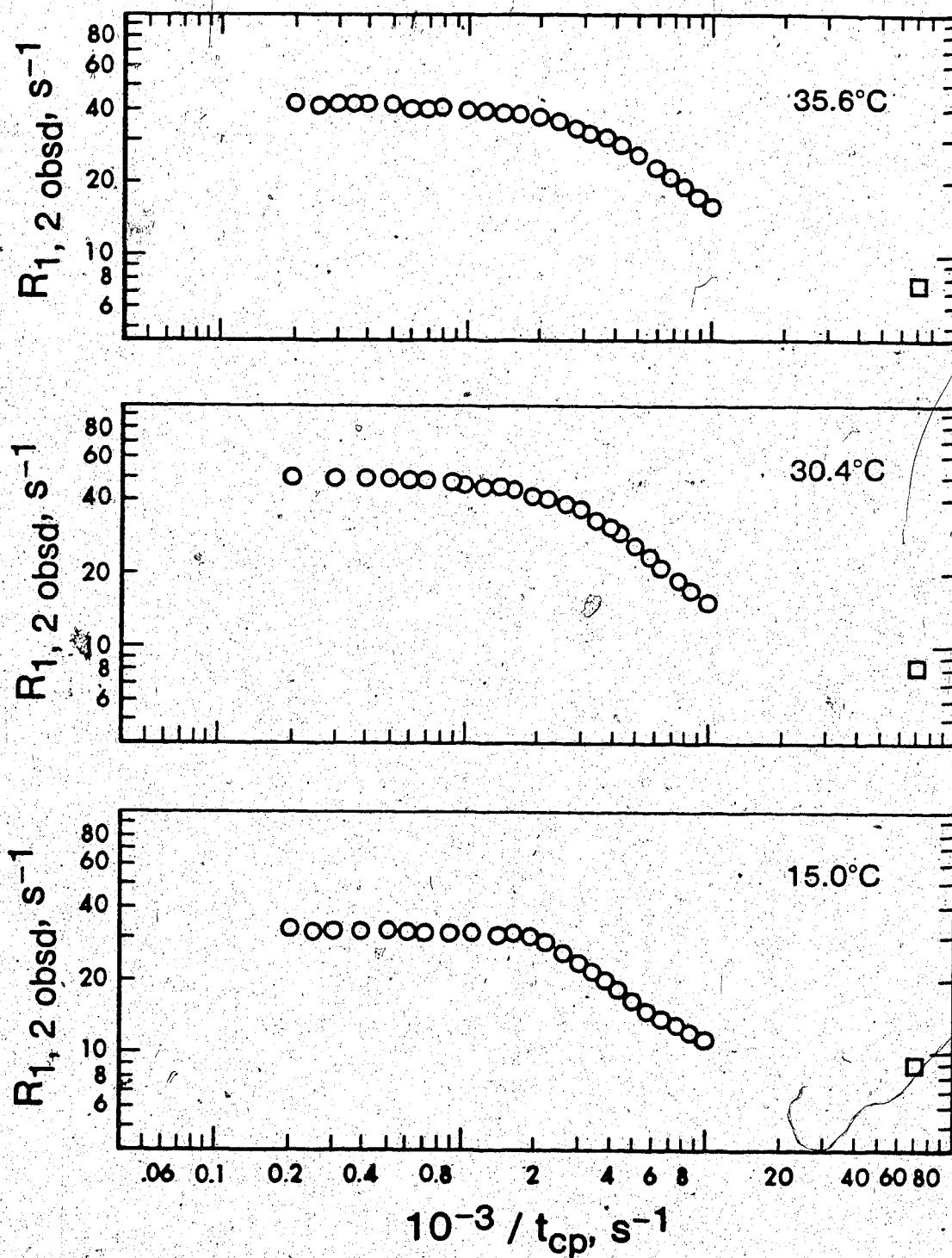
Figure 16 Plots of R_{2obsd} *versus* $1/t_{CP}$ (0) for the 0.1199 molal $NiTRI^{2+}$ solution in acetonitrile from selected data and temperatures at 53 MHz. R_{1obsd} is shown as □.
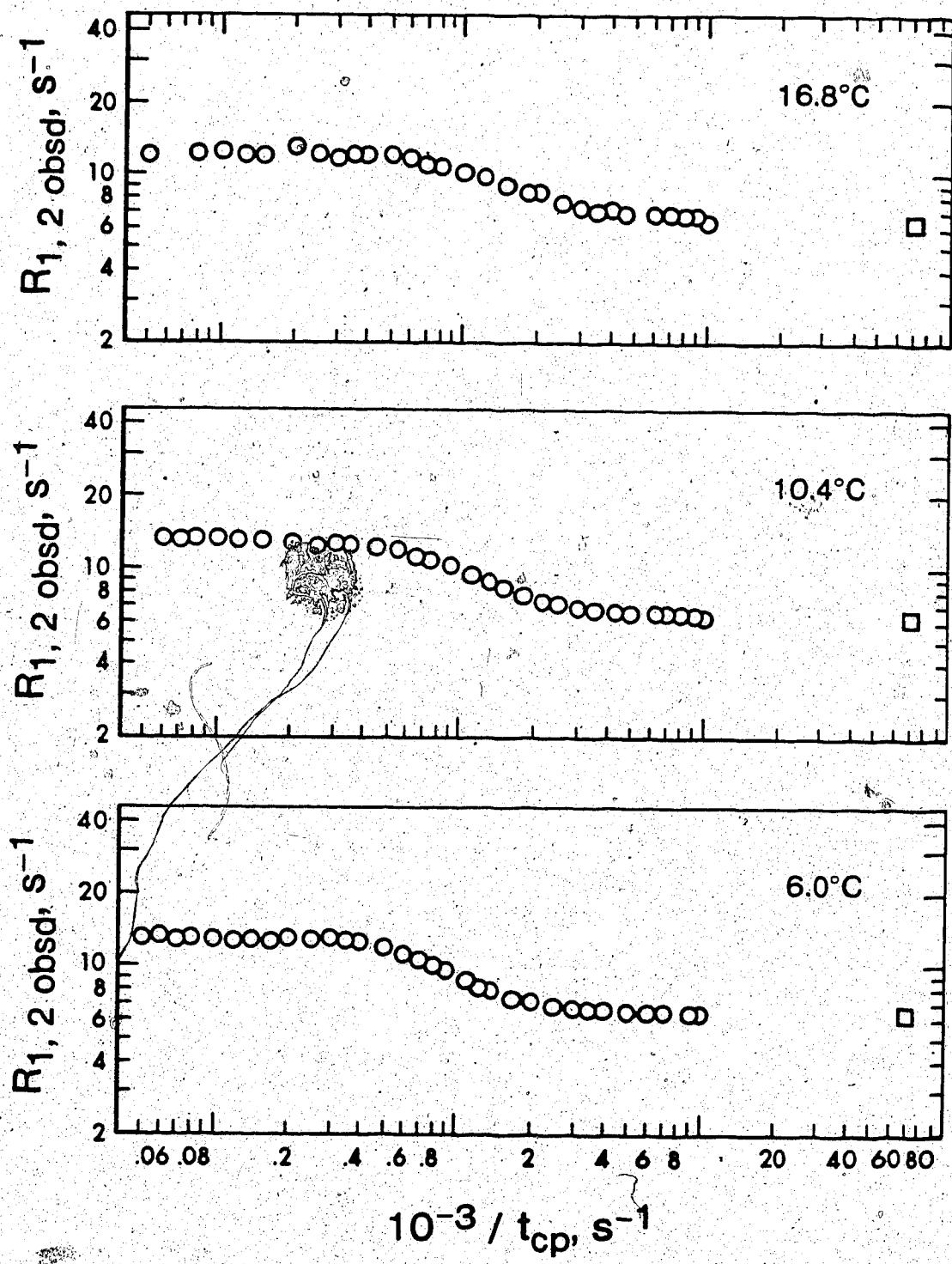
Figure 17   Plots of R_{2obsd} *versus* $1/t_{CP}$ (O) for the 0.1199 molal $NiTRI^{2+}$ solution in acetonitrile from selected data and temperatures at 10 MHz. R_{1obsd} is shown as □.

162

system is applicable to the $NiTRI^{2+}$ - acetonitrile system, the R_{2obsd} - t_{CP} least-squares analysis was carried out. The analysis procedure is the same as that described previously.

The analysis was carried out using the inner-sphere and the outer-sphere contributions given by equations (3-19) and (3-20) for the 60 MHz data, and equations (3-21) and (3-22) for the 10 MHz data. The exchange rate information obtained from the R_{2obsd} - 1/T analysis is used for the initial guesses. The initial guesses for the $\Delta\omega_m$ values were given by $\Delta\omega_m = K_\omega/(nT)$ with assumed n values of 2 and 3 and K_ω from the chemical shift studies. The results of the three-parameter $(R_{2m}, \tau_m^{-1},$ and $\Delta\omega_m)$ fits for the 53 MHz and the 10 MHz data are given in Table 31 and Table 32 respectively.

The effect of the initially assumed n value on τ_m^{-1} and $\Delta\omega_m$ parallels those observed in the nickel(II)-acetonitrile and the $NipyDPT^{2+}$ - acetonitrile systems, i.e. the quality of the fit is not significantly affected but anomalies in the temperature dependencies of τ_m^{-1} and $\Delta\omega_m$ are observed when an incorrect initial assumption of n is made.

The quality of the fits with n=2 and n=3 can be assessed from the uncertainty limits and standard errors of the fits given in Table 31 and Table 32 at 53 MHz and 10 MHz respectively. The uncertainty limits of

163

Table 31

Comparison of the results of the $R_{2obsd}-t_{CP}$ least-squares analysis assuming n=2 and n=3 for the 0.1199 molal NiTRI^{2+} solution in acetonitrile at 53 MHz.

°C	$10^{-2}R_{2m}$, s^{-1}		$10^{-3}\tau_m^{-1}$, s^{-1}		$10^{-3}\Delta\omega_m$, rad s^{-1}		10^2 S.E.^{a}	
	n=2	n=3	n=2	n=3	n=2	n=3	n=2	n=3
35.6	4.10±1.23	2.24±0.85	14.5±0.2	16.4±1.2	?±0.25	7.01±0.26	1.10	1.10
30.4	4.39±0.77	2.20±0.57	9.49±0.85	12.2±0.?	?±0.07	7.16±0.14	0.92	1.08
24.7	2.84±0.63	3.43±0.60	7.04±1.23	3.25±0.15	9.46±0.50	9.91±0.52	1.39	2.61
20.1	3.04±0.50	2.72±0.18	5.02±0.50	2.72±0.04	9.32±0.57	9.62±0.19	1.98	0.95
15.0	3.68±0.31	2.66±0.26	2.90±0.06	1.78±0.04	9.46±0.26	9.64±0.28	1.09	1.32
10.1	3.57±0.45	2.45±0.34	1.66±0.03	1.07±0.02	9.97±0.?	?1±0.9	1.51	1.65
4.7	3.96±0.31	2.68±0.21	0.950±0.014	0.626±0.008	9.78±0.?	9.81±0.35	0.84	0.84
−0.3	3.48±0.36	2.34±0.24	0.564±0.008	0.374±0.005	10.3±0.?	10.3±0.5	0.77	0.78

(a) Standard errors of the fits are based on relative residual minimization.

Table 32

Comparison of the results of the R_{2obsd}-t_{CP} least-squares analysis assuming n=2 and n=3 for the 0.1199 molal NiTRI^{2+} solution in acetonitrile at 10 MHz.

Temp, °C	$10^{-2}R_{2m}$, s^{-1}		$10^{-3}\tau_m^{-1}$, s^{-1}		$10^{-3}\Delta\omega_m$, rad s^{-1}		10^2S.E.[b]	
	n=2	n=3	n=2	n=3	n=2	n=3	n=2	n=3
20.0	2.98±0.16	1.93±0.10	4.01 ±0.45	4.28 ±0.44	1.71±0.06	1.36±0.06	1.35	1.37
12.8	2.94±0.21	1.82±0.10	2.09 ±0.30	2.64 ±0.22	1.89±0.04	1.40±0.03	1.28	1.32
5.0	2.04±0.22	1.55±0.13	1.36 ±0.56	0.603±0.037	1.85±0.30	2.12±0.17	1.86	2.42
2.3	2.12±0.12	1.55±0.10	0.890±0.061	0.504±0.016	1.96±0.13	2.02±0.11	1.31	1.40
-6.1	1.77±0.17	1.21±0.12	0.285±0.008	0.185±0.005	2.06±0.18	2.07±0.17	1.07	1.10

(a) Standard errors of the fits are based on relative residual minimization.

the parameters and the standard errors of the fits are only slightly smaller for n=2 than for n=3, yet the experimental and calculated values of R_{2obsd} with n=2 and n=3 agree quite well; the values at 24.7°C(53 MHz) and at 5.0 °C(10 MHz) where the standard errors of the fits differ most are compared in Tables 33 and 34. Thus the quality of the fits does not provide a criterion for choosing the solvation number.

When n=3 is assumed, anomalies in the temperature dependencies of τ_m^{-1} and $\Delta\omega_m$ are observed in the intermediate exchange region. Between 24.7° and 30.4°C (53 MHz) τ_m^{-1} changes by a factor of 3.7 instead of a change by a factor of 1.6 as expected from the $\Delta H^{\ddagger}$ value, and between 5.0° and 12.8°C(10 MHz) τ_m^{-1} changes by a factor of 4.4 instead of the expected change by a factor of 2.2. The abrupt changes in $\Delta\omega_{obsd}$ between such temperatures are also anomalous. When n=2 is assumed the normal temperature dependencies of τ_m^{-1} and $\Delta\omega_{obsd}$ as predicted by equations (1-6) and (1-8) are observed. The results from Tables 31 and 32 also indicate that $\Delta\omega_m$ is independent of the assumed n value in the slow exchange regions. This is very important for the determination of the solvation number.

Two important observations from this analysis are consistent with those in the studies of the nickel(II)-

Table 33

Comparison of the experimental and the calculated (least-squares) R_{2obsd} values with n=2 and n=3 for the 0.1199 molal $NiTRI^{2+}$ solution in acetonitrile at 24.7°C and 53 MHz.

t_{CP}, ms	R_{2obsd}, s^{-1}	$R_{2(calcd)}$[a], s^{-1}	
		n=2	n=3
5.00	49.3	49.2	48.3
4.00	49.1	49.0	48.2
3.33	49.8	48.8	48.1
2.86	49.8	48.6	47.9
2.50	49.9	48.4	47.8
2.00	48.6	48.0	47.6
1.67	49.0	47.5	47.3
1.43	47.2	47.1	47.0
1.25	46.9	46.7	46.8
1.11	46.8	46.2	46.6
1.00	45.7	45.8	46.2
0.909	45.8	45.4	45.8
0.833	45.4	44.9	45.7
0.769	44.2	44.5	45.6
0.714	44.4	44.1	45.6
0.667	43.9	43.8	45.7
0.588	43.5	42.9	45.4

Table 33(cont'd)

t_{CP}, ms	R_{2obsd}, s^{-1}	$R_{2(calcd)}^a$, s^{-1}	
		n=2	n=3
0.526	42.7	42.0	44.5
0.476	41.5	40.9	43.2
0.435	39.6	39.7	41.5
0.400	38.4	38.4	39.6
0.370	39.6	36.9	37.7
0.345	35.5	35.5	35.8
0.323	33.7	34.0	33.9
0.303	32.1	32.6	32.2
0.286	30.7	31.2	30.6
0.270	29.4	29.9	29.1
0.256	28.4	28.6	27.8
0.244	27.0	27.5	26.5
0.227	25.5	25.8	24.9
0.213	23.9	24.4	23.4
0.200	22.5	23.0	22.2
0.189	21.6	21.8	21.1
0.179	20.6	20.8	20.1
0.167	19.3	19.5	19.0
0.156	18.4	18.4	18.1
0.147	17.7	17.5	17.3
0.139	16.8	16.7	16.6

Table 33(cont'd)

| t_{CP}, ms | R_{2obsd}, s^{-1} | $R_{2(calcd)}$[a], s^{-1} | |
		n=2	n=3
0.128	15.7	15.6	15.7
0.116	14.5	14.5	14.8
0.111	14.1	14.0	14.5
0.106	13.8	13.6	14.2
0.100	13.3	13.0	13.7

(a) Standard errors of the fits based on relative residual minimization are 1.39×10^{-2} for n=2 and 2.61×10^{-2} for n=3.

169

Table 34

Comparison of the experimental and the calculated R_{2obsd} values with n=2 and n=3 for the 0.1199 molal $NiTRI^{2+}$ solution in acetonitrile at $5.0°C$ and 10 MHz.

t_{CP}, ms	R_{2obsd}, s^{-1}	$R_{2(calcd)}$[a], s^{-1}	
		n=2	n=3
20.0	13.5	13.0	12.7
15.0	12.8	12.9	12.6
12.5	12.6	12.9	12.6
10.0	12.7	12.8	12.6
8.00	12.4	12.7	12.5
6.67	12.6	12.6	12.4
5.71	12.3	12.5	12.4
5.00	12.4	12.4	12.3
4.44	13.0	12.3	12.2
4.00	12.1	12.2	12.2
3.64	12.0	12.1	12.2
3.33	12.3	12.0	12.2
3.08	12.2	11.9	12.2
2.86	11.9	11.8	12.2
2.50	11.4	11.6	12.0
2.27	11.2	11.4	11.8
2.08	11.0	11.2	11.6

Table 34(cont'd)

t_{CP}, ms	R'_{2obsd}, s^{-1}	$R_{2(calcd)}^{a}$, s^{-1}	
		n=2	n=3
1.92	11.0	11.0	11.3
1.75	11.2	10.7	10.9
1.67	10.5	10.6	10.7
1.54	10.3	10.3	10.4
1.43	10.1	10.0	10.0
1.33	9.65	9.75	9.70
1.26	9.55	9.53	9.45
1.18	9.34	9.28	9.16
1.11	8.98	9.07	8.93
1.05	9.07	8.88	8.73
1.00	8.71	8.70	8.54
0.870	8.22	8.25	8.10
0.769	7.87	7.91	7.77
0.687	7.55	7.64	7.52
0.620	7.49	7.42	7.32
0.556	7.13	7.22	7.15
0.526	7.08	7.14	7.07
0.500	7.04	7.06	7.01
0.454	7.00	6.94	6.90
0.417	6.81	6.85	6.82
0.385	6.87	6.77	6.76

Table 34(cont'd)

t_{CP}, ms	R_{2obsd}, s^{-1}	$R_{2(calcd)}$[a], s^{-1}	
		n=2	n=3
0.357	6.61	6.71	6.71
0.333	6.63	6.66	6.67
0.308	6.61	6.61	6.63
0.286	6.74	6.57	6.59
0.267	6.50	6.54	6.57
0.250	6.66	6.51	6.54
0.227	6.54	6.48	6.52
0.208	6.48	6.45	6.49
0.192	6.31	6.43	6.48
0.179	6.36	6.41	6.46
0.167	6.45	6.40	6.45
0.154	6.28	6.39	6.44
0.143	6.30	6.38	6.44
0.133	6.65	6.37	6.43
0.125	6.38	6.36	6.42
0.111	6.17	6.35	6.41

(a) Standard errors of the fits based on relative residual minimization are 1.86×10^{-2} for n=2 and 2.42×10^{-2} for n=3 .

acetonitrile and the NipyDPT^{2+} - acetonitrile systems. The value of $\Delta\omega_{obsd}$ is independent of the initially assumed n value in the slow exchange region. The expected temperature dependencies of τ_m^{-1} and $\Delta\omega_m$ are observed only when the correct n value has been assumed.

The solvation number now can be calculated from $K_\omega = 5.59 \times 10^6$ radians s^{-1}K at 53 MHz from the chemical shift studies and $\Delta\omega_m$ at various temperatures from the analysis of the R_{2obsd} - t_{CP} data with n=2 (Table 31 and Table 32). The results of the calculations are given in Table 35 and Table 36 for the 53 MHz and the 10 MHz data respectively. The average solvation numbers calculated from the 53 MHz and the 10 MHz data are at one standard error limits $2.0_3 \pm 0.0_4$ and $1.9_9 \pm 0.0_8$ respectively. The two average values agree well within the error limits. The solvation number of two for the NiTRI^{2+} - acetonitrile is then concluded from this analysis.

Table 35

Calculations of the solvation number for the 0.1199 molal $NiTRI^{2+}$ solution in acetonitrile at 53 MHz.

C	$10^{-3}\Delta\omega_m$	n_{calcd}^a
	rad s^{-1}	
35.6	8.62	2.1_0
30.4	9.22	2.0_0
24.7	9.46	1.9_8
20.1	9.32	2.0_5
15.0	9.46	2.0_5
10.1	9.97	1.9_8
4.7	9.78	2.0_6
-0.3	10.3	1.9_9

(a) Calculated from $n=K_\omega(\Delta\omega_m T)^{-1}$ with $K_\omega=5.59 \times 10^6$ radians s^{-1} K from the chemical shift studies and $\Delta\omega_m$ from the $R_{2obsd}-t_{CP}$ fit with $n=2$ (Table 31).

Table 36

Calculations of the solvation number for the 0.1199 molal
$NiTRI^{2+}$ solution in acetonitrile at 10 MHz.

$°C$	$10^{-3}\Delta\omega_m$ radians s^{-1}	n_{calcd} [a]
20.0	1.71	2.1_0
12.8	1.89	1.9_5
5.0	1.85	2.0_4
2.3	1.96	1.9_5
−6.1	2.06	1.9_1

(a) Calculated from $n=K_\omega(\Delta\omega_m T)^{-1}$ with $K_\omega=1.05\times10^6$
radians s^{-1}K from the chemical shift studies and
$\Delta\omega_m$ from the $R_{2obsd}-t_{CP}$ fit with $n=2$ at 10 MHz.
(Table 32).

174

D Multiple Temperature Analysis of R_{2obsd} - t_{CP} Data

In order to determine the best value for C_ω which can be combined with K_ω to calculate the solvation number, the multiple temperature analysis of the R_{2obsd} - t_{CP} data described in the study of the nickel(II)-acetonitrile system was carried out for both the 53 MHz and the 10 MHz data. The data from the R_{2obsd} - 1/T and the individual temperature R_{2obsd} - t_{CP} analysis were combined for this multiple temperature analysis. The inner-sphere and the outer-sphere contributions given by equations (3-19) and (3-20), and (3-21) and (3-22) were used in the analysis of the 53 MHz and the 10 MHz data respectively. Fits with assumed n values were carried out with C_{2m} and E_{2m} fixed since the inner-sphere contribution is not defined by the data either at 53 MHz or 10 MHz. However fits with n as a fitting parameter were done with C_{2m} varying so that the C_ω values obtained were consistently free from the assumption of n.

The results of the multiple temperature analysis are given in Table 37 and Table 38 for the 53 MHz and the 10 MHz data respectively. Fit II and Fit III of both Table 37 and Table 38 illustrate the effect of changing the assumed n value from 2 to 3. The standard error of the fit is about 2 times larger (with n=3) at

Table 37

Results of the least-squares analysis of the multiple temperature $R_{2obsd}-t_{CP}$ data[a] for the 0.1199 molal NiTRI^{2+} solution in acetonitrile at 53 MHz.

Fit[b]	$10^{-6}c_\omega$ radian s^{-1} K	$10^{-3}\Delta H^{\ddagger}$ calmol^{-1}	$\Delta S^{\ddagger}$ calmol^{-1} K^{-1}	$10^{-4}C_{2m}$[c] s^{-1}	$10^{-2}E_{2m}$ calmol^{-1}	$10^{-4}C_{2o}$[c] s^{-1}	$10^{-2}E_{2m}$ calmol^{-1}	n	$10^2 \times$ s.E.[d]
I	2.70±0.06	15.5$_6$	11.2±0.1	4.36±0.37	4.91	1.43±0.05	1.43	2.12±0.07	2.05
II	2.79±0.02	15.5$_6$	11.3±0.0$_3$	5.04	4.91	1.51±0.02	1.43	2	2.56
III	2.17±0.04	15.5$_6$	10.7±0.1	3.36	4.91	1.02±0.03	1.43	3	6.78

(a) The data consist of 388 points in the temperature range of 35.6 °C to -35 °C. The full fit of the data is given in Appendix C.

(b) If error limits are not given, parameters were held constant at the values given.

(c) The values of C_{2m}=5.04 x 10^4 and 3.36 x 10^4 s^{-1} are based on n=2 and n=3 respectively.

(d) The standard errors of the fits are based on relative residual minimization.

Table 38

Results of the least-squares analysis of the multiple temperature $R_{2obsd}-t_{CP}$ data[a] for the 0.1199 molal NiTRI^{2+} solution in acetonitrile at 10 MHz.

Fit[b]	$10^{-5}C_\omega$ rad s^{-1}K	$10^{-3}\Delta H^{\ddagger}$ calmol^{-1}	$\Delta S^{\ddagger}$ calmol^{-1}K^{-1}	$10^{-5}C_{2m}$[c] s^{-1}	$10^{-2}E_{2m}$ calmol^{-1}	$10^{-4}C_{2o}$ s^{-1}	$10^{-2}E_{2o}$ calmol^{-1}	n	$10^2\times$ S.E.[d]
I	5.25±0.37	15.5$_6$	11.4±0.2	3.59±0.26	-9.11	5.71±0.49	3.93	2.13±0.16	3.00
II	5.60±0.08	15.5$_6$	11.5±0.1	3.37	-9.11	6.20±0.07	3.93	2	3.19
III	4.02±0.09	15.5$_6$	10.9±0.1	2.24	-9.11	4.18±0.08	3.93	3	5.00

(a) The data consist of 460 points in the temperature range of 20.0°C to -41°C. The full fit of the data is given in Appendix C.

(b) If error limits are not given, parameters were held fixed at the values given.

(c) The values of $C_{2m}=3.37 \times 10^5$ and 2.24×10^5 s^{-1} are based on n=2 and n=3 respectively.

(d) Standard errors of the fits are based on relative residual minimization.

53 MHz and only 1.6 times larger (with n=3) at 10 MHz.
From the comparison of the difference between the
experimental and the calculated R_{2obsd} values given
in Appendix C, one finds that the differences between
the experimental and the calculated values are
generally about 5% for n=2 and less than 10% for n=3 at
both frequencies. Although the differences with n=2 are
generally smaller the fits with n=3 are considered
reasonable and cannot be excluded since the uncertainty
in R_{2obsd} measurement is about 5%. Thus the quality of
the fit alone does not provide a criterion for choosing
the solvation number.

The solvation number calculated from $n = K_\omega/C_\omega$,
with $K_\omega = (5.59 \pm 0.18) \times 10^6$ radians $s^{-1}K$ from the
chemical shift studies, are 2.0 ± 0.1 (n=2) and
2.6 ± 0.1 (n=3) at 53 MHz, and 1.9 ± 0.1 (n=2) and
2.6 ± 0.1 (n=3) at 10 MHz. It is clear that when n=3
is assumed the calculated solvation number is inconsistent
with the initially assumed n value. But when n=2 is
assumed the calculated solvation number is consistent
with the initially assumed n value. These observations
provide a criterion for choosing the solvation number of
2. This behavior is consistent with that observed in
the studies of the nickel(II)-acetonitrile and the
$NipyDPT^{2+}$ - acetonitrile systems.

Combination of $C_\omega = (2.70 \pm 0.06) \times 10^6$ radians $s^{-1}K$ at 53 MHz and $C_\omega = (5.25 \pm 0.37) \times 10^5$ radians $s^{-1}K$ at 10 MHz and $K_\omega = (5.59 \pm 0.18) \times 10^6$ radians $s^{-1}K$ at 53 MHz from the chemical shift studies gives the calculated solvation number of 2.1 ± 0.1 and 2.0 ± 0.2 at 53 MHz and 10 MHz respectively. The two calculated values are in good agreement within the 95% confidence limits. They are also in good agreement with the results obtained from the individual temperature fits. Accordingly it can be concluded that two acetonitrile molecules are coordinated to the NiTRI complex in the NiTRI-acetonitrile system.

Chapter IV

CONCLUSION

I Assessment and Limitaions of the Methods

The relaxation rates and chemical shifts of the three nickel(II) complexes in acetonitrile have been measured and analysed. Various types of analysis of the $R_{2obsd}-t_{CP}$ and the $\Delta\omega_{obsd}-1/T$ data and the combination of them result in three methods of determining the solvation number. The first method combines the variation of R_{2obsd} with t_{CP} and chemical shift measurements and is termed the combination method. The second method employs only the pulsed data ($R_{2obsd}-t_{CP}$) at several temperatures, including the intermediate exchange region, and assumes certain n values in the analysis of the $R_{2obsd}-t_{CP}$ data at each temperature. This method is referred to as the individual temperature method. The third method combines the pulsed and chemical shift measurements and analyses the pulsed data at all temperatures together, and therefore is referred to as the multiple temperature method.

From the analysis of the three systems studied, it was found that the combination method should only be applied if the $R_{2obsd}-t_{CP}$ variation can be measured in the slow exchange region. Then these data define $\Delta\omega_m$, and the chemical shift measurements give $n\Delta\omega_m$ so that the combination easily yields a reliable value of n. Thus the combination method requires that (i) the $R_{2obsd}-t_{CP}$

180

data be available in the slow exchange region and (ii) the chemical shift data be available in the fast exchange region where the limiting chemical shift provides $n\Delta\omega_m$. Obviously this method is applicable only to systems which have both the slow and the fast exchange regions within the liquid temperature range of the solvent. If the slow exchange region cannot be observed a non-coordinating diluent such as nitromethane can extend the low temperature liquid range of many polar solvents.[52,53] The slow exchange region can be extended to higher temperatures by increasing the magnetic field for the $R_{2obsd}-t_{CP}$ measurements. However this option is of limited use because even doubling the magnetic field only gives a 10-20°C extension for the typical $\Delta H^{\ddagger}$ values of 10-15 Kcal mol^{-1}. Similarly lowering the magnetic field is of limited use for extending the chemical shift measurements into the fast exchange region. In addition the lower field makes the observed shift proportionately smaller and less readily measureable.

The liquid range problem may be solved by studying a different solvent nucleus. To make measurements in both the slow and fast exchange regions, it requires that the intermediate exchange region ($\tau_m^{-1} \cong \Delta\omega_m$) be at least 20-30°C away from the boiling or freezing point of the solution studied. If the slow exchange region is not accessible with one nucleus because $\Delta\omega_m >> \tau_m^{-1}$, then another

nucleus with a smaller $\Delta\omega_m$ should be studied. If the fast exchange region is not observed then $\tau_m^{-1} \gg \Delta\omega_m$, and a nucleus with a larger $\Delta\omega_m$ should be studied. Obviously the practicality of these suggestions depends on the chemical nature of the solvent. For example, in acetonitrile ^2H, ^{13}C, ^{14}N, and ^{15}N would be possibilities.

A further limitation of the combination method is that the observed chemical shift in the fast exchange region must be large enough (5 Hz or larger) to be accurately measured. Since $\Delta\omega_{obsd} = P_m \Delta\omega_m$, the solute must be soluble enough to give a sufficiently large P_m value for accurate shift measurements. A lower limit of solute solubility of about 4×10^{-3} molal is estimated. The origin of this limit will be given after the general limitation of the solvation number determination methods is discussed.

The individual temperature method requires the $R_{2obsd}-t_{CP}$ variation in the intermediate exchange region. This method is based on the fact that the expected temperature dependencies of τ_m^{-1} and $\Delta\omega_m$ in the intermediate exchange region are observed only if the correct n value has been assumed. If the initially assumed n value is wrong then anomalies in the temperature dependencies of τ_m^{-1} and $\Delta\omega_m$ are observed in the intermediate exchange region. The anomaly in the temperature dependence of τ_m^{-1} is more pronounced than that of $\Delta\omega_m$ because the variation of τ_m^{-1} with temperature is larger than that of $\Delta\omega_m$. This method

of determining the solvation number is very sensitive to
even small changes in the initially assumed n value. As
illustrated in the study of the nickel(II)-acetonitrile
system the anomaly in the temperature dependence of τ_m^{-1}
is observed even when the initially assumed n value
deviates from the correct one by less than 15 %.

The individual temperature method requires
the pulsed data from at least two exchange regions: the
intermediate exchange region and either the slow exchange
region or the fast exchange region. By comparing the para-
meters τ_m^{-1} and $\Delta\omega_m$ in the intermediate exchange region
and the slow (or fast) exchange region the presence or
absence of anomalies can be determined.

The individual temperature method has a definite
advantage over the combination method in that it requires
only the $R_{2obsd}-t_{CP}$ data which give a saving in time. It
also requires measurements at only a few temperatures from
the slow (or fast) exchange region and the intermediate
exchange region. If the intermediate exchange region is
not well defined it can be brought out by one of the
methods already discussed. Since the intermediate
exchange region occupies a small temperature range, these
methods are more likely to be successful. Furthermore
the solubility limitation becomes less important because
the chemical shift is not needed.

The third method to determine the solvation number is based on the analysis of the multiple temperature $R_{2obsd}-t_{CP}$ data. The chemical shift measurements are still needed. In fact the multiple temperature method is simply a modified combination method where restrictions are placed on the temperature dependence of all the parameters involved in the analysis. The distinct feature of this method is that no assumption about the initial n value is needed. This method requires the $R_{2obsd}-t_{CP}$ data from a wide range of temperatures including the slow exchange region. Inclusion of the data from the slow exchange region is the minimum requirement of this method since $\Delta\omega_m = C_\omega/T$ is only independent of n in the slow exchange region.

The multiple temperature method provides an alternate method for the solvation number determination when an initial n value is assumed. This alternate method is based on the observation that the calculated solvation number $n = K_\omega/C_\omega$ is consistent with the initially assumed n value only if the correct n value has been assumed. The incorrect choice of n value results not only in inconsistency between the calculated solvation number and the initially assumed one but also in poor fitting of the data. However the quality of the fit as indicated by the standard error of the fit does not serve to indicate the choice of the solvation number well. Quality of the fit

is more indicative of the choice of the solvation number in the fast exchange region where $R_{2obsd} = P_m \tau_m \Delta\omega_m^2$, since the square term makes the poor fitting apparent.

The sensitivity of the multiple temperature method, based on the inconsistency between the calculated solvation number and the initially assumed n value or the lack thereof, is not as good as that of the individual temperature method. In Chapter III it was illustrated for the nickel(II)-acetonitrile system that the calculated solvation number is the weighted average between the initially assumed n value and the correct one. Thus the sensitivity of this method is limited to the closeness of the initially assumed n value and the correct one.

The three methods of extracting the solvation number for a paramagnetic metal ion in solution from $R_{2obsd}-t_{CP}$ data have been discussed. There remain three limitations common to the three methods which should be mentioned.

As described in Chapter III the magnetic field fluctuations and the necessity to keep the sample temperature constant have placed limits on t_{CP} values. With the instrumental system used in this work the upper and the lower limits on t_{CP} values are 20-50 ms and 0.1 ms respectively. The long t_{CP} limit is somewhat artificial because this limiting R_2 could be obtained from continuous wave nmr measurements. These limits on

t_{CP} values restrict the use of the nmr methods of determining the solvation number to systems with certain values of τ_m^{-1} and $\Delta\omega_m$. These instrumental limitations require the value of $\Delta\omega_m$ to be between 6×10^2 and about 3×10^4 radians s^{-1} in the slow exchange region, and τ_m^{-1} must be between 6×10^2 and 3×10^4 s^{-1} in the fast exchange region. These restrictions arise from the need to observe the variation of R_{2obsd} with t_{CP}, in the intermediate t_{CP} value region, which is necessary to obtain $\Delta\omega_m$ and τ_m^{-1} in the slow and fast exchange regions respectively.

The restriction on the value of $\Delta\omega_m$ automatically sets a lower limit on the concentration of the paramagnetic metal ion complex required for the combination method. Since $\Delta\omega_{obsd} = P_m \Delta\omega_m$ in the fast exchange region, if $\Delta\omega_{obsd} \simeq 2\pi(5Hz)$ to be measureable and $\Delta\omega_m = 3 \times 10^4$ radians s^{-1}, then a P_m of 1×10^{-3} must be attained. Then for a typical value of $n/[S] = 0.25$, [m] must be greater than about 4×10^{-3} molal.

The nmr methods of determining the solvation number presented are limited to systems whose R_{2obsd} is controlled by $\Delta\omega_m$. As mentioned in Chapter I if the limiting condition $R_{2m}^2 \gg \Delta\omega_m^2$, τ_m^{-2} applies to the slow exchange region(region II in Figure 1) then the fast exchange condition $\tau_m^{-2} \gg \Delta\omega_m^2 > R_{2m}\tau_m^{-1}$ will never

apply, and the chemical exchange is never controlled by $\Delta\omega_m$. Such systems consist of only three exchange regions: the outer-sphere control, the slow exchange, and the inner-sphere control regions. Thus the variation R_{2obsd} with t_{CP} in the slow, intermediate, and fast exchange regions (if any) cannot be used to obtain τ_m^{-1} and $\Delta\omega_m$ since the fast exchange region ($\tau_m^{-2} >> \Delta\omega_m^2 > R_{2m}\tau_m^{-1}$) does not exist and $\Delta\omega_m$ does not control R_{2obsd} in the slow exchange region. Consequently the $R_{2obsd}-t_{CP}$ method of determining the solvation number is not applicable to such exchange systems.

A less obvious limitation on the $R_{2obsd}-t_{CP}$ method occurs if solvent nuclei with nuclear spin greater than 1/2 are studied, such as ^{17}O in water or ^{14}N in ammonia. Such nuclei have inherently rather large relaxation rates due to quadrupolar relaxation. For example[54] in water at $25°C$ $R_1 = R_2 = 132$ s^{-1} for ^{17}O. If the addition of a paramagnetic ion increased this rate by say a factor of two, then $R_{2obsd} = 264$ s^{-1}. In order to accurately determine R_2 from the CPMG method about 10 echoes are required over the time (9ms) in which the echo amplitude decreases to 90% of its initial value. This means that the maximum t_{CP} would be about 1 ms for the example given, and would be proportionately shorter if more metal ion were added to increase R_{2obsd}.

This effect could reduce substantially the range of useful t_{CP} values available for solvent nuclei with natural rates of about 10^2 s^{-1}. On a more positive note it should be added that, although the deuteron has nuclear spin of 1 , deuterium natural relaxation rates are normally small enough(1 to 10 s^{-1}) to escape this limitation.

For the benefit of future work in this area it is of interest to consider what paramagnetic ions are likely candidates for R_{2obsd}-t_{CP} determinations of solvation number. It is clear from the three systems studied here that the method is applicable to nickel(II) complexes in acetonitrile. It also appears that non-reacting ligand effects are not so large as to make the method inapplicable for a solvent with a liquid range similar to or larger than that of acetonitrile. It is important to know how the R_{2obsd}-t_{CP} method might be applicable to the system in other solvents. Previous work on nickel(II) in methanol[12] indicates that the intermediate exchange region occurs at about 60 °C(60 MHz) with $\tau_m^{-1} = \Delta\omega_m = 1.3 \times 10^4$ s^{-1} for the -CH$_3$ protons, these parameters fall well within the range for an R_{2obsd}-t_{CP} study. The nickel(II)-N,N-dimethylformamide(DMF) system[55] is similar to nickel(II) in methanol with the intermediate exchange region for the C-H proton at about 40 °C(40 MHz) with $\tau_m^{-1} = \Delta\omega_m = 1 \times 10^4$ s^{-1}. The nickel(II)-dimethylsul-

foxide (DMSO) system[52] presents a special problem in that the intermediate exchange region is at about 21°C (60 MHz), close to the freezing point of DMSO (18.4°C), with $\tau_m^{-1} = \Delta\omega_m = 3 \times 10^3$ s^{-1}. Frankel[52] has shown that dilution with nitromethane or methylene chloride can be used to extend the solvent liquid range so that the system could be studied by the $R_{2obsd}-t_{CP}$ method. Van Geet[56] has studied the nickel(II)-aqueous ammonia system by proton nmr, the intermediate exchange region is at about 20°C (60 MHz) with $\tau_m^{-1} = \Delta\omega_m = 5 \times 10^4$ s^{-1}. With a modest decrease in operating frequency this system would seem to be amenable to an $R_{2obsd}-t_{CP}$ study. Such work would help to determine the extent of coordination of NH_3 in aqueous ammonia solutions. In general it seems that the $R_{2obsd}-t_{CP}$ method is applicable to nickel(II) in a range of solvents. Therefore one might expect that if a metal ion can be studied in one solvent it probably can be studied in others as well.

Richards and coworkers[6] have applied the pulsed nmr method to the cobalt(II)-CH_3OD system to obtain a solvation number of 6 in agreement with the previous conventional nmr study by Luz and Meiboom[7]. Matwiyoff and Hooker[57] studied the cobalt(II)-acetonitrile system, and found an intermediate exchange region at about -20°C (100 MHz) with $\tau_m^{-1} = \Delta\omega_m = 7 \times 10^3$ s^{-1}. Therefore,

this system could be studied by the R_{2obsd}-t_{CP} method. The cobalt(II)-DMF[55] could also be studied since $\tau_m^{-1} = \Delta\omega_m = 2.5 \times 10^4$ s^{-1} at 0°C (100 MHz).

The iron(II)-methanol system was studied by Breivogel[58] using continuous wave nmr methods and the results indicate that the conditions are excellent for an R_{2obsd}-t_{CP} study. The intermediate exchange region for the -CH$_3$ protons is at about 13°C (60 MHz) with $\tau_m^{-1} = \Delta\omega_m = 2 \times 10^4$ s^{-1}. Similarly the iron(II)-DMSO (+ CD$_3$NO$_2$) system[53] is a suitable system with the intermediate exchange region at about -35°C (60 MHz) and $\tau_m^{-1} = \Delta\omega_m = 4 \times 10^3$ s^{-1}. An increase in frequency to 100 MHz would help to move the intermediate exchange region to higher temperatures while keeping $\Delta\omega_m$ (6.7x10^3 s^{-1}) at a suitable value. The C-H proton in the iron(II)-DMF system[53] also could be studied, since the intermediate exchange region is at about -25°C with $\tau_m^{-1} = \Delta\omega_m = 2 \times 10^4$ s^{-1}. Although a proton study has not been done on iron(II) in acetonitrile the ^{14}N results[59] are sufficiently similar to those for cobalt(II) that an R_{2obsd}-t_{CP} study seems to be feasible.

The titanium(III) ion in water and methanol was studied by Chmelnick and Fiat[60]. In water, the ^{17}O relaxation measurements indicate that the intermediate exchange region is at about 4.6°C (8.13 MHz) with

$\tau_m^{-1} = \Delta\omega_m = 5 \times 10^4 \text{ s}^{-1}$, and with a substantial $\Delta\omega_m$ contribution in the fast exchange region. In CD_3OH the proton nmr measurements yield the intermediate exchange region at about $-3°C$ (54.6 MHz) with $\tau_m^{-1} = \Delta\omega_m = 4 \times 10^4$ s^{-1}. No substantial $\Delta\omega_m$ contribution in the fast exchange region is observed indicating that $\Delta\omega_m$ is not much larger than R_{2m}. The limiting chemical shift is well defined by the data in the fast exchange region in both solvents. A modest decrease in the magnetic field should bring $\Delta\omega_m$ values into the useable range for the $R_{2obsd}-t_{CP}$ study. However the titanium(III)-$^{17}OH_2$ system will suffer from the limited range of long t_{CP} values since the ^{17}O nucleus has natural relaxation rate of about 10^2 s^{-1}. In the titanium(III)-CD_3OH system a decrease in the magnetic field may eliminate the $\Delta\omega_m$ controlled region ($\tau_m^{-1} \gg \Delta\omega_m^2 > R_{2m}\tau_m^{-1}$) since $\Delta\omega_m$ is already not so large compared with R_{2m}. The combination method still may be applicable depending on whether R_{2obsd} is sufficiently different from R_{1obsd} in the slow exchange region where an $R_{2obsd}-t_{CP}$ variation may be observed. With these potential limitations in mind the $R_{2obsd}-t_{CP}$ solvation number study is considered marginally applicable to the titanium(III) systems.

Iron(III) has been studied in DMF[6,17] and DMSO[62]. Only the slow exchange region was observed up to $110°C$ in DMF and $135°C$ in DMSO respectively. The R_1 and chemical

shift measurements in DMSO show that $R_{2m} > \Delta\omega_m$ so that a $\Delta\omega_m$ controlled region will not be observed even at higher temperatures. Therefore R_{2obsd} will not show a dependence on t_{CP}. This behavior is expected to be general for iron(III) because it has a relatively long electron spin relaxation time(e.g. $T_{1e} \cong 1 \times 10^{-10}$ s for the iron(III) in water [63]) which makes the scalar relaxation mechanism very effective and R_{2m} equal to or larger than $\Delta\omega_m$.

In general the relative magnitude of R_{2m} to $\Delta\omega_m$ can be estimated from equations (1-7) and (1-9). If the scalar mechanism dominates then the ratio $(R_{2m}/\Delta\omega_m)$ $\cong 3 \times 10^2 (T_{2e})(A/\hbar)$ is estimated at $25°C$ and 14 KG field. For systems with coupling constants of about 10^7 radians s^{-1} and T_{2e} of about 10^{-9} to 10^{-10} s the condition $\Delta\omega_m^2 >> R_m^2$ will not hold. Such systems include vanadyl (VO^{2+}) [64] as well as manganese(II) and copper(II) [11] and these are unlikely to be suitable for $R_{2obsd}-t_{CP}$ determinations of solvation numbers. The same applies to chromium(III), but it also suffers from great kinetic inertness to ligand substitution $(\tau_m^{-1} = 2.1 \times 10^{-4}$ m^{-1} [65]).

II Comparison with Earlier Work

The three nmr methods of determining the solvation number presented in this work consistently give the answers of six, one, and two respectively for nickel(II), NipyDPT^{2+}, and NiTRI^{2+} complexes in acetonitrile. The solvation number of six for the nickel(II)-acetonitrile system agrees with the conclusion of Merbach et al.[49] using quite a different nmr method, but differs from the conclusion of Richards and coworkers[4]. In the latter study the R_{2obsd}-t_{CP} measurements were carried out at three temperatures and three frequencies essentially in the slow exchange region over a t_{CP} range similar to that of the present work. A comparison between the R_{2obsd} values of Richards and coworkers[4] and those of this work cannot be made because the nickel(II) concentration used in their measurements were not reported.

Richards and coworkers[4] first analysed the long t_{CP} limit R_{2obsd}-$1/T$ data to obtain the exchange parameters necessary for the numerical evaluation of the t_{CP} dependence of R_{2obsd}. Then n values of 4 and 6 were used to obtain two sets of these parameters. The chemical shift data were also analysed. Then the theoretical dependence of R_{2obsd} on t_{CP} was numerically evaluated assuming n = 4 and n = 6, and the results were compared

with the experimental variation of R_{2obsd} with t_{CP}.
Richards and coworkers concluded that a solvation number
of four gave the closest representation of the experi-
mental data.

In this work, it has been observed consistently
for the three nickel(II) complexes that the quality of
the fits with different assumed n values does not provide
a satisfactory criterion for establishing the correct
choice of the solvation number. The visual comparison
method employed by Richards and coworkers[4] is very
subjective and would be even less satisfactory than a
least-squares best fit comparison. In fact neither of the
computed $R_{2obsd}-t_{CP}$ curves with n = 4 and n = 6 appear
to match well with the experimental values even on the
small-scale plots presented by Richards *et al.* (Figure 2
of reference 4). Only at 23°C and 18°C (35 MHz and 20
MHz) do the computed curves with n = 4 appear to match
with the experimental values better than those with
n = 6.

An examination of the two sets of parameters used by Richards and coworkers[4] in computing the theoretical $R_{2obsd}-1/t_{CP}$ curves reveals that the $(A/\hbar)$ values with $n = 4$ and $n = 6$ are inconsistent with each other. Equations (1-3) and (1-7) suggest that $(A/\hbar)$ obtained from the analysis of the chemical shift data in the fast exchange region should be smaller with a larger n value. In order to determine which of the $(A/\hbar)$ values given by Richards and coworkers[4] is the correct one, a comparison of these values and those reported in the literatures is made (Table 39). The comparison indicates that the value 2.2×10^6 radians s^{-1} (with $n = 4$) is preferable over the value 3.3×10^6 radians s^{-1}. Furthermore, the $\Delta\omega_m$ value of 1.1×10^4 radians s^{-1} calculated from the $(A/\hbar)$ value with $n = 4$ of Richards and coworkers[4] agrees well with the reliable $\Delta\omega_m$ values from the $R_{2obsd}-t_{CP}$ analysis in the slow exchange region (25.1 C). This substantiates further that the value $(A/\hbar) = 2.2 \times 10^6$ radians s^{-1} of Richards and coworkers is the correct one.

Table 39

Comparison of the $(A/\hbar)$ and $\Delta\omega_m{}^a$ values (for Proton) of the nickel(II)-acetonitrile system at $25°C$ and 60 MHz.

	n=6[b]	n=4[b]	Ref 57	Ref 49	This work
$10^{-6}(A/\hbar)$, rad s^{-1}	3.3	2.2	1.6	1.8	2.2
$10^{-4}\Delta\omega_m$, rad s^{-1}	1.6	1.1	0.82	0.88	1.1
					1.1_6[c]
					1.1_5[c]

_____

(a) The values of $\Delta\omega_m$ at $25°C$ are calculated from equation (1-7) using $\mu_{eff} = 3.15$.
Except where noted the solvation number of six has been assumed in obtaining $(A/\hbar)$.

(b) From reference 4.

(c) The $\Delta\omega_m$ values at $25.1°C$ of 1.16×10^4 (n=6) and 1.15×10^4 (n=4) radians s^{-1} are obtained from the $R_{2obsd}-t_{CP}$ analysis in the slow exchange region (Table 8).

It can be speculated that Richards and coworkers[4] might have interchanged the two values of $(A/\hbar)$ and used the wrong value to evaluate the theoretical $R_{2obsd}-t_{CP}$ curves with n=6. If the value of $(A/\hbar) = 2.2 \times 10^6$ radians s^{-1} were used with n=6 and the value of 3.3×10^6 radians s^{-1} were used with n=4 then the matching of the theoretical curves with the experimental data could have been better with n=6 and worse with n=4, which ultimately made the two curves match equally well with the experimental data. This expectation is consistent with the observations in this work that the quality of the fits with different assumed n values does not provide a satisfactory criterion for the selection of n. However if Richards and coworkers used the wrong $(A/\hbar)$ value for n=6 then $\Delta\omega_m$ is too large and the mid-point of the theoretical $R_{2obsd}-t_{CP}$ curves with n=6 should appear at larger $1/t_{CP}$ values. An inspection of Figure 2 (reference 4) indicates that this is not true. Instead, the mid-point of the theoretical $R_{2obsd}-t_{CP}$ curves with n=6 appear at smaller $1/t_{CP}$ values compared with the corresponding mid-point of the experimental ones. These observations cast some doubts on the speculation mentioned above.

III <u>Solvation Number in NiTRI^{2+} in Acetonitrile</u>

The solvation number of six from the nickel(II)-acetonitrile study is consistent with an octahedral arrangement of acetonitrile ligands surrounding the nickel-(II) ion. This solvation number is consistent with the conclusion made from the study of electronic spectra of the nickel(II) solution in acetonitrile[35] and the nmr studies by Merbach et $al.$[49].

The solvation number of one concluded for the NipyDPT^{2+} complex in acetonitrile agrees with a total coordination number of six for the nickel(II) centre, since pyDPT is a pentadentate ligand. The results of the elemental analysis of the solid complex are consistent with the molecular formula [NipyDPT(CH$_3$CN)](ClO$_4$)$_2$. This supports the solvation number of one for the NipyDPT^{2+}-acetonitrile system.

However, the solvation number of two deduced for the NiTRI^{2+} complex in acetonitrile does not seem to agree with a total coordination number of six since the ligand TRI is tridentate. The conclusion from the nmr methods of determining the solvation number is inconsistent with the results of the elemental analysis of the solid complex which yields the molecular formula [NiTRI(CH$_3$CN)$_3$](ClO$_4$)$_2$. This inconsistency may be explained by considering the following possibilities.

(i) Errors in the nmr methods of determining the solvation number lead to a conclusion that the solvation number

in the NiTRI^{2+}-acetonitrile system is two instead of the expected value of three.

(ii) The perchlorate ion replaces one of the coordinated acetonitrile molecules resulting in only two acetonitrile molecules coordinated to the NiTRI^{2+} complex.

(iii) The NiTRI^{2+} complex exists as a five-coordinate complex in acetonitrile. That is, the solvation number is two.

In order to consider possibility (i) a brief summary of the results for the NiTRI^{2+}-acetonitrile system is given. The combination method gives the average values of the solvation and the one standard error limits of $2.0_3 \pm 0.0_4$ and $1.9_9 \pm 0.0_8$ at 53 MHz and 10 MHz respectively. The multiple temperature method gives the values of the solvation number and the 95% confidence error limits of 2.1 ± 0.1 and 2.0 ± 0.2 at 53 MHz and 10 MHz respectively. It is clear that within the error limits the solvation number in the NiTRI^{2+}-acetonitrile system is two. In the individual temperature method the anomalies in the temperature dependencies of τ_m^{-1} and $\Delta\omega_m$ are observed when $n=3$ is assumed in the analysis. But when $n=2$ is assumed the normal temperature dependencies of τ_m^{-1} and $\Delta\omega_m$ are observed. These observations all argue against a solvation number of three in the NiTRI^{2+}-acetonitrile system. Furthermore these observations from the study of the

NiTRI^{2+}-acetonitrile system are entirely consistent
with those from the nickel(II)-acetonitrile and the
NipyDPT^{2+}-acetonitrile systems. It is therefore difficult
to rationalize a solvation number of three in the NiTRI^{2+}-
acetonitrile system within the errors of the method
employed.

As mentioned in Chapter I, the solvation number
could be determined using the $(A/\hbar)$ constant method
employed by Hunt[2]. This method assumes that $(A/\hbar)$ is
relatively independent of other ligands on the metal ion
of the same metal ion-solvent system. Thus by comparing
the limiting chemical shift (nC_ω) of the unknown system
with those of systems of known solvation number the
unknown solvation number can be determined. The K_ω values
of the nickel(II) and NipyDPT^{2+} complexes, $(1.99\pm0.05)\times10^7$
with n=6 and $(3.32\pm0.08)\times10^6$ with n=1 radians s^{-1}K,
can be combined with the value of $K_\omega = (6.31\pm0.02)\times10^6$
radians s^{-1}K for the NiTRI^{2+}-acetonitrile system to give
the solvation numbers and the 95% confidence limits of
1.90 ± 0.11 and 2.10 ± 0.13 respectively. The solvation
number of two for the NiTRI^{2+}-acetonitrile is then
concluded. This solvation number further supports
results of the pulsed nmr methods of determining the
solvation number of this work.

The possibility that the perchlorate ion
replaces one of the acetonitrile molecules coordinated to
the NiTRI^{2+} complex is now considered. The perchlorate
ion generally is considered a non-coordinating ligand
particularly in aqueous solutions, and is considered a
weakly coordinating ligand in nonaqueous systems. When
no other donors are present to compete the perchlorate
ion exercises a donor capacity. Several examples of
perchlorate-containing transition metal complexes have
been reported[66-69]. Various perchlorate-containing nickel
(II) complexes have also been prepared and studied[68-73].

In the present study the elemental analysis of
the solid complex indicated the composition
[NiTRI(CH$_3$CN)$_3$](ClO$_4$)$_2$ and the structure of the infra-red
spectrum of the solid complex in the region 1100 cm^{-1}
does not indicate the presence of coordinated perchlorate,
whereas the nmr methods of determining the solvation
number give a solvation number of two, the perchlorate
ion must have replaced one of the coordinated
acetonitrile molecules in solution. Consequently only
two acetonitrile molecules exchange between the inner-
sphere and the bulk solvent sites. This argument
seems to require that the perchlorate ion is a stronger
coordinating ligand than acetonitrile since the
perchlorate ion population is much less than that of

of acetonitrile. The competition between the perchlorate ion and the acetonitrile solvent in binding to metal complexes is exemplified in the recent study of Bottomley and Kadish[74]. In their study of the counterion and solvent effect on reduction potential for cobalt(III)- and iron(III)-porphyrin systems, Bottomley and Kadish[74] found that the stronger the binding strength of the counterion , the larger the reduction potential will be. A strong coordinating solvent, represented by a large donor number (D.N.), displaces the counterion making reduction of the metal centre easier (smaller reduction potential). A linear relationship between the reduction potential and the D.N. value of the solvents for the α, β, γ, δ-tetraphenylporphine cobalt(III) perchlorate $\{CoTPPClO_4\}$ complex was observed. The larger the D.N. value, the smaller the reduction potential. However for the $FeTPPClO_4$ complex the reduction potential remains essentially constant in solvents of D.N. values up to 15 which include acetonitrile(D.N.=14.1). This indicates that the perchlorate ion is bound to the iron(III) centre in many solvents including acetonitrile, and serves as an indication of the competition between the perchlorate ion and the acetonitrile solvent in coordinating to the metal complex in acetonitrile.

Further studies that might help to clarify
whether the perchlorate ion replaces one of the acetoni-
trile molecules coordinated to the $NiTRI^{2+}$ complex
include conductometric measurements and ^{35}Cl relaxation
rate measurements of $NiTRI(ClO_4)_2$ in acetonitrile.

In conductometric measurements acetonitrile
solutions of the $NiTRI(ClO_4)_2$ and, for example, nickel(II)
perchlorate complexes may be studied. Then from the
charges of the two complexes in acetonitrile solution
derived from the measurements one could determine whether
the perchlorate ion replaces one of the coordinated
acetonitrile molecules in the $NiTRI^{2+}$ complex.

The R_2 measurements of ^{35}Cl of the $NiTRI(ClO_4)_2$,
and $NaClO_4$, and nickel(II) perchlorate solutions in
acetonitrile should help to determine whether R_{2obsd} of
the $NiTRI(ClO_4)_2$ solution differs from the natural R_2 of
the perchlorate ion solution in acetonitrile. The acetoni-
trile solution of nickel(II) perchlorate helps to provide
an estimate for the outer-sphere contribution. If one
perchlorate anion coordinates to the paramagnetic $NiTRI^{2+}$
complex, then a two-site exchange system is formed and
the R_{2obsd} of the ^{35}Cl nucleus should be exchange
controlled and larger than the natural R_2 of ^{35}Cl in the
perchlorate ion in acetonitrile. The ^{35}Cl relaxation
measurements would be difficult because of the poor

signal to noise ratio, and solutions would contain a small concentration of perchlorate ion because of the limited solubility of the $[NiTRI(CH_3CN)_3](ClO_4)_2$ complex in acetonitrile.

Five-coordinate complexes of cobalt(II) and nickel(II) are usually formed with polydentate ligands, or less often with bulky monodentate ligands[75]. In these complexes the steric requirements of the ligand molecule play an important role in determining the type of geometry for the coordination complexes. In spite of the large number of structures of five-coordinate complexes available, five-coordinate complexes for cobalt(II) and nickel(II) must be considered unusual, and they are favoured by the use of bulky polydentate ligands which prevent six-coordination around the metal. A total coordination number of six around the nickel(II) centre in the solid $[NiTRI(CH_3CN)_3](ClO_4)_2$ complex is in agreement with this view, and it is difficult to conceive that the $NiTRI^{2+}$ complex exists as a five-coordinate complex in acetonitrile since the same small acetonitrile ligands coordinate to the $NiTRI^{2+}$ complex in solution.

The possibility of the five-coordination of the $NiTRI^{2+}$ complex in acetonitrile was considered by examining the electronic spectra of the known five- and six-coordination complexes of nickel(II). Boge et al.[76] prepared and analysed 15 five-coordinate nickel(II)

complexes. The electronic spectra of the five-coordinate nickel(II) complexes in the solid state and in dichloromethane solution generally show absorption maxima between 600-670, 890-980, and 1150-1180 nm. The electronic spectrum of the octahedral $NiTRI^{2+}$ complex in water reported by Taylor and Busch[37b] has a broad absorption band in the region 600-1100 nm with the maximum centred at about 900 nm and a shoulder at about 780 nm. The electronic spectrum of the 2.00×10^{-3} M $[NiTRI(H_2O)_n](ClO_4)_2$ complex in acetonitrile was measured at room temperature from 400 to 1400 nm. No absorption was detected between 600 and 670 nm, but a broad absorption with two maxima at about 850 and 775 nm was observed. The spectra of the five-coordinate nickel(II) complexes, $NiTRI^{2+}$ complex in water, and $NiTRI^{2+}$ complex in acetonitrile were compared. The comparison based on the absorption between 600 and 670 nm indicates that the $NiTRI^{2+}$ complex in acetonitrile is not five-coordinate. The spectra of the $NiTRI^{2+}$ complex in acetonitrile are similar to that of the octahadral $NiTRI^{2+}$ complex in water. The broad absorption centred around 830 nm ($NiTRI^{2+}$-acetonitrile) is shifted to the shorter wavelength with respect to the maximum at about 900 nm ($NiTRI^{2+}$-H_2O). This shift in the position of the absorption band is consistent with the fact that the nitrogen donor causes a higher transition energy than the oxygen donor.

One might suspect that a small amount of water in the 2.00×10^{-3} M NiTRI^{2+} solution in acetonitrile may replace the acetonitrile molecule(s) coordinated to the nickel(II) centre, thus questioning the validity of the use of the [NiTRI(H$_2$O)$_n$](ClO$_4$)$_2$ complex for the spectral measurements. Eighteen values of relaxation rates (R_{1obsd} and R_{2obsd}) of the 0.0531 molal [NiTRI(H$_2$O)$_n$](ClO$_4$)$_2$ complex in acetonitrile were measured from 49° to -10°C at 53 MHz and compared with the relaxation data of the [NiTRI(CH$_3$CN)$_3$](ClO$_4$)$_2$ solution in acetonitrile. The comparison shows that the R_{1obsd}- and R_{2obsd}-1/T variations are identical for the two sets of data, and the concentration normalized values of R_{1obsd} and R_{2obsd} of the two solutions are the same. These observations substantiate that the acetonitrile coordination to the NiTRI^{2+} complex is not affected by a small amount of water present in the [NiTRI(H$_2$O)$_n$](ClO$_4$)$_2$ complex.

REFERENCES

1. S. F. Lincoln, *Coord. Chem. Rev.*, **6**, 309 (1971).

2. G. Liu, H. W. Dodgen, and J. P. Hunt, *Inorg. Chem.*, **16**, 2652 (1977).

3. J. H. Coates, D. A. Hadi, S. F. Lincoln, H. W. Dodgen, and J. P. Hunt, *Inorg. Chem.*, **20**, 707 (1981).

4. I. D. Campbell, J. P. Carver, R. A. Dwek, A. J. Nummelin, and R. E. Richards, *Mol. Phys.*, **20**, 913 (1971).

5. J. Reedijk, P. W. N. M. Van Leeuwen, and W. L. Groeneveld, *Recl. Trav. Chim. Pay-Bas.*, **87**, 129 (1969).

6. I. D. Campbell, P. E. Nixon, and R. E. Richards, *Mol. Phys.*, **20**, 923 (1971).

7. Z. Luz and S. Meiboom, *J. Chem. Phys.*, **40**, 1058 (1964).

8. R. K. Wangsness and F. Bloch, *Phys. Rev.*, **89**, 728 (1953).

9. F. Bloch, *Phys. Rev.*, **102**, 104 (1956).

10. H. M. McConnell, *J. Chem. Phys.*, **28**, 430 (1958).

11. T. J. Swift and R. E. Connick, *J. Chem. Phys.*, **37**, 307 (1962).

12. Z. Luz and S. Meiboom, *J. Chem. Phys.*, **40**, 2686 (1964).

13. N. Bloembergen, *J. Chem. Phys.*, **27**, 595 (1957).

14. I. Solomon, *Phys. Rev.*, 99, 559 (1955).

15. N. Bloembergen, *J. Chem. Phys.*, 27, 572 (1957).

16. R. E. Connick and D. Fiat, *J. Chem. Phys.*, 44, 4103 (1966).

17. A. D. McLauchlan, *Proc. Roy. Soc. (London)*, A280, 271 (1964).

18. N. Bloembergen and L. O. Morgan, *J. Chem. Phys.*, 34, 842 (1961).

19. L. L. Rusnak and R. B. Jordan, *Inorg. Chem.*, 14, 988 (1975).

20. L. L. Rusnak and R. B. Jordan, *Inorg. Chem.*, 10, 2686 (1971).

21. K. J. Johnson, J. P. Hunt, and H. W. Dodgen, *J. Chem. Phys.*, 51, 4493 (1969).

22. H. Y. Carr and E. M. Purcell, *Phys. Rev.*, 94, 630 (1954).

23. S. Meiboom and D. Gill, *Rev. Sci. Instrum.*, 29, 688 (1958).

24. T. C. Farrar and E. D. Becker, *Pulse and Fourier Transform NMR*, Academic Press, New York, Chapter 2.

25. J. P. Carver and R. E. Richards, *J. Mag. Res.*, 6, 89 (1972).

26. J. Jen, *Adv. Mol. Rel. Proc.*, 6, 171 (1974).

27. Z. Luz and S. Meiboom, *J. Chem. Phys.*, 39, 366 (1963).

28. A. Allerhand and H. S. Gutowsky, *J. Chem. Phys.*, 41, 2115 (1964).

29. A. Allerhand and Gutowsky, *J. Chem. Phys.*, <u>42</u>, 1587 (1965).

30. H. S. Gutowksy, R. L. Vold, and E. J. Wells, *J. Chem. Phys.*, <u>43</u>, 4107 (1965).

31. A. Allerhand and E. Thiele, *J. Chem. Phys.*, <u>45</u>, 902 (1966).

32. J. Jen, *J. Mag. Res.*, <u>30</u>, 111 (1978).

33. J. Frahm, *J. Mag. Res.*, <u>47</u>, 209 (1982).

34. D. E. Woessner, *J. Chem. Phys.*, <u>35</u>, 41 (1961).

35. A. E. Wickenden and R. A. Krause, *Inorg. Chem.*, <u>39</u>, 404 (1962).

36. C. T. Spencer and L. T. Taylor, *Inorg. Chem.*, <u>10</u>, 2407 (1971).

37. (a) L. T. Taylor, S. C. Vergez, and D. H. Busch, *J. Am. Chem. Soc.*, <u>88</u>, 3170 (1966).

    (b) L. T. Taylor and D. H. Busch, *J. Am. Chem. Soc.*, <u>89</u>, 5372 (1967).

38. L. I. Smith and J. W. Opie, *Org. Syn.*, <u>28</u>, 11 (1948).

39. J. Kowalewski, G. C. Levy, L. F. Johnson, and L. Palmer, *J. Mag. Res.*, <u>26</u>, 553 (1977).

40. R. L. Streever and H. Y. Carr, *Phys. Rev.*, <u>121</u>, 20 (1961).

41. Dinesh and M. T. Rogers and G. D. Vickers, *Rev. Sci. Instrum.*, <u>43</u>, 555 (1972).

42. Dinesh and M. T. Rogers, *J. Chem. Phys.*, <u>56</u>, 542 (1972).

43. N. Boden, J. Deck, E. Gore, and H. S. Gutowsky, *J. Chem. Phys.*, 45, 3875 (1966).

44. T. T. Bopp, *J. Chem. Phys.*, 47, 3621 (1967).

45. D. E. Woessner, B. S. Snowden, Jr., and E. T. Strom, *Mol. Phys.*, 14, 265 (1968).

46. W. B. Moniz and H. S. Gutowsky, *J. Chem. Phys.*, 38, 1155 (1963).

47. M. D. Zeidler, *Ber. Bunsenges. Physik. Chem.*, 69, 659 (1965).

48. G. Binsch, J. B. Lambert, B. W. Roberts, and J. D. Roberts, *J. Am. Chem. Soc.*, 86, 5564 (1964).

49. K. E. Newman, F. K. Meyer, and A. E. Merbach, *J. Am. Chem. Soc.*, 101, 1470 (1979).

50. L. L. Rusnak and R. B. Jordan, *Inor. Chem.*, 15, 709 (1976).

51. L. L. Rusnak, E. S. Yang, and R. B. Jordan, *Inorg. Chem.*, 17, 1810 (1978).

52. L. S. Frankel, *Inorg. Chem.*, 10, 814 (1971).

53. S. Funahashi and R. B. Jordan, *Inorg. Chem.*, 16, 1301 (1977).

54. M. Grant and R. B. Jordan, *Inorg. Chem.*, 20, 55 (1981).

55. N. A. Matwiyoff, *Inorg. Chem.*, 5, 788 (1966).

56. Van Geet, *Inorg. Chem.*, 7, 2026 (1968).

57. N. A. Matwiyoff and S. V. Hooker, *Inorg. Chem.*, 6, 1127 (1967).

58. F. W. Breivogel, Jr., *J. Chem. Phys.*, 51, 445 (1969).

59. R. J. West and S. F. Lincoln, *Aust. J. Chem.*, 24, 1169 (1971).

60. A. M. Chmelnick and D. Fiat, *J. Chem. Phys.*, 51, 4238 (1969).

61. J. Hodgkinson and R. B. Jordan, *J. Am. Chem. Soc.*, 95, 763 (1973).

62. J. C. Boubel, J. J. Delpuech, and G. Mathis, *Mol. Phys.*, 33, 1729 (1977).

63. M. Rubinstein, A. Baram, and Z. Luz, *Mol. Phys.*, 20, 67 (1971).

64. N. S. Angerman and R. B. Jordan, *J. Chem. Phys.*, 54, 837 (1971).

65. J. P. Hunt and R. A. Plane, *J. Am. Chem. Soc.*, 76, 5960 (1954).

66. R. C. Elder, M. J. Heeg, and E. Deutsch, *Inorg. Chem.*, 17, 427 (1978).

67. W. C. Jones and W. E. Bull, *J. Chem. Soc. (A)*, 1849 (1968).

68. J. Lewis, R. S. Nyholm, and G. A. Rodley, *Nature (London)*, 207, 72 (1965).

69. P. Pauling, G. B. Robertson, and G. A. Rodley, *Nature (London)*, 207, 73 (1965).

70. A. V. Butcher, D. J. Phillips, and J. P. Redfern, *J. Chem. Soc. (A)*, 1064 (1968).

71. L. E. Moore, R. B. Gayhart, and W. E. Bull, *J. Inorg. Nucl. Chem.*, <u>26</u>, 896 (1964).

72. B. J. Hathaway, D. G. Holah, and M. Hudson, *J. Chem. Soc.*, 4586 (1963).

73. C. M. Harris and E. D. McKenzie, *J. Inorg. Nucl. Chem.*, <u>19</u>, 372 (1961).

74. L. A. Bottomley and K. M. Kadish, *Inorg. Chem.*, <u>20</u>, 1348 (1981).

75. P. L. Orioli, *Coord. Chem. Rev.*, <u>6</u>, 285 (1971).

76. E. M. Boge, D. P. Freyberg, E. Kokot, G. M. Mockler, and E. Sinn, *Inorg. Chem.*, <u>16</u>, 1655 (1977).

APPENDIX A

Comparison of the experimental and calulated (multiple temperature least-squares) R_{2obsd} values with n=6 and n=4 at various temperatures and t_{CP} values for the nickel(II) solutions in acetonitrile at 60 and 15 MHz.

I. At 60 MHz

Temp °C	Sample Molality	t_{CP} s	Exptl s^{-1}	$R_{2(calcd)}$ s^{-1} n=6	n=4
50.4	0.1278	2.000E-03	1.141E+02	1.151E+02	1.012E+02
		1.667E-03	1.127E+02	1.144E+02	1.007E+02
		1.429E-03	1.133E+02	1.137E+02	1.002E+02
		1.250E-03	1.133E+02	1.130E+02	9.974E+01
		1.111E-03	1.125E+02	1.123E+02	9.925E+01
		1.000E-03	1.126E+02	1.116E+02	9.877E+01
		8.333E-04	1.112E+02	1.103E+02	9.780E+01
		7.143E-04	1.093E+02	1.089E+02	9.683E+01
		6.250E-04	1.094E+02	1.075E+02	9.586E+01
		5.556E-04	1.075E+02	1.061E+02	9.489E+01
		5.000E-04	1.063E+02	1.047E+02	9.392E+01
		4.545E-04	1.052E+02	1.034E+02	9.296E+01
		4.167E-04	1.024E+02	1.020E+02	9.199E+01
		3.846E-04	1.019E+02	1.006E+02	9.102E+01
		3.448E-04	1.002E+02	9.853E+01	8.957E+01
		3.448E-04	9.875E+01	9.853E+01	8.957E+01
		3.125E-04	9.727E+01	9.646E+01	8.811E+01
		2.899E-04	9.541E+01	9.472E+01	8.690E+01
		2.667E-04	9.291E+01	9.263E+01	8.544E+01
		2.500E-04	9.155E+01	9.088E+01	8.422E+01
		2.326E-04	8.820E+01	8.879E+01	8.276E+01
		2.174E-04	8.615E+01	8.670E+01	8.129E+01
		2.041E-04	8.418E+01	8.462E+01	7.982E+01
		1.923E-04	8.187E+01	8.255E+01	7.834E+01
		1.818E-04	8.080E+01	8.050E+01	7.686E+01
		1.724E-04	7.791E+01	7.849E+01	7.539E+01
		1.613E-04	7.589E+01	7.587E+01	7.343E+01
		1.538E-04	7.289E+01	7.394E+01	7.196E+01
		1.471E-04	7.060E+01	7.209E+01	7.054E+01
		1.389E-04	6.864E+01	6.966E+01	6.862E+01
		1.316E-04	6.602E+01	6.734E+01	6.676E+01
		1.220E-04	6.243E+01	6.406E+01	6.404E+01
		1.163E-04	6.130E+01	6.198E+01	6.227E+01
		1.111E-04	5.864E+01	6.001E+01	6.055E+01
		1.053E-04	5.627E+01	5.771E+01	5.850E+01
		1.000E-04	5.492E+01	5.553E+01	5.651E+01
40.0	0.2907	7.692E-04	3.010E+02	3.245E+02	2.924E+02
		6.667E-04	3.118E+02	3.179E+02	2.879E+02
		6.250E-04	3.024E+02	3.146E+02	2.856E+02
		5.714E-04	3.022E+02	3.097E+02	2.823E+02
		5.405E-04	2.998E+02	3.063E+02	2.801E+02
		5.000E-04	3.054E+02	3.012E+02	2.767E+02
		4.878E-04	2.969E+02	2.995E+02	2.756E+02

213

Temp °C	Sample Molality	t_{CP} s	Exptl s^{-1}	$R_{2(calcd)}$, s^{-1} n=6	n=4
		4.545E-04	2.947E+02	2.942E+02	2.723E+02
		4.255E-04	2.873E+02	2.886E+02	2.689E+02
		4.000E-04	2.882E+02	2.829E+02	2.655E+02
		4.000E-04	2.844E+02	2.829E+02	2.655E+02
		3.704E-04	2.815E+02	2.750E+02	2.608E+02
		3.448E-04	2.725E+02	2.669E+02	2.558E+02
		3.226E-04	2.654E+02	2.586E+02	2.507E+02
		3.030E-04	2.562E+02	2.502E+02	2.454E+02
		2.667E-04	2.353E+02	2.316E+02	2.328E+02
		2.500E-04	2.216E+02	2.216E+02	2.255E+02
		2.500E-04	2.222E+02	2.216E+02	2.255E+02
		2.410E-04	2.189E+02	2.158E+02	2.212E+02
		2.326E-04	2.142E+02	2.101E+02	2.168E+02
		2.174E-04	2.016E+02	1.993E+02	2.080E+02
		2.083E-04	1.920E+02	1.924E+02	2.023E+02
		2.000E-04	1.847E+02	1.859E+02	1.967E+02
		1.887E-04	1.757E+02	1.766E+02	1.885E+02
		1.786E-04	1.663E+02	1.681E+02	1.806E+02
		1.695E-04	1.602E+02	1.602E+02	1.731E+02
		1.613E-04	1.518E+02	1.530E+02	1.659E+02
		1.538E-04	1.460E+02	1.462E+02	1.591E+02
		1.471E-04	1.387E+02	1.402E+02	1.528E+02
		1.389E-04	1.322E+02	1.327E+02	1.449E+02
		1.333E-04	1.261E+02	1.276E+02	1.394E+02
		1.282E-04	1.216E+02	1.229E+02	1.343E+02
		1.220E-04	1.160E+02	1.173E+02	1.280E+02
		1.176E-04	1.114E+02	1.134E+02	1.235E+02
		1.111E-04	1.053E+02	1.076E+02	1.168E+02
		1.053E-04	1.005E+02	1.025E+02	1.108E+02
39.0	0.1278	1.667E-03	1.473E+02	1.568E+02	1.375E+02
		1.250E-03	1.439E+02	1.539E+02	1.356E+02
		1.111E-03	1.438E+02	1.524E+02	1.346E+02
		1.000E-03	1.426E+02	1.510E+02	1.336E+02
		8.333E-04	1.436E+02	1.481E+02	1.317E+02
		7.407E-04	1.418E+02	1.459E+02	1.302E+02
		6.667E-04	1.379E+02	1.438E+02	1.287E+02
		5.882E-04	1.372E+02	1.410E+02	1.268E+02
		5.714E-04	1.359E+02	1.403E+02	1.263E+02
		5.000E-04	1.329E+02	1.366E+02	1.239E+02
		4.444E-04	1.302E+02	1.327E+02	1.215E+02
		4.000E-04	1.274E+02	1.284E+02	1.191E+02
		3.636E-04	1.233E+02	1.239E+02	1.165E+02
		3.333E-04	1.184E+02	1.191E+02	1.137E+02
		3.077E-04	1.145E+02	1.142E+02	1.107E+02
		2.857E-04	1.089E+02	1.092E+02	1.075E+02
		2.857E-04	1.100E+02	1.092E+02	1.075E+02
		2.667E-04	1.049E+02	1.044E+02	1.042E+02
		2.500E-04	1.003E+02	9.968E+01	1.009E+02
		2.326E-04	9.441E+01	9.430E+01	9.677E+01
		2.174E-04	9.059E+01	8.921E+01	9.269E+01
		2.041E-04	8.556E+01	8.448E+01	8.870E+01
		1.923E-04	8.084E+01	8.009E+01	8.483E+01
		1.818E-04	7.694E+01	7.604E+01	8.112E+01
		1.724E-04	7.220E+01	7.232E+01	7.760E+01
		1.639E-04	6.977E+01	6.891E+01	7.425E+01
		1.563E-04	6.649E+01	6.581E+01	7.114E+01
		1.493E-04	6.336E+01	6.295E+01	6.818E+01
		1.429E-04	6.059E+01	6.032E+01	6.541E+01
		1.351E-04	5.709E+01	5.712E+01	6.196E+01
		1.266E-04	5.370E+01	5.366E+01	5.813E+01
		1.220E-04	5.222E+01	5.181E+01	5.603E+01

215

Temp °C	Sample Molality	t_{CP} s	Exptl s^{-1}	R_2(calcd), s^{-1} n=6	n=4
		1.163E-04	4.981E+01	4.954E+01	5.343E+01
		1.111E-04	4.766E+01	4.750E+01	5.105E+01
		1.053E-04	4.521E+01	4.527E+01	4.840E+01
		1.000E-04	4.312E+0.1	4.327E+01	4.600E+01
40.2	0.1278	1.429E-03	1.496E+02	1.549E+02	1.363E+02
		1.111E-03	1.460E+02	1.520E+02	1.343E+02
		1.000E-03	1.454E+02	1.505E+02	1.334E+02
		8.000E-04	1.441E+02	1.469E+02	1.309E+02
		6.667E-04	1.403E+02	1.434E+02	1.285E+02
		5.882E-04	1.383E+02	1.405E+02	1.265E+02
		5.000E-04	1.330E+02	1.362E+02	1.236E+02
		5.000E-04	1.349E+02	1.362E+02	1.236E+02
		4.545E-04	1.334E+02	1.332E+02	1.217E+02
		4.617E-04	1.305E+02	1.337E+02	1.220E+02
		4.000E-04	1.266E+02	1.284E+02	1.188E+02
		3.774E-04	1.250E+02	1.258E+02	1.173E+02
		3.571E-04	1.187E+02	1.232E+02	1.157E+02
		3.448E-04	1.215E+02	1.215E+02	1.146E+02
		3.333E-04	1.160E+02	1.197E+02	1.136E+02
		3.125E-04	1.160E+02	1.160E+02	1.113E+02
		3.077E-04	1.103E+02	1.151E+02	1.107E+02
		2.857E-04	1.096E+02	1.105E+02	1.078E+02
		2.667E-04	1.050E+02	1.059E+02	1.047E+02
		2.500E-04	1.008E+02	1.015E+02	1.016E+02
		2.326E-04	9.611E+01	9.633E+01	9.777E+01
		2.326E-04	9.525E+01	9.633E+01	9.777E+01
		2.128E-04	8.911E+01	8.986E+01	9.268E+01
		2.000E-04	8.521E+01	8.533E+01	8.893E+01
		1.923E-04	7.738E+01	8.249E+01	8.649E+01
		1.852E-04	7.856E+01	7.980E+01	8.411E+01
		1.754E-04	7.404E+01	7.597E+01	8.063E+01
		1.667E-04	7.028E+01	7.248E+01	7.735E+01
		1.563E-04	6.614E+01	6.821E+01	7.321E+01
		1.471E-04	6.273E+01	6.437E+01	6.935E+01
		1.389E-04	5.897E+01	6.092E+01	6.578E+01
		1.299E-04	5.516E+01	5.713E+01	6.174E+01
		1.220E-04	5.155E+01	5.382E+01	5.810E+01
		1.136E-04	4.863E+01	5.033E+01	5.418E+01
		1.075E-04	4.648E+01	4.784E+01	5.132E+01
		1.042E-04	4.514E+01	4.652E+01	4.976E+01
		1.000E-04	4.320E+01	4.485E+01	4.780E+01
35.4	0.06597	2.500E-03	7.132E+01	7.854E+01	6.835E+01
		2.000E-03	7.113E+01	7.789E+01	6.791E+01
		1.667E-03	7.115E+01	7.724E+01	6.747E+01
		1.429E-03	7.011E+01	7.659E+01	6.704E+01
		1.250E-03	7.000E+01	7.594E+01	6.660E+01
		1.000E-03	6.880E+01	7.464E+01	6.573E+01
		8.000E-04	6.981E+01	7.300E+01	6.463E+01
		7.692E-04	6.726E+01	7.269E+01	6.441E+01
		7.143E-04	6.860E+01	7.208E+01	6.396E+01
		6.667E-04	6.803E+01	7.150E+01	6.352E+01
		5.882E-04	6.804E+01	7.034E+01	6.268E+01
		5.405E-04	6.636E+01	6.941E+01	6.208E+01
		5.000E-04	6.596E+01	6.837E+01	6.151E+01
		4.651E-04	6.567E+01	6.718E+01	6.093E+01
		4.348E-04	6.449E+01	6.586E+01	6.033E+01
		4.167E-04	6.383E+01	6.490E+01	5.989E+01
		4.000E-04	6.292E+01	6.389E+01	5.942E+01
		3.774E-04	6.154E+01	6.230E+01	5.866E+01
		3.571E-04	5.926E+01	6.062E+01	5.781E+01
		3.333E-04	5.792E+01	5.833E+01	5.656E+01
		3.125E-04	5.584E+01	5.601E+01	5.519E+01
		2.941E-04	5.379E+01	5.370E+01	5.371E+01
		2.703E-04	5.012E+01	5.036E+01	5.138E+01
		2.500E-04	4.723E+01	4.721E+01	4.898E+01

Temp °C	Sample Molality	t_{CP} s	Exptl s^{-1}	$R_{2(calcd)}$, s^{-1} n=6	n=4
		2.381E-04	4.549E+01	4.524E+01	4.738E+01
		2.273E-04	4.352E+01	4.338E+01	4.581E+01
		2.128E-04	4.021E+01	4.079E+01	4.351E+01
		2.041E-04	3.954E+01	3.920E+01	4.203E+01
		1.961E-04	3.779E+01	3.771E+01	4.061E+01
		1.887E-04	3.637E+01	3.631E+01	3.925E+01
		1.786E-04	3.471E+01	3.440E+01	3.731E+01
		1.724E-04	3.346E+01	3.321E+01	3.609E+01
		1.667E-04	3.227E+01	3.213E+01	3.494E+01
		1.667E-04	3.236E+01	3.213E+01	3.494E+01
		1.613E-04	3.154E+01	3.110E+01	3.384E+01
		1.563E-04	2.993E+01	3.015E+01	3.281E+01
		1.471E-04	2.872E+01	2.841E+01	3.088E+01
		1.471E-04	2.841E+01	2.841E+01	3.088E+01
		1.429E-04	2.799E+01	2.763E+01	2.999E+01
		1.389E-04	2.757E+01	2.689E+01	2.915E+01
		1.351E-04	2.655E+01	2.620E+01	2.834E+01
		1.229E-04	2.593E+01	2.401E+01	2.576E+01
		1.250E-04	2.483E+01	2.438E+01	2.620E+01
		1.220E-04	2.428E+01	2.386E+01	2.557E+01
		1.176E-04	2.334E+01	2.309E+01	2.465E+01
		1.149E-04	2.280E+01	2.263E+01	2.409E+01
		1.111E-04	2.218E+01	2.199E+01	2.331E+01
		1.099E-04	2.185E+01	2.180E+01	2.306E+01
		1.053E-04	2.133E+01	2.104E+01	2.213E+01
		1.000E-04	2.044E+01	2.020E+01	2.107E+01
35.0	0.1278	2.000E-03	1.365E+02	1.491E+02	1.301E+02
		1.250E-03	1.387E+02	1.▓▓▓E+02	1.276E+02
		1.220E-03	1.394E+02	1.▓▓▓E+02	1.274E+02
		1.053E-03	1.371E+02	1.43▓E+02	1.264E+02
		1.000E-03	1.380E+02	1.429E+02	1.259E+02
		9.091E-04	1.364E+02	1.416E+02	1.251E+02
		8.333E-04	1.362E+02	1.404E+02	1.243E+02
		7.407E-04	1.348E+02	1.386E+02	1.230E+02
		6.250E-04	1.308E+02	1.358E+02	1.209E+02
		5.556E-04	1.310E+02	1.335E+02	1.194E+02
		5.000E-04	1.286E+02	1.309E+02	1.179E+02
		4.545E-04	1.267E+02	1.277E+02	1.165E+02
		4.348E-04	1.263E+02	1.259E+02	1.157E+02
		4.167E-04	1.240E+02	1.240E+02	1.148E+02
		4.000E-04	1.213E+02	1.220E+02	1.139E+02
		3.571E-04	1.175E+02	1.155E+02	1.108E+02
		3.226E-04	1.110E+02	1.087E+02	1.070E+02
		3.125E-04	1.045E+02	1.065E+02	1.056E+02
		3.030E-04	1.054E+02	1.042E+02	1.041E+02
		2.941E-04	1.045E+02	1.020E+02	1.027E+02
		2.778E-04	1.009E+02	9.761E+01	9.964E+01
		2.632E-04	9.607E+01	9.342E+01	9.654E+01
		2.564E-04	9.420E+01	9.138E+01	9.496E+01
		2.381E-04	8.800E+01	8.562E+01	9.027E+01
		2.273E-04	8.476E+01	8.206E+01	8.721E+01
		2.174E-04	8.092E+01	7.871E+01	8.421E+01
		2.041E-04	7.694E+01	7.408E+01	7.990E+01
		1.923E-04	7.311E+01	6.989E+01	7.582E+01
		1.786E-04	6.746E+01	6.497E+01	7.082E+01
		1.613E-04	6.053E+01	5.873E+01	6.418E+01
		1.429E-04	5.451E+01	5.221E+01	5.686E+01
		1.250E-04	4.694E+01	4.611E+01	4.967E+01
		1.111E-04	4.184E+01	4.163E+01	4.420E+01
		1.000E-04	3.843E+01	3.828E+01	3.999E+01
29.8	0.1278	2.500E-03	1.149E+02	1.209E+02	1.052E+02
		2.500E-03	1.135E+02	1.209E+02	1.052E+02

Temp °C	Sample Molality	t_{CP} / s	Exptl / s^{-1}	$R_{2(calcd)}$ / s^{-1} n=6	n=4
		1.000E-03	1.128E+02	1.163E+02	1.023E+02
		6.667E-04	1.090E+02	1.134E+02	9.952E+01
		5.000E-04	1.085E+02	1.100E+02	9.816E+01
		4.348E-04	1.086E+02	1.054E+02	9.720E+01
		3.846E-04	1.056E+02	9.947E+01	9.515E+01
		3.571E-04	9.705E+01	9.516E+01	9.315E+01
		3.333E-04	9.332E+01	9.080E+01	9.074E+01
		3.030E-04	8.821E+01	8.443E+01	8.660E+01
		2.857E-04	8.371E+01	8.041E+01	8.365E+01
		2.632E-04	7.928E+01	7.484E+01	7.916E+01
		2.500E-04	7.377E+01	7.141E+01	7.618E+01
		2.222E-04	6.707E+01	6.393E+01	6.915E+01
		2.000E-04	6.207E+01	5.783E+01	6.290E+01
		1.818E-04	5.823E+01	5.284E+01	5.748E+01
		1.667E-04	5.349E+01	4.879E+01	5.287E+01
		1.563E-04	5.105E+01	4.606E+01	4.967E+01
		1.471E-04	4.849E+01	4.371E+01	4.686E+01
		1.429E-04	4.675E+01	4.266E+01	4.558E+01
		1.389E-04	4.635E+01	4.168E+01	4.437E+01
		1.316E-04	4.569E+01	3.992E+01	4.219E+01
		1.250E-04	4.379E+01	3.838E+01	4.025E+01
		1.176E-04	4.327E+01	3.671E+01	3.813E+01
		1.111E-04	4.288E+01	3.530E+01	3.631E+01
30.2	0.06597	2.500E-03	6.098E+01	6.376E+01	5.549E+01
		2.000E-03	5.730E+01	6.336E+01	5.522E+01
		1.000E-03	5.992E+01	6.133E+01	5.389E+01
		5.882E-04	5.810E+01	5.922E+01	5.201E+01
		5.000E-04	5.746E+01	5.789E+01	5.164E+01
		4.545E-04	5.623E+01	5.643E+01	5.133E+01
		4.167E-04	5.350E+01	5.460E+01	5.082E+01
		3.704E-04	5.107E+01	5.142E+01	4.956E+01
		3.333E-04	4.734E+01	4.804E+01	4.778E+01
		3.030E-04	4.401E+01	4.473E+01	4.565E+01
		2.703E-04	4.154E+01	4.065E+01	4.258E+01
		2.381E-04	3.740E+01	3.622E+01	3.874E+01
		2.083E-04	3.276E+01	3.191E+01	3.455E+01
		1.852E-04	3.000E+01	2.853E+01	3.09?E+01
		1.724E-04	2.781E+01	2.668E+01	2.891E+01
		1.389E-04	2.248E+01	2.206E+01	2.347E+01
		1.282E-04	2.101E+01	2.069E+01	2.177E+01
		1.190E-04	1.986E+01	1.956E+01	2.035E+01
		1.124E-04	1.902E+01	1.878E+01	1.935E+01
		1.053E-04	1.795E+01	1.799E+01	1.832E+01
29.8	0.06597	1.000E-04	1.726E+01	1.741E+01	1.757E+01
		5.000E-03	5.891E+01	6.336E+01	5.500E+01
		2.500E-03	5.891E+01	6.258E+01	5.447E+01
		2.000E-03	5.909E+01	6.220E+01	5.422E+01
		1.852E-03	5.821E+01	6.204E+01	5.411E+01
		1.667E-03	5.936E+01	6.181E+01	5.396E+01
		1.515E-03	5.813E+01	6.158E+01	5.381E+01
		1.429E-03	5.853E+01	6.143E+01	5.370E+01
		1.250E-03	5.793E+01	6.106E+01	5.345E+01
		1.111E-03	5.792E+01	6.068E+01	5.319E+01
		1.000E-03	5.702E+01	6.025E+01	5.294E+01
		9.524E-04	5.666E+01	6.002E+01	5.283E+01
		9.091E-04	5.636E+01	5.979E+01	5.270E+01
		8.333E-04	5.680E+01	5.938E+01	5.243E+01
		7.692E-04	5.613E+01	5.907E+01	5.213E+01
		7.143E-04	5.617E+01	5.885E+01	5.182E+01
		6.250E-04	5.578E+01	5.851E+01	5.130E+01

Temp °C	Sample Molality	t_{CP} s	Exptl s^{-1}	$R_{2(calcd)}$, s^{-1} n=6	s^{-1} n=4
		5.556E-04	5.480E+01	5.797E+01	5.101E+01
		5.000E-04	5.528E+01	5.700E+01	5.082E+01
		5.000E-04	5.681E+01	5.700E+01	5.082E+01
		4.545E-04	5.600E+01	5.555E+01	5.054E+01
		4.000E-04	5.379E+01	5.273E+01	4.970E+01
		3.846E-04	5.329E+01	5.167E+01	4.929E+01
		3.571E-04	5.099E+01	4.947E+01	4.827E+01
		3.333E-04	4.954E+01	4.724E+01	4.704E+01
		3.125E-04	4.782E+01	4.504E+01	4.567E+01
		2.941E-04	4.494E+01	4.292E+01	4.418E+01
		2.778E-04	4.313E+01	4.091E+01	4.266E+01
		2.564E-04	3.968E+01	3.811E+01	4.034E+01
		2.326E-04	3.636E+01	3.483E+01	3.738E+01
		2.174E-04	3.430E+01	3.268E+01	3.528E+01
		2.000E-04	3.190E+01	3.019E+01	3.273E+01
		1.887E-04	2.919E+01	2.858E+01	3.100E+01
		1.754E-04	2.789E+01	2.669E+01	2.891E+01
		1.667E-04	2.681E+01	2.548E+01	2.753E+01
		1.563E-04	2.522E+01	2.406E+01	2.587E+01
		1.471E-04	2.375E+01	2.283E+01	2.440E+01
		1.370E-04	2.205E+01	2.153E+01	2.281E+01
		1.282E-04	2.077E+01	2.043E+01	2.145E+01
		1.190E-04	1.972E+01	1.934E+01	2.007E+01
		1.111E-04	1.885E+01	1.844E+01	1.891E+01
		1.053E-04	1.778E+01	1.781E+01	1.809E+01
		1.000E-04	1.701E+01	1.725E+01	1.737E+01
24.7	0.1278	2.000E-03	8.398E+01	8.768E+01	7.683E+01
		1.000E-03	8.356E+01	8.581E+01	7.570E+01
		6.667E-04	8.323E+01	8.484E+01	7.399E+01
		5.556E-04	8.320E+01	8.476E+01	7.394E+01
		5.000E-04	8.374E+01	8.350E+01	7.427E+01
		4.545E-04	8.263E+01	8.131E+01	7.430E+01
		4.000E-04	7.795E+01	7.693E+01	7.334E+01
		3.636E-04	7.462E+01	7.282E+01	7.162E+01
		3.333E-04	6.968E+01	6.867E+01	6.928E+01
		3.030E-04	6.657E+01	6.395E+01	6.602E+01
		2.778E-04	6.246E+01	5.964E+01	6.258E+01
		2.500E-04	5.640E+01	5.461E+01	5.806E+01
		2.273E-04	5.230E+01	5.038E+01	5.387E+01
		2.000E-04	4.743E+01	4.528E+01	4.841E+01
		1.942E-04	4.647E+01	4.421E+01	4.721E+01
		1.786E-04	4.410E+01	4.138E+01	4.394E+01
		1.667E-04	4.102E+01	3.927E+01	4.143E+01
		1.575E-04	3.961E+01	3.769E+01	3.950E+01
		1.493E-04	3.886E+01	3.632E+01	3.781E+01
		1.429E-04	3.753E+01	3.528E+01	3.650E+01
		1.351E-04	3.616E+01	3.405E+01	3.493E+01
		1.250E-04	3.554E+01	3.252E+01	3.296E+01
		1.176E-04	3.537E+01	3.146E+01	3.157E+01
25.1	0.06597	5.000E-03	4.551E+01	4.711E+01	4.114E+01
		2.000E-03	4.572E+01	4.651E+01	4.074E+01
		2.000E-03	4.565E+01	4.651E+01	4.074E+01
		2.000E-03	4.569E+01	4.651E+01	4.074E+01
		1.000E-03	4.449E+01	4.550E+01	4.012E+01
		7.143E-04	4.377E+01	4.484E+01	3.940E+01
		5.000E-04	4.434E+01	4.420E+01	3.930E+01
		4.545E-04	4.458E+01	4.307E+01	3.930E+01
		4.167E-04	4.309E+01	4.160E+01	3.904E+01
		3.846E-04	4.147E+01	3.993E+01	3.848E+01
		3.571E-04	3.979E+01	3.819E+01	3.767E+01

Temp °C	Sample Molality	t_{CP} s	Exptl s^{-1}	$R_{2(calcd)}$, s^{-1} n=6	n=4
		3.333E-04	3.854E+01	3.645E+01	3.667E+01
		3.125E-04	3.679E+01	3.477E+01	3.556E+01
		2.857E-04	3.411E+01	3.240E+01	3.376E+01
		2.632E-04	3.173E+01	3.028E+01	3.195E+01
		2.273E-04	2.817E+01	2.674E+01	2.855E+01
		2.000E-04	2.547E+01	2.401E+01	2.564E+01
		1.667E-04	2.188E+01	2.078E+01	2.192E+01
		1.563E-04	2.104E+01	1.982E+01	2.075E+01
		1.429E-04	1.986E+01	1.863E+01	1.928E+01
		1.351E-04	1.913E+01	1.797E+01	1.844E+01
		1.250E-04	1.864E+01	1.715E+01	1.738E+01
		1.163E-04	1.818E+01	1.647E+01	1.650E+01
		1.087E-04	1.734E+01	1.591E+01	1.576E+01
19.6	0.1278	2.000E-03	6.301E+01	6.108E+01	5.425E+01
		1.000E-03	6.107E+01	6.029E+01	5.379E+01
		6.667E-04	5.973E+01	5.999E+01	5.273E+01
		5.556E-04	5.994E+01	6.033E+01	5.293E+01
		5.000E-04	5.727E+01	5.963E+01	5.337E+01
		4.545E-04	5.759E+01	5.826E+01	5.358E+01
		4.167E-04	5.594E+01	5.646E+01	5.336E+01
		3.704E-04	5.262E+01	5.337E+01	5.227E+01
		3.333E-04	5.214E+01	5.020E+01	5.050E+01
		2.941E-04	4.663E+01	4.630E+01	4.765E+01
		2.500E-04	4.289E+01	4.144E+01	4.327E+01
		2.381E-04	4.142E+01	4.008E+01	4.191E+01
		2.000E-04	3.662E+01	3.574E+01	3.719E+01
		1.667E-04	3.224E+01	3.212E+01	3.286E+01
		1.429E-04	3.016E+01	2.972E+01	2.983E+01
		1.250E-04	2.800E+01	2.808E+01	2.767E+01
		1.111E-04	2.707E+01	2.692E+01	2.611E+01
		1.000E-04	2.676E+01	2.606E+01	2.494E+01
16.4	0.1278	5.000E-03	5.066E+01	4.876E+01	4.382E+01
		2.500E-03	5.088E+01	4.858E+01	4.370E+01
		2.500E-03	4.905E+01	4.858E+01	4.370E+01
		1.000E-03	4.649E+01	4.806E+01	4.337E+01
		5.882E-04	4.769E+01	4.822E+01	4.263E+01
		5.000E-04	4.637E+01	4.777E+01	4.317E+01
		4.762E-04	4.700E+01	4.736E+01	4.331E+01
		4.348E-04	4.494E+01	4.625E+01	4.336E+01
		4.000E-04	4.359E+01	4.490E+01	4.309E+01
		3.704E-04	4.186E+01	4.343E+01	4.253E+01
		3.448E-04	4.037E+01	4.195E+01	4.174E+01
		3.125E-04	3.840E+01	3.982E+01	4.032E+01
		2.857E-04	3.705E+01	3.787E+01	3.875E+01
		2.632E-04	3.496E+01	3.614E+01	3.719E+01
		2.500E-04	3.316E+01	3.510E+01	3.618E+01
		2.381E-04	3.192E+01	3.415E+01	3.522E+01
		2.174E-04	2.946E+01	3.250E+01	3.344E+01
		2.000E-04	2.836E+01	3.113E+01	3.188E+01
		1.852E-04	2.595E+01	2.998E+01	3.052E+01
		1.667E-04	2.444E+01	2.860E+01	2.882E+01
		1.429E-04	2.333E+01	2.694E+01	2.668E+01
		1.351E-04	2.232E+01	2.643E+01	2.601E+01
		1.250E-04	2.106E+01	2.580E+01	2.516E+01
		1.111E-04	2.047E+01	2.499E+01	2.406E+01
4.9	0.02433	5.000E-03	4.797E+00	4.596E+00	4.472E+00
		2.500E-03	4.659E+00	4.577E+00	4.455E+00
		1.000E-03	4.913E+00	4.565E+00	4.438E+00
		6.667E-04	4.687E+00	4.547E+00	4.414E+00
		5.000E-04	4.750E+00	4.562E+00	4.432E+00

Temp °C	Sample Molality	t_{CP} s	Exptl s^{-1}	$R_{2(calcd)}$, s^{-1}	
				n=6	n=4
		4.000E-04	4.728E+00	4.471E+00	4.443E+00
		3.333E-04	4.581E+00	4.343E+00	4.385E+00
		2.857E-04	4.396E+00	4.222E+00	4.293E+00
		2.500E-04	4.203E+00	4.121E+00	4.195E+00
		2.273E-04	4.088E+00	4.054E+00	4.123E+00
		2.000E-04	3.919E+00	3.973E+00	4.028E+00
		1.905E-04	3.903E+00	3.946E+00	3.993E+00
		1.667E-04	3.824E+00	3.879E+00	3.907E+00
		1.429E-04	3.798E+00	3.816E+00	3.822E+00
		1.250E-04	3.724E+00	3.773E+00	3.761E+00

II. At 15 MHz

Temp °C	Sample Molality	t_{CP} s	Exptl s^{-1}	R_2 (calcd), s^{-1} n=6	n=4
30.1	0.1278	5.000E-03	5.259E+01	4.853E+01	4.622E+01
		4.000E-03	5.046E+01	4.815E+01	4.597E+01
		3.333E-03	4.980E+01	4.778E+01	4.572E+01
		2.857E-03	5.057E+01	4.740E+01	4.547E+01
		2.500E-03	5.035E+01	4.703E+01	4.522E+01
		2.222E-03	4.873E+01	4.666E+01	4.498E+01
		2.000E-03	4.968E+01	4.629E+01	4.473E+01
		2.000E-03	4.759E+01	4.629E+01	4.473E+01
		1.818E-03	4.846E+01	4.592E+01	4.448E+01
		1.667E-03	4.716E+01	4.555E+01	4.424E+01
		1.538E-03	4.665E+01	4.517E+01	4.399E+01
		1.429E-03	4.650E+01	4.480E+01	4.374E+01
		1.250E-03	4.538E+01	4.405E+01	4.325E+01
		1.111E-03	4.419E+01	4.329E+01	4.275E+01
		1.000E-03	4.238E+01	4.253E+01	4.226E+01
		8.696E-04	4.186E+01	4.138E+01	4.151E+01
		7.692E-04	4.022E+01	4.024E+01	4.074E+01
		6.666E-04	3.904E+01	3.878E+01	3.972E+01
		5.882E-04	3.709E+01	3.741E+01	3.871E+01
		5.405E-04	3.565E+01	3.646E+01	3.796E+01
		5.000E-04	3.486E+01	3.559E+01	3.723E+01
		4.444E-04	3.342E+01	3.428E+01	3.608E+01
		4.000E-04	3.173E+01	3.316E+01	3.503E+01
		3.636E-04	3.078E+01	3.220E+01	3.406E+01
		3.333E-04	3.006E+01	3.138E+01	3.320E+01
		2.941E-04	2.952E+01	3.031E+01	3.201E+01
		2.703E-04	2.830E+01	2.967E+01	3.125E+01
		2.500E-04	2.789E+01	2.913E+01	3.060E+01
		2.273E-04	2.716E+01	2.854E+01	2.986E+01
		2.105E-04	2.674E+01	2.812E+01	2.931E+01
		2.000E-04	2.570E+01	2.786E+01	2.897E+01
		1.852E-04	2.598E+01	2.752E+01	2.851E+01
		1.724E-04	2.625E+01	2.723E+01	2.811E+01
		1.666E-04	2.588E+01	2.711E+01	2.793E+01
		1.666E-04	2.611E+01	2.711E+01	2.793E+01
		1.563E-04	2.638E+01	2.689E+01	2.763E+01
		1.538E-04	2.563E+01	2.684E+01	2.756E+01
		1.429E-04	2.560E+01	2.662E+01	2.725E+01
		1.250E-04	2.494E+01	2.630E+01	2.677E+01
		1.111E-04	2.494E+01	2.607E+01	2.643E+01
		1.000E-04	2.442E+01	2.590E+01	2.617E+01
30.2	0.06597	1.000E-02	2.639E+01	2.579E+01	2.434E+01
		1.000E-02	2.638E+01	2.579E+01	2.434E+01
		6.667E-03	2.528E+01	2.557E+01	2.419E+01
		5.000E-03	2.494E+01	2.537E+01	2.405E+01
		4.000E-03	2.500E+01	2.517E+01	2.392E+01
		3.333E-03	2.444E+01	2.497E+01	2.379E+01
		2.500E-03	2.382E+01	2.459E+01	2.353E+01
		2.000E-03	2.320E+01	2.420E+01	2.328E+01
		1.666E-03	2.300E+01	2.381E+01	2.302E+01
		1.429E-03	2.238E+01	2.343E+01	2.277E+01
		1.250E-03	2.268E+01	2.304E+01	2.252E+01

Temp °C	Sample Molality	t_{CP} s	Exptl s^{-1}	R_2(calcd), s^{-1} n=6	n=4
		1.250E-03	2.246E+01	2.304E+01	2.252E+01
		1.111E-03	2.167E+01	2.265E+01	2.226E+01
		1.111E-03	2.223E+01	2.265E+01	2.226E+01
		1.000E-03	2.223E+01	2.225E+01	2.201E+01
		1.000E-03	2.164E+01	2.225E+01	2.201E+01
		9.090E-04	2.146E+01	2.185E+01	2.175E+01
		8.333E-04	2.063E+01	2.146E+01	2.149E+01
		7.143E-04	1.953E+01	2.068E+01	2.097E+01
		6.250E-04	1.895E+01	1.994E+01	2.044E+01
		5.555E-04	1.792E+01	1.926E+01	1.992E+01
		5.000E-04	1.744E+01	1.864E+01	1.942E+01
		4.444E-04	1.677E+01	1.795E+01	1.882E+01
		4.000E-04	1.655E+01	1.736E+01	1.827E+01
		3.571E-04	1.563E+01	1.676E+01	1.768E+01
		3.226E-04	1.560E+01	1.627E+01	1.716E+01
		2.857E-04	1.581E+01	1.574E+01	1.656E+01
		2.857E-04	1.511E+01	1.574E+01	1.656E+01
		2.500E-04	1.470E+01	1.524E+01	1.596E+01
		2.500E-04	1.442E+01	1.524E+01	1.596E+01
		2.174E-04	1.350E+01	1.480E+01	1.541E+01
		2.174E-04	1.416E+01	1.480E+01	1.541E+01
		2.000E-04	1.395E+01	1.457E+01	1.511E+01
		2.000E-04	1.441E+01	1.457E+01	1.511E+01
		1.818E-04	1.384E+01	1.435E+01	1.481E+01
		1.818E-04	1.321E+01	1.435E+01	1.481E+01
		1.666E-04	1.313E+01	1.417E+01	1.457E+01
		1.429E-04	1.334E+01	1.392E+01	1.421E+01
		1.250E-04	1.331E+01	1.374E+01	1.395E+01
		1.111E-04	1.349E+01	1.362E+01	1.377E+01
25.0	0.1278	1.000E-04	1.326E+01	1.353E+01	1.364E+01
		5.000E-03	5.022E+01	4.983E+01	4.665E+01
		4.444E-03	5.149E+01	4.958E+01	4.648E+01
		4.000E-03	5.168E+01	4.932E+01	4.632E+01
		3.636E-03	5.167E+01	4.907E+01	4.616E+01
		3.333E-03	5.044E+01	4.882E+01	4.599E+01
		3.077E-03	4.997E+01	4.857E+01	4.583E+01
		2.857E-03	4.993E+01	4.831E+01	4.567E+01
		2.667E-03	4.945E+01	4.806E+01	4.551E+01
		2.500E-03	4.945E+01	4.781E+01	4.535E+01
		2.273E-03	4.896E+01	4.741E+01	4.509E+01
		2.000E-03	4.821E+01	4.680E+01	4.470E+01
		1.666E-03	4.652E+01	4.578E+01	4.406E+01
		1.429E-03	4.579E+01	4.472E+01	4.342E+01
		1.250E-03	4.474E+01	4.361E+01	4.277E+01
		1.111E-03	4.324E+01	4.246E+01	4.209E+01
		1.000E-03	4.136E+01	4.130E+01	4.140E+01
		8.696E-04	3.973E+01	3.959E+01	4.031E+01
		7.692E-04	3.768E+01	3.797E+01	3.919E+01
		6.666E-04	3.495E+01	3.602E+01	3.770E+01
		5.882E-04	3.279E+01	3.435E+01	3.628E+01
		5.263E-04	3.224E+01	3.293E+01	3.497E+01
		4.762E-04	3.086E+01	3.174E+01	3.378E+01
		4.348E-04	3.030E+01	3.074E+01	3.272E+01
		4.000E-04	2.909E+01	2.990E+01	3.179E+01
		3.636E-04	2.772E+01	2.904E+01	3.078E+01
		3.333E-04	2.762E+01	2.833E+01	2.992E+01
		3.077E-04	2.728E+01	2.776E+01	2.920E+01
		2.857E-04	2.711E+01	2.728E+01	2.858E+01
		2.857E-04	2.701E+01	2.728E+01	2.858E+01
		2.667E-04	2.652E+01	2.688E+01	2.805E+01

Temp °C	Sample Molality	t_{CP} s	Exptl s^{-1}	$R_{2(calcd)}$, s^{-1} n=6	n=4
		2.632E-04	2.635E+01	2.681E+01	2.795E+01
		2.500E-04	2.595E+01	2.654E+01	2.759E+01
		2.273E-04	2.551E+01	2.611E+01	2.699E+01
		2.083E-04	2.458E+01	2.577E+01	2.651E+01
		1.887E-04	2.489E+01	2.544E+01	2.604E+01
		1.852E-04	2.471E+01	2.538E+01	2.595E+01
		1.667E-04	2.426E+01	2.510E+01	2.554E+01
		1.429E-04	2.359E+01	2.477E+01	2.505E+01
		1.250E-04	2.345E+01	2.455E+01	2.472E+01
		1.163E-04	2.359E+01	2.446E+01	2.458E+01
		1.034E-04	2.332E+01	2.433E+01	2.438E+01
25.0	0.06597	1.000E-04	2.357E+01	2.429E+01	2.433E+01
		1.000E-02	2.628E+01	2.649E+01	2.457E+01
		6.666E-03	2.585E+01	2.620E+01	2.438E+01
		5.714E-03	2.622E+01	2.607E+01	2.429E+01
		5.000E-03	2.592E+01	2.593E+01	2.420E+01
		4.348E-03	2.602E+01	2.577E+01	2.410E+01
		3.704E-03	2.539E+01	2.556E+01	2.396E+01
		3.333E-03	2.528E+01	2.540E+01	2.386E+01
		2.857E-03	2.454E+01	2.514E+01	2.369E+01
		2.500E-03	2.494E+01	2.488E+01	2.352E+01
		2.000E-03	2.436E+01	2.436E+01	2.319E+01
		1.667E-03	2.384E+01	2.383E+01	2.286E+01
		1.429E-03	2.270E+01	2.329E+01	2.253E+01
		1.250E-03	2.170E+01	2.271E+01	2.219E+01
		1.111E-03	2.162E+01	2.211E+01	2.184E+01
		1.000E-03	2.114E+01	2.150E+01	2.148E+01
		9.090E-04	2.036E+01	2.090E+01	2.111E+01
		8.333E-04	1.962E+01	2.032E+01	2.072E+01
		7.692E-04	1.985E+01	1.976E+01	2.033E+01
		7.692E-04	1.942E+01	1.976E+01	2.033E+01
		6.897E-04	1.891E+01	1.898E+01	1.975E+01
		6.250E-04	1.772E+01	1.828E+01	1.918E+01
		5.555E-04	1.684E+01	1.748E+01	1.847E+01
		5.000E-04	1.643E+01	1.680E+01	1.782E+01
		4.545E-04	1.713E+01	1.623E+01	1.723E+01
		4.167E-04	1.595E+01	1.576E+01	1.672E+01
		3.774E-04	1.528E+01	1.527E+01	1.616E+01
		3.448E-04	1.552E+01	1.487E+01	1.568E+01
		3.333E-04	1.530E+01	1.473E+01	1.552E+01
		3.077E-04	1.443E+01	1.443E+01	1.514E+01
		3.030E-04	1.410E+01	1.438E+01	1.507E+01
		2.857E-04	1.459E+01	1.419E+01	1.482E+01
		2.778E-04	1.508E+01	1.410E+01	1.470E+01
		2.500E-04	1.414E+01	1.381E+01	1.431E+01
		2.326E-04	1.410E+01	1.363E+01	1.407E+01
		2.222E-04	1.443E+01	1.353E+01	1.393E+01
		2.174E-04	1.442E+01	1.349E+01	1.387E+01
		2.128E-04	1.388E+01	1.344E+01	1.381E+01
		2.000E-04	1.385E+01	1.333E+01	1.364E+01
		1.923E-04	1.345E+01	1.326E+01	1.355E+01
		1.724E-04	1.355E+01	1.310E+01	1.331E+01
		1.667E-04	1.351E+01	1.306E+01	1.325E+01
		1.563E-04	1.284E+01	1.298E+01	1.314E+01
		1.429E-04	1.332E+01	1.289E+01	1.300E+01
		1.250E-04	1.326E+01	1.278E+01	1.283E+01
		1.111E-04	1.283E+01	1.270E+01	1.271E+01
		1.000E-04	1.298E+01	1.264E+01	1.263E+01
20.7	0.1278	5.000E-03	4.876E+01	4.705E+01	4.350E+01
		4.000E-03	4.867E+01	4.656E+01	4.319E+01

Temp °C	Sample Molality	t_{CP} s	Exptl s^{-1}	R_2(calcd), s^{-1} n=6	n=4
		3.333E-03	4.719E+01	4.606E+01	4.288E+01
		2.857E-03	4.698E+01	4.557E+01	4.258E+01
		2.500E-03	4.645E+01	4.509E+01	4.227E+01
		2.222E-03	4.643E+01	4.462E+01	4.196E+01
		2.000E-03	4.538E+01	4.414E+01	4.166E+01
		1.818E-03	4.527E+01	4.363E+01	4.136E+01
		1.667E-03	4.507E+01	4.309E+01	4.107E+01
		1.538E-03	4.445E+01	4.250E+01	4.077E+01
		1.428E-03	4.402E+01	4.188E+01	4.047E+01
		1.333E-03	4.320E+01	4.123E+01	4.015E+01
		1.250E-03	4.247E+01	4.056E+01	3.981E+01
		1.111E-03	4.101E+01	3.917E+01	3.909E+01
		1.000E-03	3.894E+01	3.779E+01	3.829E+01
		9.090E-04	3.783E+01	3.648E+01	3.745E+01
		7.692E-04	3.556E+01	3.413E+01	3.571E+01
		6.666E-04	3.341E+01	3.219E+01	3.405E+01
		5.882E-04	3.189E+01	3.064E+01	3.255E+01
		5.263E-04	3.103E+01	2.939E+01	3.124E+01
		5.000E-04	3.040E+01	2.886E+01	3.066E+01
		4.651E-04	2.917E+01	2.817E+01	2.986E+01
		4.444E-04	2.853E+01	2.776E+01	2.938E+01
		4.166E-04	2.739E+01	2.723E+01	2.874E+01
		3.846E-04	2.786E+01	2.663E+01	2.799E+01
		3.703E-04	2.647E+01	2.637E+01	2.766E+01
		3.448E-04	2.651E+01	2.592E+01	2.707E+01
		3.125E-04	2.550E+01	2.538E+01	2.635E+01
		2.857E-04	2.608E+01	2.496E+01	2.577E+01
		2.703E-04	2.573E+01	2.473E+01	2.544E+01
		2.500E-04	2.497E+01	2.444E+01	2.503E+01
		2.134E-04	2.501E+01	2.396E+01	2.434E+01
		2.000E-04	2.482E+01	2.380E+01	2.411E+01
		1.818E-04	2.466E+01	2.360E+01	2.381E+01
		1.563E-04	2.425E+01	2.334E+01	2.343E+01
		1.389E-04	2.396E+01	2.319E+01	2.320E+01
		1.250E-04	2.361E+01	2.308E+01	2.303E+01
		1.111E-04	2.476E+01	2.298E+01	2.288E+01
		1.000E-04	2.410E+01	2.291E+01	2.277E+01
21.0	0.06597	1.000E-02	2.440E+01	2.513E+01	2.308E+01
		8.333E-03	2.430E+01	2.502E+01	2.301E+01
		6.666E-03	2.462E+01	2.486E+01	2.290E+01
		6.666E-03	2.395E+01	2.486E+01	2.290E+01
		5.882E-03	2.465E+01	2.475E+01	2.283E+01
		5.000E-03	2.379E+01	2.459E+01	2.273E+01
		4.545E-03	2.417E+01	2.449E+01	2.266E+01
		4.000E-03	2.425E+01	2.433E+01	2.256E+01
		3.333E-03	2.378E+01	2.408E+01	2.240E+01
		2.857E-03	2.340E+01	2.382E+01	2.224E+01
		2.500E-03	2.326E+01	2.357E+01	2.208E+01
		2.000E-03	2.267E+01	2.307E+01	2.176E+01
		1.666E-03	2.239E+01	2.253E+01	2.145E+01
		1.429E-03	2.176E+01	2.193E+01	2.114E+01
		1.250E-03	2.076E+01	2.125E+01	2.080E+01
		1.111E-03	1.993E+01	2.054E+01	2.043E+01
		1.111E-03	1.988E+01	2.054E+01	2.043E+01
		1.000E-03	1.987E+01	1.984E+01	2.003E+01
		1.000E-03	1.968E+01	1.984E+01	2.003E+01
		9.090E-04	1.908E+01	1.916E+01	1.959E+01
		8.333E-04	1.858E+01	1.853E+01	1.915E+01
		7.143E-04	1.687E+01	1.741E+01	1.827E+01
		6.250E-04	1.629E+01	1.649E+01	1.745E+01

Temp °C	Sample Molality	t_{CP} s	Exptl s^{-1}	$R_{2(calcd)}$, s^{-1} n=6	n=4
		5.556E-04	1.551E+01	1.576E+01	1.672E+01
		5.000E-04	1.469E+01	1.517E+01	1.608E+01
		4.444E-04	1.426E+01	1.458E+01	1.541E+01
		4.000E-04	1.363E+01	1.413E+01	1.487E+01
		3.571E-04	1.328E+01	1.372E+01	1.434E+01
		3.223E-04	1.327E+01	1.340E+01	1.392E+01
		2.857E-04	1.281E+01	1.309E+01	1.350E+01
		2.500E-04	1.318E+01	1.281E+01	1.311E+01
		2.273E-04	1.244E+01	1.264E+01	1.287E+01
		2.000E-04	1.237E+01	1.246E+01	1.261E+01
		1.666E-04	1.221E+01	1.227E+01	1.233E+01
		1.428E-04	1.222E+01	1.215E+01	1.215E+01
		1.250E-04	1.225E+01	1.208E+01	1.203E+01
		1.111E-04	1.198E+01	1.202E+01	1.195E+01
15.4	0.06597	1.000E-04	1.185E+01	1.198E+01	1.189E+01
		1.000E-02	2.058E+01	2.076E+01	1.898E+01
		8.000E-03	2.065E+01	2.067E+01	1.892E+01
		6.667E-03	2.029E+01	2.058E+01	1.886E+0.1
		5.714E-03	2.033E+01	2.049E+01	1.880E+01
		5.000E-03	1.990E+01	2.040E+01	1.874E+01
		4.444E-03	2.045E+01	2.032E+01	1.869E+01
		4.000E-03	1.992E+01	2.023E+01	1.864E+01
		3.333E-03	1.962E+01	2.006E+01	1.853E+01
		2.857E-03	1.932E+01	1.989E+01	1.843E+01
		2.500E-03	1.939E+01	1.976E+01	1.832E+01
		2.000E-03	1.900E+01	1.947E+01	1.813E+01
		1.667E-03	1.874E+01	1.905E+01	1.796E+01
		1.429E-03	1.814E+01	1.847E+01	1.777E+01
		1.250E-03	1.781E+01	1.780E+01	1.751E+01
		1.111E-03	1.667E+01	1.712E+01	1.717E+01
		1.000E-03	1.720E+01	1.648E+01	1.678E+01
		9.090E-04	1.583E+01	1.589E+01	1.637E+01
		8.333E-04	1.551E+01	1.536E+01	1.596E+01
		7.407E-04	1.473E+01	1.469E+01	1.536E+01
		6.667E-04	1.408E+01	1.414E+01	1.482E+01
		6.061E-04	1.389E+04	1.370E+01	1.435E+01
		5.556E-04	1.356E+01	1.333E+01	1.393E+01
		5.000E-04	1.312E+01	1.294E+01	1.347E+01
		4.545E-04	1.270E+01	1.263E+01	1.309E+01
		4.082E-04	1.245E+01	1.234E+01	1.271E+01
		3.636E-04	1.195E+01	1.207E+01	1.235E+01
		3.333E-04	1.170E+01	1.190E+01	1.212E+01
		3.077E-04	1.168E+01	1.177E+01	1.193E+01
		2.740E-04	1.133E+01	1.161E+01	1.170E+01
		2.500E-04	1.119E+01	1.150E+01	1.155E+01
		2.273E-04	1.097E+01	1.141E+01	1.141E+01
		2.000E-04	1.090E+01	1.131E+01	1.127E+01
		1.786E-04	1.108E+01	1.124E+01	1.116E+01
		1.613E-04	1.075E+01	1.118E+01	1.108E+01
		1.429E-04	1.092E+01	1.113E+01	1.101E+01
		1.250E-04	1.058E+01	1.109E+01	1.094E+01
		1.111E-04	1.069E+01	1.106E+01	1.090E+01
		1.000E-04	1.064E+01	1.104E+01	1.086E+01
10.3	0.06597	1.000E-02	1.682E+01	1.619E+01	1.491E+01
		6.667E-03	1.647E+01	1.609E+01	1.484E+01
		5.000E-03	1.626E+01	1.600E+01	1.477E+01
		4.000E-03	1.642E+01	1.591E+01	1.472E+01
		3.333E-03	1.587E+01	1.581E+01	1.467E+01
		2.857E-03	1.614E+01	1.574E+01	1.462E+01
		2.500E-03	1.600E+01	1.570E+01	1.455E+01

Temp °C	Sample Molality	t_{CP} s	Exptl s^{-1}	$R_{2(calcd)}$, s^{-1} n=6	n=4
		2.222E-03	1.593E+01	1.567E+01	1.450E+01
		2.000E-03	1.578E+01	1.561E+01	1.447E+01
		1.786E-03	1.616E+01	1.546E+01	1.445E+01
		1.667E-03	1.597E+01	1.532E+01	1.443E+01
		1.515E-03	1.564E+01	1.507E+01	1.439E+01
		1.429E-03	1.533E+01	1.488E+01	1.434E+01
		1.333E-03	1.529E+01	1.464E+01	1.427E+01
		1.250E-03	1.491E+01	1.439E+01	1.417E+01
		1.111E-03	1.448E+01	1.390E+01	1.392E+01
		1.000E-03	1.396E+01	1.346E+01	1.364E+01
		9.090E-04	1.386E+01	1.307E+01	1.334E+01
		8.000E-04	1.335E+01	1.258E+01	1.291E+01
		7.143E-04	1.254E+01	1.218E+01	1.252E+01
		6.667E-04	1.275E+01	1.197E+01	1.229E+01
		6.061E-04	1.213E+01	1.170E+01	1.199E+01
		5.405E-04	1.181E+01	1.142E+01	1.165E+01
		5.000E-04	1.163E+01	1.126E+01	1.145E+01
		4.545E-04	1.123E+01	1.108E+01	1.122E+01
		4.167E-04	1.094E+01	1.094E+01	1.104E+01
		3.846E-04	1.097E+01	1.083E+01	1.089E+01
		3.571E-04	1.120E+01	1.074E+01	1.077E+01
		3.571E-04	1.106E+01	1.074E+01	1.077E+01
		3.333E-04	1.093E+01	1.067E+01	1.067E+01
		3.333E-04	1.087E+01	1.067E+01	1.067E+01
		3.030E-04	1.064E+01	1.058E+01	1.054E+01
		2.740E-04	1.155E+01	1.051E+01	1.043E+01
		2.500E-04	1.050E+01	1.045E+01	1.035E+01
		2.000E-04	1.045E+01	1.034E+01	1.019E+01
		1.667E-04	1.004E+01	1.028E+01	1.011E+01
		1.429E-04	9.984E+00	1.025E+01	1.006E+01
		1.250E-04	1.008E+01	1.022E+01	1.002E+01
		1.111E-04	1.006E+01	1.021E+01	9.997E+00
		1.000E-04	9.987E+00	1.020E+01	9.979E+00

Comparison of the experimental and calculated (multiple temperature least-squares) R_{2obsd} values with n=1 and n=2 at various temperatures and t_{CP} values for the 0.04936 molal NipyDPT^{2+} solution in acetonitrile at 60 MHz.

Temp °C	t_{CP} s	Exptl s^{-1}	$R_{2(calcd)}$, s^{-1}	
			n=1	n=2
-32.3	1.000E-02	1.464E+01	1.431E+01	1.671E+01
	6.667E-03	1.397E+01	1.426E+01	1.662E+01
	5.000E-03	1.450E+01	1.421E+01	1.653E+01
	4.000E-03	1.439E+01	1.417E+01	1.645E+01
	3.333E-03	1.462E+01	1.412E+01	1.637E+01
	2.857E-03	1.428E+01	1.408E+01	1.630E+01
	2.500E-03	1.439E+01	1.404E+01	1.622E+01
	2.000E-03	1.425E+01	1.396E+01	1.607E+01
	1.667E-03	1.400E+01	1.389E+01	1.592E+01
	1.429E-03	1.389E+01	1.381E+01	1.578E+01
	1.250E-03	1.389E+01	1.373E+01	1.563E+01
	1.111E-03	1.387E+01	1.366E+01	1.548E+01
	1.000E-03	1.392E+01	1.358E+01	1.534E+01
	8.000E-04	1.367E+01	1.339E+01	1.497E+01
	6.667E-04	1.353E+01	1.320E+01	1.460E+01
	5.713E-04	1.320E+01	1.301E+01	1.423E+01
	5.000E-04	1.307E+01	1.282E+01	1.387E+01
	4.444E-04	1.300E+01	1.263E+01	1.349E+01
	4.000E-04	1.259E+01	1.244E+01	1.312E+01
	3.636E-04	1.233E+01	1.225E+01	1.273E+01
	3.333E-04	1.208E+01	1.206E+01	1.234E+01
	3.077E-04	1.179E+01	1.187E+01	1.194E+01
	2.857E-04	1.160E+01	1.168E+01	1.155E+01
	2.667E-04	1.141E+01	1.148E+01	1.116E+01
	2.500E-04	1.100E+01	1.128E+01	1.077E+01
	2.273E-04	1.076E+01	1.096E+01	1.017E+01
	2.083E-04	1.053E+01	1.063E+01	9.599E+00
	1.923E-04	1.009E+01	1.030E+01	9.066E+00
	1.754E-04	9.728E+00	9.886E+00	8.450E+00
	1.613E-04	9.340E+00	9.477E+00	7.897E+00
	1.471E-04	8.839E+00	8.999E+00	7.308E+00
	1.333E-04	8.176E+00	8.463E+00	6.711E+00
	1.250E-04	7.872E+00	8.105E+00	6.344E+00
	1.176E-04	7.437E+00	7.763E+00	6.013E+00
	1.111E-04	7.222E+00	7.445E+00	5.722E+00
	1.053E-04	6.965E+00	7.147E+00	5.463E+00
	1.000E-04	6.546E+00	6.866E+00	5.229E+00
-38.1	1.000E-02	1.552E+01	1.531E+01	1.854E+01
	6.667E-03	1.544E+01	1.525E+01	1.844E+01
	5.000E-03	1.549E+01	1.520E+01	1.834E+01
	4.000E-03	1.587E+01	1.515E+01	1.824E+01
	3.333E-03	1.542E+01	1.510E+01	1.814E+01
	2.500E-03	1.547E+01	1.500E+01	1.795E+01
	2.000E-03	1.522E+01	1.491E+01	1.777E+01
	1.667E-03	1.519E+01	1.482E+01	1.759E+01
	1.429E-03	1.501E+01	1.473E+01	1.740E+01
	1.250E-03	1.526E+01	1.465E+01	1.722E+01

Temp °C	t_{CP} s	Exptl s^{-1}	$R_{2(calcd)}$, s^{-1} n=1	n=2
	1.000E-03	1.478E+01	1.447E+01	1.685E+01
	8.000E-04	1.502E+01	1.425E+01	1.641E+01
	6.667E-04	1.462E+01	1.403E+01	1.597E+01
	5.713E-04	1.402E+01	1.381E+01	1.551E+01
	5.000E-04	1.395E+01	1.360E+01	1.499E+01
	4.444E-04	1.370E+01	1.339E+01	1.440E+01
	4.000E-04	1.368E+01	1.318E+01	1.376E+01
	3.636E-04	1.331E+01	1.296E+01	1.309E+01
	3.333E-04	1.293E+01	1.272E+01	1.242E+01
	3.077E-04	1.265E+01	1.246E+01	1.176E+01
	2.857E-04	1.250E+01	1.218E+01	1.113E+01
	2.667E-04	1.210E+01	1.188E+01	1.053E+01
	2.500E-04	1.173E+01	1.156E+01	9.970E+00
	2.273E-04	1.119E+01	1.103E+01	9.162E+00
	2.083E-04	1.060E+01	1.049E+01	8.452E+00
	1.923E-04	1.004E+01	9.961E+00	7.838E+00
	1.786E-04	9.500E+00	9.455E+00	7.306E+00
	1.613E-04	8.761E+00	8.745E+00	6.634E+00
	1.493E-04	8.061E+00	8.211E+00	6.174E+00
	1.351E-04	7.390E+00	7.542E+00	5.643E+00
	1.250E-04	6.860E+00	7.048E+00	5.278E+00
	1.176E-04	6.483E+00	6.679E+00	5.019E+00
	1.111E-04	6.159E+00	6.354E+00	4.799E+00
	1.064E-04	6.019E+00	6.119E+00	4.644E+00
-42.2	1.000E-04	5.647E+00	5.800E+00	4.440E+00
	1.000E-02	1.263E+01	1.305E+01	1.609E+01
	6.667E-03	1.284E+01	1.300E+01	1.601E+01
	5.000E-03	1.225E+01	1.296E+01	1.594E+01
	4.000E-03	1.283E+01	1.293E+01	1.587E+01
	3.333E-03	1.241E+01	1.289E+01	1.580E+01
	2.857E-03	1.258E+01	1.286E+01	1.573E+01
	2.381E-03	1.244E+01	1.281E+01	1.563E+01
	2.000E-03	1.213E+01	1.276E+01	1.553E+01
	1.667E-03	1.231E+01	1.270E+01	1.539E+01
	1.429E-03	1.244E+01	1.264E+01	1.526E+01
	1.250E-03	1.242E+01	1.258E+01	1.513E+01
	1.000E-03	1.211E+01	1.246E+01	1.486E+01
	8.333E-04	1.217E+01	1.234E+01	1.463E+01
	6.667E-04	1.188E+01	1.215E+01	1.433E+01
	5.713E-04	1.178E+01	1.200E+01	1.397E+01
	5.000E-04	1.182E+01	1.188E+01	1.344E+01
	4.444E-04	1.174E+01	1.177E+01	1.278E+01
	4.000E-04	1.154E+01	1.165E+01	1.206E+01
	3.636E-04	1.144E+01	1.149E+01	1.133E+01
	3.333E-04	1.121E+01	1.128E+01	1.062E+01
	3.030E-04	1.096E+01	1.096E+01	9.827E+00
	2.667E-04	1.050E+01	1.039E+01	8.785E+00
	2.500E-04	1.019E+01	1.004E+01	8.281E+00
	2.381E-04	9.594E+00	9.760E+00	7.916E+00
	2.222E-04	9.194E+00	9.340E+00	7.423E+00
	2.083E-04	8.892E+00	8.931E+00	6.992E+00
	1.961E-04	8.349E+00	8.542E+00	6.615E+00
	1.786E-04	7.650E+00	7.939E+00	6.084E+00
	1.667E-04	7.268E+00	7.503E+00	5.732E+00
	1.563E-04	6.891E+00	7.110E+00	5.433E+00
	1.471E-04	6.467E+00	6.755E+00	5.176E+00
	1.389E-04	6.235E+00	6.436E+00	4.955E+00
	1.316E-04	5.877E+00	6.151E+00	4.764E+00
	1.220E-04	5.590E+00	5.778E+00	4.523E+00
	1.136E-04	5.129E+00	5.455E+00	4.322E+00
-46.8	1.064E-04	4.993E+00	5.185E+00	4.159E+00
	1.000E-02	9.777E+00	9.438E+00	1.166E+01
	6.667E-03	9.523E+00	9.412E+00	1.162E+01
	5.000E-03	9.615E+00	9.389E+00	1.158E+01
	4.000E-03	9.519E+00	9.369E+00	1.155E+01

Temp °C	t_{CP} s	Exptl s^{-1}	R_2 (calcd), s^{-1}	
			n=1	n=2
	3.333E-03	9.535E+00	9.351E+00	1.151E+01
	2.000E-03	9.504E+00	9.287E+00	1.138E+01
	1.667E-03	9.525E+00	9.258E+00	1.132E+01
	1.429E-03	9.516E+00	9.229E+00	1.126E+01
	1.250E-03	9.390E+00	9.202E+00	1.120E+01
	1.111E-03	9.355E+00	9.173E+00	1.111E+01
	1.000E-03	9.430E+00	9.144E+00	1.103E+01
	6.667E-04	9.283E+00	8.988E+00	1.095E+01
	5.000E-04	9.230E+00	8.900E+00	1.029E+01
	4.000E-04	9.170E+00	8.877E+00	9.153E+00
	3.636E-04	9.142E+00	8.783E+00	8.576E+00
	3.333E-04	9.141E+00	8.625E+00	8.038E+00
	3.077E-04	8.865E+00	8.417E+00	7.550E+00
	2.857E-04	8.559E+00	8.173E+00	7.113E+00
	2.667E-04	8.482E+00	7.912E+00	6.726E+00
	2.500E-04	8.001E+00	7.641E+00	6.384E+00
	2.273E-04	7.509E+00	7.216E+00	5.919E+00
	2.128E-04	7.187E+00	6.912E+00	5.626E+00
	2.000E-04	6.868E+00	6.625E+00	5.372E+00
	1.852E-04	6.425E+00	6.277E+00	5.086E+00
	1.724E-04	6.103E+00	5.964E+00	4.847E+00
	1.563E-04	5.680E+00	5.562E+00	4.560E+00
	1.471E-04	5.400E+00	5.331E+00	4.404E+00
	1.351E-04	5.054E+00	5.032E+00	4.210E+00
	1.250E-04	4.714E+00	4.785E+00	4.056E+00
	1.190E-04	4.623E+00	4.642E+00	3.969E+00
	1.111E-04	4.426E+00	4.457E+00	3.859E+00
	1.053E-04	4.300E+00	4.326E+00	3.783E+00

APPENDIX C

Comparison of the experimental and calculated(multiple temperature least-squares) R_{2obsd} values with n=2 and n=3 at various temperatures and t_{CP} values for the 0.1199 molal NiTRI^{2+} solution in acetonitrile at 53 and 10 MHz.

I. At 53 MHz

Temp °C	t_{CP} s	Exptl s^{-1}	$R_{2(calcd)}$, s^{-1}	
			n=2	n=3
35.6	5.000E-03	4.227E+01	4.136E+01	4.568E+01
	4.000E-03	4.145E+01	4.120E+01	4.547E+01
	3.333E-03	4.268E+01	4.105E+01	4.525E+01
	2.857E-03	4.270E+01	4.090E+01	4.504E+01
	2.500E-03	4.177E+01	4.075E+01	4.483E+01
	2.000E-03	4.197E+01	4.046E+01	4.441E+01
	1.667E-03	4.232E+01	4.016E+01	4.399E+01
	1.429E-03	4.182E+01	3.986E+01	4.357E+01
	1.250E-03	4.054E+01	3.957E+01	4.315E+01
	1.111E-03	4.014E+01	3.927E+01	4.273E+01
	1.000E-03	3.994E+01	3.897E+01	4.231E+01
	9.091E-04	3.889E+01	3.868E+01	4.189E+01
	8.333E-04	3.950E+01	3.838E+01	4.147E+01
	7.692E-04	3.901E+01	3.808E+01	4.105E+01
	7.143E-04	3.896E+01	3.779E+01	4.063E+01
	6.667E-04	3.777E+01	3.749E+01	4.022E+01
	6.250E-04	3.705E+01	3.720E+01	3.979E+01
	6.061E-04	3.726E+01	3.705E+01	3.958E+01
	5.882E-04	3.709E+01	3.690E+01	3.937E+01
	5.556E-04	3.671E+01	3.660E+01	3.895E+01
	5.000E-04	3.654E+01	3.601E+01	3.810E+01
	4.545E-04	3.606E+01	3.542E+01	3.725E+01
	4.167E-04	3.523E+01	3.482E+01	3.639E+01
	3.846E-04	3.465E+01	3.422E+01	3.552E+01
	3.571E-04	3.325E+01	3.362E+01	3.465E+01
	3.333E-04	3.266E+01	3.302E+01	3.379E+01
	3.125E-04	3.164E+01	3.241E+01	3.293E+01
	2.941E-04	3.115E+01	3.179E+01	3.208E+01
	2.703E-04	3.018E+01	3.087E+01	3.083E+01
	2.500E-04	2.936E+01	2.995E+01	2.962E+01
	2.326E-04	2.843E+01	2.903E+01	2.847E+01
	2.128E-04	2.659E+01	2.783E+01	2.702E+01
	2.000E-04	2.565E+01	2.695E+01	2.600E+01
	1.887E-04	2.488E+01	2.610E+01	2.505E+01
	1.754E-04	2.388E+01	2.500E+01	2.387E+01
	1.667E-04	2.301E+01	2.421E+01	2.307E+01
	1.563E-04	2.166E+01	2.322E+01	2.208E+01
	1.471E-04	2.073E+01	2.228E+01	2.118E+01
	1.351E-04	1.874E+01	2.097E+01	1.997E+01
	1.282E-04	1.886E+01	2.018E+01	1.927E+01

230

Temp °C	t_{CP} s	Exptl s^{-1}	$R_{2(calcd)}$, s^{-1}	
			n=2	n=3
	1.190E-04	1.809E+01	1.909E+01	1.833E+01
	1.111E-04	1.716E+01	1.812E+01	1.753E+01
	1.053E-04	1.658E+01	1.739E+01	1.695E+01
	1.000E-04	1.565E+01	1.672E+01	1.642E+01
30.4	5.000E-03	4.965E+01	4.912E+01	5.358E+01
	3.333E-03	4.915E+01	4.867E+01	5.295E+01
	2.500E-03	4.932E+01	4.823E+01	5.232E+01
	2.000E-03	4.914E+01	4.779E+01	5.170E+01
	1.667E-03	4.850E+01	4.735E+01	5.108E+01
	1.429E-03	4.838E+01	4.692E+01	5.045E+01
	1.111E-03	4.719E+01	4.604E+01	4.921E+01
	1.000E-03	4.637E+01	4.560E+01	4.859E+01
	8.333E-04	4.490E+01	4.473E+01	4.735E+01
	7.143E-04	4.448E+01	4.385E+01	4.610E+01
	6.250E-04	4.372E+01	4.298E+01	4.483E+01
	5.556E-04	4.258E+01	4.211E+01	4.350E+01
	5.263E-04	4.110E+01	4.166E+01	4.282E+01
	5.000E-04	4.154E+01	4.122E+01	4.212E+01
	4.545E-04	4.029E+01	4.031E+01	4.070E+01
	4.167E-04	3.939E+01	3.937E+01	3.925E+01
	3.846E-04	3.859E+01	3.839E+01	3.780E+01
	3.751E-04	3.734E+01	3.806E+01	3.732E+01
	3.333E-04	3.682E+01	3.636E+01	3.496E+01
	3.077E-04	3.465E+01	3.507E+01	3.328E+01
	2.857E-04	3.316E+01	3.377E+01	3.169E+01
	2.667E-04	3.195E+01	3.249E+01	3.021E+01
	2.500E-04	3.053E+01	3.124E+01	2.882E+01
	2.326E-04	2.892E+01	2.979E+01	2.730E+01
	2.000E-04	2.575E+01	2.669E+01	2.430E+01
	1.887E-04	2.458E+01	2.550E+01	2.322E+01
	1.754E-04	2.340E+01	2.403E+01	2.194E+01
	1.667E-04	2.229E+01	2.304E+01	2.111E+01
	1.563E-04	2.105E+01	2.182E+01	2.011E+01
	1.429E-04	1.967E+01	2.021E+01	1.884E+01
	1.333E-04	1.852E+01	1.904E+01	1.796E+01
	1.250E-04	1.777E+01	1.803E+01	1.721E+01
	1.176E-04	1.690E+01	1.713E+01	1.656E+01
	1.111E-04	1.629E+01	1.636E+01	1.600E+01
	1.053E-04	1.573E+01	1.567E+01	1.552E+01
	1.000E-04	1.505E+01	1.505E+01	1.510E+01
24.7	5.000E-03	4.928E+01	4.904E+01	5.316E+01
	4.000E-03	4.912E+01	4.883E+01	5.285E+01
	3.333E-03	4.983E+01	4.861E+01	5.254E+01
	2.857E-03	4.976E+01	4.840E+01	5.223E+01
	2.500E-03	4.990E+01	4.818E+01	5.193E+01
	2.000E-03	4.859E+01	4.776E+01	5.132E+01
	1.667E-03	4.902E+01	4.733E+01	5.071E+01
	1.429E-03	4.719E+01	4.691E+01	5.009E+01
	1.250E-03	4.694E+01	4.648E+01	4.948E+01
	1.111E-03	4.683E+01	4.606E+01	4.888E+01
	1.000E-03	4.570E+01	4.563E+01	4.830E+01
	9.091E-04	4.577E+01	4.520E+01	4.774E+01
	8.333E-04	4.538E+01	4.479E+01	4.716E+01
	7.692E-04	4.421E+01	4.439E+01	4.656E+01
	7.143E-04	4.443E+01	4.400E+01	4.590E+01
	6.667E-04	4.388E+01	4.361E+01	4.517E+01
	5.882E-04	4.346E+01	4.281E+01	4.352E+01
	5.263E-04	4.267E+01	4.189E+01	4.166E+01
	4.762E-04	4.150E+01	4.083E+01	3.969E+01
	4.348E-04	3.961E+01	3.961E+01	3.769E+01
	4.000E-04	3.840E+01	3.827E+01	3.573E+01
	3.704E-04	3.691E+01	3.686E+01	3.387E+01
	3.448E-04	3.546E+01	3.541E+01	3.212E+01
	3.226E-04	3.371E+01	3.397E+01	3.051E+01
	3.030E-04	3.206E+01	3.255E+01	2.902E+01

Temp °C	t_{CP} s	Exptl s^{-1}	$R_{2\text{(calcd)}}$, s^{-1} n=2	n=3
	2.857E-04	3.074E+01	3.118E+01	2.766E+01
	2.703E-04	2.944E+01	2.987E+01	2.643E+01
	2.564E-04	2.844E+01	2.863E+01	2.530E+01
	2.439E-04	2.704E+01	2.745E+01	2.428E+01
	2.273E-04	2.546E+01	2.583E+01	2.292E+01
	2.128E-04	2.391E+01	2.437E+01	2.175E+01
	2.000E-04	2.249E+01	2.305E+01	2.072E+01
	1.887E-04	2.162E+01	2.187E+01	1.983E+01
	1.786E-04	2.059E+01	2.081E+01	1.905E+01
	1.667E-04	1.934E+01	1.956E+01	1.815E+01
	1.563E-04	1.840E+01	1.849E+01	1.739E+01
	1.471E-04	1.767E+01	1.755E+01	1.675E+01
	1.389E-04	1.679E+01	1.673E+01	1.619E+01
	1.282E-04	1.570E+01	1.568E+01	1.549E+01
	1.163E-04	1.447E+01	1.457E+01	1.477E+01
	1.111E-04	1.414E+01	1.411E+01	1.446E+01
	1.064E-04	1.381E+01	1.369E+01	1.420E+01
	1.000E-04	1.333E+01	1.315E+01	1.386E+01
20.1	4.000E-03	4.257E+01	4.159E+01	4.493E+01
	3.333E-03	4.229E+01	4.145E+01	4.472E+01
	2.857E-03	4.214E+01	4.130E+01	4.452E+01
	2.500E-03	4.225E+01	4.116E+01	4.431E+01
	2.000E-03	4.179E+01	4.088E+01	4.390E+01
	1.667E-03	4.192E+01	4.060E+01	4.350E+01
	1.429E-03	4.055E+01	4.032E+01	4.307E+01
	1.111E-03	4.118E+01	3.975E+01	4.226E+01
	9.091E-04	4.102E+01	3.914E+01	4.173E+01
	8.333E-04	4.134E+01	3.890E+01	4.141E+01
	7.692E-04	4.122E+01	3.871E+01	4.099E+01
	7.143E-04	4.134E+01	3.855E+01	4.044E+01
	6.667E-04	4.070E+01	3.839E+01	3.976E+01
	5.882E-04	4.013E+01	3.793E+01	3.807E+01
	5.263E-04	3.903E+01	3.716E+01	3.612E+01
	4.762E-04	3.760E+01	3.611E+01	3.410E+01
	4.348E-04	3.633E+01	3.482E+01	3.213E+01
	4.000E-04	3.480E+01	3.340E+01	3.027E+01
	3.704E-04	3.348E+01	3.192E+01	2.856E+01
	3.448E-04	3.038E+01	3.044E+01	2.701E+01
	3.333E-04	2.996E+01	2.972E+01	2.629E+01
	3.030E-04	2.766E+01	2.764E+01	2.437E+01
	2.778E-04	2.562E+01	2.575E+01	2.275E+01
	2.632E-04	2.463E+01	2.460E+01	2.182E+01
	2.500E-04	2.358E+01	2.353E+01	2.098E+01
	2.326E-04	2.226E+01	2.210E+01	1.989E+01
	2.128E-04	2.021E+01	2.045E+01	1.869E+01
	2.000E-04	1.944E+01	1.938E+01	1.793E+01
	1.887E-04	1.851E+01	1.844E+01	1.729E+01
	1.786E-04	1.780E+01	1.762E+01	1.673E+01
	1.667E-04	1.680E+01	1.667E+01	1.609E+01
	1.613E-04	1.648E+01	1.624E+01	1.581E+01
	1.515E-04	1.585E+01	1.549E+01	1.532E+01
	1.429E-04	1.500E+01	1.485E+01	1.491E+01
	1.333E-04	1.432E+01	1.416E+01	1.447E+01
	1.250E-04	1.381E+01	1.359E+01	1.411E+01
	1.176E-04	1.333E+01	1.310E+01	1.381E+01
	1.111E-04	1.305E+01	1.269E+01	1.355E+01
	1.064E-04	1.271E+01	1.240E+01	1.338E+01
	1.000E-04	1.232E+01	1.202E+01	1.315E+01
15.0	5.000E-03	3.234E+01	3.135E+01	3.375E+01
	4.000E-03	3.146E+01	3.127E+01	3.365E+01
	3.333E-03	3.163E+01	3.120E+01	3.354E+01
	2.500E-03	3.144E+01	3.107E+01	3.335E+01
	2.000E-03	3.207E+01	3.094E+01	3.315E+01
	1.667E-03	3.182E+01	3.080E+01	3.299E+01

Temp °C	t_{CP} s	Exptl s^{-1}	$R_{2(calcd)}$, s^{-1}	
			n=2	n=3
	1.429E-03	3.113E+01	3.067E+01	3.271E+01
	1.250E-03	3.114E+01	3.058E+01	3.243E+01
	1.111E-03	3.120E+01	3.039E+01	3.232E+01
	1.000E-03	3.096E+01	3.016E+01	3.234E+01
	9.091E-04	3.099E+01	2.998E+01	3.236E+01
	8.333E-04	3.101E+01	2.992E+01	3.229E+01
	7.143E-04	3.027E+01	3.001E+01	3.166E+01
	6.650E-04	3.056E+01	3.005E+01	3.109E+01
	5.882E-04	3.025E+01	2.987E+01	2.974E+01
	5.263E-04	2.991E+01	2.932E+01	2.818E+01
	5.000E-04	2.930E+01	2.892E+01	2.739E+01
	4.545E-04	2.838E+01	2.793E+01	2.585E+01
	4.167E-04	2.757E+01	2.680E+01	2.443E+01
	3.846E-04	2.538E+01	2.562E+01	2.313E+01
	3.751E-04	2.444E+01	2.523E+01	2.274E+01
	3.333E-04	2.337E+01	2.331E+01	2.097E+01
	3.125E-04	2.233E+01	2.225E+01	2.007E+01
	2.941E-04	2.159E+01	2.127E+01	1.928E+01
	2.778E-04	2.038E+01	2.037E+01	1.859E+01
	2.632E-04	1.971E+01	1.955E+01	1.798E+01
	2.500E-04	1.902E+01	1.879E+01	1.743E+01
	2.326E-04	1.790E+01	1.780E+01	1.673E+01
	2.128E-04	1.691E+01	1.667E+01	1.597E+01
	2.000E-04	1.635E+01	1.595E+01	1.549E+01
	1.887E-04	1.563E+01	1.533E+01	1.509E+01
	1.754E-04	1.475E+01	1.461E+01	1.464E+01
	1.667E-04	1.427E+01	1.416E+01	1.435E+01
	1.563E-04	1.387E+01	1.364E+01	1.403E+01
	1.449E-04	1.343E+01	1.308E+01	1.369E+01
	1.429E-04	1.342E+01	1.299E+01	1.363E+01
	1.333E-04	1.290E+01	1.255E+01	1.336E+01
	1.250E-04	1.257E+01	1.219E+01	1.314E+01
	1.176E-04	1.220E+01	1.188E+01	1.296E+01
	1.111E-04	1.192E+01	1.162E+01	1.281E+01
	1.000E-04	1.140E+01	1.120E+01	1.256E+01
10.1	5.000E-03	2.282E+01	2.301E+01	2.453E+01
	4.000E-03	2.313E+01	2.298E+01	2.448E+01
	3.333E-03	2.295E+01	2.295E+01	2.444E+01
	2.222E-03	2.285E+01	2.286E+01	2.430E+01
	2.000E-03	2.284E+01	2.284E+01	2.426E+01
	1.818E-03	2.275E+01	2.282E+01	2.426E+01
	1.667E-03	2.288E+01	2.277E+01	2.424E+01
	1.563E-03	2.285E+01	2.273E+01	2.419E+01
	1.429E-03	2.266E+01	2.272E+01	2.406E+01
	1.333E-03	2.260E+01	2.274E+01	2.394E+01
	1.250E-03	2.206E+01	2.273E+01	2.386E+01
	1.176E-03	2.247E+01	2.269E+01	2.383E+01
	1.111E-03	2.154E+01	2.262E+01	2.385E+01
	1.000E-03	2.193E+01	2.243E+01	2.395E+01
	9.091E-04	2.236E+01	2.231E+01	2.406E+01
	8.333E-04	2.139E+01	2.231E+01	2.407E+01
	7.692E-04	2.224E+01	2.240E+01	2.396E+01
	7.143E-04	2.236E+01	2.251E+01	2.372E+01
	7.143E-04	2.190E+01	2.251E+01	2.372E+01
	6.667E-04	2.121E+01	2.260E+01	2.337E+01
	6.250E-04	2.246E+01	2.262E+01	2.295E+01
	5.882E-04	2.168E+01	2.256E+01	2.248E+01
	5.556E-04	2.190E+01	2.242E+01	2.199E+01
	5.260E-04	2.216E+01	2.221E+01	2.147E+01
	5.000E-04	2.116E+01	2.195E+01	2.097E+01
	4.545E-04	2.107E+01	2.129E+01	2.000E+01
	4.250E-04	2.063E+01	2.071E+01	1.932E+01
	4.000E-04	1.964E+01	2.014E+01	1.871E+01

Temp °C	t_{CP} s	Exptl s^{-1}	R_2 (calcd), s^{-1}	
			n=2	n=3
	3.704E-04	1.925E+01	1.936E+01	1.796E+01
	3.448E-04	1.857E+01	1.861E+01	1.731E+01
	3.333E-04	1.809E+01	1.825E+01	1.701E+01
	3.125E-04	1.740E+01	1.757E+01	1.647E+01
	2.857E-04	1.665E+01	1.665E+01	1.579E+01
	2.632E-04	1.584E+01	1.585E+01	1.523E+01
	2.500E-04	1.539E+01	1.538E+01	1.491E+01
	2.326E-04	1.463E+01	1.476E+01	1.450E+01
	2.128E-04	1.409E+01	1.406E+01	1.405E+01
	2.000E-04	1.386E+01	1.362E+01	1.377E+01
	1.887E-04	1.320E+01	1.324E+01	1.354E+01
	1.750E-04	1.289E+01	1.279E+01	1.327E+01
	1.667E-04	1.258E+01	1.253E+01	1.311E+01
	1.563E-04	1.236E+01	1.221E+01	1.292E+01
	1.429E-04	1.190E+01	1.182E+01	1.269E+01
	1.330E-04	1.183E+01	1.154E+01	1.254E+01
	1.250E-04	1.146E+01	1.133E+01	1.242E+01
	1.176E-04	1.128E+01	1.115E+01	1.231E+01
	1.111E-04	1.107E+01	1.099E+01	1.222E+01
	1.000E-04	1.079E+01	1.074E+01	1.208E+01
4.7	5.000E-03	1.641E+01	1.684E+01	1.762E+01
	4.000E-03	1.662E+01	1.682E+01	1.760E+01
	3.333E-03	1.645E+01	1.681E+01	1.758E+01
	2.857E-03	1.636E+01	1.679E+01	1.756E+01
	2.500E-03	1.658E+01	1.679E+01	1.756E+01
	2.000E-03	1.644E+01	1.677E+01	1.750E+01
	1.667E-03	1.663E+01	1.674E+01	1.753E+01
	1.429E-03	1.668E+01	1.671E+01	1.744E+01
	1.250E-03	1.671E+01	1.676E+01	1.731E+01
	1.136E-03	1.647E+01	1.672E+01	1.730E+01
	1.000E-03	1.651E+01	1.657E+01	1.739E+01
	8.690E-04	1.646E+01	1.648E+01	1.750E+01
	8.333E-04	1.681E+01	1.650E+01	1.750E+01
	7.692E-04	1.657E+01	1.656E+01	1.746E+01
	6.897E-04	1.638E+01	1.668E+01	1.727E+01
	6.061E-04	1.654E+01	1.674E+01	1.686E+01
	5.556E-04	1.636E+01	1.666E+01	1.648E+01
	5.000E-04	1.622E+01	1.642E+01	1.597E+01
	4.545E-04	1.595E+01	1.607E+01	1.548E+01
	4.167E-04	1.534E+01	1.567E+01	1.504E+01
	3.846E-04	1.491E+01	1.525E+01	1.464E+01
	3.751E-04	1.458E+01	1.511E+01	1.452E+01
	3.333E-04	1.430E+01	1.445E+01	1.398E+01
	3.125E-04	1.397E+01	1.408E+01	1.371E+01
	2.941E-04	1.362E+01	1.375E+01	1.348E+01
	2.778E-04	1.333E+01	1.345E+01	1.327E+01
	2.632E-04	1.319E+01	1.317E+01	1.309E+01
	2.500E-04	1.289E+01	1.292E+01	1.293E+01
	2.326E-04	1.264E+01	1.259E+01	1.273E+01
	2.128E-04	1.228E+01	1.222E+01	1.251E+01
	2.000E-04	1.204E+01	1.198E+01	1.237E+01
	1.887E-04	1.185E+01	1.178E+01	1.225E+01
	1.786E-04	1.159E+01	1.161E+01	1.215E+01
	1.667E-04	1.149E+01	1.141E+01	1.204E+01
	1.563E-04	1.141E+01	1.124E+01	1.195E+01
	1.471E-04	1.125E+01	1.109E+01	1.187E+01
	1.389E-04	1.117E+01	1.097E+01	1.180E+01
	1.282E-04	1.103E+01	1.082E+01	1.172E+01
	1.190E-04	1.092E+01	1.070E+01	1.165E+01
	1.111E-04	1.074E+01	1.060E+01	1.160E+01

Temp $^\circ$C	t_{CP} s	Exptl s^{-1}	$R_{2(calcd)}$, s^{-1} n=2	n=3
	1.000E-04	1.067E+01	1.046E+01	1.153E+01
-0.3	5.000E-03	1.335E+01	1.345E+01	1.378E+01
	4.000E-03	1.391E+01	1.344E+01	1.377E+01
	3.333E-03	1.359E+01	1.344E+01	1.376E+01
	2.857E-03	1.342E+01	1.343E+01	1.375E+01
	2.500E-03	1.329E+01	1.343E+01	1.375E+01
	2.222E-03	1.340E+01	1.342E+01	1.373E+01
	2.000E-03	1.337E+01	1.341E+01	1.372E+01
	1.818E-03	1.348E+01	1.342E+01	1.373E+01
	1.667E-03	1.332E+01	1.341E+01	1.374E+01
	1.539E-03	1.331E+01	1.338E+01	1.373E+01
	1.429E-03	1.349E+01	1.338E+01	1.370E+01
	1.333E-03	1.334E+01	1.340E+01	1.366E+01
	1.250E-03	1.351E+01	1.342E+01	1.364E+01
	1.111E-03	1.353E+01	1.340E+01	1.363E+01
	1.000E-03	1.344E+01	1.333E+01	1.367E+01
	9.091E-04	1.337E+01	1.328E+01	1.371E+01
	8.333E-04	1.332E+01	1.328E+01	1.374E+01
	7.692E-04	1.353E+01	1.331E+01	1.372E+01
	6.897E-04	1.337E+01	1.337E+01	1.365E+01
	6.250E-04	1.338E+01	1.341E+01	1.351E+01
	5.713E-04	1.346E+01	1.340E+01	1.335E+01
	5.000E-04	1.334E+01	1.328E+01	1.306E+01
	4.545E-04	1.311E+01	1.311E+01	1.283E+01
	4.167E-04	1.288E+01	1.292E+01	1.263E+01
	3.846E-04	1.272E+01	1.271E+01	1.244E+01
	3.571E-04	1.256E+01	1.251E+01	1.228E+01
	3.333E-04	1.244E+01	1.232E+01	1.214E+01
	3.125E-04	1.218E+01	1.213E+01	1.201E+01
	2.941E-04	1.203E+01	1.197E+01	1.190E+01
	2.703E-04	1.171E+01	1.175E+01	1.176E+01
	2.500E-04	1.163E+01	1.155E+01	1.165E+01
	2.326E-04	1.139E+01	1.139E+01	1.155E+01
	2.128E-04	1.121E+01	1.120E+01	1.145E+01
	2.000E-04	1.114E+01	1.108E+01	1.138E+01
	1.852E-04	1.102E+01	1.095E+01	1.131E+01
	1.724E-04	1.094E+01	1.084E+01	1.125E+01
	1.613E-04	1.084E+01	1.075E+01	1.121E+01
	1.471E-04	1.071E+01	1.063E+01	1.115E+01
	1.333E-04	1.060E+01	1.053E+01	1.110E+01
	1.250E-04	1.048E+01	1.047E+01	1.107E+01
	1.163E-04	1.034E+01	1.041E+01	1.104E+01
	1.064E-04	1.039E+01	1.035E+01	1.101E+01
	1.000E-04	1.042E+01	1.031E+01	1.099E+01
-10.2	5.000E-03	1.049E+01	1.083E+01	1.067E+01
	4.000E-03	1.114E+01	1.082E+01	1.066E+01
	3.333E-03	1.084E+01	1.082E+01	1.066E+01
	3.000E-03	1.080E+01	1.081E+01	1.065E+01
	2.857E-03	1.086E+01	1.081E+01	1.065E+01
	2.500E-03	1.081E+01	1.081E+01	1.065E+01
-15.1	5.000E-03	1.077E+01	1.067E+01	1.038E+01
	4.000E-03	1.054E+01	1.066E+01	1.038E+01
	3.333E-03	1.074E+01	1.066E+01	1.037E+01
	3.000E-03	1.056E+01	1.065E+01	1.037E+01
	2.857E-03	1.061E+01	1.065E+01	1.037E+01
	2.500E-03	1.075E+01	1.065E+01	1.037E+01
	2.000E-03	1.094E+01	1.065E+01	1.036E+01
	1.667E-03	1.099E+01	1.065E+01	1.036E+01
	1.250E-03	1.070E+01	1.065E+01	1.036E+01
	1.000E-03	1.088E+01	1.064E+01	1.036E+01

Temp °C	t_{CP} s	Exptl s^{-1}	$R_2 \text{(calcd)}, s^{-1}$	
			n=2	n=3
-20.3	5.000E-03	1.096E+01	1.095E+01	1.058E+01
	4.000E-03	1.117E+01	1.094E+01	1.057E+01
	3.333E-03	1.096E+01	1.094E+01	1.056E+01
	2.857E-03	1.105E+01	1.094E+01	1.056E+01
	2.500E-03	1.097E+01	1.093E+01	1.056E+01
	2.000E-03	1.088E+01	1.093E+01	1.056E+01
-24.9	5.000E-03	1.107E+01	1.149E+01	1.105E+01
	4.000E-03	1.110E+01	1.148E+01	1.104E+01
	3.333E-03	1.112E+01	1.147E+01	1.104E+01
	3.000E-03	1.122E+01	1.147E+01	1.103E+01
	2.857E-03	1.122E+01	1.147E+01	1.103E+01
	2.500E-03	1.126E+01	1.147E+01	1.103E+01
	2.000E-03	1.118E+01	1.146E+01	1.103E+01
	1.000E-03	1.119E+01	1.146E+01	1.102E+01
	5.000E-04	1.113E+01	1.146E+01	1.102E+01
	2.000E-04	1.109E+01	1.145E+01	1.101E+01
-28.6	5.000E-03	1.179E+01	1.205E+01	1.157E+01
	4.000E-03	1.197E+01	1.204E+01	1.156E+01
	3.333E-03	1.203E+01	1.203E+01	1.155E+01
	3.000E-03	1.214E+01	1.203E+01	1.155E+01
	2.857E-03	1.201E+01	1.203E+01	1.155E+01
	2.500E-03	1.193E+01	1.203E+01	1.155E+01
	2.000E-03	1.197E+01	1.203E+01	1.155E+01
	1.000E-03	1.184E+01	1.202E+01	1.154E+01
	5.000E-04	1.188E+01	1.202E+01	1.154E+01
	2.000E-04	1.188E+01	1.202E+01	1.154E+01
-35.1	5.000E-03	1.360E+01	1.326E+01	1.271E+01
	4.000E-03	1.377E+01	1.325E+01	1.270E+01
	3.333E-03	1.341E+01	1.324E+01	1.270E+01
	3.000E-03	1.341E+01	1.324E+01	1.269E+01
	2.857E-03	1.345E+01	1.324E+01	1.269E+01
	2.500E-03	1.305E+01	1.324E+01	1.269E+01
	2.000E-03	1.281E+01	1.324E+01	1.269E+01
	1.000E-03	1.335E+01	1.323E+01	1.268E+01
	5.000E-04	1.335E+01	1.323E+01	1.268E+01
	2.000E-04	1.332E+01	1.323E+01	1.268E+01

II. At 10 MHz°

Temp °C	t_{CP} s	Exptl s^{-1}	$R_{2(calcd)}$, s^{-1} n=2	n=3
20.0	2.000E-02	1.186E+01	1.180E+01	1.202E+01
	1.500E-02	1.158E+01	1.175E+01	1.196E+01
	1.429E-02	1.183E+01	1.174E+01	1.195E+01
	1.250E-02	1.173E+01	1.171E+01	1.192E+01
	1.060E-02	1.155E+01	1.167E+01	1.187E+01
	7.692E-03	1.162E+01	1.159E+01	1.177E+01
	7.000E-03	1.142E+01	1.156E+01	1.174E+01
	6.667E-03	1.156E+01	1.155E+01	1.172E+01
	5.556E-03	1.134E+01	1.149E+01	1.164E+01
	5.000E-03	1.145E+01	1.145E+01	1.159E+01
	4.000E-03	1.145E+01	1.136E+01	1.147E+01
	3.333E-03	1.129E+01	1.126E+01	1.135E+01
	2.857E-03	1.109E+01	1.118E+01	1.124E+01
	2.500E-03	1.113E+01	1.109E+01	1.112E+01
	2.222E-03	1.087E+01	1.100E+01	1.101E+01
	2.000E-03	1.059E+01	1.091E+01	1.089E+01
	1.818E-03	1.073E+01	1.082E+01	1.078E+01
	1.539E-03	1.064E+01	1.065E+01	1.055E+01
	1.333E-03	1.016E+01	1.047E+01	1.032E+01
	1.220E-03	1.044E+01	1.035E+01	1.016E+01
	1.136E-03	1.033E+01	1.024E+01	1.002E+01
	1.053E-03	9.934E+00	1.012E+01	9.873E+00
	9.521E-04	9.790E+00	9.939E+00	9.663E+00
	8.690E-04	9.444E+00	9.766E+00	9.464E+00
	8.000E-04	9.422E+00	9.598E+00	9.279E+00
	7.143E-04	9.020E+00	9.355E+00	9.024E+00
	6.250E-04	9.014E+00	9.054E+00	8.728E+00
	5.882E-04	8.753E+00	8.914E+00	8.597E+00
	5.556E-04	8.419E+00	8.782E+00	8.478E+00
	4.995E-04	8.237E+00	8.538E+00	8.267E+00
	4.450E-04	7.991E+00	8.282E+00	8.057E+00
	4.082E-04	7.930E+00	8.099E+00	7.915E+00
	3.700E-04	7.801E+00	7.903E+00	7.769E+00
	3.448E-04	7.662E+00	7.772E+00	7.674E+00
	3.175E-04	7.692E+00	7.630E+00	7.574E+00
	2.942E-04	7.555E+00	7.509E+00	7.491E+00
	2.700E-04	7.478E+00	7.385E+00	7.408E+00
	2.485E-04	7.431E+00	7.278E+00	7.338E+00
	2.326E-04	7.485E+00	7.201E+00	7.289E+00
	2.222E-04	7.515E+00	7.151E+00	7.258E+00
	2.083E-04	7.292E+00	7.087E+00	7.217E+00
	2.000E-04	7.329E+00	7.050E+00	7.194E+00
	1.887E-04	7.006E+00	7.001E+00	7.164E+00
	1.724E-04	7.176E+00	6.933E+00	7.122E+00
	1.563E-04	7.036E+00	6.870E+00	7.085E+00
	1.429E-04	7.060E+00	6.821E+00	7.055E+00
	1.316E-04	7.113E+00	6.783E+00	7.033E+00
	1.163E-04	6.848E+00	6.735E+00	7.004E+00
	1.010E-04	6.894E+00	6.692E+00	6.979E+00
12.8	2.000E-02	1.368E+01	1.381E+01	1.416E+01
	1.800E-02	1.357E+01	1.378E+01	1.412E+01
	1.600E-02	1.366E+01	1.375E+01	1.408E+01

238

Temp °C	t_{CP} s	Exptl s^{-1}	$R_{2(calcd)}$, s^{-1} n=2	n=3
	1.429E-02	1.346E+01	1.371E+01	1.403E+01
	1.250E-02	1.325E+01	1.367E+01	1.398E+01
	1.111E-02	1.368E+01	1.362E+01	1.392E+01
	9.995E-03	1.379E+01	1.358E+01	1.386E+01
	8.000E-03	1.372E+01	1.348E+01	1.372E+01
	6.667E-03	1.345E+01	1.338E+01	1.359E+01
	5.714E-03	1.299E+01	1.328E+01	1.346E+01
	5.556E-03	1.319E+01	1.326E+01	1.343E+01
	5.174E-03	1.345E+01	1.321E+01	1.336E+01
	5.000E-03	1.334E+01	1.319E+01	1.333E+01
	4.444E-03	1.321E+01	1.310E+01	1.320E+01
	3.995E-03	1.295E+01	1.300E+01	1.307E+01
	3.636E-03	1.260E+01	1.291E+01	1.295E+01
	3.333E-03	1.272E+01	1.282E+01	1.282E+01
	3.077E-03	1.267E+01	1.273E+01	1.269E+01
	2.857E-03	1.255E+01	1.264E+01	1.256E+01
	2.███E-03	1.263E+01	1.255E+01	1.243E+01
	2.500E-03	1.241E+01	1.246E+01	1.230E+01
	2.326E-03	1.212E+01	1.235E+01	1.214E+01
	2.128E-03	1.200E+01	1.221E+01	1.192E+01
	2.000E-03	1.182E+01	1.209E+01	1.175E+01
	1.852E-03	1.184E+01	1.194E+01	1.153E+01
	1.695E-03	1.151E+01	1.175E+01	1.126E+01
	1.563E-03	1.119E+01	1.155E+01	1.100E+01
	1.429E-03	1.115E+01	1.130E+01	1.069E+01
	1.333E-03	1.105E+01	1.110E+01	1.045E+01
	1.220E-03	1.058E+01	1.082E+01	1.014E+01
	1.124E-03	1.047E+01	1.055E+01	9.850E+00
	1.053E-03	1.006E+01	1.032E+01	9.626E+00
	1.000E-03	1.004E+01	1.014E+01	9.454E+00
	9.091E-04	9.628E+00	9.806E+00	9.148E+00
	8.333E-04	9.554E+00	9.501E+00	8.887E+00
	7.692E-04	9.071E+00	9.228E+00	8.663E+00
	7.143E-04	8.892E+00	8.984E+00	8.472E+00
	6.667E-04	8.729E+00	8.767E+00	8.308E+00
	6.061E-04	8.614E+00	8.486E+00	8.103E+00
	5.556E-04	8.166E+00	8.250E+00	7.937E+00
	5.000E-04	7.902E+00	7.993E+00	7.762E+00
	4.545E-04	7.884E+00	7.788E+00	7.627E+00
	4.000E-04	7.552E+00	7.551E+00	7.475E+00
	3.704E-04	7.383E+00	7.428E+00	7.398E+00
	3.333E-04	7.378E+00	7.282E+00	7.308E+00
	3.077E-04	7.321E+00	7.187E+00	7.250E+00
	2.850E-04	7.352E+00	7.107E+00	7.202E+00
	2.667E-04	7.275E+00	7.046E+00	7.165E+00
	2.500E-04	7.272E+00	6.993E+00	7.134E+00
	2.353E-04	7.138E+00	6.949E+00	7.107E+00
	1.990E-04	7.202E+00	6.848E+00	7.049E+00
	1.667E-04	6.903E+00	6.771E+00	7.004E+00
	1.429E-04	7.118E+00	6.722E+00	6.976E+00
	1.111E-04	7.000E+00	6.668E+00	6.945E+00
8.2	1.600E-02	1.338E+01	1.354E+01	1.406E+01
	1.429E-02	1.360E+01	1.351E+01	1.401E+01
	1.250E-02	1.387E+01	1.346E+01	1.395E+01
	1.111E-02	1.330E+01	1.342E+01	1.389E+01
	1.000E-02	1.376E+01	1.338E+01	1.383E+01
	9.995E-03	1.362E+01	1.337E+01	1.383E+01
	8.000E-03	1.386E+01	1.327E+01	1.368E+01
	7.000E-03	1.299E+01	1.320E+01	1.357E+01
	6.000E-03	1.302E+01	1.310E+01	1.344E+01

Temp $^\circ$C	t_{CP} s	Exptl s^{-1}	R_2(calcd), s^{-1} n=2	n=3
	5.000E-03	1.291E+01	1.298E+01	1.325E+01
	4.444E-03	1.347E+01	1.288E+01	1.311E+01
	4.000E-03	1.358E+01	1.279E+01	1.298E+01
	3.636E-03	1.263E+01	1.270E+01	1.284E+01
	3.333E-03	1.264E+01	1.261E+01	1.269E+01
	3.077E-03	1.254E+01	1.252E+01	1.254E+01
	2.857E-03	1.252E+01	1.243E+01	1.237E+01
	2.667E-03	1.236E+01	1.234E+01	1.220E+01
	2.326E-03	1.216E+01	1.212E+01	1.180E+01
	2.128E-03	1.200E+01	1.194E+01	1.150E+01
	2.000E-03	1.184E+01	1.180E+01	1.128E+01
	1.852E-03	1.163E+01	1.160E+01	1.099E+01
	1.724E-03	1.133E+01	1.140E+01	1.071E+01
	1.563E-03	1.098E+01	1.108E+01	1.033E+01
	1.429E-03	1.060E+01	1.077E+01	9.978E+00
	1.351E-03	1.050E+01	1.056E+01	9.764E+00
	1.250E-03	1.013E+01	1.026E+01	9.478E+00
	1.176E-03	1.005E+01	1.003E+01	9.262E+00
	1.064E-03	9.641E+00	9.646E+00	8.932E+00
	1.000E-03	9.586E+00	9.414E+00	8.743E+00
	9.091E-04	9.116E+00	9.071E+00	8.476E+00
	8.333E-04	8.723E+00	8.778E+00	8.257E+00
	7.692E-04	8.550E+00	8.527E+00	8.078E+00
	7.143E-04	8.345E+00	8.312E+00	7.929E+00
	6.667E-04	8.188E+00	8.128E+00	7.805E+00
	6.061E-04	8.034E+00	7.898E+00	7.654E+00
	5.540E-04	7.714E+00	7.708E+00	7.531E+00
	5.000E-04	7.602E+00	7.519E+00	7.412E+00
	4.545E-04	7.611E+00	7.368E+00	7.319E+00
	4.255E-04	7.428E+00	7.277E+00	7.264E+00
	4.000E-04	7.500E+00	7.200E+00	7.217E+00
	3.636E-04	7.348E+00	7.096E+00	7.155E+00
	3.333E-04	7.509E+00	7.015E+00	7.107E+00
	3.077E-04	7.252E+00	6.951E+00	7.070E+00
	2.632E-04	7.331E+00	6.851E+00	7.011E+00
	2.500E-04	7.209E+00	6.824E+00	6.995E+00
	2.222E-04	7.335E+00	6.770E+00	6.965E+00
	2.000E-04	7.236E+00	6.732E+00	6.942E+00
5.0	2.000E-02	1.349E+01	1.256E+01	1.318E+01
	1.500E-02	1.275E+01	1.250E+01	1.309E+01
	1.250E-02	1.255E+01	1.245E+01	1.302E+01
	1.000E-02	1.268E+01	1.238E+01	1.291E+01
	8.000E-03	1.241E+01	1.229E+01	1.279E+01
	6.667E-03	1.265E+01	1.221E+01	1.266E+01
	5.713E-03	1.229E+01	1.213E+01	1.254E+01
	5.000E-03	1.245E+01	1.205E+01	1.243E+01
	4.444E-03	1.302E+01	1.198E+01	1.233E+01
	4.000E-03	1.206E+01	1.190E+01	1.222E+01
	3.636E-03	1.196E+01	1.184E+01	1.210E+01
	3.333E-03	1.232E+01	1.177E+01	1.196E+01
	3.077E-03	1.219E+01	1.171E+01	1.180E+01
	2.857E-03	1.188E+01	1.164E+01	1.163E+01
	2.500E-03	1.143E+01	1.148E+01	1.125E+01
	2.273E-03	1.116E+01	1.132E+01	1.094E+01
	2.083E-03	1.096E+01	1.114E+01	1.062E+01
	1.923E-03	1.104E+01	1.094E+01	1.033E+01
	1.754E-03	1.119E+01	1.067E+01	9.980E+00
	1.667E-03	1.047E+01	1.051E+01	9.790E+00
	1.539E-03	1.032E+01	1.024E+01	9.496E+00
	1.429E-03	1.013E+01	9.974E+00	9.235E+00

Temp °C	t_{CP} s	Exptl s^{-1}	$R_{2(calcd)}$, s^{-1} n=2	n=3
	1.333E-03	9.651E+00	9.723E+00	9.002E+00
	1.260E-03	9.551E+00	9.519E+00	8.823E+00
	1.176E-03	9.340E+00	9.273E+00	8.616E+00
	1.111E-03	8.985E+00	9.075E+00	8.458E+00
	1.053E-03	9.068E+00	8.894E+00	8.317E+00
	1.000E-03	8.711E+00	8.725E+00	8.191E+00
	8.696E-04	8.222E+00	8.306E+00	7.890E+00
	7.692E-04	7.869E+00	7.987E+00	7.673E+00
	6.879E-04	7.552E+00	7.736E+00	7.509E+00
	6.200E-04	7.487E+00	7.535E+00	7.381E+00
	5.556E-04	7.132E+00	7.355E+00	7.269E+00
	5.263E-04	7.080E+00	7.277E+00	7.222E+00
	5.000E-04	7.042E+00	7.210E+00	7.181E+00
	4.545E-04	7.003E+00	7.099E+00	7.114E+00
	4.167E-04	6.809E+00	7.012E+00	7.062E+00
	3.846E-04	6.870E+00	6.944E+00	7.022E+00
	3.571E-04	6.613E+00	6.888E+00	6.989E+00
	3.333E-04	6.626E+00	6.843E+00	6.963E+00
	3.077E-04	6.613E+00	6.798E+00	6.937E+00
	2.857E-04	6.738E+00	6.761E+00	6.916E+00
	2.667E-04	6.499E+00	6.732E+00	6.898E+00
	2.500E-04	6.661E+00	6.707E+00	6.884E+00
	2.273E-04	6.541E+00	6.676E+00	6.867E+00
	2.083E-04	6.481E+00	6.653E+00	6.853E+00
	1.923E-04	6.310E+00	6.634E+00	6.843E+00
	1.786E-04	6.364E+00	6.619E+00	6.834E+00
	1.667E-04	6.448E+00	6.607E+00	6.827E+00
	1.539E-04	6.285E+00	6.595E+00	6.821E+00
	1.429E-04	6.304E+00	6.586E+00	6.815E+00
	1.333E-04	6.654E+00	6.578E+00	6.811E+00
	1.250E-04	6.376E+00	6.572E+00	6.807E+00
	1.111E-04	6.169E+00	6.562E+00	6.802E+00
2.3	2.000E-02	1.138E+01	1.141E+01	1.201E+01
	1.800E-02	1.148E+01	1.139E+01	1.198E+01
	1.600E-02	1.139E+01	1.137E+01	1.195E+01
	1.400E-02	1.152E+01	1.134E+01	1.192E+01
	1.250E-02	1.132E+01	1.132E+01	1.188E+01
	1.111E-02	1.155E+01	1.129E+01	1.184E+01
	7.690E-03	1.148E+01	1.119E+01	1.168E+01
	7.143E-03	1.157E+01	1.116E+01	1.164E+01
	6.667E-03	1.143E+01	1.114E+01	1.161E+01
	5.882E-03	1.132E+01	1.109E+01	1.153E+01
	5.405E-03	1.136E+01	1.105E+01	1.148E+01
	5.000E-03	1.142E+01	1.102E+01	1.144E+01
	4.545E-03	1.142E+01	1.097E+01	1.139E+01
	4.000E-03	1.146E+01	1.091E+01	1.130E+01
	3.636E-03	1.127E+01	1.087E+01	1.120E+01
	3.333E-03	1.125E+01	1.083E+01	1.108E+01
	3.030E-03	1.106E+01	1.078E+01	1.090E+01
	2.778E-03	1.100E+01	1.073E+01	1.069E+01
	2.500E-03	1.073E+01	1.062E+01	1.040E+01
	2.273E-03	1.050E+01	1.047E+01	1.010E+01
	2.128E-03	1.041E+01	1.034E+01	9.887E+00
	2.000E-03	1.031E+01	1.021E+01	9.679E+00
	1.852E-03	9.978E+00	1.001E+01	9.421E+00
	1.724E-03	9.824E+00	9.807E+00	9.185E+00
	1.587E-03	9.550E+00	9.556E+00	8.921E+00
	1.429E-03	9.292E+00	9.226E+00	8.608E+00
	1.333E-03	8.946E+00	9.006E+00	8.416E+00
	1.250E-03	8.722E+00	8.806E+00	8.250E+00

Temp $^{\circ}$C	t_{CP} s	Exptl s^{-1}	$R_{2(calcd)}$, s^{-1}	
			n=2	n=3
	1.111E-03	8.365E+00	8.455E+00	7.977E+00
	1.000E-03	8.096E+00	8.167E+00	7.768E+00
	9.090E-04	7.939E+00	7.931E+00	7.603E+00
	8.333E-04	7.660E+00	7.738E+00	7.473E+00
	7.692E-04	7.483E+00	7.578E+00	7.369E+00
	7.143E-04	7.213E+00	7.445E+00	7.284E+00
	6.667E-04	7.270E+00	7.334E+00	7.214E+00
	6.065E-04	7.102E+00	7.199E+00	7.130E+00
	6.061E-04	7.211E+00	7.199E+00	7.130E+00
	5.556E-04	6.920E+00	7.092E+00	7.065E+00
	5.120E-04	6.871E+00	7.005E+00	7.013E+00
	4.651E-04	6.827E+00	6.918E+00	6.961E+00
	4.625E-04	6.882E+00	6.913E+00	6.958E+00
	4.348E-04	6.632E+00	6.865E+00	6.929E+00
	3.995E-04	6.647E+00	6.807E+00	6.895E+00
	3.704E-04	6.534E+00	6.762E+00	6.869E+00
	3.333E-04	6.456E+00	6.709E+00	6.838E+00
	3.077E-04	6.574E+00	6.676E+00	6.819E+00
	2.703E-04	6.634E+00	6.631E+00	6.793E+00
	2.700E-04	6.663E+00	6.631E+00	6.793E+00
	2.500E-04	6.411E+00	6.609E+00	6.781E+00
	2.222E-04	6.390E+00	6.582E+00	6.765E+00
	2.000E-04	6.351E+00	6.562E+00	6.754E+00
-6.1	2.500E-02	7.643E+00	8.059E+00	8.367E+00
	1.667E-02	7.711E+00	8.034E+00	8.335E+00
	1.429E-02	7.666E+00	8.022E+00	8.320E+00
	1.250E-02	7.609E+00	8.010E+00	8.305E+00
	1.111E-02	7.628E+00	7.999E+00	8.290E+00
	1.000E-02	7.595E+00	7.988E+00	8.276E+00
	9.091E-03	7.684E+00	7.979E+00	8.266E+00
	8.333E-03	7.567E+00	7.969E+00	8.256E+00
	6.897E-03	7.703E+00	7.948E+00	8.215E+00
	6.667E-03	7.730E+00	7.945E+00	8.206E+00
	5.882E-03	7.558E+00	7.934E+00	8.183E+00
	5.405E-03	7.675E+00	7.921E+00	8.178E+00
	5.000E-03	7.479E+00	7.904E+00	8.181E+00
	4.545E-03	7.665E+00	7.883E+00	8.184E+00
	4.000E-03	7.698E+00	7.869E+00	8.171E+00
	3.636E-03	7.645E+00	7.873E+00	8.134E+00
	3.333E-03	7.682E+00	7.880E+00	8.075E+00
	3.077E-03	7.568E+00	7.882E+00	8.001E+00
	2.857E-03	7.473E+00	7.875E+00	7.918E+00
	2.703E-03	7.524E+00	7.860E+00	7.848E+00
	2.500E-03	7.487E+00	7.825E+00	7.741E+00
	2.326E-03	7.371E+00	7.776E+00	7.638E+00
	2.222E-03	7.293E+00	7.738E+00	7.571E+00
	2.000E-03	7.260E+00	7.630E+00	7.418E+00
	1.818E-03	7.232E+00	7.515E+00	7.285E+00
	1.667E-03	7.150E+00	7.402E+00	7.171E+00
	1.539E-03	6.912E+00	7.296E+00	7.074E+00
	1.429E-03	6.935E+00	7.198E+00	6.992E+00
	1.333E-03	6.835E+00	7.109E+00	6.921E+00
	1.250E-03	6.721E+00	7.029E+00	6.860E+00
	1.176E-03	6.727E+00	6.958E+00	6.808E+00
	1.111E-03	6.691E+00	6.895E+00	6.764E+00
	1.020E-03	6.549E+00	6.807E+00	6.703E+00
	9.091E-04	6.381E+00	6.703E+00	6.635E+00
	8.333E-04	6.343E+00	6.635E+00	6.591E+00
	7.692E-04	6.244E+00	6.579E+00	6.556E+00
	7.143E-04	6.290E+00	6.534E+00	6.528E+00

Temp °C	t_{CP} s	Exptl s^{-1}	$R_2(calc)$, s^{-1}	
			n=	n=3
	6.667E-04	6.274E+00	6.496E+00	6.505E+00
	6.250E-04	6.256E+00	6.464E+00	6.485E+00
	5.882E-04	6.233E+00	6.437E+00	6.469E+00
	5.405E-04	6.214E+00	6.405E+00	6.450E+00
	5.000E-04	6.119E+00	6.379E+00	6.435E+00
	4.444E-04	6.151E+00	6.346E+00	6.415E+00
	4.000E-04	6.134E+00	6.322E+00	6.402E+00
	3.636E-04	6.055E+00	6.304E+00	6.391E+00
	3.333E-04	6.063E+00	6.290E+00	6.383E+00
	2.857E-04	6.053E+00	6.270E+00	6.372E+00
	2.500E-04	6.150E+00	6.258E+00	6.365E+00
	2.222E-04	5.914E+00	6.249E+00	6.360E+00
	2.000E-04	5.930E+00	6.243E+00	6.357E+00
	1.667E-04	5.834E+00	6.234E+00	6.352E+00
	1.429E-04	5.927E+00	6.229E+00	6.349E+00
31.9	2.000E-02	8.668E+00	8.509E+00	8.820E+00
	1.800E-02	8.668E+00	8.499E+00	8.810E+00
	1.600E-02	8.856E+00	8.488E+00	8.797E+00
	1.429E-02	8.617E+00	8.476E+00	8.785E+00
	1.250E-02	8.457E+00	8.462E+00	8.771E+00
	1.111E+02	8.668E+00	8.450E+00	8.758E+00
	7.685E-03	8.854E+00	8.415E+00	8.721E+00
	7.000E-03	8.805E+00	8.407E+00	8.712E+00
28.6	2.000E-02	9.443E+00	9.219E+00	9.501E+00
	1.800E-02	9.302E+00	9.208E+00	9.489E+00
	1.600E-02	9.476E+00	9.195E+00	9.476E+00
	1.500E-02	9.275E+00	9.188E+00	9.468E+00
	1.250E-02	9.545E+00	9.167E+00	9.445E+00
	1.111E-02	9.331E+00	9.153E+00	9.430E+00
	7.692E-03	9.465E+00	9.110E+00	9.383E+00
	5.000E-03	9.450E+00	9.060E+00	9.323E+00
24.2	2.000E-02	1.054E+01	1.040E+01	1.064E+01
	1.500E-02	1.066E+01	1.036E+01	1.060E+01
	1.429E-02	1.062E+01	1.036E+01	1.059E+01
	1.250E-02	1.060E+01	1.034E+01	1.057E+01
	1.111E-02	1.024E+01	1.032E+01	1.055E+01
	7.000E-03	1.026E+01	1.024E+01	1.046E+01
	6.250E-03	1.049E+01	1.022E+01	1.043E+01
	5.556E-03	1.049E+01	1.019E+01	1.040E+01
	5.000E-03	1.051E+01	1.017E+01	1.038E+01
	3.995E-03	1.048E+01	1.012E+01	1.031E+01
23.5	2.000E-02	1.080E+01	1.062E+01	1.086E+01
	1.667E-02	1.052E+01	1.060E+01	1.083E+01
	1.250E-02	1.062E+01	1.055E+01	1.078E+01
	1.000E-02	1.013E+01	1.052E+01	1.074E+01
	8.000E-03	1.081E+01	1.047E+01	1.069E+01
17.4	2.000E-02	1.243E+01	1.270E+01	1.294E+01
	1.800E-02	1.251E+01	1.268E+01	1.291E+01
	1.500E-02	1.230E+01	1.264E+01	1.286E+01
	1.400E-02	1.261E+01	1.262E+01	1.284E+01
	1.250E-02	1.286E+01	1.259E+01	1.281E+01
16.8	2.000E-02	1.193E+01	1.288E+01	1.312E+01
	1.250E-02	1.226E+01	1.276E+01	1.298E+01
	1.000E-02	1.263E+01	1.270E+01	1.290E+01
	8.000E-03	1.222E+01	1.262E+01	1.279E+01
	6.667E-03	1.210E+01	1.254E+01	1.270E+01
	5.000E-03	1.295E+01	1.240E+01	1.251E+01
	4.000E-03	1.220E+01	1.227E+01	1.233E+01
15.2	2.000E-02	1.364E+01	1.333E+01	1.361E+01
	1.800E-02	1.364E+01	1.331E+01	1.358E+01

Temp °C	t_{CP} s	Exptl s^{-1}	$R_{2(calcd)}$, s^{-1} n=2	n=3
	1.600E-02	1.351E+01	1.328E+01	1.354E+01
	1.400E-02	1.312E+01	1.325E+01	1.350E+01
	1.250E-02	1.342E+01	1.321E+01	1.345E+01
	1.111E-02	1.302E+01	1.317E+01	1.340E+01
	1.000E-02	1.302E+01	1.313E+01	1.335E+01
9.8	1.500E-02	1.361E+01	1.378E+01	1.423E+01
	1.250E-02	1.383E+01	1.372E+01	1.414E+01
	1.000E-02	1.374E+01	1.363E+01	1.402E+01
	8.000E-03	1.327E+01	1.352E+01	1.386E+01
	6.667E-03	1.380E+01	1.341E+01	1.372E+01
	5.713E-03	1.318E+01	1.331E+01	1.357E+01
5.7	2.000E-02	1.230E+01	1.285E+01	1.346E+01
	1.250E-02	1.277E+01	1.273E+01	1.329E+01
	1.000E-02	1.272E+01	1.266E+01	1.318E+01
	6.667E-03	1.239E+01	1.248E+01	1.291E+01
	5.000E-03	1.221E+01	1.231E+01	1.267E+01
0.1	2.500E-02	1.034E+01	1.045E+01	1.101E+01
	2.000E-02	1.043E+01	1.043E+01	1.097E+01
	1.500E-02	1.050E+01	1.039E+01	1.092E+01
	1.250E-02	1.090E+01	1.036E+01	1.087E+01
	1.000E-02	1.083E+01	1.031E+01	1.081E+01
	8.000E-03	1.048E+01	1.026E+01	1.074E+01
	5.000E-03	1.037E+01	1.013E+01	1.055E+01
	4.000E-03	1.004E+01	1.004E+01	1.046E+01
-5.0	2.500E-02	9.197E+00	8.423E+00	8.776E+00
	2.000E-02	8.314E+00	8.409E+00	8.758E+00
	1.500E-02	8.534E+00	8.386E+00	8.728E+00
	1.250E-02	8.995E+00	8.368E+00	8.706E+00
	1.000E-02	8.874E+00	8.344E+00	8.673E+00
	8.000E-03	9.623E+00	8.316E+00	8.640E+00
	5.000E-03	8.756E+00	8.247E+00	8.558E+00
-5.4	2.500E-02	8.389E+00	8.276E+00	8.611E+00
	2.000E-02	8.185E+00	8.263E+00	8.594E+00
	1.000E-02	8.839E+00	8.200E+00	8.513E+00
	8.000E-03	9.126E+00	8.174E+00	8.483E+00
-10.2	2.500E-02	7.158E+00	7.052E+00	7.218E+00
	2.000E-02	7.386E+00	7.043E+00	7.207E+00
	1.000E-02	7.540E+00	7.000E+00	7.157E+00
	8.000E-03	7.175E+00	6.984E+00	7.142E+00
	5.000E-03	7.802E+00	6.945E+00	7.100E+00
	2.000E-03	7.649E+00	6.803E+00	6.691E+00
-15.3	2.500E-02	6.517E+00	6.322E+00	6.364E+00
	2.000E-02	6.508E+00	6.314E+00	6.356E+00
	1.000E-02	6.239E+00	6.281E+00	6.321E+00
	5.000E-03	6.507E+00	6.242E+00	6.280E+00
-18.7	3.500E-02	6.297E+00	6.073E+00	6.061E+00
	3.000E-02	6.207E+00	6.070E+00	6.058E+00
	2.857E-02	6.178E+00	6.069E+00	6.056E+00
	2.500E-02	6.112E+00	6.065E+00	6.053E+00
	2.000E-02	6.185E+00	6.059E+00	6.047E+00
	1.800E-02	6.386E+00	6.055E+00	6.043E+00
	1.500E-02	6.259E+00	6.048E+00	6.036E+00
	1.250E-02	6.134E+00	6.040E+00	6.028E+00
	1.111E-02	6.326E+00	6.035E+00	6.022E+00
-22.6	3.636E-02	5.907E+00	5.932E+00	5.877E+00
	2.857E-02	5.969E+00	5.928E+00	5.873E+00
	2.500E-02	5.967E+00	5.925E+00	5.870E+00
	2.000E-02	6.048E+00	5.920E+00	5.864E+00
	1.800E-02	6.066E+00	5.917E+00	5.861E+00
	1.500E-02	6.085E+00	5.910E+00	5.855E+00

Temp °C	t_{CP} s	Exptl s^{-1}	$R_{2(calcd)}$, s^{-1} n=2	n=3
	1.250E-02	5.999E+00	5.903E+00	5.848E+00
-26.8	3.000E-02	5.826E+00	5.904E+00	5.818E+00
	2.857E-02	5.894E+00	5.903E+00	5.818E+00
	2.500E-02	6.003E+00	5.900E+00	5.815E+00
	2.000E-02	5.934E+00	5.895E+00	5.810E+00
	1.800E-02	5.919E+00	5.893E+00	5.807E+00
	1.500E-02	6.071E+00	5.887E+00	5.802E+00
	8.000E-03	6.095E+00	5.862E+00	5.777E+00
	5.000E-03	5.846E+00	5.842E+00	5.756E+00
	4.000E-03	5.967E+00	5.834E+00	5.750E+00
	2.500E-03	6.011E+00	5.825E+00	5.734E+00
-30.4	2.500E-02	5.851E+00	5.951E+00	5.847E+00
	2.000E-02	5.876E+00	5.946E+00	5.843E+00
	1.800E-02	6.188E+00	5.944E+00	5.840E+00
	1.700E-02	6.019E+00	5.942E+00	5.839E+00
	1.600E-02	5.982E+00	5.941E+00	5.837E+00
	1.500E-02	6.009E+00	5.939E+00	5.836E+00
	1.250E-02	5.862E+00	5.933E+00	5.830E+00
	1.111E-02	6.193E+00	5.929E+00	5.826E+00
	1.000E-02	6.192E+00	5.925E+00	5.821E+00
-33.9	3.000E-02	6.295E+00	6.041E+00	5.926E+00
	2.857E-02	6.019E+00	6.041E+00	5.926E+00
	2.845E-02	6.075E+00	6.040E+00	5.926E+00
	2.500E-02	6.064E+00	6.039E+00	5.924E+00
	2.000E-02	6.060E+00	6.034E+00	5.919E+00
	1.800E-02	6.082E+00	6.032E+00	5.917E+00
	1.500E-02	6.081E+00	6.028E+00	5.913E+00
	1.250E-02	6.068E+00	6.022E+00	5.908E+00
	1.111E-02	6.099E+00	6.019E+00	5.904E+00
-36.8	3.000E-02	6.091E+00	6.141E+00	6.018E+00
	2.857E-02	6.117E+00	6.140E+00	6.018E+00
	2.500E-02	6.159E+00	6.138E+00	6.016E+00
	2.000E-02	6.072E+00	6.135E+00	6.012E+00
	1.800E-02	6.215E+00	6.133E+00	6.010E+00
	1.500E-02	6.129E+00	6.129E+00	6.006E+00
	1.250E-02	6.091E+00	6.124E+00	6.001E+00
-40.2	2.500E-02	6.345E+00	6.275E+00	6.145E+00
	2.000E-02	6.239E+00	6.271E+00	6.141E+00
	1.800E-02	6.372E+00	6.269E+00	6.139E+00
	1.600E-02	6.294E+00	6.267E+00	6.137E+00
	1.400E-02	6.228E+00	6.264E+00	6.134E+00
-41.6	3.000E-02	6.219E+00	6.340E+00	6.208E+00
	2.857E-02	6.157E+00	6.340E+00	6.207E+00
	2.500E-02	6.295E+00	6.338E+00	6.206E+00
	2.000E-02	6.304E+00	6.335E+00	6.202E+00
	1.800E-02	6.362E+00	6.333E+00	6.201E+00
	1.500E-02	6.309E+00	6.330E+00	6.197E+00
	1.250E-02	6.307E+00	6.326E+00	6.193E+00